GRIGORE T. POPA UNIVERSITY OF
MEDICINE AND PHARMACY IASI

HABILITATION THESIS

HEPATO-BILIO-PANCREATIC IMAGING – BEYOND A SIMPLE DIAGNOSTIC TOOL

Associate Professor
CORINA-VERONICA LUPASCU-URSULESCU, MD, PhD

2023

CONTENTS

ABBREVIATION LIST

ADK == Adenosine kinase
AFP == Serum a-fetoprotein
aFRS == alternative Fistula Risk Score
ALBI == Albumin Bilirubin
ALT == Alanine Transaminase
ANOVA == Analysis of Variance
ASA == American Surgical Association
AST == Aspartate Aminotransferase
AUC == Area Under the Curve
AUROC == Area Under the Receiver Operating Characteristic Curve
BCLC == Barcelona Clinic Liver Cancer
BCNHL == B-cell non-Hodgkin's Lymphoma
BMI == Body Mass index
CHASM == Associated Systemic Manifestations
CHC == Chronic Hepatitis C
CI == Confidence Interval
CMBS == Computer-Based Medical Systems
CNN == Convolutional Layer
COPD == Chronic Obstructive Pulmonary Disease
CRPF == Clinically Relevant Pancreatic Fistula
CPT == Child-Pugh-Turcotte
CRO == Contract Research Organization
CT == Computer Tomography
DAA == Direct-acting antiviral
DMFT == Dilatable Multifunction Trocal
DOAJ == Directory of Open Access Journals
EASL == European Association for the Study of the Liver
EBD == External Bile Drainage
EIBD == External-Internal Bile Drainage
EORTC == European Organization of Research and Treatment of Cancer
EOSL == European Association for the Study of the Liver
EOT == End of Treatment
EPRV == Estimated Pancreatic Remnant Volume
ERCP == Endoscopic Retrograde Cholangiopancreatography
FDG == F-fluorodeoxyglucose
G == Grade
GDA == Gastroduenal Artery
GGT == Gamma-glutamyl Transferase
GRE == Gradient Echo
GSH == Glutathione

HA == Hepatic Artery
HBV == Hepatitis B Virus
HCC == Hepatocellular Carcinoma
HCV == Hepatitis C Virus
HGB == Hemoglobin
HPB == Hepato-pancreato-biliary
HR == Hazard Ratio
HU == Hounsfield Unit
IASGO == International Association of Surgeons , Gastroenterologists and Oncologists
IEEE == Institute of Electrical and Electronics Engineers
IFN == Interferons
INR == International Normalized Ratio
IPMN == Intraductal Papillary and Mucinous Neoplasms
IQR == Interquartile range
ISBN == International Standard Book Number
ISI == International Scientific Indexing
L == Level
LGA = left gastric artery
LHA ==Left Hepatic Artery
LI-RADS == Liver Imaging Reporting and Data Systems
LSM == Liver Stiffness Measurements
LT == Liver Transplantation
MALT == marginal zone B-cell lymphoma of the mucosa-associated lymphoid tissue
MCN == Mucinous Cystic Neoplasm
MDCT == Multidetector Computed Tomography
MD-IPMN == Intraductal Papillary and Mucinous Neoplasm of the Main Duct
MELD == Model of End-stage Liver Disease
MMF == Mycophenolic Acid
MPD == Main Pancreatic Duct
MRI == Magnetic Resonance Imaging
OR == Odds ratio
PAIR == Percutaneous Aspiration-Injection-Reaspiration Drainage
PBD == Percutaneous Bile Drainage
PD == Pancreaticoduodenectomy
PDA == Pancreaticoduodenal Artery
PET-CT == Positron Emission Computed Tomography
PET-MRI == Positron Emission Tomograpy -Magnetic Resonance Imaging
PEVAC == Percutaneous Evacuation
PF == Pacreatic Fistula
PHA ==Proper hepatic artery
PHT == Portal Hypertension
PLT == Paletet Count
POPF == Postoperative Pancreatic Fistula

PPA == Pancreatic Pseudoaneurysm
PPC == Pancreatic Pseudocyst
PRL == primary renal lymphoma
PrOD == paritaprevir/ritonavir-ombitasvir and dasabuvir
PV == Portal Vein
PVA == polyvinyl alcohol
PVT == Portal Vein Trombosis
RBV == Ribavirin
ReLu == Rectified Linear Units
RF == Radiofrequency
RHA == Right Hepatic Artery
RNA == Ribonucleic Acid
ROC == Receiver Operating Characteristic
ROI == Region of Interest
rRHA == Replaced Right Hepatic Artery
SCVIR == Society of International Cardiovascular Radiology
SD == Standard Deviation
SMA == Super Mesenteric Artery
SMI == Skeletal Muscle Index
SMV == Superior Mesenteric Vein
SPIO == SuperMagnetic Iron Oxide
SPSS == Statistical Package for the Social Sciences
SRIM == Societatea de Radiologie si Imagistica din Romania
SVR == Sustained Virological Response
TACE == Transarterial Chemoembolization
TAE == Transcatheter Arterial Embolization
TMA == Total Muscle Area
TNM == Tumor Nodes Metastasis
TSE == Turbo-spin Echo
U/L == Units per Liter
UDL == Unenhanced Density of the Liver
UPD == Unenhanced Pancreatic Density
US == Ultrasonography
VGG == Oxford Visual Geometry Group
WHO == World Health Organization

REZUMAT

Teza de abilitare cu titlul „ ***Imagistica hepato-bilio-pancreatică – mai mult decât o simplă modalitate de diagnostic***” este o teză cumulativă, ce trece în revistă realizările profesionale, academice și științifice din perioada postdoctorală, dar se axează pe prezentarea preocupărilor mele într-un domeniu al radiologiei și imagisticii medicale (explorarea imagistică a ficatului, căilor biliare si pancreasului), unde diagnosticul se îmbină cu tratamentul asistat/ ghidat imagistic sau realizat prin metode de radiologie intervențională. Majoritatea activității de cercetare în acest domeniu a fost rezultatul colaborării cu colegii mei de aceeași specialitate dar, mai ales, în echipe multidisciplinare (alături de chirurgi, anatomo-patologi, gastroenterologi, anesteziști).

Am structurat lucrarea, în concordanță cu recomandările Consiliului Național de Atestare a Titlurilor, Diplomelor și Certificatelor Universitare (CNATDCU), pe trei secțiuni: Secțiunea I - Realizările pe plan academic, profesional și științific din perioada postdoctorală; - Secțiunea II - Direcții de dezvoltare și proiecte de cercetare viitoare; - Secțiunea III - Referințe bibliografice.

Secțiunea întâi a tezei de abilitare prezintă o sinteză a rezultatelor din domeniile academic și medical, dar și a celor științifice obținute pe parcursul celor 18 ani de activitate post-doctorală (2005-2023) în cadrul Universității de Medicină și Farmacie „Grigore T. Popa” din Iași și a Spitalului Clinic Județean de Urgențe ”Sf. Spiridon” Iași. Am evidențiat principalele elemente ale activității clinice si academice, precum și realizările științifice, concretizate în lucrări publicate. Sunt medic primar radiologie-imagistică medicală și am atestate de studii complementare în ultrasonografie generală, tomografie computerizată, imagistică prin rezonanță magnetică și radiologie intervențională. Obiectivele mele profesionale sunt în strânsă legătură cu direcțiile de dezvoltare în activitatea de învățământ postuniversitar, dar și în cea de cercetare științifică. După susținerea tezei de doctorat în 2004 și confirmarea titlului de doctor în medicină în 2005, activitatea științifică s-a axat pe imagistica abdominală, în special hepato-bilio-pancreatică, oncologică și pe radiologia intervențională abdominală. Rezultatele activității științifice in aceste domenii au fost publicate în 31 articole în reviste indexate ISI, dintre care 15 în calitate de autor principal, și 36 articole în reviste indexate în baze de date internaționale. De asemenea, sunt autor și coautor la 9 monografii și cursuri, dar și autor a 20 de capitole de carte, publicate în special în Editura ”UMF Iași” și Editura Academiei Române.

Recunoașterea activității științifice este dovedită de factorul de impact cumulat pentru articolele în care sunt autor principal de 31,752 și indicele Hirsch – 6.

Parcursul meu academic s-a desfășurat în cadrul disciplinei de Radiologie și Imagistică Medicală, Facultatea de Medicină, Universitatea de Medicină și Farmacie “Grigore T. Popa” Iaşi, pe o durată de 23 de ani, în care am parcurs etapele de asistent, șef lucrări și, ulterior, conferențiar din anul 2017. Activitatea didactică a inclus lucrări practice și cursuri din domeniul Radiologiei și Imagisticii Medicale pentru studenții Facultății de Medicină (anul IV seriile de predare în limbile română, engleză și franceză, anul III specializarea asistență medicală), cursuri postuniversitare (pentru rezidenți sau tip EMC), dar și participarea la un proiect Erasmus+ ce și-a propus crearea unei rețele europene de învățământ în domeniul oncogeneticii.

Am coordonat și primii pași în activitatea de cercetare a studenților (redactarea tezelor de licență, prezentări orale sau poster la congrese), a rezidenților (prezentări și postere la manifestări științifice naționale) și a studenților doctoranzi (ca membru in comisia de îndrumare).

Prezentarea activității științifice este structurată în 2 mari capitole, dedicate realizărilor în plan științific din principalele arii de interes ce fac subiectul acestei teze – explorarea imagistică hepato-biliară și pancreatică.

Primul capitol, referitor la **imagistica hepato-biliară**, este divizat în subcapitole: 1) rolul metodelor imagistice în patologia cronică hepatică (ce include a) evaluarea răspunsului la terapia cu agenți direcți antivirali; b) asocieri între hepatita cronică și alte patologii ; c) imagistica hipertensiunii portale); 2) diagnosticul imagistic și radiologia intervențională în tumorile hepatice ; 3) radiologia intervențională hepatică non-oncologică ; 4) radiologia intervențională biliară și 5) monitorizarea imagistică după chirurgia hepato-biliară.

Al doilea capitol este dedicat prezentării contribuțiilor personale din domeniul **imagisticii pancreatice**, fiind subdivizat în 1) importanța implicării vasculare și a prezenței variantelor arteriale în stadializarea tumorilor pancreatice; 2) imagistica postoperatorie pancreatică, cu accent pe aspectele normale și diagnosticul fistulei pancreatice postoperatorii; 3) tumori pancreatice rare.

Secțiunea a doua prezintă principalele direcții de dezvoltare viitoare a activității didactice, clinice și de cercetare științifică. Pe plan didactic, îmi propun implicarea tot mai activă în activitățile didactice complexe (studenți, rezidenți, cursuri postuniversitare/ EMC, proiecte ERASMUS), crearea unei noi linii de studiu în cadrul Universității pentru asistenții de radiologie, actualizarea permanentă a materialelor didactice. În planul activității medicale, îmi propun să dezvolt în special tehnicile de radiologie intervențională și colaborarea cu alte specialități în echipele multidisciplinare vizând tratamentul complex al patologiei oncologice. Pe plan științific, voi continua o parte din direcțiile de studiu actuale (in domeniile radiologiei intervenționale, al imagisticii transplantului hepatic și al diagnosticului complicațiilor postoperatorii pancreatice), dar voi încerca să dezvolt si implicarea inteligenței artificiale în diagnosticul imagistic și crearea unor algoritmi de selecție a pacienților pentru optimizarea tratamentului. Intenționez să completez gama procedurilor de radiologie intervențională, deschizând astfel și noi oportunități de cercetare.

Secțiunea a treia cuprinde o selecție a referințelor bibliografice corespunzătoare articolelor utilizate în elaborarea tezei de abilitare.

ABSTRACT

The habilitation thesis entitled "**Hepato-bilio-pancreatic imaging – beyond a simple diagnostic tool**" is a cumulative thesis, which reviews the professional, academic and scientific achievements of the postdoctoral period, but focuses on my involvement in a field of radiology and medical imaging (hepato-bilio-pancreatic imaging) that combines diagnosis with image-assisted / guided treatment and interventional radiology.
The research activity in this field was the result of fruitful and constant collaboration with my colleagues from Radiology Department but, also, within multidisciplinary teams (with surgeons, pathologists, gastroenterologists, anesthesiologists) concerning the hepato-bilio-pancreatic pathology and liver transplantation.
The thesis is structured, in accordance with the recommendations of the National Council for Attesting of University Titles, Diplomas and Certificates (CNATDCU), on three sections: Section I - Academic, professional and scientific achievements during the postdoctoral period; - Section II - Development directions and future research projects; - Section III - References.

The **first section** of the habilitation thesis presents a synthesis of the results from the academic and medical fields, but also the scientific achievements during the 18 years of post-doctoral activity (2005-2023) at the University of Medicine and Pharmacy "Grigore T. Popa" Iasi and the County Clinical Emergency Hospital "Sf. Spiridon" Iasi. I am a consultant radiologist and I have 4 certifications and competencies, namely general ultrasonography, computed tomography, magnetic resonance imaging and interventional radiology. My professional objectives are closely related to the directions of development in postgraduate education, but also in scientific research. The main elements of clinical and academic activity are highlighted, as well as scientific achievements, especially the published papers. After defending my doctoral thesis in 2004 and confirming my PhD in 2005, my scientific activity focused on abdominal imaging, especially hepato-bilio-pancreatic, oncology and interventional radiology. The results of the scientific activity were published in 31 articles in ISI indexed journals (15 as main author and 16 as co-author), and 36 articles in journals indexed in international databases. I am also author and co-author of 9 books, and author of 20 book chapters, mainly published by "UMF Iași" Publishing House and Romanian Academy Publishing House.
As a recognition of scientific activity, I would like to mention the cumulative impact factor (calculated for articles published as a main author) of 31,752 and the Hirsch index – 6.
My whole academic career is related to the Department of Radiology and Medical Imaging, Faculty of Medicine, University of Medicine and Pharmacy "Grigore T. Popa" Iasi. During the last 23 years I went through all academic steps, as an assistant, lecturer and, subsequently, associate professor since 2017. The teaching activity included practical workshops and courses in the field of Radiology and Medical Imaging for the students of the Faculty of Medicine (fourth year, teaching series in Romanian, English and French languages, and third year nursing specialization), postgraduate courses (for residents or CME type), but also participation in one Erasmus + project that aimed to create a European education network in the field of oncogenetics. I coordinated the first steps in the research activity for students (for graduation thesis, oral presentations or posters at congresses), residents (presentations and posters at national scientific events) and two doctoral students.
The presentation of the scientific activity is structured in 2 main chapters, dedicated to the main areas of interest that are the subject of this thesis – hepatobiliary and pancreatic imaging.

The **first chapter** – **the hepatobiliary imaging -** is divided into the following subchapters: **1)** The role of imaging methods in chronic liver disease (includes a) evaluation of response to therapy with direct antiviral agents; b) associations between chronic hepatitis and other pathologies; c) imaging of portal hypertension); **2)** Imaging diagnosis and interventional radiology in liver tumors ; **3)** Non-oncological interventional radiology for liver; **4)** Biliary interventional radiology; and **5)** Imaging follow-up after hepatic surgery.
The **second chapter** is dedicated to personal contributions in the field of **pancreatic imaging**, being divided into **1)** Staging of pancreatic tumors and diagnosis of vascular involvement/variants; **2)** Postoperative imaging and its implications in management of the complications; and **3)** rare lesions of the pancreas.

The **second section** presents the main directions of future development of teaching, clinical and scientific research activity. On teaching level, I intend to get more and active involvement in complex teaching activities (students, residents, ERASMUS projects, postgraduate courses), to create a new line of study within the University for radiographers (radiology technicians), to permanently update teaching materials. Concerning the medical activity, I aim to develop in our hospital the range of interventional radiology techniques, and the collaboration with other specialties in multidisciplinary teams. As projects for scientific research, I will continue some of the current study directions (concerning interventional radiology, liver transplantation imaging and diagnosis of postoperative pancreatic complications), and I will try to develop the involvement of artificial intelligence in imaging diagnosis and the creation of patient selection algorithms. The extension of the interventional radiology procedures practiced in our department will also open up new research opportunities.

The **third section** contains a selection of references corresponding to the articles used in the elaboration of the habilitation thesis.

SECTION I

PROFESSIONAL, SCIENTIFIC AND ACADEMIC ACHIEVEMENTS OVER THE POSTDOCTORAL PERIOD

A. SYNTHESIS OF PROFESSIONAL, SCIENTIFIC AND ACADEMIC ACTIVITY

BIOGRAPHICAL DATA

I was born on October 9, 1968, in Ianca, Braila.

In 1987 I graduated "C. Negruzzi" High School in Iasi – Science (mathematics and physics). Subsequently, I was admitted, based on exam, on Faculty of Medicine within the 'Gr T Popa' University of Medicine and Pharmacy Iasi, which I graduated in 1993.

1. PROFESSIONAL (MEDICAL) ACTIVITY

Upon completion of my undergraduate studies, I had one year of internship (1993-1994, employed by the Hospital of obstetrics and gynecology "Elena Doamna" Iasi, with stages in obstetrics and gynecology, internal medicine, orthopedics, and pediatrics). In November 1994 I was admitted, through the national residency exam, as a resident in Radiology-Imaging, employed by "Sf. Spiridon" Emergency University Hospital of Iasi. After completion of the 5-years training period (1995-1999), I became specialist in Radiology-Imaging (MS Order 900/1999), and since 2005 I have served as an attending radiologist (MS Order 1067/2004).

My entire clinical activity since 2000 was related to "Sf. Spiridon" Emergency County Hospital of Iasi, a tertiary referral center for Moldova, and I have provided imaging reports (emergency and inpatient) covering almost the entire spectrum of pathology, as well as treatment by interventional radiology methods for abdominal pathology. I performed thousands of radiological and imaging exams (performing and reporting radiographs during the first years of on-call duties, abdominal, vascular and small parts ultrasonography, computed tomography, both diagnostic and therapeutic interventional radiology procedures, etc.).

I have never ceased my professional development, since Radiology is a very dynamic specialty, with new techniques emerging and imaging protocols changing regularly. I have constantly attended specialization courses and obtained professional certifications and professional competencies. Several stages in other European countries allowed me to develop new competencies:

- in June-August 1996, as a part of TEMPUS program JEP 7094 coordinated by the University of Rouen, France, a stage at the University Hospital "S.Joao" Porto, Portugal, regarding the organization of health services;
- between November 1999 and April 2000 at Hopital Hautepierre, Department of Radiology (prof. F. Veillon), Faculty of Medicine Strasbourg, France; during 1999-2000 I have attended two postgraduated courses at the Faculty of Medicine Strasbourg, France: Attestation de Formation Spécialisée Approfondie (AFSA), Radiologie abdominale et des urgences, Universite „Louis Pasteur" Strasbourg, France and Diplome d'Universite d'Imagerie par Resonance Magnetique Clinique, Universite „Louis Pasteur" Strasbourg, France;
- August-November 2003 – an internship in emergency radiology at the University Cantonal Hospital (Department of Radiology) of Geneva, Switzerland.

Over 35 national and international courses completed my expertise in the field of ultrasonography (Ultrasound in medical and surgical emergencies , Craiova, 1999; Training course in General ultrasound, University "Gr.T.Popa " Iasi 2000-2001;) computed tomography (Training course in Computed tomography, University "Carol Davila " Bucharest, 2003), magnetic resonance (Magnetic Resonance Permanent European School - 1st course Prague
1996; Summer School of Imaging and Magnetic Resonance Spectroscopy, Sinaia, 2005; Basic training in MRI (SRIM) 2009; UMF "Carol Davila" Bucharest 2012), interventional radiology (Training course in Interventional Radiology, University "Gr.T.Popa " Iasi, 2000-2001), radiation protection in diagnostic and interventional radiology (2004, 2009, 2013, 2019) or in various fields of pathology (4th Refresher Course on Musculoskeletal Radiology – Halley Project – Continuing Education on Radiology in East Europe (European Association of Radiology) 1995; 5th Refresher Course on Chest, Musculoskeleton, GI, Urinary Tract and Abdominal Radiology, Halley Project - Continuing Education on Radiology in East Europe - Budapest, Hungary 1996; Armed Forces Institute of Pathology AFIP'96 - Lisbon , Portugal 1996; 2nd Refresher Course Series on Musculoskeletal, Neuro and Interventional, Halley Project - Continuing Education in Radiology in Eastern Europe, Budapest, Hungary 1998; Imaging thoracic pathology – GREF, Iasi, 2006; CNS-Spine Workshop, European School of Radiology, St. Petersburg 2006; ESOR Visiting Professorship Programme – Imaging neoplastic Diseases in GI Tract 2016; IASGO course „Advances in hepato-pancreatico-biliary malignancies" 2019).
I have 4 national certifications and competencies, in general ultrasonography, computed tomography, magnetic resonance imaging and interventional radiology.
A course on "Management of the modern health organization" attended at the University of Medicine and Pharmacy "Grigore T. Popa" Iasi in 2017 was a very useful tool to improve my activity as a coordinator of the National Health Program on Interventional Radiology in our hospital, as well as the course on "Management of European projects" (2014).
I am affiliated to several scientific and professional societies:

1. Society of Physicians and Naturalists, Iasi;
2. Romanian Society of Radiology-Imaging (SRIM) – secretary of the local section (2008-2012); member of the national committee 2006-2008; 2011-2013; 2015-2019; 2021-2023;
3. Romanian Society of Neuroradiology and Interventional Radiology – founding member and vice-president 2007;
4. European Society of Radiology – ESR;
5. CIRSE (Cardiovascular and Interventional Radiology European Society);
6. Societe Francaise de Radiologie;
7. International Association of Surgeons and Gastroenterologists (IASGO).

I was involved in the organizing committee for several international scientific manifestations:
- The 6th Francofon Congress of Medical Imaging for Central and Eastern European Countries, Iaşi, 2006;
- European School of Radiology - Iasi 2011;
- tutor for European School of Radiology - Training Center in Emergency Radiology (2012, 2014, 2015);
- Gastroenterology Summer School, Iasi, 24-27 July 2013, organized by the Romanian Society of Digestive Oncology, Partner European Society of Digestive Oncology.

As a member of national societies, I was involved in the organizing or scientific committee for national scientific manifestations: National Congresses and Conferences of the Romanian Society of Radiology-Imaging 2000, 2006, 2011, 2015, 2016, 2017, 2018, 2019; the 7th Conference of the Cross-sectional Imaging Society 2010; Summer School of Radiology 2014; Updates in Oncology, Iasi, 2019; The XIII Congress of the Romanian Association of Hepato- Biliary and

Pancreatic Surgery and Liver Transplantation, Iasi 2019; The XIth Congress of Romtransplant Association, Iasi, 2020.
During my daily medical practice, I coordinate the activity of residents in Radiology -Imaging, contributing to their professional training.

2. TEACHING ACTIVITY

My academic career began with enrollment in postgraduate study program– PhD in 1997, at the "Grigore T. Popa" University of Medicine and Pharmacy of Iasi.
In 1999, during my last year of residency, I obtained, by exam, the position of teaching assistant in the discipline of Radiology-Imaging at the Faculty of Medicine, University of Medicine and Pharmacy "Grigore T. Popa" Iasi. I have developed my teaching skills by attending the Course on psycho-pedagogy at the University "Al. I. Cuza" Iasi, 2001-2002. In 2008 I became lecturer and in 2017 associate professor in the same discipline.
Throughout this period of 24 years, I oversaw the practical activities, and I was teaching the course of Radiology for the fourth-year students in Medicine and for third year students of the General Nursing Program. Alongside the teaching activity with general medicine students and general medicine nursing students, I am involved in teaching for residents (radiology, gastroenterology, pneumology, internal medicine, general medicine, etc), supervising and coordinating their medical activity. Since 2022 I am also coordinator for residency in Radiology at the University of Medicine and Pharmacy "Grigore T. Popa" Iasi.
I had involved the students in case reports for clinical sessions and case series presentation for medical students' congresses and I coordinated more than 30 undergraduate students to elaborate their graduation theses in radiology.
Apart from the teaching and coordination of medical rounds for teaching purposes, I have contributed as an author to seven textbooks for students and young doctors and I wrote ten chapter in textbooks of radiology, semiology, oncogenetics.
As part of my teaching activity, I have contributed to the development of exam topics (multiple choice questions) for students of all grade levels who came under the scope of my teaching activity. I am also involved in all the activities concerning the admission process (for Romanian students, and for foreign students), the graduation exam, the residency exam, the specialty exam. Since 2022 I coordinate the activity of the discipline of Radiology-Imaging at the Faculty of Medicine Iasi.

3. RESEARCH ACTIVITY

My structured research activity began during 1997-2004, with doctoral studies on the topic "The value of imaging studies for diagnostic of postoperative complications after abdominal surgery", under the coordination of MD PhD M.R. Galesanu. The results of the clinical research carried out in the field of the doctoral dissertation research topic led to the publication of 3 articles in extenso in BDI journals as well as in oral presentations and scientific poster communications at national and international events.
To date, my scientific and research activity is summarized by: author and co-author of 9 specialty textbooks, 20 chapters, 31 articles (15 main author and 16 coauthor) published in extenso in ISI indexed journals with impact factor, 37 articles published in BDI indexed journals and 7 articles published in extenso in other CNCSIS recognized journals. I should also mention 16 abstracts published in supplements of ISI-indexed journals and 85 abstracts in the publications of scientific events with ISBN, as well as more than 100 communicated papers at various national and international conferences.
I attended all the specialty national symposiums and congresses, and I gave many lectures as invited speaker. Some of these presentations were awarded: Prize of the Romanian Society of Radiology and Medical Imaging and Schering Prize for poster at the National Congress of

Radiology and Medical Imaging (1999), Magna Cum Laudae and Cum Laudae Award; National Congress of Radiology and Medical Imaging "Millennium 2000", Iasi, Mention at the National Congress of Radiology and Medical Imaging 2006, Prize of the Society of Radiology and Medical Imaging in Romania at the 16th National Congress of the Society of Radiology and Medical Imaging.

In the same regard, I emphasize that the scientific articles have attracted more than 100 citations in Clarivate Analytics Web of Science Core Collection and over 200 citations in Google Scholar, which have generated a Hirsch index of 6 according to Clarivate Analytics.

My activity has also been directed toward research/educational projects and I have been actively involved in national and international projects obtained through competition.

A. INTERNATIONAL PROJECTS

1. ERA NET EuroNanoMED JTC-3 (2011): "Chemo-Hyperthermal delivery combined chemo-hyperthermal control of hepatic tumors, based on microwave-activated subendothelial-targeted nano-assemblies" (Che Ther Del) – 02.05.2012 - 20.12.2014 – project manager for Partner 2 (Institute of Oncology Iasi) ;
2. Réseau partenaire francophone pour la validation clinique des protocoles diagnostiques et thérapeutiques de la médecine fœtale dans la région de l'Europe Orientale, 01.10.2012-01.10.2014, UMF Iasi, UMF Testemitanu Chisinau, UM Descartes Paris, Franta - research team member;
3. Promoters of advanced oncogenetics open online training and multimedia raise awareness on multidisciplinary assessment of patients and their families at risk of hereditary or familial cancer" - HOPE - How Oncogenetics Predicts & Educates ; Proiect ERASMUS + (2018-1-RO01-KA202-049189)- research team member.

B. NATIONAL PROJECTS

1. CEEX 122/2006: "Selection criteria of the therapeutic methods in secondary hepatic cancer - clinic-biologic and molecular substantiation" – research team member;
2. CEEX - M1 - C2 – 5482 (tip P-CD)" Textiles with drugs controlled issue in the treatment of dermatological diseases" DERMACTIVTEX contract code 192/1.09.2006; research team member;
3. IMAGO-MOL Regional Cluster; team member.

C. INTERNATIONAL MULTICENTER STUDIES – coinvestigator

1. A multicenter multinationale phase 3 randomized study to evaluate the safety and efficacy of treating colorectal cancer patients recurrent liver metastases using the LitxTm system plus chemotherapy as compared to chemotherapy only; LSO-OL006
2. HGS 1012-C1103 „A randomized, multi-center, blinded, placebo-controlled study of Mapatamumab ([HGS1012], a fully-human monoclonal antibody to TRAIL-R1) in combination with sorafenib as a first-line therapy in subjects with advanced hepatocellular carcinoma" ClinicalTrials.gov Identifier: HGS1012-C1103; Sponsor: Human Genome Sciences, Inc; PSI CRO AG ; 2010 – 2013;

Chapter 1.

DIAGNOSTIC AND INTERVENTIONAL RADIOLOGY IN HEPATO-BILIARY PATHOLOGY S

1. 1. CONTEXT AND RATIONALE OF THE RESEARCH TOPIC

During my postdoctoral period, the liver and biliary tree pathology represented a constant line of research in close relationship with my clinical activity. This direction is one of the most consistent, with various scientific achievements.

The role of the radiologist and of the interventional radiology in hepatic pathology represented for me a constant interest even before my graduation, driving me to the subject of "Chemoembolization for treatment of hepatic tumors" in 1993 for my graduation thesis. At that time, chemoembolization for hepatic tumors, introduced in 1983 in Japan, was a completely new method of treatment in Romania, as well as the subspecialty of interventional radiology. Having the opportunity to work between 1992 and 2004 with Professor Cezar Daniil, one of the pioneers of the interventional radiology in Romania, this line of research came as a natural development of my interest and continued to be among my challenging research directions even today.

On the other hand, the focus on this pathology has been kept up by the increasing incidence and prevalence of the liver chronic disease and of the hepatocellular carcinoma in Romania, due to its complex etiopathogenesis, to the significant progress in diagnostic, including imaging diagnosis, and by steady progress in the management of diffuse and focal liver disease in recent decades, with new drugs and new focal therapies developed and successfully implemented.

Furthermore, the development of the liver transplant activity in "St. Spiridon" Hospital (authorized for organ procurement activity since 2013 and for liver transplantation since 2016) represented an additional encouragement for this line of research as part of the multidisciplinary team involved in evaluation of transplant recipients and donors.

The research in this field in my postdoctoral period was accomplished in multidisciplinary teams, together with gastroenterologists from Institute of Hepatology and Gastroenterology Iași and surgeons from 2nd Surgical Clinic, St. Spiridon Hospital Iași.

The research I have been involved in 18 years aimed to establish the role of imaging in chronic liver diseases, liver tumors, as well as in postoperative follow-up. Other studies have capitalized the clinical experience in the field of abdominal interventional radiology, regarding oncological and non-oncological procedures, endovascular and non-vascular.

1.2. SCIENTIFIC ACHIEVEMENT IN THE FIELD OF RESEARCH

Below is presented the research carried out in this field and the results published in original articles to which I contributed as main author or co-author, as well as in books.

I have divided the research I have conducted on hepato-biliary imaging into five main subdivisions: 1. The role of imaging studies in chronic liver disease; 2. Diagnostic and interventional radiology for liver tumors; 3. Non-oncological interventional radiology for liver; 4. Interventional radiology for biliary system; 5. Imaging follow-up after hepatic surgery.

1.2.1. Is there a role for imaging studies in chronic liver disease?

Liver cirrhosis, characterized by significant change of the parenchymal and vascular architecture with formation of septae and regenerative nodule, is a major cause of morbidity and mortality worldwide and is still the 11th most common cause of death in the world (Asrani, et al. J. Hepatol. 2019). One main cause of cirrhosis is the infection with hepatitis C virus (HCV) [Sebastiani, et al. World J. Gastroenterol. 2014).

Cross-sectional imaging techniques, such as computed tomography (CT), magnetic resonance imaging (MRI), and ultrasonography (US) have been used for diagnosis and staging of cirrhosis with variable rates of success. US is the most accessible and widely used imaging method for the evaluation of patients with chronic liver disease; liver cirrhosis diagnosis using US has an accuracy, sensitivity, and specificity of 64–79%, 52–69%, and 74–89%, respectively (Kudo M, et al. Intervirology 2008; Sangster GP, et al. HPB Surg. 2013). MRI sensitivity and specificity in liver cirrhosis are 87% and 54%, respectively, similar to CT (Kudo M, et al. Intervirology 2008). Contrast-enhanced abdominal CT is frequently indicated for cirrhotic patients due to its ability to diagnose and stage HCC. Additionally, CT is useful to evaluate the extrahepatic complications of cirrhosis, such as portal hypertension and its effect on the abdominal organs.

Different independent predictive imaging signs were described for the diagnosis of liver cirrhosis (Kudo M, et al. Intervirology 2008; Mihai F, et al. Rev. Med. Chir. 2017). Imaging features, such as the hypertrophy of the caudate lobe, the hypertrophy of the lateral segments of the left lobe (II and III) with atrophy of the medial segment (IV) and of the posterior segments (VI and VII) of the right lobe were considered typical for cirrhosis (Sangster GP, et al. HPB Surg. 2013). Volume changes in the left lobe medial segment and right lobe segments lead to the widening of gallbladder fossa and the enlargement of central periportal space (defined as the distance between the anterior wall of the right portal vein and the posterior edge of the medial segment of the left hepatic lobe, assessed with a cut-off value of 10 mm) (Tan KC, Radiology 2008; Ito K, et al. Radiology 1999). Alteration of the caudate and right lobe morphology results in the presence of the right hepatic posterior notch sign, representing the functional lateral boundary of the hypertrophied caudate lobe and can be used as a simple and specific sign of cirrhosis (Tan KC, Radiology 2008). The regenerative nodules, formed during the repair process, determine the compression of the central hepatic veins, with decrease of hepatic veins diameters; a diameter of the right liver vein below 7 mm raises the suspicion of cirrhosis (Zhang Y, et al. J. Magn. Reson. Imaging 2009).

Beyond descriptive features, several imaging-based scores were developed to quantify cirrhosis, all based on the caudate lobe hypertrophy. The caudate-right lobe ratio (C/RL), developed by Harbin et al, is based on axial imaging measurements and calculated by dividing the width of the caudate lobe to the width of the right lobe at bifurcation of portal vein; a ratio $\geq$0.65 is a positive diagnostic indicator for cirrhosis, with 100% specificity, good sensitivity (84%), and accuracy (94%) (Harbin WP, et al. Radiology 1980). A modified caudate-right lobe ratio (C/RL-m) is calculated using the right portal vein bifurcation instead of main portal as lateral boundary; it was reported to be more accurate both for diagnosis and for assessment of clinical severity of cirrhosis (Awaya H, et al. Radiology 2002). The latest imaging score for cirrhosis proposed by Huber et al. combines both morphological and vascular changes, dividing the sum of liver vein diameters by the C/RL-m (Huber A, et al. Swiss Med. Wkly. 2014). Other findings, as splenic volume enlargement, the presence of ascites, the portal hypertension, and the sarcopenia, are also accurately assessed by imaging studies.

Direct acting antivirals (DAAs) were introduced in 2014 and changed the paradigm of the treatment for patients with HCV due to high sustained virologic response (SVR) rate (95–100% in genotype 1) and excellent tolerability (Stanciu C, et al. Hepat. Mon. 2015; Gheorghe L, et al. J. Gastrointest. Liver Dis. 2017).

Despite the proven SVR, the constant risk of developing HCC justifies a close follow-up of these patients, including imaging follow-up [Kogiso T, et al. JGH Open 2018). Furthermore, the irreversibility of cirrhosis is no longer considered a "dogma" as liver fibrosis is potentially reversible once the trigger is removed (Desmet VJ, et al. J. Hepatol. 2004). Evidence that patients who achieve SVR are less likely to develop liver-related complications, due to the regression of fibrosis after HCV eradication was previously reported (Trivedi HD, et al. Gastroenterol. Hepatol. 2017). The non-invasive methods used to assess liver fibrosis confirmed the regression in patients with SVR (Bachofner JA, et al. Liver Int. 2017; Mauro E, et al. Hepatology 2018; Trifan A, Stanciu, C. World J. Gastroenterol. 2012).

This direction of research has been accomplished through the following contributions:

Articles

1. Zabara M, Trofin AM, Cadar R, Nastase A, Blaj M, Ciuntu BM, Garleanu I, **Lupascu-Ursulescu C**, Lupascu C. Prognostic factors for outcome of liver transplantion hepatitis C cirrhosis. Chirurgia 2023;36(1): 5-9 DOI: 10.23736/S0394-9508.22.05393-1
2. Muzica CM, Stanciu C, Cijevschi-Prelipcean C, Girleanu I, Huiban L, Petrea OC, Singeap AM, Cojocariu C, Cuciureanu T, Sfarti C, Zenovia S, Chriac S, Stefanescu G, Ciortescu I, **Lupascu-Ursulescu C**, Miftode E, Trifan A. Long-Term Risk of Hepatocellular Carcinoma Following Direct-Acting Antiviral Therapy in Compensated Liver Cirrhosis Induced by Hepatitis C Virus Infection. Hepatitis Monthly 2021; 21 (6); e115910 DOI: 10.5812/hepatmon.115910 (**IF 2021- 1.214**)
3. Mihai F, Trifan A, Stanciu C, Huiban L, Muzica C, **Lupascu-Ursulescu C**, Negru D, Savin M.L, Gîrleanu I, Cuciureanu T et al. L3 Skeletal Muscle Index Dynamics in Patients with HCV-Related Compensated Cirrhosis Following Sustained Virological Response after Direct Acting Antiviral Treatment. Medicina 2021, 57, 1226. (**IF 2021 - 2.948**)
4. Mihai F, Trifan A, Stanciu C, Singeap AM, Cucuteanu B, **Lupascu Ursulescu C**, et al. Liver Remodeling on CT Examination in Patients with HCV Compensated Cirrhosis Who Achieved Sustained Virological Response after Direct-Acting Antivirals Treatment. MEDICINA-LITHUANIA 2020; 56 (4); DOI: 10.3390/medicina5604017 (**IF 2020 = 2.43**)
5. Liţescu M, Baboi ID, Paverman L, Vrabie CD, Iordache N, Coman IS, **Lupaşcu-Ursulescu CV**, Dina I, Grigorean VT. Incidental case of primary renal lymphoma (PRL) in a patient with chronic hepatitis C infection. Report of a rare case. Rom J Morphol Embryol. 2020 Jul-Sep;61(3):929-934. doi: 10.47162/RJME.61.3.33. (**IF 2020 -1,033**)
6. Mihai F, Cucuteanu B, **Lupascu-Ursulescu C**, et al. Reduction of splenic volume after direct acting antivirals treatment in patients with HCV compensated cirrhosis. Revista medico-chirurgicala 2020; 124 (2): 225-230
7. **Lupascu-Ursulescu C,** Trofin AM, Zabara M, Vornicu A, Cadar R, Apopei O, Stefanescu G, Lupascu C. Bleeding from isolated gastric varices as complication of a mucinous cystic neoplasm of the pancreas. A case report. Medicine 2017; 96:47(e8775) (IF 2017 – **2,028**)

Abstracts in ISI journals

Mihai F, Trifan A, Stanciu C, Huiban L, Muzica CM, **Lupascu- Ursulescu C**, Negru D, Girleanu I, Cuciureanu T, Singeap AM. CT evaluation of skeletal muscle mass dynamics following sustained virological response in patients with hcv-related compensated cirrhosis treated with direct acting antivirals. Gastroenterology 2021; 160 (6): S792-S792 **(IF 2020 – 22,682)**
Books **Ursulescu C,** V.Drug, C.Stanciu. Investigaţii paraclinice în hipertensiunea portală. În: C.Stanciu (ed) Esenţialul în hipertensiunea portală. Ed. Junimea, Iaşi, 2007: 32-48, ISBN 978-973-37-1207-7

1.2.1.1 Assessment of treatment response to direct acting antiviral agents in patients with chronic hepatitis

The studies concerning the treatment response to direct acting antiviral agents in patients with chronic hepatitis, who have achieved SVR, were triggered by the need to follow-up patients enrolled in Institute of Gastroenterology and Hepatology in Iași for this treatment. They were achieved in collaboration with the gastroenterology team and aimed to assess the changes of some morphological parameters after treatment, evaluated by imaging methods. Correlation with reversibility of fibrosis of the liver was assessed, as well as the prevalence of hepatocellular carcinoma (HCC).

1.2.1.1.1 Liver and spleen remodeling after DAA therapy

Methods

Study Design

A prospective study on patients with genotype 1 HCV-related compensated cirrhosis who have achieved SVR after treatment with DAAs (Ombitasvir/ Paritaprevir/ ritonavir + Dasabuvir) was conducted.

Patients were enrolled according to the criteria of National Health Insurance Agency, also recommended by international guidelines: adult, treatment experienced or naïve patients with Child–Pugh class A cirrhosis assessed by Fibromax® Biopredictive (cut-off of 0.71 for F4) or liver biopsy (F4 by METAVIR). Decompensated liver cirrhosis or evidence of hepatocellular carcinoma were exclusion criteria.

An abdominal CT was performed before treatment to exclude liver malignancy and to evaluate liver morphology.

After the completion of the treatment, the imaging follow-up protocol included US at every 6 months and a second abdominal CT, within 6 and 18 months following SVR achievement, to characterize nodular lesions or other parenchymal abnormalities detected by US.

All CT scans, anonymized, were independently reviewed by three senior radiologists with experience in hepatobiliary radiology, blinded to all patient information. A fourth reader provided consensus when disagreement in measurement occurred.

Scanning Protocols

The scanning protocol, achieved on a Siemens Sensation® 16 slice configuration CT scanner (Siemens AG Medical Solution, Erlangen, Germany), was optimized for detection of potential malignant liver lesion, according with CT/MRI Diagnostic LI-RADS® recommendation, and included a non-enhanced scan followed by i.v. administration of iodine-based contrast medium and a tri-phase liver scan (arterial at 30–35 s, portal at 75 s and equilibrium phase at about 4 min

after contrast injection). The contrast medium was administered in bolus with an injection rate of 3–5 mL/s. Patients were examined in the supine position, in post inspiratory apnea.

Data Analytic Strategy for Imaging Interpretation

The following liver morphological changes were evaluated: liver volume estimation (maximum dimension in cranio-caudal × latero-lateral × antero-posterior × 0.31 in cm3) [Muggli D, 2009]; C/RL and C/RL-m (the width of the caudate lobe in proportion to the width of the right hepatic lobe); hepatic veins diameter; central periportal space width; combination of hepatic vein diameter sums and caudate-right lobe ratio; assessment of right posterior hepatic notch variation; manifestations of portal hypertension: dilatation of portal system, including portal trunk, splenic vein, and superior mesenteric vein diameter and splenomegaly using the index value (product of maximum cranio-caudal dimension and length and thickness in axial plane) and the splenic volume (index value × 0.58 + 30) in cm3 [Liu P, 2009].

Statistical Analysis

The inspection of the continuous variables assessed the normality of the distributions, including the distributions of the differences between two repeated measurements. Since most of the differences did not meet the normality requirement, comparisons between the two sets of measurements were performed with the Wilcoxon signed-rank test, to search for changes in parameter levels; p value < 0.05 was considered statistically significant.

Results

Patients

There were 56 patients enrolled (24 men and 32 women), mean age 57.78 ± 9.048 years (range 42–79). All the results are summarized in Table 1.I.

Table 1.I Liver morphological changes before and after treatment

Variable	Pre-Treatment		Post-Treatment		*p*
	Median	IQR	Median	IQR	
Liver volume (cm^3)	1786.77	879.23	1716.44	840.50	0.049
Caudate-right lobe ratio	0.65	0.19	0.65	0.17	ns
Modified caudate-right lobe ratio	0.98	0.28	0.99	0.31	ns
Right hepatic vein diameter (mm)	6.36	3.94	8.12	4.20	<0.001
Middle hepatic vein diameter (mm)	5.70	2.48	5.91	2.51	ns
Left hepatic vein diameter (mm)	6.69	3.17	6.65	3.19	ns
Sum of hepatic vein diameters (mm)	19.29	9.52	21.44	9.06	0.028
Huber's score	19.16	11.50	20.58	9.73	0.035
Central periportal space widening (mm)	11.85	5.75	11.7	6.47	ns
Right posterior hepatic notch (degrees)	126.3	26.05	136.9	17.30	ns
Splenic volume (cm^3)	564.79	342.54	474.45	330.00	0.012
Portal trunk diameter (mm)	14	2.70	14.2	2.90	ns
Superior mesenteric vein diameter (mm)	12.7	2.90	12.2	2.70	ns
Splenic vein diameter (mm)	9.85	3.31	10.2	3.73	ns

ns: nonsignificant; IQR: interquartile range.

1.2.1.1.2 Hepatic Veins Diameters

Only the right hepatic vein diameter showed a statistically significant widening after treatment (median: 8.12 mm, IQR: 4.20), compared to the diameter recorded before treatment (median: 6.36 mm, IQR: 3.94), $z = -3.894$, $p < 0.001$. No significant changes were found for diameters of the middle and left hepatic veins (Fig. 1.1).

The overall scores for the vein diameters were statistically significantly higher after treatment (median: 21.44 mm, IQR: 9.06) than before treatment (median: 19.29 mm, IQR: 9.52), z = −2.194, p = 0.028.

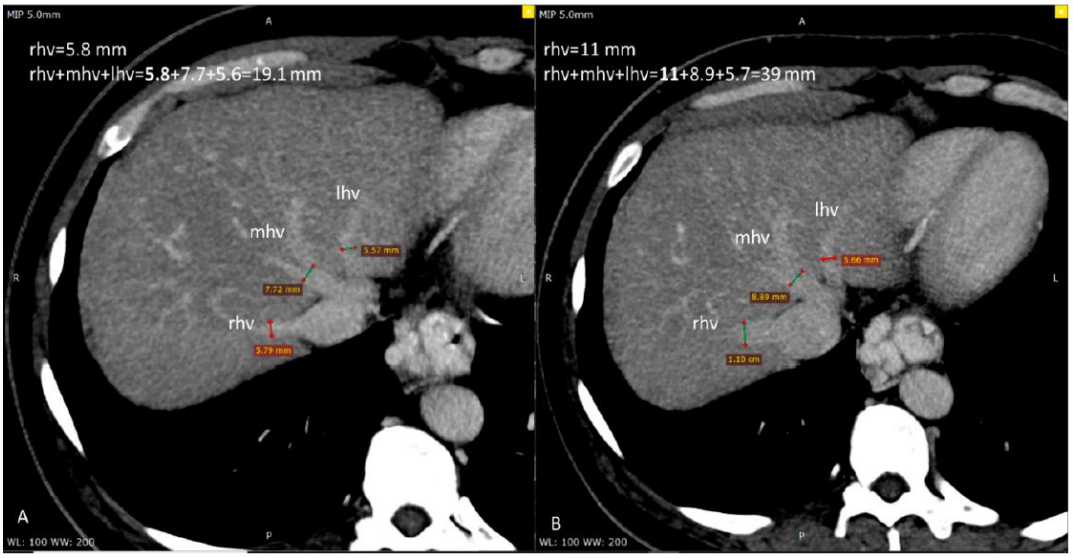

(**A**) (**B**)

Fig. 1.1. Computed tomography (CT) axial section at the level of hepatic veins before (A) and after (B) treatment. Only the right hepatic vein (rhv) showed significant widening after treatment (11 mm) compared to before (5.8 mm), while the middle hepatic vein (mhv) and left hepatic vein (lhv) showed no significant changes

The Caudate-Right Lobe Ratio and Modified Caudate-Right Lobe Ratio

There were no statistically significant differences between the C/RL before (median: 0.65, IQR: 0.19) and after treatment (median: 0.65, IQR: 0.17), z = −1.283, p = 0.2, as well as between C/RL-m before (median: 0.98, IQR: 0.28) and after treatment (median: 0.99, IQR: 0.31), z = −0.597, p = 0.551.

Huber's Score

Huber's score before treatment (median: 19.16, IQR: 11.50) was significantly lower than after treatment (median: 20.58, IQR: 9.73), z = −2.106, p = 0.035, probably due to changes in hepatic vein diameters, because C/RL-m did not show meaningful changes (Fig. 1.2).

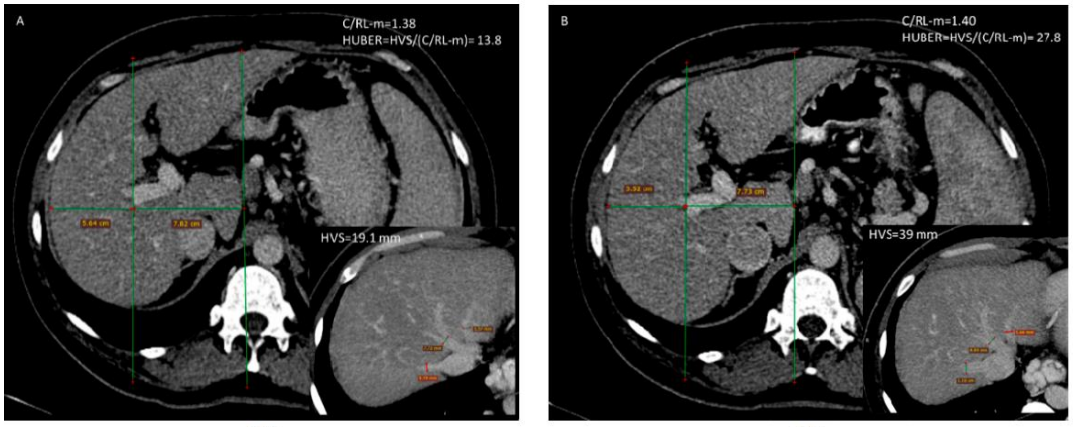

(**A**) (**B**)

Fig. 1.2 Huber's score—before (A) and after (B) treatment in one patient. HVS: hepatic veins sum; C/RL m: caudate right lobe ratio modified.

Liver Volume

Liver volume was significantly higher before (median: 1786.77 cm3, IQR: 879.23) than after treatment (median: 1716.44 cm3, IQR: 840.50), $z = -1.970$, $p = 0.049$.

Central Periportal Space Widening

We found no differences between central periportal space widening measured before (median: 11.85 mm, IQR: 5.75) and after treatment (median: 11.7 mm, IQR: 6.47), $z = -0.368$, $p = 0.713$.

Right Posterior Hepatic Notch Variation

There were no significant differences between right posterior hepatic notch angle before (median: 126.3, IQR: 26.05) and after treatment (median: 136.9, IQR: 17.30), $z = -1.783$, $p = 0.075$.

Indicators of Portal Hypertension

We found significant difference only for ***splenic volume*** before and after treatment (median: 564.79 cm3, IQR: 342.54 vs. median: 474.45 cm3, IQR: 330, $z = -2.500$, $p = 0.012$).

There were no differences between the portal trunk, splenic vein, and superior mesenteric vein diameter before and after treatment.

Discussion

During these past decades, cirrhosis has evolved from an irreversible liver disease into a potentially reversible one.

The main question is what happens after SVR with the liver: will the morphological changes remain as such, or will there be further morphological hepatic improvement?

Our study showed improvements of some of the morphological changes such as decrease of the liver and spleen volume, widening of the right hepatic vein diameter, increase of the sum of hepatic vein diameters and of Huber's score. The first morphological improvement after treatment was the decrease in liver volume. Although the decrease in volume was statistically significant, it is small in value and therefore we consider that it is more likely secondary to the reduction of inflammation. The most dynamic changing parameter was the hepatic veins diameter, especially the right hepatic vein, significantly increased from a median of 6.36 mm at baseline to 8.12 mm ($p < 0.001$) after treatment. This variation has been also reported by other studies evaluating the fibrotic changes in pre-cirrhotic or cirrhotic patients [Huber A et al, 2014]. We estimate that this parameter is the most sensitive one and can be used as an early marker of liver recovery. It is unclear whether this improvement is secondary to inflammation, or if it is a true indicator of fibrosis reduction. Secondary, the Huber's score also improved after treatment.

The widening of the periportal space consequently to atrophy in segment IV, the caudate-right lobe ratio and the presence of the hepatic notch show no significant variation. It is however premature to set the boundaries of the reversibility in short-term follow up, as it could take longer to see a change in this parameter.

Regarding the portal system, no significant changes were noted for vessel diameter. This lack of modifications may reflect a balance between two opposite tendencies: one towards a reduction in diameter because of flow reduction and the other towards an enlargement due to portal hypertension. The improvement of portal hypertension status was revealed only by decrease in splenic volume.

1.2.1.1.2 L3 Skeletal Muscle Index Dynamics after DAA treatment

Introduction

Sarcopenia, a syndrome characterized by progressive and generalized loss of skeletal muscle mass and impairment of muscular strength, is a remarkably frequent abnormality, ranging from 40–70%, depending on the definition criteria, the type of study population, and the assessment methods (Ponziani et al, 2018; Kim et al, 2015; Montano-Loza et al, 2015). Sarcopenia is seen as a prevalent complication, a proven predictor for morbidity and mortality of cirrhotic patients

(Mauro et al, 2020; DiMartini et al, 2013). For these reasons routine assessment of sarcopenia is highly recommended, involving measurement of muscle mass, in addition to muscle strength and function.

The introduction of direct-acting antivirals (DAAs) for the treatment of patients with HCV-related cirrhosis gives hopes for the improvement of cirrhosis-associated comorbidities, including sarcopenia. Moreover, for cirrhotic patients treated with antiviral therapies, maintaining muscle mass is crucial and identifying pretreatment factors linked to the improvement in skeletal muscle mass is important in nutritional strategy.

CT is currently the most widely used method for evaluating sarcopenia (Sinclair et al, 2016; Paternostro et al, 2019). It is easy to access, does not require preparation of the patient before scanning, and allows the evaluation of muscle mass even on non-enhanced examinations. Different muscle groups were considered to quantify muscle mass, but the most widely used method measures total muscle area (TMA) at a section level passing through the third lumbar vertebra (L3), calculating the skeletal muscle index (SMI) (Paternostro et al, 2019). The L3-SMI is easy to assess and there are well-established cutoff values depending on gender (Boutin et al, 2015).

Our study evaluated patients with HCV-related cirrhosis who achieved SVR after DAA treatment, aiming to identify the changes in L3-SMI as a quantitative marker of sarcopenia, and the pretreatment predictive factors for the evolution of L3-SMI.

Materials and Methods

Study Design

A single center retrospective study was conducted in patients with genotype 1 HCV-related compensated cirrhosis who obtained SVR after treatment with DAAs. Demographic and biological parameters were assessed for all patients at baseline.

To evaluate the dynamics of muscle mass, we included in the study patients who had at least two CT evaluations: one before treatment with DAAs, and another after obtaining SVR. The interval between these CT examinations ranged from 5 to 24 months.

Scanning Protocols

Patients were examined in the supine position, in post-inspiratory apnea. The scanning protocol includes a non-enhanced scan followed by intravenous administration of iodine-based contrast medium. The contrast medium was administered in bolus with an injection rate of 3–5 mL/s and a three-phase acquisition were made after contrast injection.

Assessment of L3-SMI (Skeletal Muscle Index)

All imaging data were acquired from venous phase images using a single slice axial CT scan of the abdomen. The third lumbar vertebral body, with both transverse processes visible was chosen as a reference for processing. The designated axial slice, 3 mm in thickness, was evaluated in the soft tissue window (WL 60 WW 360) and the truncal muscles (psoas muscle, erector spinae, quadratus lumborum, transversus abdominis, external and internal obliques and rectus abdominis) were delimited (Fig. 1.3).

A semi-automated demarcation of the muscle tissue was based on Hounsfield unit (HU) thresholds from −29 to +150. We used for demarcation a 3D Slicer® image computing platform, a free, open source and multi-platform software package used for medical and related imaging research. Manual corrections were applied by the reader when needed. The calculated total muscle area (TMA) was expressed in cm^2. Skeletal muscle index (L3-SMI) was calculated dividing TMA to square height (H2) of patient expressed in m^2 as follows: $SMI=TMA(cm^2)/H^2(m^2)$

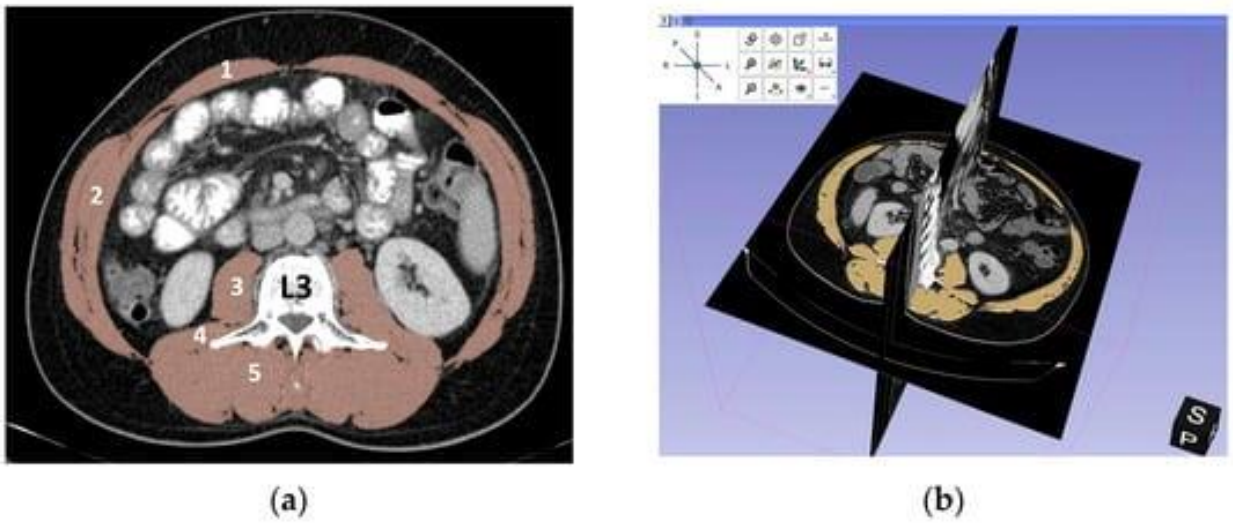

Fig. 1.3 Axial cross-section at third lumbar vertebra (L3): (a) Total muscle area included: (1) rectus abdominis, (2) transversus abdominis, internal and external oblique, (3) psoas, (4) quadratus lumborum, (5) erector spine; (b) 3D representation of the axial section of interest at L3 level.

Low muscle mass was defined according to established SMI cut-offs for each sex: males: <52.4 cm^2/m^2, females: <38.5 cm^2/m^2 [Sinclair et al, 2016; Paternostro et al, 2019].

Statistical Analysis

The Shapiro–Wilk test was used to assess the normality of the distribution of the continuous variables. The differences between two independent groups for the continuous variable were assessed with the non-parametric Mann–Whitney U test, given the small sample size. For predicting changes in L3-SMI, candidate variables were identified by creating a linear regression model. Throughout the analysis a 95% confidence level was considered satisfying, setting the significance at $p < 0.05$.

Results

Baseline Data

The study group included 52 patients (20 men and 32 women) with a median age of 59 years (range 42–79). L3-SMI in males at baseline ranged from 29.96 to 73.39 cm2/m2 (median 50.73 cm2/m2), whereas for women the baseline ranged from 21.74 to 60.52 cm2/m2 (median 37 cm2/m2). Considering the cut-off values specific for each sex, the overall percentage of patients with low L3-SMI value at baseline was 63.46% (33/52), with 80% (16/20) in the male group and 53.12% (17/32) in the female group.

Comparison of Baseline Characteristics between Patients with Low L3-SMI and Normal L3-SMI

The following parameters were evaluated: age, body mass index (BMI) and laboratory values for total bilirubin, serum albumin, platelets, total cholesterol, INR, alpha-fetoprotein, serum creatinine, AST and ALT 9 (Table 1.II).

The statistical analysis showed that there was a significant difference for the laboratory values of serum creatinine between the two groups. Patients with normal L3-SMI values had higher serum creatinine (median 0.73) compared to patients with low baseline L3-SMI (median 0.68, $p = 0.031$).

The other parameters investigated did not reveal significant differences between the two groups of patients at baseline.

Table 1.II Comparison between patients with low L3-SMI and normal L3-SMI.

	Normal L3-SMI (*n* = 19)		Low L3-SMI (*n* = 33)		Mann-Whitney	
	Median (Range)	Mean Rank	Median (Range)	Mean Rank	U	*p*
Age (years)	55.6 (42–73)	22.58	60 (42–79)	28.76	239.000	0.156
BMI	28.32 (20.2–34.42)	30.16	26.82 (19.27–38.67)	24.39	244.000	0.187
Total bilirubin	0.99 (0.6 -2.3)	24.29	1.16 (0.43–2.47)	27.77	271.500	0.425
Serum albumin	3.9 (2.49–5.25)	26.79	3.94 (2.28–4.75)	26.33	308.000	0.917
Platelets	10.6 (5.6–29.3)	26.76	10.9 (3.7–26.10)	26.35	308.500	0.924
Total cholesterol	148 (98–221)	23.61	158 (80–212)	28.17	258.500	0.296
INR	1.2 (0.95–1.55)	29.71	1.12 (0.97–2.27)	24.65	252.500	0.246
Alpha-fetoprotein	10.15 (3.82–131)	25.71	13.06 (2.14–110)	26.95	298.500	0.776
Serum creatinine	0.73 (0.53–1.06)	29.94	0.68 (0.4–0.92)	20.53	200.000	0.031 *
AST	84 (28–197)	25.34	78 (35–224)	27.17	291.500	0.676
ALT	68 (33–264)	27.74	75 (15–229)	25.79	290.000	0.655

INR, international normalized ratio; AST, aspartate aminotransferase; ALT, alanine aminotransferase, * significant.

Comparison of Baseline Characteristics between Patients with Decreased L3-SMI and with Increased L3-SMI Assessed after Sustained Virological Response (SVR)

The dynamics of L3-SMI after treatment was assessed by the difference between L3-SMI values at baseline and those obtained after SVR, reported as a percentage of the initial value. The results were grouped in increased and decreased groups depending on the positive or negative values. The loss of muscle mass had a median of −7.5% (−1% to −28%) and in group with growth the median was 7.2% (0.9% to 34%).

After obtaining SVR, only 14 patients showed an increase of L3-SMI, and 38 patients had a decrease in L3-SMI values.

The differences between patients with decreasing muscle mass (according to L3-SMI values) and those with increasing muscle mass with respect to the initial values of the collected parameters, were assessed by the Mann–Whitney U test. The results are summarized in Table 1.III.

Table 1.III. Comparison between patients with decreased L3-SMI and increased L3-SMI.

	Decreased (*n* = 38)		Increased (*n* = 14)		Mann-Whitney	
	Median (Range)	Mean Rank	Median (Range)	Mean Rank	U	*p*
Age (years)	59.5 (42–79)	27.04	57.07 (45–69)	25.04	245.500	0.672
BMI	26.17 (19.27–36)	23.55	28.84 (23.94–38.67)	34.50	154.000	0.021 *
Total bilirubin	1.1 (0.48–2.47)	26.71	1.0 (0.43–2.4)	25.93	258.000	0.869
Serum albumin	4.04 (2.28–5.25)	28.79	3.69 (2.44–4.5)	20.29	179.000	0.073
Platelets	11.6 (5.6–29.3)	27.20	10.25 (3.7–17.5)	24.61	239.500	0.584
Total cholesterol	150.5 (80–221)	26.51	157.5 (102–198)	25.93	265.500	0.992
INR	1.14 (0.95–1.98)	26.13	1.14 (0.97–2.27)	27.50	252.000	0.772
Alpha-fetoprotein	11.2 (2.14–131)	24.26	26.15 (3.07–110)	32.57	181.000	0.080
Serum creatinine	0.71 (0.4–0.95)	26.39	0.7 (0.52–1.06)	26.79	262.000	0.934
AST	69 (28–224)	24.05	107.5 (38–146)	33.14	173.000	0.055
ALT	66.5 (15–264)	23.95	88 (38–229)	33.43	169.000	0.045 *

INR, international normalized ratio; AST, aspartate aminotransferase; ALT, alanine aminotransferase, * significant.

BMI in the decreased L3-SMI group was significantly lower (median 26.17) than those without decreased L3-SMI (median 28.84, p = 0.021).

Similarly, ALT values in the decreased L3-SMI group (median 66.5) were significantly lower than those without a decrease in L3-SMI (median 88, p = 0.045).

Linear Regression Model

All parameters available at baseline were assessed as predictive factors in multiple linear regression and multiple logistic regression models. The only viable model was linear regression with a single predictor represented by BMI.

Linear regression (Fig1.4) targeting the percentage change in L3-SMI values after SVR showed significant prediction ability of the independent variable assessing the BMI at baseline (ANOVA F (1.50) = 14.83, sig = 0.00).

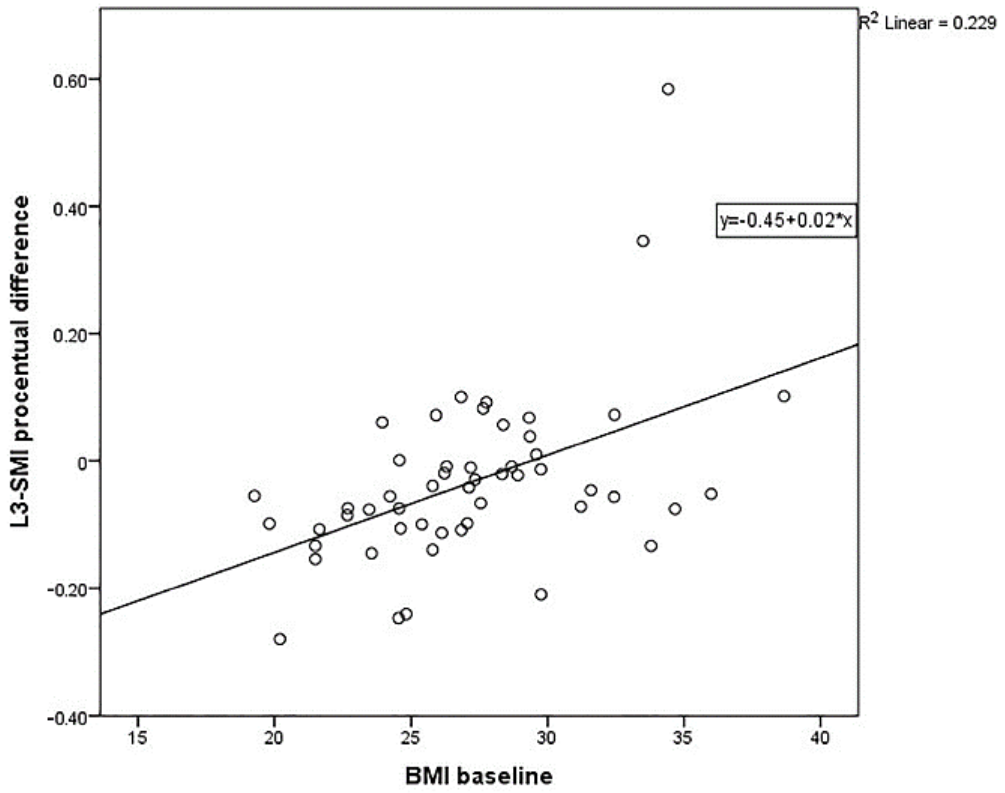

Fig. 1.4. Linear regression for L3-SMI percentage change and BMI values at baseline.

The variance of the single significant predictor obtained through the model, BMI at baseline, is able to predict at least 23% of the variance in the target variable L3-SMI (R2 = 0.229).

Comparison of Muscle Mass Dynamics after SVR between Groups with Low L3-SMI and Normal L3-SMI at Baseline

Comparing the evolution of L3-SMI values after treatment according to baseline groups, normal L3-SMI and low L3-SMI, we found a significant difference between patients with low L3-SMI values (median −1.3) and patients with normal L3-SMI (median −3.98, p = 0.02).

A higher number of patients in the sarcopenic group at baseline showed a post-SVR increase in L3-SMI values compared to the number of patients with normal baseline values. In patients with baseline low L3-SMI, 11 (33%) presented increased values after SVR while in patients with normal L3-SMI only 3 (16%) had an increase.

Discussion

Analysis of baseline data showed the global predominance of patients with low L3-SMI (63.5% of all patients were underneath definition values, and median L3-SMI was inferior to cut-off

values for both male and female patients' groups), with a higher percentage of male patients with low L3-SMI values (80% compared to 53.1%, in female group).
Since sarcopenia is associated with poor clinical outcome, such a high incidence of sarcopenia in a selected group of compensated cirrhosis must trigger an early nutritional care. A special concern is necessary in male patients, which are more predisposed to sarcopenia, as our study and previous data have shown, both in general population and in patients with liver cirrhosis (Du et al, 2019; Chen et al, 2021).
Furthermore, baseline data showed significant difference regarding serum creatinine levels according to L3-SMI values, patients with low L3-SMI also having decreased serum creatinine levels compared to those with normal L3-SMI. The results of our study are consistent with the current association between low creatinine levels and sarcopenia, serum creatinine being described as a classical biomarker for the body's muscle tissue mass (Shafiee et al, 2017). No other conditions that could have interfered with serum creatinine level dosage, such as advanced liver disease, fluid overload, and augmented renal clearance, were identified in our study, consequently low serum creatinine levels found in the low L3-SMI group of patients are interpreted as a direct marker of their poor muscle mass status.
Our analysis on the dynamics of muscle mass status following antiviral treatment showed that most patients (72%) presented a decrease of L3-SMI values, while only a few more than a quarter (28%) obtained an increase of L3-SMI values. According to baseline muscle mass status, more patients with initial low L3-SMI presented an increased index after SVR, compared to patients with normal muscular status at baseline (33% vs 16%, respectively). Therefore, even if a benefit in terms of muscle mass was noted only in a minority of all patients, improvements were more frequent in patients who were most in need of muscle mass status correction. It should be noted that although most patients in the baseline group with normal L3-SMI values showed a decrease after treatment, only three patients fell below the threshold values, the rest remaining within the normal range.
Even if other recent evidence suggests an increase or no more loss of skeletal muscle mass after antiviral treatment (Sakamori et al, 2021; Tokuchi et al, 2021), the muscular improvement cannot be guaranteed solely by the viral clearance, and supplementary nutritional interventions are necessary. All efforts to counteract underweight and malnutrition must be made.
ALT has gained recognition as surrogate marker of frailty and shortened survival. In our study, lower ALT levels were predictive for the lack of benefit regarding muscle mass dynamics after SVR. In our relatively homogenous study group based on stage of liver disease, where all our patients had compensated cirrhosis, lower ALT levels appear to have predictive power concerning sarcopenia.

1.2.1.1.3 Long-term risk of hepatocellular carcinoma following DAA Therapy

Introduction
According to Globocan 2020, HCC is the sixth most frequent malignancy and one of the most lethal malignancies, being the third leading cause of neoplasia-related death in 2020 worldwide (Sung et al, 2021). Therefore, identification and management of the modifiable major risk factors such as viral hepatitis B (HBV) or C (HCV) chronic infection, excessive alcohol consumption, aflatoxin, type 2 diabetes mellitus, obesity, and smoking are of essence to interrupt the upward dynamics of the HCC rates (Sung et al, 2021).
The carcinogenic potential of HCV has been extensively studied. According to previous studies, its pro-oncogenic effects on the infected cells are caused by both direct (i.e., DNA damage, oxidative mechanisms) and indirect (i.e., liver injury and fibrosis) mechanisms (Muzica et al, 2020). Data from the IFN era showed that achieving viral eradication (SVR) significantly reduced the risk of HCC (Janjua et al, 2017; Brown et al, 2000). However, the IFN-based therapy

was ranked as suboptimal considering the low SVR rate (approximately 40 - 50%) and poor tolerance and limited access caused by strict criteria for the eligibility of patients (Janjua et al, 2017). The discovery of direct-acting antivirals (DAAs) was considered a significant advance in clinical medicine, associated with high efficacy (SVR rates > 95%), acceptable tolerability, short treatment duration (8 - 12 weeks), and simple administration (once-daily oral dosage) (Laursen et al, 2020). However, in 2016, shadows were cast over such fantastic therapeutic triumph when two articles from Spain and Italy reported that the DAA therapy might favor the HCC occurrence or recurrence (Reig et al, 2916; Conti et al, 2016). This issue was since a hotbed of debate in more than 100 papers, letters, or communications; however, no conclusive result was achieved.

Methods

Patients

This multicentric cohort study analyzed the data from 479 consecutive patients with chronic HCV genotype 1b infection and compensated liver cirrhosis, treatment-experienced or naïve, treated with paritaprevir/ritonavir/ombitasvir, and dasabuvir (PrOD) +/- ribavirin (RBV) for 12 weeks in two tertiary centers in Northeastern Romania. The patients were prospectively followed up in The Institute of Gastroenterology Iasi, Romania, from November 2015 to December 2020.

Monitoring During and After DAA Treatment

Clinical parameters and laboratory tests (namely HCV RNA level, aspartate and alanine aminotransferases, bilirubin, alkaline phosphatase, gamaglutamyl transpeptidase, albumin, and international normalized ratio, serum creatinine, hemoglobin, platelet count, and alpha-fetoprotein) were monitored before DAAs, at the end of treatment (EOT), three months after EOT (SVR), and whenever it was necessary. The scores of Child–Pugh-Turcotte (CPT) and model of end-stage liver disease (MELD) were calculated at the baseline, end of treatment, and 12 weeks after the therapy. Transient elastography (FibroScan; Echosens, Paris, France) was used to perform the liver stiffness measurement (LSM) with 13 kPa as the cutoff point for cirrhosis.

HCC Surveillance

The HCC screening was performed at the baseline in all patients using abdominal US, CT or MRI. US and serum a-fetoprotein (AFP) were performed every 3 - 6 months for all patients after the initiation of treatment.

Statistical Analysis

All data were statistically analyzed using SPSS software version 22.0 (IBM SPSS Inc., Chicago, IL, USA). The continuous variables were expressed as median (first-third quartiles) and compared using Student's t-test; however, the categorical variables were reported as frequencies and percentages and compared using chi-squared or Fisher's exact tests. The Kaplan-Meier method was used to calculate and plot the cumulative HCC incidence. Only complete data were analyzed in this study.

To compare the differences among the groups, the log-rank test was used. In this regard, a Cox proportional hazard model with a hazard ratio (HR) and 95% confidence interval (CI) generated by Cox regression was calculated in both univariate and multivariate analysis to detect the risk factors associated with the HCC occurrence. Moreover, we evaluated the relationship between AFP and the HCC occurrence using the area under the receiver operating characteristic curve (AUROC) analysis, and the optimal cutoff value was selected at the highest specificity and sensitivity from the receiver operating characteristic (ROC). Statistically, two-tailed $P < 0.05$ was set as the significance level in this study. Kolmogorov-Smirnov test was performed to check the normality of the data distributions.

Results

Participants' Characteristics

The study included 479 patients treated with PrOD ± RBV, with a median age of 60 (52-73) years, who mainly encompassed female patients (54.5 %). Of the research participants, 32% had a history of antiviral treatment with IFN, and 16.5% received RBV associated with PrOD. The participants' body mass index (BMI) was 27.76 ± 4.04 kg/m2. More than half of the patients (57.2%) had comorbidities, the most common being hypertension (36.5%) and type 2 diabetes mellitus (14%). All patients had compensated liver cirrhosis (according to CPT, 88.5% had a score of 5, and 11.5% had a score of 6).

The mean follow-up period was 60.11 ± 3.87 months. A statistically significant decrease was recorded at the ALT, AST, GGT, and AFP levels and LSM ($P < 0.001$) in SVR compared to baseline.

Incidence and Risk Factors of HCC Occurrence

After the mean follow-up of 60.11 ± 3.87 months, 23 patients (4.8%) developed HCC. The 1-, 3-, and 5-year cumulative incidence rates of HCC were 1.1, 1.9, and 2.6%, respectively. The mean period from the beginning of the treatment to the HCC diagnosis was 19.6 ± 13.7 months.

All patients in our cohort study had compensated liver cirrhosis (Child-Pugh A 5 or 6). The patients who were diagnosed with HCC (n = 23) were older (63 vs 59 years, P = 0.022) and more likely to be male (57 vs 55%, P = 0.448) compared to the non-HCC patients (n = 456). Furthermore, higher AST and AFP levels, and lower PLT counts were observed at baseline in the HCC patients than the non-HCC patients (table 1.IV).

Table 1.IV. Baseline Factors with Possible Impact on HCC Occurrence

Variables	HCC = 23	No HCC = 456	P-Value
Age	63.04 ± 10.	59 ± 8.14	0.022
Gender, male/female, (male%)	13/10 (57)	251/205 (55)	0.448
PLT, × 10^4/μL	12.6 ± 50.4	14.8 ± 63.9	0.109
BMI	26.9 ± 3.7	27.7 ± 4.04	0.156
AFP baseline	15.8 ± 23.5	13.9 ± 9.7	0.696
ALT, U/L	112.78 ± 69.07	103.54 ± 71.56	0.545
AST, U/L	110.87 ± 51.68	101.25 ± 66.88	0.497

Abbreviations: PLT, platelets; BMI, body mass index; ALT, alanine aminotransferase; AST, aspartate aminotransferase; AFP, alpha-fetoprotein; a Values are expressed as mean ± SD unless otherwise indicated.

HCC Features and Management

Of the patients who developed HCC, 12 patients (52.2%) met the Milan criteria, and according to the BCLC classification, most of them were in class A (39.1%). Regarding the imaging characteristics of the tumor, most patients had a single nodule (65.2%), and the presence of the capsule was highlighted in 82.6%. Malignant portal vein thrombosis (PVT) was demonstrated in 26% of the patients, and local/distant metastases was noticed in 13% of the patients.

The therapeutic management of the patients with HCC was performed according to the BCLC classification. Most patients (n = 11; 47.8%) received curative treatment by surgical resection; the histopathological examination of the resected specimen depicted a moderately differentiated tumor (G2) in five patients, a poorly differentiated tumor (G3) in five patients, and a well-differentiated tumor (G1) only in one patient. Three patients (27%) had HCC recurrence after a mean of 6 ± 5.2 months and were subsequently addressed for systemic therapy.

Discussion

The cumulative 5-year risk for HCC in HCV-free cirrhotic patients after the DAA treatment was 2.6%, and this value exceeded the cutoff beyond which HCC surveillance was cost-effective. Nonetheless, the findings of the present study support the incidence of HCC, with no evidence on the high occurrence of de novo HCC after the DAA therapy.

Only few reports assessed the behavior of HCC and access to curative therapy after the DAA treatment (Renzulli et al, 2018; Nakao et al, 2018). Regarding tumor aggression, the patients with HCC in the present study revealed aggression less frequently than those reported in other studies (Nakao et al, 2018). Most HCC patients in the present study had a single nodule (65.2%). The portal vein invasion was observed in 26% of patients, and there were local and distant metastases in 13% of the patients. Furthermore, most patients were in classes O and A BCLC, implying access to curative treatment.

The main limitation of the present study was the presence of no control group of untreated patients to compare the characteristics and the prognosis of HCC after DAAs. Other limitations were the lack of patients with decompensated cirrhosis and the use of a single DAA regimen in our cohort.

Conclusions

SVR in patients with HCV-related compensated cirrhosis treated with DAAs is associated with some improvements of hepatic morphology detectable by CT, the most constant being the increase of right hepatic vein diameter.

Sarcopenia, a frequent comorbidity in patients with advanced liver disease, can be objectively assessed by CT-based measurements. Even if the skeletal mass index is partially influenced by the viral clearance, some improvements were recorded in patients with baseline sarcopenia. Low creatinine serum level correlates with sarcopenia. Lower BMI and ALT serum levels at baseline were predictive for no benefit in terms of muscle mass dynamics.

Regarding the HCC occurrence after long-term follow-up of patients with HCV genotype 1b infection and liver cirrhosis, who achieved SVR following the DAA treatment we found no higher incidence. However, the cumulative 5-year risk remained above the cutoff point, making the HCC screening cost-effective. Accordingly, clinical and imaging follow-up should be maintained for patients with liver cirrhosis at the time of SVR. The tumor phenotype does not seem to be more aggressive after DAAs, and the access to curative therapy is similar to that of the HCC associated with other liver diseases.

Originality and applicability of the results in medical practice

As far as we know, these were the first studies related to HCV-related cirrhosis patients achieving SVR after DAAs treatment that evaluated prospectively by CT the morphological changes in liver, portal system and spleen, as well as L3-SMI dynamics.

Understanding all the mechanisms involved in sarcopenia and identifying the most vulnerable cirrhotic patients could ensure optimal adapted care strategies.

Furthermore, our results supported the paradigm of the reversibility of cirrhotic changes.

Limitations of the studies

Limitations were given mainly by the low number of patients included. Other limitations concerned the one-dimensional measurements, which may not accurately reflect all intrahepatic morphological changes, the variable CT scan follow-up interval, in the retrospective study regarding sarcopenia.

Future directions

These results are promising but should be validated by further studies based on a larger number of patients and a longer follow-up. Larger datasets are necessary to propose imaging-based scores of cirrhosis reversibility.

The evaluation of the HCC pattern requires prospective case-control studies comparing the clinical-biological and imaging markers of tumor aggression between the HCC cases after DAAs and naïve patients.

1.2.1.2. Chronic hepatitis C infection associated with other pathologies

Introduction

Virus C infection has well-known hepatic manifestations – cirrhosis and liver cancer – but the extrahepatic ones should not be overlooked, these being responsible for a significant morbidity burden in the infected patients. Associated systemic manifestations (CHASMs) are present in 40% to 75% of CHC infections, more in women and in older patients (Cacoub et al, 1999). Besides its hepatotropism, hepatitis C virus (HCV) also has lymphotropism and that could be the reason for the most frequently described extrahepatic manifestations – mixed cryoglobulinemia and B-cell non-Hodgkin's lymphoma (BCNHL) (Durant et al, 2010).

1.2.1.2.1 Primary renal lymphoma and chronic hepatitis C infection

PRL is a very rare disease. We reported a case of PRL discovered during evaluation of a patient with HCV in order to start direct-acting antiviral (DAA) therapy. The patient was asymptomatic. The initial abdominal US revealed hepatomegaly with increased echogenicity and a homogenous structure, 14 mm portal vein diameter measured at the hepatic hilum and moderate splenomegaly with a homogenous structure (longitudinal splenic diameter of 185 mm) and no ascites. Surprisingly, we also found a slightly hypoechoic right renal mass of 40/20 mm. The mass was further characterized by contrast-enhanced abdominal CT scan showing moderate enhancement (Fig. 1.5).

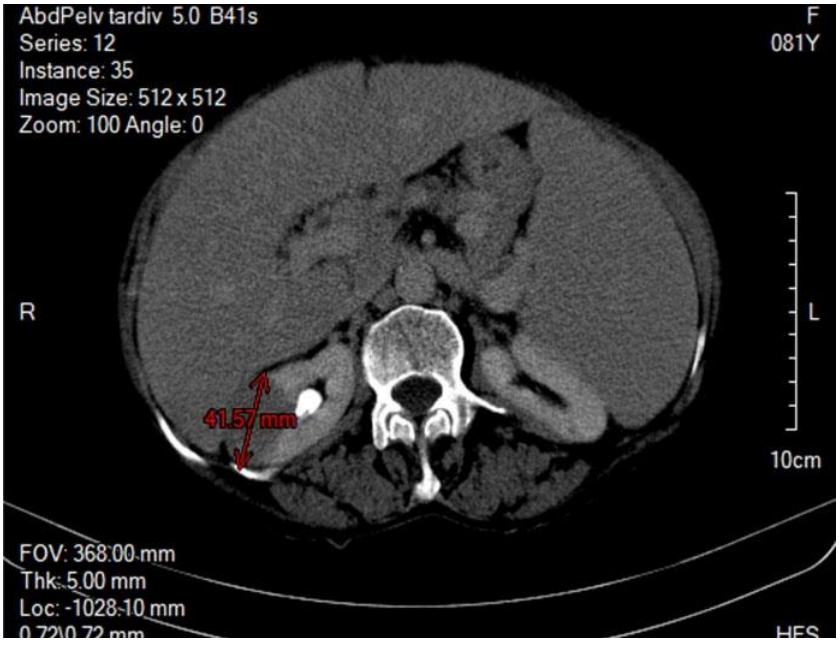

Fig. 1.5 Abdominal CT: right renal tumor of 42/25 mm, splenomegaly of 184/89 mm.

Since malignancy was not ruled out, the patient was addressed for surgical resection. The histopathological exam described lymphoid proliferation with small lymphocytes suggestive for marginal zone (MALT) BCNHL (table 1.V).

Table 1.V Immunohistochemical characterization of the tumor – PRL

Immunomarker	Positive	Negative
CD3		✓
CD5		✓
CD10		✓
CD20	✓	
CD34		✓
CD138		✓
BCL2	✓	
BCL6		✓
MUM1		✓
Ki67	<10% in "hotspot"	

BCL: B-cell lymphoma; CD: Cluster of differentiation; MUM1: Multiple myeloma oncogene 1; PRL: Primary renal lymphoma.

Because we did not find any other extrarenal lesions (visceral or lymph nodes) and no leukemic blood picture or sign of myelosuppression, the final diagnostic of PRL was established. A subsequent interdisciplinary evaluation after the surgical procedure decided that the patient must follow DAA therapy for HCV and then follow-up and hematological treatment if it is necessary. One year later, no sign of local recurrence could be identified during follow-up.

Discussion

Numerous extrahepatic manifestations (HCV–EHMs) have been reported along the time. Some authors consider these phenomena as being CHASMs. Whatever name they bear, in some studies up to three-quarters of the patients experienced such events of different severity,
from infraclinical to incapacitating conditions (Cacoub et al, 1999; Cacoub et al, 2016).
We can split these conditions into three categories: well-documented and more common, conditions with strong scientific proofs of the association and others that are infrequent, whose association with HCV has yet to be proven.
Even if the association of CHC with mixed cryoglobulinemia and BCNHL is most frequently described, the mechanisms behind this occurrence in HCV infection is not yet completely understood. There are three theories formulated today: (i) lymphocytes proliferation driven by continuous viral antigens stimulation; (ii) invasion of lymphocytes by the virus and viral replication leading to oncogenic effects; (iii) the "hit and run" theory that implies a transient invasion of lymphocytes by a virus that leads to permanent damage similar to a mutation in tumor-suppressing genes (Gill K et al, 2016).
NHL was associated with HCV for the first time back in 1994 (Zignego AL et al, 1999). Since then, scientific interest grew and now there are described multiple histological subtypes of HCV-associated lymphomas: marginal zone lymphomas (MZLs), lymphoplasmacytic lymphoma (rare) and diffuse large B-cell lymphoma (DLBCL) – an aggressive type (Gill K et al, 2016). MZL is the most frequent type and usually has an indolent course. Currently, we know three different types of MZL: (i) the extranodal type – MALT; (ii) nodal type – that implies exclusive lymph node involvement and (iii) splenic type (Peveling-Oberhag J et al, 2013).
The MALT-type NHBL is the most frequently diagnosed among HCV-infected patients (de Sanjose S et al, 2008). Different studies reported a prevalence of 28% HCV versus 2.9% in general population (Lizardi-Cervera J et al, 2006). The top three locations according to a study [14] are the skin, salivary glands, and the orbit; less than 15% represents other sites.

PRL is a very rare entity, to date being described in medical literature worldwide less than 70 cases of PRL and only a few associated with HCV infection upon our knowledge (Chen X et al, 2011; Wang XJ et al, 2016; Cyriac S et al, 2010; Okuno SH et al, 1995).
Renal involvement is frequent as a dissemination site in patients with advanced stages of NHL, but PRL appears extremely rare. For a while, scientists believed that this entity does not exist due to anatomical characteristics of kidneys, which normally are lacking lymphoid tissue.
The particularity of our case is the presence of renal lymphoma, not the usually secondary one, but the primary one in association with HCV infection. In the case of chronic HCV infection, like in our patient, mechanisms underlying the occurrence of the PRL appear to be a mix of invasion of lymphocytes by the virus, lymphocytes proliferation driven by continuous viral antigens stimulation and viral replication leading to oncogenic effects (lymphotropism of the virus). Some authors consider that preexisting inflammatory processes
mobilize lymphoid cells into the renal parenchyma, and while there, "the untimely oncogenic event takes place" (Okuno SH et al, 1995).
Diagnosis of a unique nodular PRL is always difficult because usually PRL appears as kidney with multiple renal masses (60%); less frequently as a diffuse infiltration of renal tissue (25%), and only the least common variant is a solitary mass (15%) (Nguyen DD et al, 2013). Also, the solitary type is usually mistaken for RCC because neither clinical manifestations, nor the US or other radiological findings are specific (Chen X et al, 2016).
US, even if non-specific, is usually the first method to detect the lesion. It can only describe diffuse nephromegaly or the presence of an inhomogeneous hypoechoic mass (Sheth S et al, 2006). The CT frequently depicts a hypovascularized tumor, which is an important detail in the differential diagnosis with RCC and other renal tumors that are hypervascularized. In our case, the CT described a mass with moderate enhancement. Magnetic resonance imaging (MRI), useful for patients with a history of contrast medium allergy or suffering of renal insufficiency, shows lesions that are typically T1 hypointense and T2 isointense to hypointense (Nguyen DD et al, 2013; Sheth S et al, 2006; Ganeshan D et al, 2013). Positron emission tomography (PET)–CT is another imaging technique that is very useful in detecting small lesions therefore with an important role in the staging of the disease, exclusion of other concomitant localization, and follow-up after treatment but with the disadvantage of lower accessibility (Ganeshan D et al, 2013).
Since clinical manifestations and imaging features lack specificity for the PRL, the final diagnostic is established histological examination. In most reported cases, DLBCL is the HP diagnosis, but in our case a non-Hodgkin's small cell lymphoma with marginal zone (MALT) B-cell type was certified (Geetha N et al, 2014).
In order to diagnose a primary renal lymphoma, the following criteria must be met esides the presence of the renal mass: (*i*) exclusion of concomitant lesions affecting extrarenal visceral organs or lymph nodes at first admission, with the observation that some authors accept the presence of alongside adenopathy, (*ii*) the absence of leukemic blood picture, and (iii) the absence of any sign of myelosuppression (Pinggera GM et al, 2009; Shaikh AB et al, 2016).
The latest large-scale analysis of the PRL survival revealed that the relative survival (RS) rates of PRL at one year, five years and 10 years were 78%, 64% and 55%, respectively. In addition, the RS for patients diagnosed between 2000 and 2013 was better than that of patients diagnosed during the last two decades before 2000. On the other hand, the survival analysis also demonstrated an advantage for patients who were younger, females, had disease in early stages (stage I and II),received surgical treatment and had the MZL form (Chen J et al, 2019).

Conclusions

PRL is a very rare disease. A moderate enhancing mass in the kidney, incidentally discovered, raises the suspicion of RCC, and only the pathological exam od the resected specimen can describe lymphoid proliferation with small lymphocytes suggestive for marginal zone (MALT)

BCNHL. The exclusion of other extrarenal lesions (visceral or lymph nodes) and of leukemic blood picture is in favor of PRL.

1.2.1.3 Prognostic factors in liver transplantation for virus C hepatitis

Introduction
Hepatitis C virus represents one of the main causes of end-stage liver disease and liver transplant remains the curative treatment in this stage. Identifying the predictor factors for the best postoperative outcome is important for better recipient selection. Objectives: This paper aims to study the perioperative parameters as prognostic factors for the outcome of liver transplantation in patients with postviral C cirrhosis.

Methods: We identified from the Romanian Liver Transplant Registry patients with viral C cirrhosis, who received a liver transplant from a brain death donor or living donor, between 2013-2018. MELD and ALBI scores and intraoperative data were extracted from the computerized database and statistically analysed.

Results: Eighty patients with a history of HCV infection and the median age of 47.93 +/- 8.78 years, were enrolled in this study. 30% of cases of hepatocellular carcinoma were associated with virus C cirrhosis. The correlation revealed no statistical significance ($P>0.05$) between the occurrence of general complications and the high ALBI grade or MELD score, but a high ALBI score was associated with an increased risk of acute rejection and chronic rejection ($P<0.05$). There is a strong correlation between intraoperative blood loss, blood transfusion and postoperative complications.

Conclusions
The data reveal that the ALBI score may be a better tool than the MELD score to assess the risk stratification in LT patients. Both intraoperative blood loss and blood product transfusion are predictors for the postoperative outcome.

1.2.1.4 Portal hypertension – a continuous imaging challenge beyond the chronic liver disease frame

Imaging studies (ultrasound, CT and MRI) are able to identify and characterize the portal system, including anatomical variants, focal or global dilation, patency or thrombosis, presence of collaterals, as well as other associate signs (ascites) or pathology.
The thrombosis in portal system may be secondary to cirrhosis, hepatocellular carcinoma, pancreatic cancer, lymphadenopathy, infections (cholecystitis, appendicitis, diverticulitis), pancreatitis, inflammatory bowel disease, trauma, stenosis of the portal anastomosis in liver recipients.
When intrahepatic portal flow is diminished or obstructed, there are some typical groups of porto-systemic derivation:

- Superior: left gastric, esophagial varices, short gastric veins;
- Anterior: umbilical, anterior abdominal wall;
- Posterior: direct and indirect spleno-renal shunts (spleno-gastro-freno-adreno-renal);
- Inferior: Superior rectal, transperitoneal, mesenterico-gonadal/ mesenterico-lumbar, gastro-epiploic.

1.2.1.4.1. Left-side portal hypertension

Isolated gastric varices due to splenic vein thrombosis are usually related to the short gastric veins connecting the hilum of the spleen to the greater curvature of the stomach (Al-Osaimi AMS et al, 2011). The outflow is usually directed to the systemic territory, as a part of a portosystemic shunt, draining into the inferior phrenic vein at the level of gastrophrenic ligament and then forming a gastrorenal shunt terminating into the left renal vein, or a gastrocaval shunt terminating into the inferior vena cava (Johns TN et al, 1962; Wani ZA et al, 2015). Anastomoses with left pericardiophrenic veins, other peridiaphragmatic and retroperitoneal veins, including the subcostal and intercostal veins, right inferior phrenic vein, or azygos venous system were also described.

We have **reported a case** with large gastric varices as part of a spleno-mesenteric shunt to overcome a short splenic vein thrombosis due to a mucinous cystadenoma of the pancreas.

A 37-year old woman presented to the emergency unit with 4 episodes of hematemesis and melena over the last 4 hours. Her medical history included a pancreatic body thin-walled cyst of 5 cm, discovered 2 years ago on a routine ultrasound and characterized by CT as a benign lesion (Fig. 1A). As there were no indication of other associated pancreatic or hepatobiliary conditions, the portal system was patent, and the patient refused invasive examinations, a follow-up of the lesion was decided at that time. A follow-up abdominal ultrasound at 1 year showed stability of the lesion. On examination, she was alert and oriented, with a blood pressure of 100/55 mm Hg and heart rate of 110 min1. She was pale, without any jaundice, lymphadenopathy, or pedal edema. Abdominal examination revealed an enlarged spleen 7cm below the left costal margin. The digital rectal examination revealed melena and the nasogastric tube detected a coffee ground aspirate with bright red blood. The rest of the systemic examination was unremarkable and without peripheral stigma of chronic liver disease. She had hemoglobin level of 3.9 g/dL, white blood cell counts of 3.35_103 L_1, and platelets count of 86.000 mm_3. Her liver function tests, including prothrombin time, were normal, except for albumin level of 3.0 g/dL. Hepatitis B and C serology was negative, as well as the seric levels of tumor markers (carcinoembriogenic antigen [CEA] 19–9 antigen). The patient was admitted in the intensive care unit (ICU) for blood volume restitution with blood transfusion, crystalloid, and colloid solutions and started on intravenous omeprazole infusions. The upper tract endoscopy revealed large gastric varices located at the fornix with nipple and red wale signs, indicating the site of bleeding, looking like “varicose veins in varicose veins”. Abdominal US and CT revealed changes of the size (measuring 7/6 cm in diameter) and morphology of the pancreatic cyst in the body/tail of the pancreas (still well defined, thin walled, but with enhancing internal septa), associated with segmental occlusion of the splenic vein and homogeneous splenomegaly (Fig. 1.6). Dilated veins were identified in the fundus of the stomach (up to 7 mm), without esophageal varices (Fig. 1.6). Maximum intensity projection (MIP) reconstructions identify the inflow at the level of short gastric veins and the outflow to the omental veins and right gastroepiploic veins, draining in the distal part of the dilated superior mesenteric vein and developing a spleno-mesenteric shunt. The diagnosis was cystic pancreatic tumor with left-side segmental portal hypertension. As far as the patient was actively bleeding with difficulties in endoscopic management through sclerosis, ligation, or embolization, and 2 high-risk features of the cystic tumor were present (size >3cm and increasing of the solid component represented by septa) a salvage surgery was decided and distal pancreatectomy and splenectomy were performed with lymphadenectomy along the splenic, common hepatic, and celiac.

Discussions

The two commonest clinical features in gastric varices due to splenic vein thrombosis are gastrointestinal blood loss and splenomegaly. Since isolated gastric varices may be observed in up to 5% of patients with cirrhosis, and up to 10% of patients with non-cirrhotic portal hypertension, further imaging studies are always necessary to evaluate the portal system, as well as the underlying pathology.

Segmental left-sided portal hypertension represents a clinical entity involving the development of gastric varices in the context of splenic vein thrombosis due to pancreatic pathology. The difference from other forms of portal hypertension resides in the presence of normal liver function and permeable extrahepatic portal vein. Regularly, the reported causes of segmental left-sided portal hypertension include acute and chronic pancreatitis, pancreatic carcinomas, and pancreatic pseudocysts. Less frequently reported are benign pancreatic tumors, although various types of pancreatic cysts, like cystadenoma, choledochal cyst, echinococcal cyst, and also pseudotumor and pancreatic abscesses have all been reported as causing this particular type of portal hypertension and subsequent bleeding.

Confirmed segmental left-sided portal hypertension does not always require surgical intervention in case of benign lesions and the "wait-and-watch" strategy is legitimate in asymptomatic patients. Yet, the presented case required surgical management, due to the presence of 2 high-risk features of the pancreatic cyst and to the difficulty in performing optimal endoscopic management of bleeding. We opted for an oncologic resection of the lesion, considering the inconclusive intraoperative pathology examination of the lymph nodes and cystic wall and the well-known errors due to regressive changes within MCNs. MCNs of the pancreas are uncommon (10% of cystic lesions of the pancreas and 1% of pancreatic neoplasms) but with potential to progress to pancreatic adenocarcinoma [Naveed S et al, 2014]. There are scarce reports in the literature associating MCNs with left-side portal hypertension [Thrainsdottir H et al, 2014].

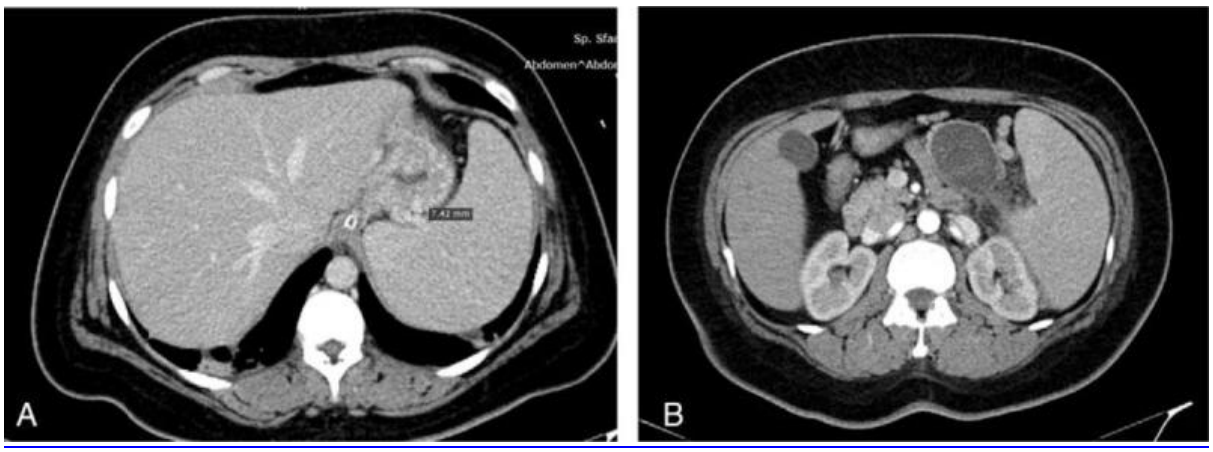

Fig. 1.6 Abdominal CT. January 2015: Patent splenic vein and normal-sized spleen in a patient with incidental finding of a well defined pancreatic cystic lesion located in the tail of the pancreas (A). January 2017: enlargement of the cystic lesion, with internal enhanced septa and wall (B).

Conclusions

Segmental portal hypertension may prompt the identification of an extrahepatic cause. Every pancreatic lesion, even with typical appearance of benignity, may produce splenic vein thrombosis and left-side portal hypertension, with life-threatening digestive bleeding; therefore, vascular complications should be included in the follow-up criteria for cystic lesions of the pancreas.

1.2.2. Liver tumors – diagnostic and interventional radiology

Liver cancer is the fifth most common cancer and the second most frequent cause of cancer-related death globally (EASL guidelines, 2018). HCC represents the most frequent primary liver neoplasia, and the third leading cause of neoplasia-related death in 2020 worldwide (Bray et al., 2018). The incidence of HCC has risen worldwide over the last 20 years and is expected to increase until 2030 in some countries. The incidence of HCC is highest in Asia and Africa, where the endemic high prevalence of hepatitis B and hepatitis C strongly predisposes to the development of chronic liver disease and subsequent development of HCC.

Traditionally, the main risk factor for HCC is liver cirrhosis, but HCC is diagnosed even in non-cirrhotic patients. The leading risk factor for HCC is HCV infection with a 3% annual risk in patients with HCV liver cirrhosis (El-Serag, 2011). Current international vaccination strategies for HBV and advances in the management of HCV will have a major impact on the incidence of HCC, but their benefit will be seen probably in the next 20-30 years.

Non-invasive criteria of diagnostic can be applied to cirrhotic patients for nodule(s) ≥1 cm, in light of the high pre-test probability and are based on imaging techniques obtained by multiphasic CT, dynamic contrast-enhanced MRI (evidence high; recommendation strong) or CEUS (evidence moderate; recommendation weak) (EASL guidelines, 2018). The Liver Imaging Reporting and Data System (LI-RADS) was created to standardize the reporting and data collection of CT and MR imaging for patients at risk for HCC (Li-RADS 2018). LI-RADS advocates the term "arterial phase hyperenhancement (APHE)" which is descriptive and non-ambiguous replacing other frequently used descriptors such as "hypervascularity", "intense arterial phase uptake", or "wash-in" LI-RADS 2018). Diagnosis is based on the identification of the typical hallmarks of HCC, which differ according to imaging techniques or contrast agents (APHE with washout in the portal venous or delayed phases on CT and MRI using extracellular contrast agents or gadobenate dimeglumine, APHE with washout in the portal venous phase on MRI using gadoxetic acid, APHE with late-onset (>60 s) washout of mild intensity on CEUS). Because of their higher sensitivity and the analysis of the whole liver, CT or MRI should be used first (evidence high; recommendation strong) (EASL guidelines, 2018). LR-5 is an important category because LR-5 nodules can be treated as HCC without biopsy or further imaging. LR-4 (probable HCC) nodules usually require biopsy, but alternative imaging or short-term (<3 months) imaging follow-up can be applied if neither biopsy nor treatment is implemented immediately based on multidisciplinary discussion. LR-3 (intermediated probability of malignancy) generally requires alternative imaging or follow-up but may require biopsy in selected cases based on multidisciplinary discussion (LI-RADS).

In the last 10 years the therapeutic management of HCC considerably improved leading to extended access to therapeutic options that increase the life expectancy of these patients. However, HCC still remains an aggressive malignant tumor with a high rate of cumulative recurrence over 5 years (70%) after curative therapies (El-Serag, 2011, Marrero JA et al, 2018, EASL guidelines 2018).

Articles

1. Muzica CM, Stanciu C, Cijevschi-Prelipcean C, Girleanu I, Huiban L, Petrea OC, Singeap AM, Cojocariu C, Cuciureanu T, Sfarti C, Zenovia S, Chriac S, Stefanescu G, Ciortescu I, **Lupascu-Ursulescu C**, Miftode E, Trifan A. Long-Term Risk of Hepatocellular Carcinoma Following Direct-Acting Antiviral Therapy in Compensated Liver Cirrhosis Induced by Hepatitis C Virus Infection. Hepatitis Monthly 2021; 21 (6); e115910 DOI: 10.5812/hepatmon.115910 (**IF 2021- 1.214**)
2. **Lupașcu-Ursulescu C**, Fotea V, Vasiluță C, Georgescu Șt, Lozneanu LG, Lupașcu C, Grigorean V, Negru D. Hepatocellular carcinoma with central severe arterioportal shunt – endovascular approach. Rev. Med. Chir. Soc. Med.Nat. 2017; 121 (1): 148-152

3. **Ursulescu C**, Lupaşcu C. Liver metastasis imaging. Jurnalul de Chirurgie 2008; 4: 194-200 (IndexCopernicus, DOAJ şi EBSCO Academic) E-ISSN: 1584-9341
4. Negru D, **Ursulescu C**, Fotea V. Puncţia percutană diagnostică ghidată radioimagistic. Rev. Med. Chir. Soc. Med. Nat., 2007; 111(4):833-44
5. **Ursulescu C**, Fotea V, Platon A, Negru D, Daniil C. Chemoembolizarea arterială terapeutică în cancerul hepatic. Jurnalul de Chirurgie, 2005; 1 (4): 411-418

Books

1. **Ursulescu C**. Diagnosticul carcinomului hepatocelular: punctia ghidată imagistic. In: Stanciu, C. Cijevschi, G. Bălan, A. Trifan (sub red.) Curs intensiv de boli digestive. Editura "Gr.T.Popa" UMF Iași, 2013, ISBN 978-606-544-154-5
2. **Ursulescu C**, Lupașcu C. Terapia ablativă locală pentru carcinomul hepatocelular. In: Stanciu, C. Cijevschi, G. Bălan, A. Trifan (sub red.) Curs intensiv de boli digestive. Editura "Gr.T.Popa" UMF Iași, 2013, ISBN 978-606-544-154-5
3. Lupascu C, **Lupascu-Ursulescu C.** Tumorile benigne ale ficatului. In Popescu I. Tratat de chirurgie hepato-bilio-pancreatică și transplant hepatic. Editura Academiei Române, București 2016, 221-238 ISBN 978-973-27-2592-4

Projects

1. **ERA NET EuroNanoMED JTC-3 (2011): "Chemo-Hyperthermal delivery combined chemo-hyperthermal control of hepatic tumors, based on microwave-activated subendothelial-targeted nano-assemblies " (Che Ther Del)** – 02.05.2012 - 20.12.2014 – project manager for Partner 2 (Institute of Oncology Iasi) ;
2. **CEEX 122/2006:** "Selection criteria of the therapeutic methods in secondary hepatic cancer - clinic-biologic and molecular substantiation" (manager project PhD MD E. Târcoveanu) – research team member;
3. **"A multicenter multinationale phase 3 randomized study to evaluate the safety and efficacy of treating colorectal cancer patients recurrent liver metastases using the LitxTm system plus chemotherapy as compared to chemotherapy only; LSO-OL006**
4. **HGS 1012-C1103 „A randomized, multi-center, blinded, placebo-controlled study of Mapatamumab ([HGS1012], a fully-human monoclonal antibody to TRAIL-R1) in combination with sorafenib as a first-line therapy in subjects with advanced hepatocellular carcinoma**" ClinicalTrials.gov Identifier: HGS1012-C1103; Sponsor: Human Genome Sciences, Inc; PSI CRO AG ; 2010 – 2013;

1.2.2.1 Image-guided percutaneous biopsy

Introduction

Liver biopsy for diagnostic purpose, first reported in 1923, has been widely influenced over the past 40 years by the advances in imaging techniques and therapy. The percutaneous biopsy of a focal liver lesion benefits from the guidance of cross-sectional imaging, especially ultrasound (US) and computed tomography (CT), necessary to plan and to secure the path, to avoid the passage through other structures, to optimize the accuracy, and to minimize the complications. Together with technical improvements in imaging, the indications for biopsy constantly evolved, especially for focal lesions. Since the rationale of the biopsy is to confirm the nature of an indeterminate lesion and to facilitate the choice of the appropriate treatment, the suspicion of the malignancy, based on multiphase CT or MR imaging, is a major indication. For patients at risk for hepatocellular carcinoma (HCC), the American College of Radiology has published in 2011

guidelines for performing and standardized reporting multiphase CT and MR exams, the LI-RADS (CT/MRI LI-RADS v2018). Consequently, since 2012, EASL-EORTC guidelines for the management of hepatocellular carcinoma changed the paradigm for the diagnosis of HCC, and unlike most solid cancers, this type of cancer may be diagnosed based on noninvasive imaging without biopsy confirmation when the imaging criteria are met (EASLguidelines 2012; Marrero et al, 2018). Biopsy is still indicated in some patients with cirrhosis and an indeterminate nodule (as an alternative to follow-up imaging), for categories LI-RADS 4, LI-RADS-M, nodules with imaging features overlapping HCC in vascular form of cirrhosis or congenital liver fibrosis, and nodules with enhancement and wash-out in the absence of cirrhosis (Marrero et al, 2018).

Technical notes

Imaging methods used to guide the biopsy

Diagnostic percutaneous puncture can be guided by fluoroscopy, ultrasound, CT and MRI. The first fluoroscopically guided fine-needle puncture was reported in 1930 (McGahan JP et al, 1990). For liver, fluoroscopy is used to guide the transjugular approach.

Ultrasound is the most used method for guiding percutaneous puncture. The first ultrasound probes used to guide percutaneous puncture were made in 1972 by Goldberg and Holm (McGahan JP et al, 1990) and contained a central hole through which a special needle was inserted for aspiration or biopsy. The impressive technical development in recent years has led to the emergence of high-performance ultrasound equipment with high resolution in real-time. At the same time, devices attached to transducers allow better visualization of the needle during the procedure.

The advantages of ultrasound as a method of guiding method are short examination time, real-time needle visualization and control, possibility to perform percutaneous puncture at the patient's bedside (portable devices) and low cost.

The disadvantages of ultrasound are represented by the impossibility of exploring structures containing air or gas and there are also limits in recently operated patients (scars, drainage tubes).

CT was first used to guide a diagnostic percutaneous puncture in 1976 (Haaga JR et al, 1976). Today, the method plays a central role in percutaneous biopsy and drainage of abscesses or various fluid collections. CT has excellent density resolution, which allows precise location of focal masses. Adjacent vital structures are easily recognizable, so planning the access path is very accurate. Intravenous contrast administration also allows visualization of blood vessels and type of vascularization of masses to be biopsied.

A great advantage of CT is the ability to locate the tip of the puncture needle, which allows biopsy of small structures with great accuracy and low risk of complications (Silverman SG et al, 1992). Postoperative scars and drainage tubes are not limitations of the method.

CT has some disadvantages in guiding biopsy: is relatively expensive, does not operate in real time, exposes the patient and the radiologist to radiation, and is more time consuming.

MRI is not routinely used for liver biopsy, requiring equipment with "open magnet" and special non-ferromagnetic biopsy instruments.

Indication

Percutaneous biopsy is indicated for diagnostic purposes to determine whether a mass:

a. is primitively neoplastic or inflammatory.

b. represents metastatic disease, a second malignant primitive tumor or a benign entity in a known neoplastic patient.

c. represents viable residual tissue or necrotic tissue.

The choice of the guiding method depends on the available equipment in the radiology department when biopsy is scheduled, on the experience of the interventional radiologist and must be in direct correlation with the cost-efficiency ratio.
In our department, ultrasound-guided biopsy is the preferred method. CT is used for guidance when a mass has a diameter less than 3 cm, is located near large vessels, bile ducts or diaphragm.

Contraindications
Absolute contraindications are represented by patient refusal, major uncorrectable coagulopathy and coma. Heart failure, liver cirrhosis, uremia and decompensated diabetes mellitus are relative contraindications and percutaneous biopsy can be postponed until some major imbalances are corrected.

Preparation for procedure
In order to have a high success rate, the interventional procedure must be prepared in detail and involves the following steps:
A. Preparation of the patient
B. Analysis of the clinical and imaging file
C. Choice of method of guidance.
The preparation of the patient is particularly important and consists of:
- anamnesis (anticoagulant medication, significant bleeding from tooth extractions or previous surgery);
- the radiologist offers to the patient information about the method, purpose and usefulness of the examination, accidents and possible incidents and obtains an informed consent.
- clinical examination (highlighting possible hematoma);
- biological assessment (bleeding time, prothrombin time, partial thromboplastin time, kidney function, blood glucose, platelets);
- stop feeding 4-6 hours before the procedure.
- discontinue the anticoagulant treatment before the procedure according to the type of treatment, the underlying disease and the guides;
- ensure the presence of an anesthesiologist for children (under 3 years) and anguish patients, for short-term general anesthesia.
The analysis of the imaging file is a mandatory step and allows to choose the best guiding method and to plan the access path.

Materials
Regardless of the method of guiding a percutaneous puncture, the materials necessary for such an intervention are: sterile gloves, lancet, skin marker, distance measuring line, sterile fields, sterile compresses, xyline 1%, solution of iodopovidone, sterile needles (18, 20, 22 gauge), sterile syringes (5, 10, 20 and possibly 50 ml), puncture needles (will be described below), container with formalin (to preserve the biopsy specimen).
There is a wide variety of needles used for percutaneous puncture (Bernardino ME, 1984; Ferrucci JT Jr et al., 1980; Makuuchi M et al, 1987). The selection is very important for the success of the procedure and depends on the following factors:
- lesion size (a bulky lesion requires a larger amount of harvested tissue, therefore a thicker needle – 14-17 gauge diameter);
- type of vascularization (for hypervascularized masses we use thinner needles to minimize the hemorrhage risk – 18-22 gauge diameter)
- location of the lesion and neighboring elements (if the lesion is in the vicinity of intestinal loops, large vessels, pleura and the access route is difficult, it is preferable to use thinner needles).
Finally, the choice of puncture needles is made according to the examiner's experience and collaboration with the histopathologist.

Puncture needles can be classified into:
A. Aspiration needles;
B. Modified aspiration needles;
C. Biopsy needles.
The aspiration needles are the thinnest, with a diameter of 20-22 gauge. They are used only to collect specimens for cytology and, rarely, small tissue fragments. The most used is Chiba needle. They have the advantage of limited complications, but they are very flexible, bend and are difficult to use for deep lesions. However, the use of Chiba needles is generally very reliable, with success rates ranging from 80 to 100% according to literature (Bernardino ME, 1984; Ferrucci JT Jr et al., 1980; Makuuchi M et al, 1987).
Modified aspiration needles combine the safety of aspiration needles with the possibility of sampling tissue. They have a diameter of 18-20-22 gauge, the thicker ones being reserved for biopsy paths that avoid intestinal loops or important vascular structures. The most used modified aspiration needles are Turner (the tip at a sharp angle of 45 degrees), Madayag and Greene (90-degree tip and different types of mandren), Franseen and Rotex (with a screwdriver-shaped stiletto at the tip). They are not routinely used for liver biopsy.
Biopsy needles are those that harvest tissue fragments in the form of cylinders of varying length, with diameter 14 to 20 gauge. The most used are Trucut needles; the coating cuts the tissue sample and brings it and deposits it in the hollow of the needle. They can be attached to a biopsy gun, making the procedure easier. After inserting the biopsy needle in the immediate vicinity of the lesion, the gun is armed and then triggered, the internal trocar advances 2-3 cm followed almost instantly by the external trocar with the role of cutting the tissue. The biopsy gun is easy to handle and reduces the time required for biopsy (Bernardino ME, 1984; Ferrucci JT Jr et al., 1980; Makuuchi M et al, 1987).

Methods
The puncture technique depends on the chosen method of guiding.

Ultrasound-guided percutaneous puncture technique
There are two main ultrasound-guided techniques for liver biopsy: indirect guidance, and "free hand" technique with the use of special guidance systems.

Indirect guidance
Once the puncture site is selected by ultrasound (the angle and length of the puncture path), the puncture site is marked with a marker and the transducer is withdrawn from the skin. The puncture site is disinfected and covered with a sterile field. With the transducer wrapped in a sterile cup filled with gel, the puncture site is checked again. The local anesthesia with 1% xyline is performed, followed by a small skin incision to facilitate the insertion of the puncture needle. The patient is asked to suspend breathing and the biopsy needle is inserted at the periphery of the lesion. The position of the needle tip is checked again, and the gun is triggered (Fig. 1.7). After removal of the needle. The tissue sample is placed in formalin to be preserved for pathology.
If an aspiration needle is used, it is placed inside the lesion, a syringe is attached, negative pressure is produced by raising the syringe plunger and simultaneously several push-withdraw movements of the needle over 1 cm are performed. The circular movement of the needle increases the chances of harvesting a tissue fragment. At the end, the negative pressure in the syringe is diminished as the needle is withdrawn. The material for cytology is stretched on a slide and distributed over the entire surface of the blade.

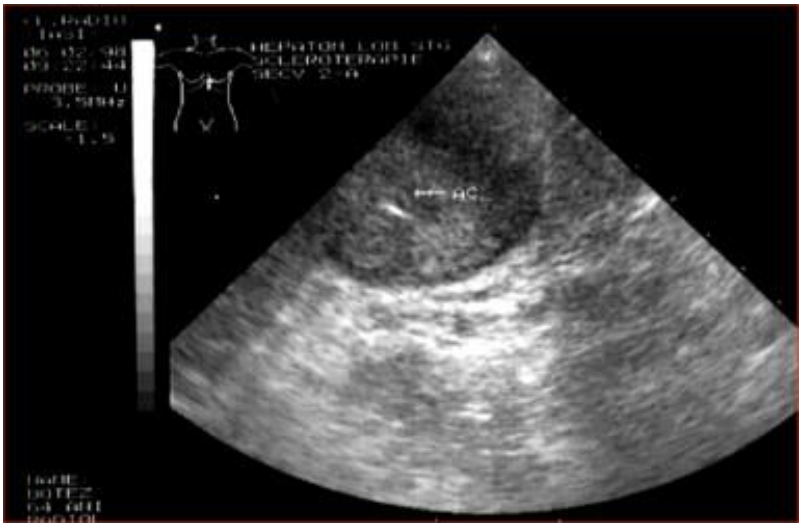

Fig. 1.7 Ultrasound-guided percutaneous biopsy of HCC

The "free hand" technique

This technique allows direct visualization of the puncture needle, ultrasound examination following both the lesion and the needle. The needle can be positioned in close proximity to the transducer parallel to the section plane. The aspiration or biopsy is performed in the same way as described in the indirect guidance technique.

There are two main types of puncture needle guidance systems:

- dedicated biopsy transducers with holes or grooves for biopsy needles built inside the transducer; they have several disadvantages: difficult sterilization, large contact surface, the impossibility of directly viewing the needle on the puncture site;
- systems that are attached to the transducer; they are more useful and easier to sterilize. The placement of the biopsy needle in the lesion is done in the same way as described in the indirect guidance technique, except that here the needle is continuously viewed on the ultrasound monitor.

CT-guided percutaneous puncture technique

On CT examination performed for diagnostic purposes we planned the access route and the patient's position during the procedure (dorsal or lateral decubitus, procubitus) to insure the shorter path to the lesion avoiding the surrounding structures. We prefer to biopsy a lesion located deeper into the parenchyma to minimize the bleeding.

Once the patient is placed on the table in the established position, the area of interest is scanned. The respiratory command should be kept throughout the procedure.

Once the biopsy section plan has been chosen, the needle entry site on the skin is marked with a metal marker. A new scan is performed to confirm the position of the metal marker. The distance to the lesion and the input angle are calculated as the shortest route to the lesion avoiding vital structures such as large vessels.

After local disinfection of the skin and anesthesia with 1% xyline, with the anesthesia needle inserted into the abdominal wall structures, we take another scan to reconfirm the position and angle. If these parameters are correct, the anesthesia needle is removed, the puncture needle is inserted and pushed into the lesion/ at the periphery of the lesion. When the needle moves toward the lesion, the patient does the same respiratory command used in control scans.

A new scan is performed to confirm the position of the needle tip. The appearance of a black linear artifact confirms that the needle tip is in the section plane.

At this moment the biopsy needle is triggered, and the tissue sample is collected. The needle is withdrawn, and the sample is placed in a formalin recipient.

After completing the procedure, a sterile dressing is applied to the skin and the area of interest is rescanned to highlight any acute complication.
The CT-guided biopsy is a time-consuming technique because there is no possibility of real-time guidance, and each step is verified by a new scan for the precise location of the biopsy needle.

Post-procedural care
An image-guided percutaneous biopsy is a safe interventional procedure with low complication rate. After completion of the procedure, the following measures shall be required:
a. bed rest 4-6 hours
b. monitoring vital functions – pulse, blood pressure
c. Pulmonary X-ray in expiration if the percutaneous puncture targeted the diaphragmatic area.
For liver biopsy, we prefer a 24-hours surveillance due to the risk of late bleeding. If after 24 hours the patient is stable in terms of vital functions, he can be discharged.

Results and complications
Image-guided percutaneous puncture is mainly used to establish a clear diagnosis of malignancy or benignity of a mass. The success rate of puncture is 80-95%, even under optimal cytological technique and analysis. The false-negative rate varies between 5 and 20%, caused by:
- failure of biopsy of small nodules (less than 1 cm);
- hypervascularized and necrotic lesion, when the chance to collect blood cells or necrosis is higher, with insufficient tumor cells;
- histological type of lesion (lesion with desmoplastic or inflammatory reaction).
In benign tumors or inflammatory lesions, cytology is less specific than in malignant tumors.
Besides percutaneous biopsy, intraoperative ultrasound can be extremely useful in the diagnosis and biopsy of hepatocellular carcinoma developed on a cirrhotic liver. On a batch of 203 hepatocellular carcinomas Makuuchi reported intraoperative ultrasound sensitivity of 99% compared to preoperative ultrasound (89.3%), angiography (84.1%) and CT (89.6%) (Makuuchi M et al, 1987). Also, in the diagnosis of daughter nodules, intraoperative ultrasound is clearly superior to other methods with a sensitivity of 41.7% compared to preoperative ultrasound (12.5%), angiography (14%) or CT (22.4%) (Makuuchi M et al, 1987).
Most liver biopsies are performed under ultrasound guidance with puncture needles of 18-20 gauge diameter. Solid nodules can be biopsied, or liver cysts and abscesses discharged with 70 and 95% accuracy (Lindgren PG et al, 1996).
CT is used in guiding hepatic biopsy when the lesion is not visible on ultrasound or is located deep in the hilar plaque and in the vicinity of the diaphragm.
The use of a 18-gauge needle ensures enough tissue for pathological diagnosis both for focal and diffuse liver disease (cirrhosis, chronic hepatitis, hemochromatosis or Budd-Chiari disease). In Budd-Chiari disease, a biopsy must be done in both lobes of the liver for a correct diagnosis.
CT has an accuracy of 85-95% in guidance of percutaneous puncture (Martino CR et al, 1984).
Complications that may occur after image-guided liver biopsy are rare and minor – bleeding, hypotension, fistula formation. In a percentage of 0-2.4%, septic shock, biliary peritonitis and massive bleeding may occur. (Pagani JJ 1983).

Conclusion
In non-cirrhotic patients, diagnosis of HCC or of other indefinite lesions should be confirmed by pathology. Image-guided percutaneous biopsy is effective for sampling the focal liver lesions.

1.2.2.2 Endarterial treatment of hepatocellular carcinoma

Introduction

HCC is the 5th most common of all cancers, with an annual incidence exceeding 7‰ (EASL guidelines 2018). The prognosis depends both on the size and extent of the tumor, as well as on liver function, 90% of HCC evolving on a background of chronic hepatopathy (hepatitis B and C virus infections, ethanolic consumption). Because most tumors are discovered at relatively large sizes, surgical treatment (resection, liver transplantation) is only possible in less than 20% of cases. Alternative treatment is offered by systemic chemotherapy, intraarterial procedures (therapeutic arterial chemoembolization, selective portal embolization), percutaneous ablation techniques (thermal ablation, such as radiofrequency or microwave, and chemical ablation, such as alcoholization), external radiotherapy or radioembolization Transarterial chemoembolisation (TACE) is the most widely used primary treatment for unresectable HCC and was the recommended first-line therapy for patients with intermediate-stage disease in the previous guidelines (EASL guidelines 2018). HCC exhibits intense arterial neo-angiogenic activity during its progression. The rationale for TACE is that the intra-arterial infusion of a cytotoxic agent followed by embolisation of the tumour-feeding blood vessels will result in a strong cytotoxic and ischaemic effect targeted to the tumour since this tends to become entirely fed by arterial inflow, unlike the surrounding parenchyma which receives the majority of inflow through the portal system. TACE should be distinguished from chemo-lipiodolisation, which involves the delivery of an emulsion of chemotherapy mixed with Lipiodol®, bland transcatheter embolisation (TAE), where no chemotherapeutic agent is delivered, and intra-arterial chemotherapy, where no embolisation is performed.

This method of interventional radiology is well tolerated due to the double vascularization of the hepatic parenchyma (hepatic artery and portal vein), and effective since the tumor is supplied almost exclusively by branches of the hepatic artery. Therefore, tumor ischemia can be achieved without major harm of the remaining liver parenchyma, provided that portal system is patent, and the portal flow is hepatopedal. In addition, selective intraarterial injection of an emulsion of iodized oil and cytostatic or of drug-eluting beads determines its predominant concentration in hypervascularized tumors, with gradually persistent release of cytostatic, improving the therapeutic effect and avoiding the adverse effects of systemic chemotherapy. Nowadays, TACE is the standard of care for patients with intermediate stage HCC (BCLC B - large or multifocal HCC without macrovascular invasion or extrahepatic metastasis) (Sieghart W et al, 2015). In Romania, this interventional procedure was first performed by prof. Cezar Daniil in 1987, at the Emergency Hospital “Sf. Spiridon” Iasi, 4 years after the first report by Yamada et al. (Yamada et al, 1983). The series published in 2005 was among the first reported in our country.

1.2.2.2.1 Chemoembolisation for HCC

Material. Methods

The study group included 82 patients (66 men, 16 women) with HCC treated by conventional TACE, in the Department of Interventional Radiology of "Sf. Spiridon" Hospital during 1993-2005. The age of patients ranged from 39 to 80 years, with a mean of 58.8 years. Most of them had pre–existing liver damage, due to ethanol (32 cases), viral infection (hepatitis virus B -10 cases, C - 2 cases), association ethanol – hepatitis B in 4 cases. Thirty-four cases had non-specified etiology of the underlying chronic liver disease. Most patients were classified as Okuda II (61 patients).

Pre-procedural imaging diagnosis was based on detection by ultrasound and characterization by another cross-sectional method with intravenous contrast injection (CT and/or MRI).

The criteria for patient selection have been modified as experience has gained, and more studies were published in the literature. The patients at increased risk of postprocedural liver failure have

been excluded in recent years. The procedure was indicated in patients with inoperable HCC due to tumor volume, reduced remnant volume, presence of tumor nodules in both lobes, and impaired liver function.

The exclusion criteria were very important, and they include the presence of extrahepatic extension (abdominal or thoracic adenopathy, lung metastases), jaundice or elevated bilirubin (above 3 mg/dL), ascites, portal vein thrombosis. Also, due to the increased risk of postprocedural liver failure, patients with tumour volume exceeding 50% of liver volume, and elevated transaminase enzyme (AST and ALT over 100 IU/L) were excluded from this interventional procedure.

The procedure was performed under fluoroscopic guidance and local anesthesia, in the angiography suite, by Seldinger technique, with femoral approach in all cases. The right femoral approach was preferred in the first procedures; the left femoral approach was used in case of obstruction of the right side or in iterative procedures (3-4), due to fibrosis. The classical materials were used for the angiography of the hepatic artery (introducer kit, guidewires, Cobra or multipurpose 4F/5 F catheters), as well as microcatheters (3F) for selective and supraselective access in the hepatic artery branches supplying the lesion. For embolization we used Lipiodol UF 5 – 10 ml, PVA particles and spongel particles (obtained by scarification), combined with chemotherapy (Farmorubicin: 50 – 100 mg; Mitomycin C: 5 – 10 mg).

Arteriography of the celiac trunk and superior mesenteric artery were routinely performed at the beginning of the procedure, in order to identify tumoral arterial feeders and anatomical variants of the hepatic artery. Selective catheterization of the proper hepatic artery was then performed in 54 cases (45 emergent from celiac trunk and 9 from the superior mesenteric artery) (Fig. 1.8, Fig. 1.10), followed by the catheterization of the right hepatic artery (RHA) in 19 cases and left hepatic artery (LHA) in 10 cases (fig.1.9).

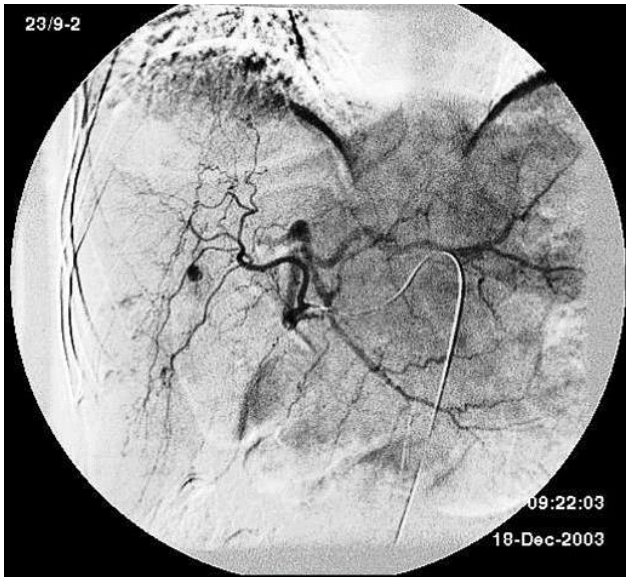

Fig. 1.8 Selective arteriography of the hepatic artery: the HCC occupies the left hepatic lobe, but daughter nodules are identified in the right lobe;

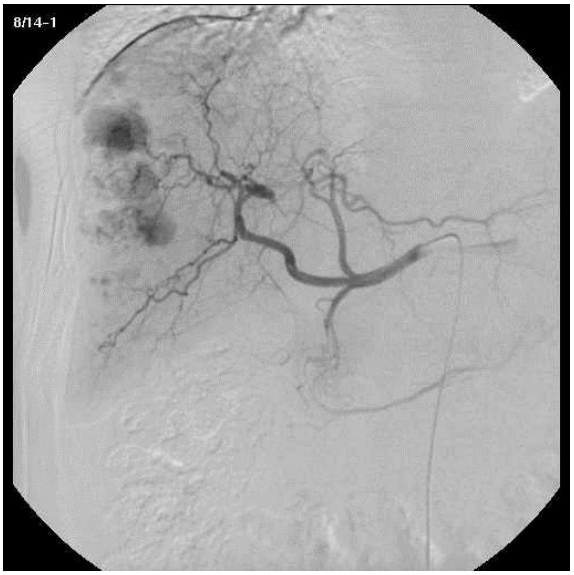

Fig. 1.9 Selective catheterization of the right hepatic artery: arterial supply of multinodular HCC from segmental branches V and VIII.

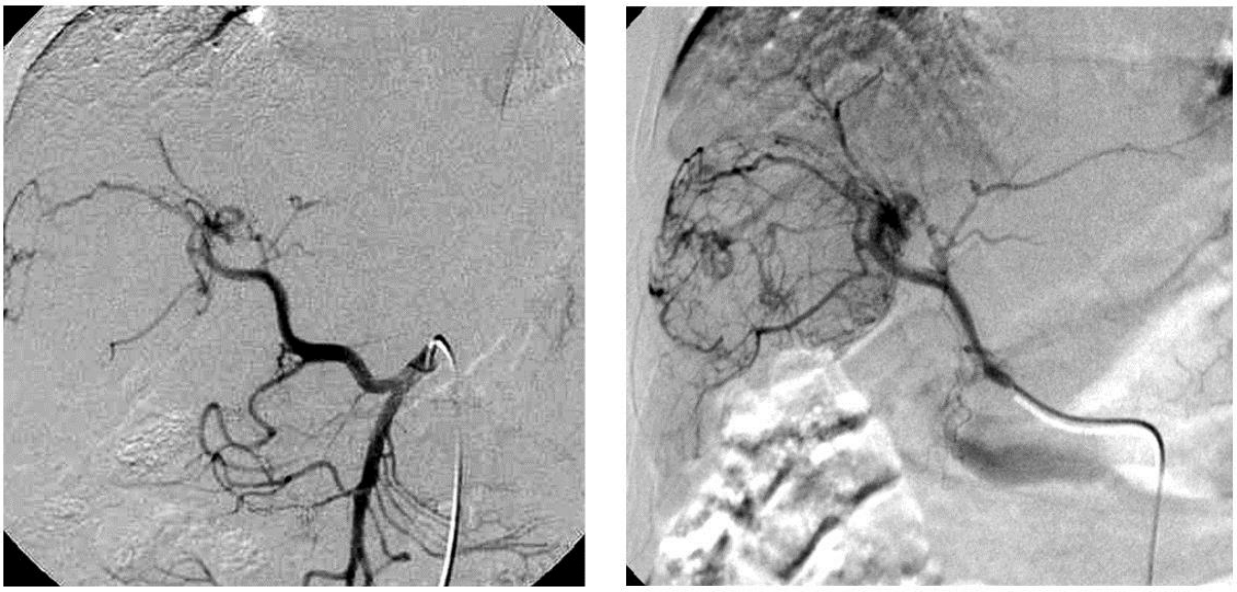

Fig 1.10 a) Selective arteriography of the superior mesenteric artery: hepatic artery originating from the superior mesenteric artery; b) Selective catheterization of the right hepatic artery with tumor vascularization.

The position of the catheter as selectively as possible was assessed by supraselective angiography, to confirm the inclusion of all arterial feeders and to avoid the embolization of not targeted branches, especially those responsible for complications or persistent postembolization syndrome (i.e. gastroduodenal artery, cystic artery, gastric branches).
We then perform the slow injection, intraarterially, of the chemotherapy + embolic emulsion, following through intermittent fluoroscopy its flow and distribution; the procedure was stopped when emulsion stasis or reflux was revealed (Fig. 1.11). The embolization of all arterial feeders of the tumor was assessed by another angiography at the site of injection and then, more proximal. If incomplete, the embolization was completed with gelatin sponge particles.

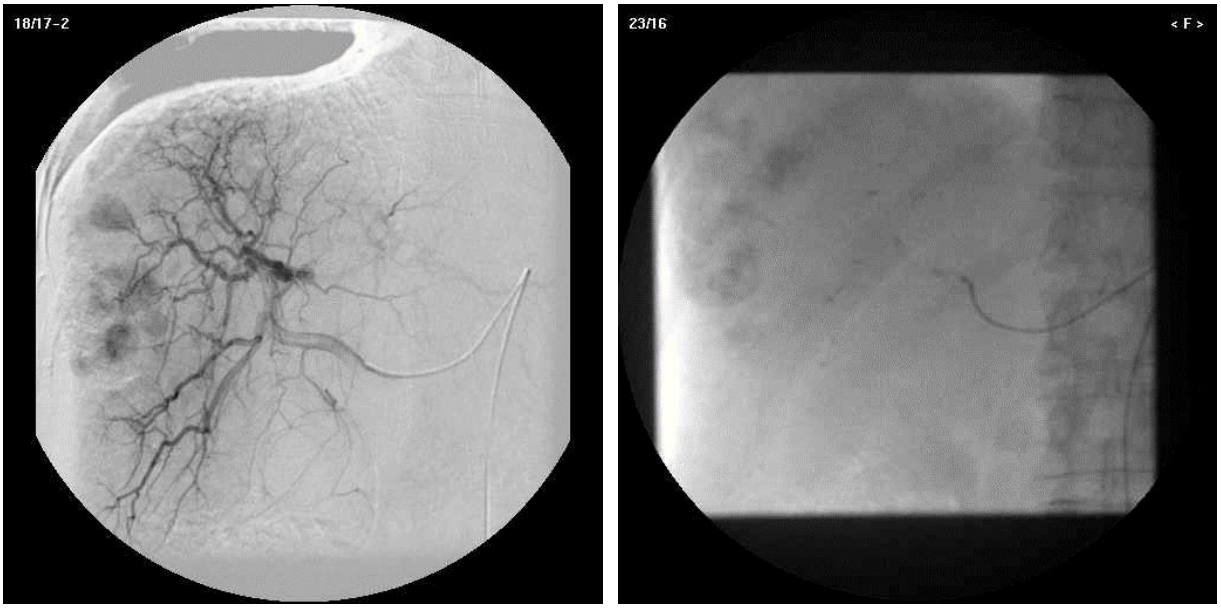

Fig.1.11 a) Selective right hepatic arteriography: hypervascularized tumor nodules; b) Fluoroscopic control of lipiodolate emulsion injection revealed concentration of the emulsion in nodules;

In all cases where Lipiodol was used, a plain X-ray of the right upper quadrant was taken at the end, to assess the intrahepatic and intratumoral contrast distribution. The postprocedural follow-up included clinical monitoring for 1-3 days, depending on the extent and severity of the post-embolization syndrome, as well as biological reassessment at 24 hours and imaging (color Doppler ultrasound at 24 h). In hypovascular lesions, a native CT at 48 h was used to assess distribution of emulsion inside the tumor. The patients were reassessed at 1 month clinically, biologically and by contrast-enhanced CT or MRI. The lesions with stability or partial response were re-evaluated at 3 months. The lesions incompletely/ partially devascularized were scheduled for a new TACE procedure. The patients with progressive lesions, as well as those treated initially only by intraarterial chemotherapy, were referred to the oncological team to assess the opportunity for another oncological treatment.

Results

For the 82 patients included in the study group, a total of 189 procedures were performed (1 to 6 procedures/patient), with a significant percentage of patients (46%) who benefited from only 1 procedure (table 1.VI). Fifty-five percent of the patients benefits from repeated procedure. The hepatic lesions treated by TACE sized 5 – 18 cm (mean 8.35 cm), but lesions sized more than 10 cm were included in the study group in the first part of the interval, when TACE was considered only a palliative method. The most common macroscopic type was macronodular (52 cases), followed by multinodular (19 cases), nodular conglomerate (9 cases) and diffuse (2 cases).

Table 1.VI Number of procedures/patient

No. procedures	1	2	3	4	5	6
No. / % patients	38/ 46%	7 / 8%	20 / 24.4%	10 / 12.2%	5 / 6%	2 / 2.4%

The substances used were: lipiodol + chemotherapy emulsion followed by embolization with gelatin sponge particles in 43 cases, lipiodol + chemotherapy emulsion in 17 cases, mixture of gelatin sponge particles with chemotherapy in 2 cases.

The presence of anatomical variants or the large tumoral volume made the selective approach inappropriate in 20 cases, the intraarterial injection of chemotherapy being the therapeutic option. Immediate results (reduction of tumour vasculature) were confirmed by post-embolisation angiography and abdominal ultrasound performed at 24h with evidence of gas and tumour necrosis, as well as reduction of vascularisation in the Doppler study in all cases where the embolic mixture was injected. The distribution of the emulsion was assessed by the upper right quadrant X-ray (in all 60 cases using lipiodol) and by CT scan at 48 h (in 42 patients), with evidence of intratumoral, intrahepatic, extrahepatic lipiodol distribution. Lipiodol was distributed mainly inside the tumor in 36 cases out of 42 examined by CT, with an intense and homogeneous distribution in 24 cases. Also, postprocedural CT examination detected new daughter nodules in 6 cases, with good distribution of the lipiodolate emulsion (fig. 1.12).

Extratumoral intrahepatic distribution was observed in 6 cases, all hypovascular nodules on pre-procedural cross-sectional and angiographic exams (fig. 1.13). Non-targeted vessels were embolized in one case, with contrast present in the spleen and gastric wall.

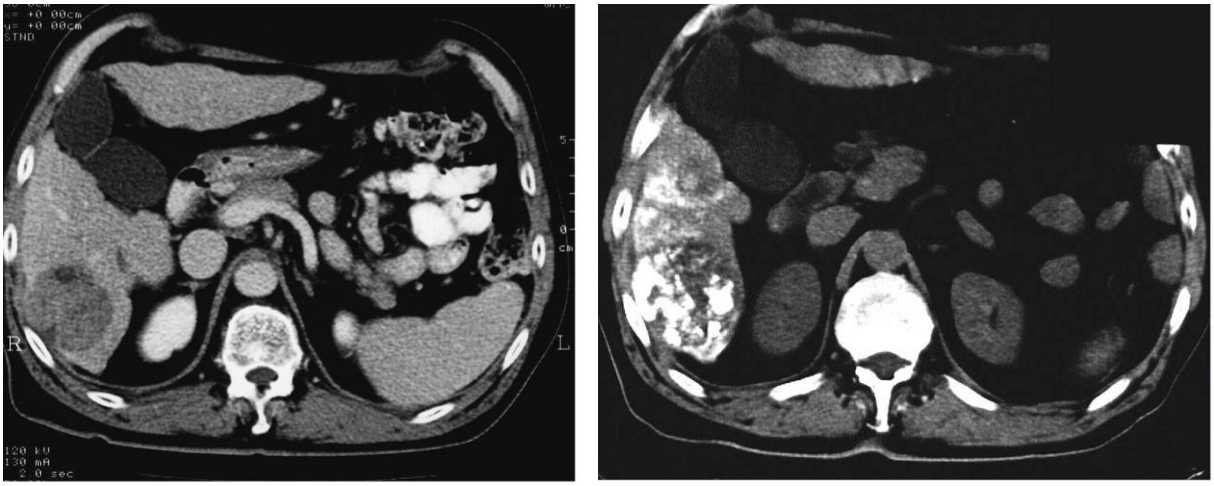

Fig. 1.12 a) HCC located in the right lobe, 6th segment: contrast-enhanced CT; b) Non-enhanced CT follow-up at 48 hours post-embolization: concentration of lipiodolate emulsion predominantly in tumor, with delimitation of adjacent daughter nodules.

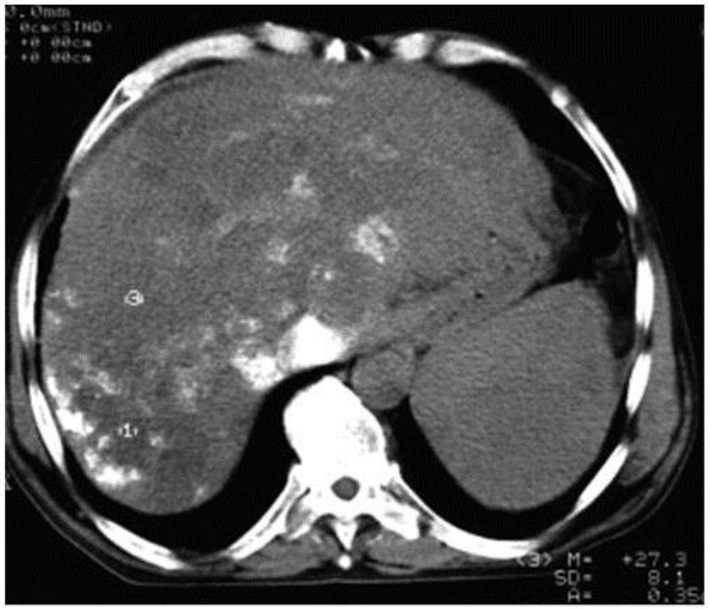

Fig. 1.13 CT follow-up at 48 hours: poor concentration of lipiodol in the periphery of the lesion, corresponding to hypovascularization displayed by angiography.

Post-embolisation syndrome (fever, abdominal pain, vomiting, ileus) was minor and conservatively treated by hydration, antiemetics, analgesics in 77 cases.

Partial reduction of tumour volume was seen in 25 (30.4%) cases after the first TACE sequence. In 24 (29.2%) of cases, there were no changes in tumour volume at 1 month.

Both color Doppler ultrasound and contrast-enhanced CT performed 3-4 weeks after TACE showed the pesistance of tumor vascularization in 44 cases, mainly peripheral, indicating the need to complete the embolization by a new procedure, regardless the evolution of the tumoral volume (fig. 1.14).

The complications encountered in the study group were: vascular - 5 cases (4 patients with hematoma at the puncture site and 1 patient with lesions consistent with stricture of the hepatic artery after the third sequence), local (2 patients with cholecystitis regressed under conservative treatment) and general (1 patient with persistent alteration of the general status 3 weeks after TACE and impaired liver function, 1 patient with ileus conservatively treated). The study group recorded an early post-procedural death by acute myocardial infarction.

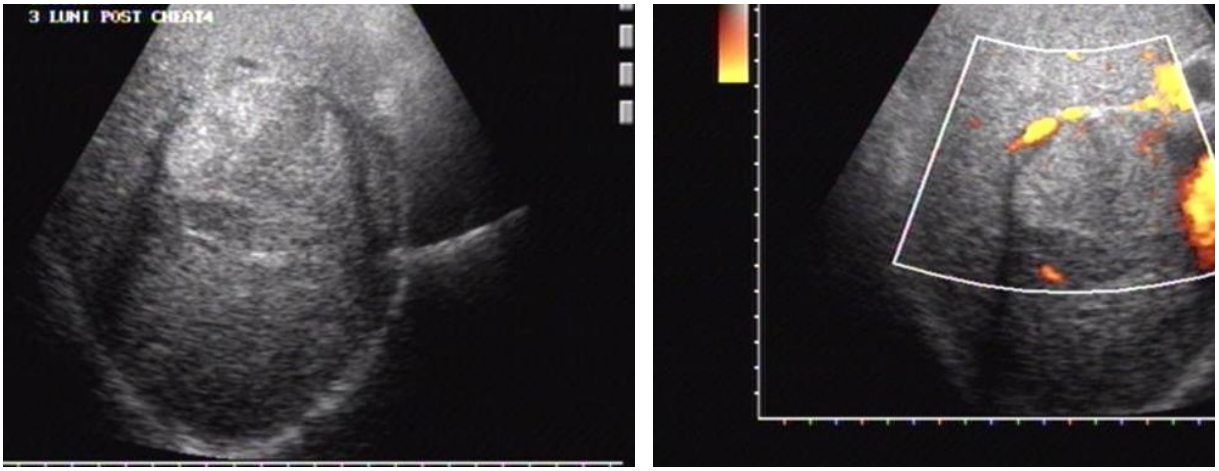

Fig. 1.14 a) Liver US: HCC; b) Follow-up y Doppler ultrasound revealed diminished intratumoral vascularization, with persistence of peripheral vascularization.

Late results are difficult to assess due to the lack of a strict protocol for patient follow-up and of a multidisciplinary team in the hospital. The period for follow-up in our department was 1-58 months (mean 9.95 months). Poor results were recorded for hypovascularized lesions, diffuse type and large lesions (more than 50% of liver volume), all these cases benefited from a single TACE or intraarterial chemotherapy procedure without stabilization of tumor volume.

Discussion

A TACE procedure combines two therapeutic principles: embolization of the arterial tumoral feeders and intraarterial, local, administration of the chemotherapy. In 1976, Goldstein reported the use of therapeutic embolization in the treatment of abdominal tumors, using gelatin sponge particles as an embolizing agent.

Studies performed on a emulsion of chemotherapy and iodized oil have shown the stability and the slowly realesing of the chemotherapy when intraarterially injected into HCC feeders. A study published by Takayasu in 1987 compared the results of intraarterial treatment with lipiodol, lipiodolate emulsion, and lipiododolate emulsion followed by embolization with gelatin sponge particles, with better results (more extensive necrosis) in the group of patients receiving the complete variant (Takayasu K et al, 1987).

This method of treatment has the advantage that it can be repeated, the total number of procedures and their frequency varying in different studies. Actually, this heterogeneity of the TACE technique and schedules used in world wide clinical practice prevents standardization. One European study performed conventional TACE with the chemotherapeutic agent doxorubicin at dosages adjusted to bilirubin levels with a fixed schedule at baseline, 2 months and 6 months, while an Asian study performed TACE with cisplatin, repeated every 2–3 month until disease progression, serious adverse events or hepatic decompensation (Llovet JM et al, 2002; Lo CM et al, 2002). The selectivity of TACE (lobar vs. segmental vs. subsegmental embolization) is another subject of debate, but is an important factor to decide the tolerance and efficacy of the procedure. In our group, the large number of patients with only one procedure is explained by less rigorous selection criteria in the early period, when patients with large tumour volume were not excluded for procedure, as well as those with impaired hepatic function. Also, patients without overt benefit after the first procedure (hypovascularized tumor with no intratumoral concentration of lipiodol, anatomical variants precluding the selective catheterization of tumoral feeders) were excluded from the follow-up in the interventional radiology department and were referred to the oncology team.

The distribution of lipiodol in the postprocedural CT study correlates with the degree of tumor vascularization on pre-procedural imaging and angiography. The intense and homogeneous uptake

of lipiodol correlates with a complete response to the procedure (amputation of tumor vessels, also demonstrated by color Doppler ultrasound and contrast-enhanced CT or MRI), while partial and inhomogeneous distribution correlates with persistence of vascularized neoplasic tissue (Cioni D et al, 2000). The extent of tumor destruction after TACE is difficult to assess only by imaging studies. The rate of tumor necrosis varies in different studies from minimal destruction to 100% (Geschwind JFH et al, 2000). MRI with diffusion-weighted sequences allows non-invasive detection of areas with viable tumor cells (Geschwind JFH et al, 2000). The local recurrence rate is 18% and 30% at 1 and 3 years, respectively, mainly caused by arterial collateral supply to tumors from the neighboring arteries (Terayama N et al, 1998; Yoshida K et al, 2018). Recurrence and partial response is also explained by persistence of portal blood supply in some tumor tissues, such as well-differentiated tumor portions and tumors invading the surrounding liver through the capsule (capsular/extracapsular invasion) mainly located in the periphery of the tumor, as well as microsatellite lesions (Kuroda C et al, 1991).
TACE survival is 54% to 88% at 1 year and decreases to approximately 18 to 50% at 3 years (Terayama N et al, 1998; Geschwind JFH et al, 2000). Variations in percentages in different studies are explained by heterogeneity of study groups, especially in liver function, Okuda stage being the most useful criterion in assessing it (Ngan H et al, 1996). In addition, recurrence may also be caused by underlying chronic liver disease (cirrhosis) or portal tumor extension, with the appearance of nodules distant from the primary tumor (Ngan H et al, 1996).
Recent studies associates TACE with local ablative techniques (radiofrequency or microwave ablation) to improve survival of inoperable CHC (Sieghart W et al, 2015).

Conclusions
TACE is an effective interventional radiology procedure used for the treatment of intermediate stage HCC. Since its introduction, 40 years ago, constant advancements in technique, radiologic response evaluation and patient selection improved the therapeutic efficacy of TACE.

1.4.2.3 Endarterial treatment in HCC with arterioportal shunt

HCC frequently involves portal vein (PV) and creates arterioportal shunts (APS), worsening portal hypertension (PHT) and increasing the risk of gastrointestinal bleeding and hepatic encephalopathy.
HCC and central severe APS require complex interventional procedure, with embolization of the shunt followed by transcatheter arterial embolization of the tumor.
We reported the case of a 70-year-old woman, diagnosed with C virus - related cirrhosis 8 years before, referred to our hospital for rapid deterioration of liver function with refractory ascites and upper digestive tract bleeding. Child's classification status was B (Child-Pugh score 8). Upper gastrointestinal endoscopy revealed severe esophageal varices and emergent sclerotherapy was performed to control bleeding. Abdominal ultrasound (US) identified a hypervascular lesion in the 4th segment of the liver, and hepatofugal high velocity flow in PV trunk and branches (up to 190 cm/s) with arterial waveform (fig.1.15). No thrombus was found in PV. Massive ascites was noticed in all peritoneal spaces. Tri-phasic abdominal CT identified a low-density lesion in the 4th segment only on non-enhanced and late scan. An APS located in porta hepatis with early and strong enhancement of enlarged PV trunk at early hepatic arterial phase was seen, as well as an arterial variant, with replaced common hepatic artery (HA) originating from superior mesenteric artery (SMA).

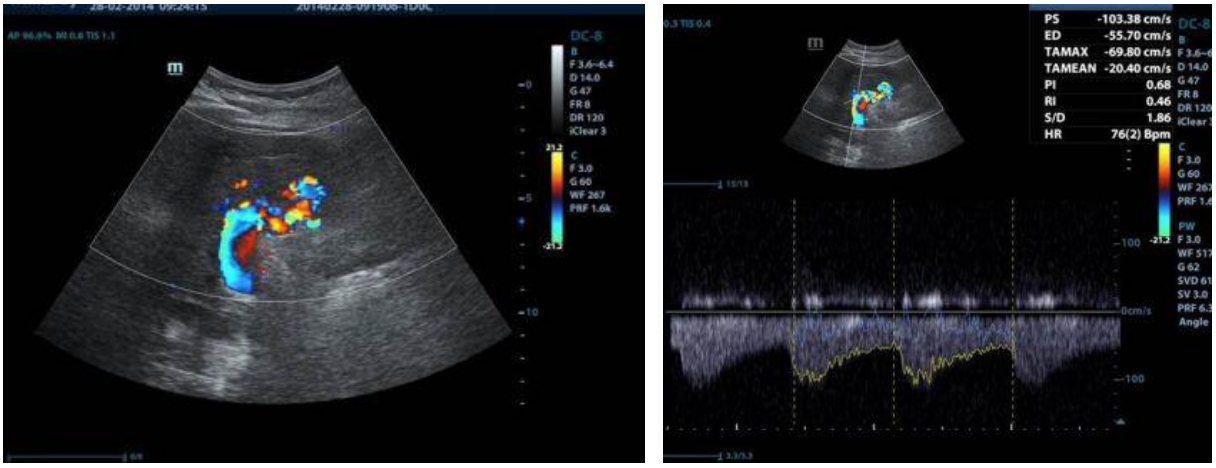

Fig 1.15 Liver Doppler ultrasound: a) mixed arterial and venous flow in PV; b) hepatofugal PV flow with high velocity arterial waveform in the portal trunk and branches .

The patient was referred to the interventional radiology unit. The common HA arteriography showed a major APS centrally located (between right HA and PV trunk with multiple feeders), but a tumor stain was not visible because of flow diversion by the shunt (fig. 1.16a). A superselective catheterization of the right HA was performed with microcatheter (3F, Renegade) followed by angiography. Due to the numerous feeders and enlarged right HA and PV, we decided to perform coils transcatheter arterial embolization (TAE) for the major APS. Three coils (Azur Pure, 4 mm in diameter, length 4 and 6 mm) were introduced into the right HA with partial occlusion of the APS (approximately 80%) (fig. 1.16b).

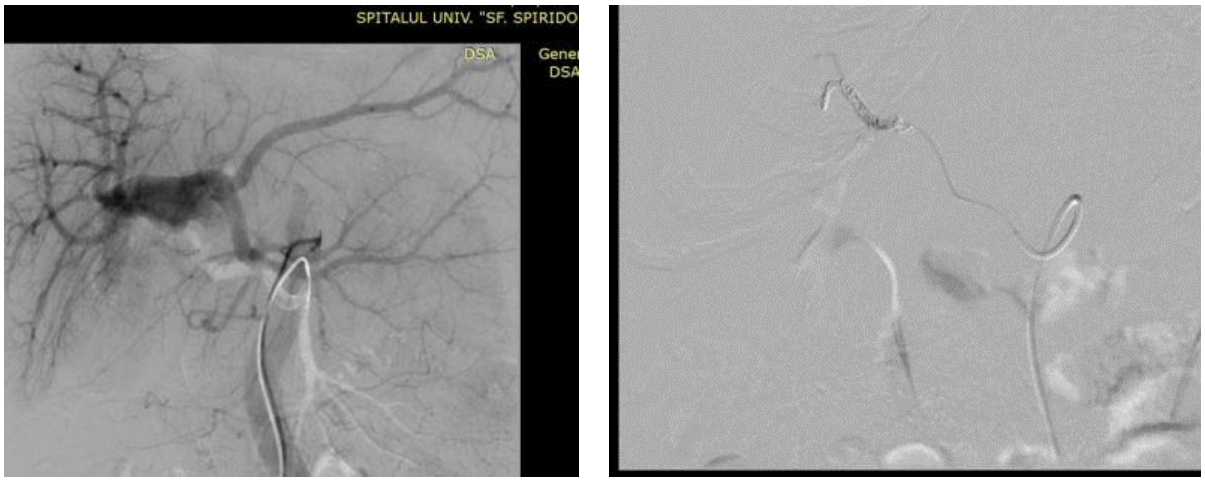

Fig. 1.16 Digital subtraction hepatic arteriography: major APS centrally located (between right HA and PV trunk with multiple feeders)

The follow-up Doppler US performed 1 week after revealed lower velocity in PV but with persistent APS. Clinical status slowly improved with diminishing rate of ascites recurrence.
Consequently, we have performed a second TAE within 3 weeks, completing the embolization with Gelfoam and occluding the shunt (fig. 1.17). The left HA arteriography showed HCC feeders, which were superselective embolized with Embosphere microspheres 300-500µm. The celiac trunk (splenic, left gastric and left phrenic arteries) was catheterized, but no tumor feeders were depicted.
After treatment, ascites and esophageal varices, as well as laboratory findings improved (table.1.VII). Doppler US revealed reduced sized PV (14 mm), without thrombosis (fig. 1.18). The patient was discharged one week after with a small amount of ascites.

Table 1.VII Laboratory data at the admission, after initial embolization and at 1 month follow-up

Laboratory data	Admission	2 days after TAE1	9 days after TAE 1	3 days after TAE. 2
Total bilirubin level mg/dL (N: 0.2-1.2)	1.50	1.08	1.02	0.96
AST IU/L (N: 5-31)	73	43	35	27
ALT IU/L (N: 5-32)	112	72	52	46
GGTP IU/L (N: 8〜59)		119	203	
WBC count /μL,	4010	5910		
RBC count × $10^{4/}$ μL	362	346	377	325
HGB level g/dL	11.3	10.7	11.7	11
hematocrit %	33.1	31.3	33.4	33
platelet count × 0^{3}/μL	90	82	132	85

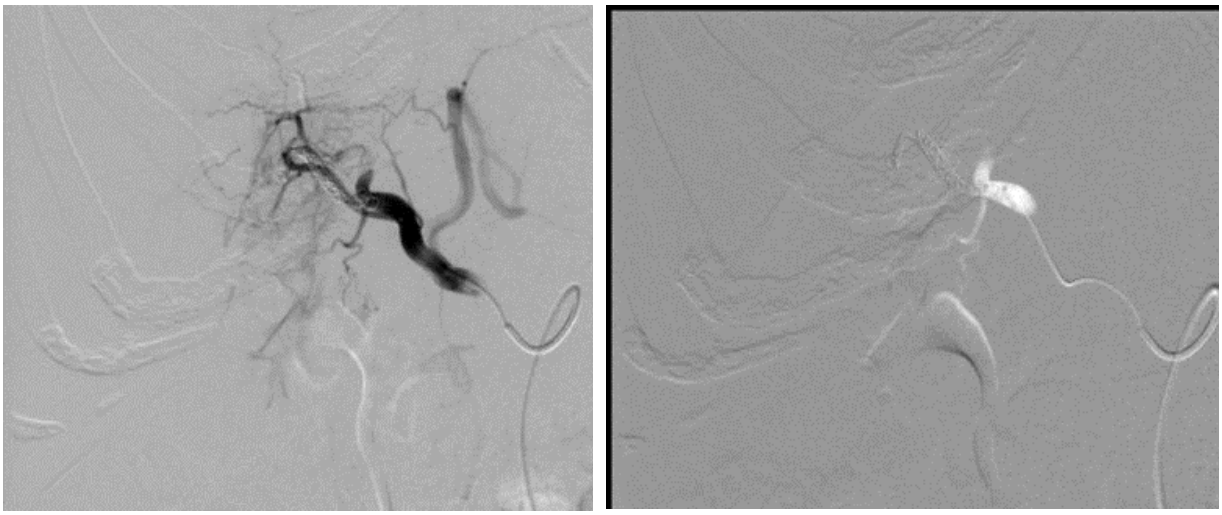

Fig 1.17 . a) Hepatic arteriography after 3 weeks: persistence of APS; b) completion of the embolization with Gelfoam and occlusion of the shunt.

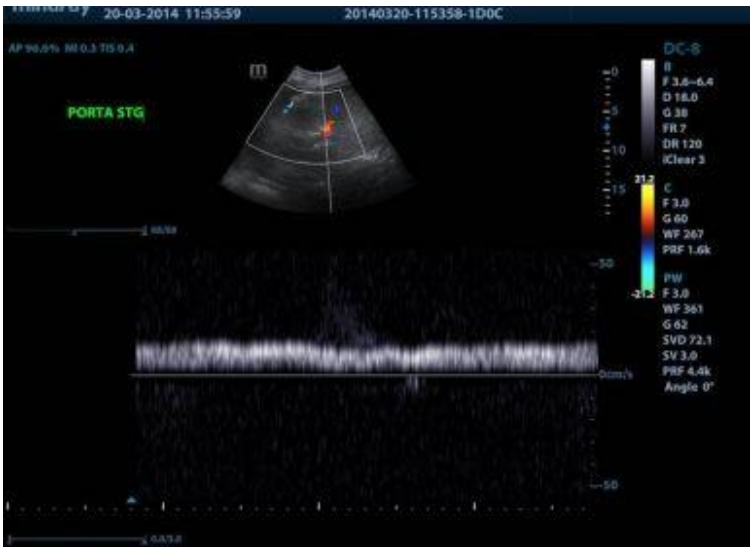

Fig. 1.18 Liver Doppler US – follow-up after embolization: reduced sized PV (14 mm), without thrombosis and normal hepatopetal flow in the left portal branch

Discussion

Several clinical and imaging classifications of APS are available (Luo MY et al, 2005). The central APS is located in porta hepatis and a severe APS consists in opacification of PV trunk and/or the first-order branches with enhancement at the early hepatic arterial phase, without or with early enhancement of HCC foci (Luo MY et al, 2005).

APS occurs in 60% of patients with HCC, marked APS of the main, right or left PV accounting for half of these patients (Ngan H et al, 1997). Lesions associated with severe APS shows no enhancement at the arterial phase in dynamic CT due to reduced arterial flow to the tumor (Luo MY et al, 2005).

TAE is the standard treatment for intermediate stage HCC, but there is no consensus about optimal treatment of HCC associated with central severe APS (1). EASL–EORTC Clinical Practice Guidelines have no reference related to the treatment of this complication of HCC, even if microscopic vascular invasion involves 20% of tumors of 2 cm in diameter and APS occurs in more than half of patients with HCC (EASL guidelines).

Moreover, HCC associated with central severe APS is a challenge for interventional radiologist since embolic material can pass through the shunt reducing the effectiveness of the treatment and producing damage of PV branches with higher risk of liver ischemia. Therefore, temporary or permanent occlusion of the supplying arteries of the APS is required before endovascular treatment of the lesion. For severe APS the procedure is also mandatory in order to ameliorate PHT (Huang MS et al, 2004; Izaki K et al, 2004; Senokuchi T et al, 2011; Hirakawa M et al, 2013).

TAE of severe APS can be achieved by several embolic materials used alone or combined: gelatin sponge, ethanol, PVA particles, N-butyl cyanoacrylate, coils (Huang MS et al, 2004; Izaki K et al, 2004; Senokuchi T et al, 2011; Hirakawa M et al, 2013). The choice of embolic agent is based on shunt size, velocity, location, angio-architecture and specific actions of each embolic agent. Coils are generally recommended only for simple APS owing to the difficulty to reach each feeder in complex shunts, but we choose them because of severity of the APS and multitude of feeders which render the selective embolization impossible.

The prognosis of HCC patients with severe APS is related to severe PHT and subsequently, to variceal bleeding, refractory ascites and portal encephalopathy (EASL guidelines). Surgical treatment is reported only for some severe resistant or recanalized APS with recurrent uncontrolled esophageal variceal hemorrhage (Ishii H et al, 2010). For centrally located APS the procedure of choice should be a major hepatectomy, unsafe in patients with poor liver function.

Conclusions

HCC with central severe APS is a challenging situation. Embolization of the shunt is the first option in order to reduce the pressure in the portal system, as well to render the endovascular treatment of the tumor more efficient and to favor patient survival.

1.2.2.3 Liver metastasis

Introduction

Liver metastases are the most common malignant liver lesions, 20 times more frequent than primitive malignant tumors (Albrecht T, 2005). The source is frequently represented by neoplasms of the digestive tract (colon, stomach, pancreas), breast, lung or kidney. But not all lesions in a neoplastic patient are necessarily secondary, autopsy studies reporting up to 25-50% benign liver lesions below 2 cm in patients with known malignancies (Albrecht T, 2005). Therefore, imaging studies of liver metastasis often implies different imaging techniques and thorough assessment of examinations, aiming: detection of focal liver lesions, morphological and functional assessment, evaluation of resectability (segmental anatomy, size and number of metastasis, relationship with vascular structures and diaphragm), assessment of vascularity,

volumetric studies of metastasis (for follow-up and assessment of treatment response) and liver remnant after surgery, guiding percutaneous or laparoscopic treatment (thermal ablation, ethanol injection, injection of monoclonal antibodies or chemotherapy with nanoparticles).
Ultrasound (transabdominal and intraoperative), CT and MRI are the methods of choice to achieve these objectives. For each method, specific intravascular contrast media injection improves the accuracy. The latest method, PET-CT, is used to identify metabolic active tumoral tissue, especially for recurrence diagnosis and for guiding biopsies and local treatments. Techniques, typical features of hypo- and hypervascular metastasis in native and postcontrast examination, sensitivity and specificity for each method are discussed, as well as their place in the diagnostic algorithm.

Methods

A. Ultrasound is used as a first intention method for detection of liver tumors, being non-invasive, efficient, and low cost.
Two US modalities are used:

a) transabdominal US, with 2-5 MHz transducer, which allows detection and morphological assessment of focal lesions: border, size, echostructure, relationship with intrahepatic vessels, as well as evaluation of underlying diffuse pathology: cirrhosis, portal hypertension. Examination in B-mode is improved, in terms of spatial and contrast resolution, by using tissue harmonics (Albrecht T, 2005: Badea R, 2004). The association of Doppler technique allows characterization of lesion vascularization and contrast-enhanced US increases the acoustic impedance of tumor vessels and allow accurate assessment of metastasis vascularization (Albrecht T, 2005: Badea R, 2004). For ultrasound the reported sensitivity in detection is 50-75%, and the specificity is 50-65%, but the use of contrast increases the sensitivity to over 90% (Albrecht T, 2005: Albrecht T,et al, 2003; Kinkel K et al, 2002).
b) intraoperative US uses 5-7.5 MHz transducer, with shapes and sizes that allow exploration in narrow spaces. It has high accuracy for detecting small lesions (from 3-5 mm), as well as for their characterization (better localization in liver segments, better assessment of the relationship with vascular structures and identification of vascular resection plan), therefore it is considered the imaging method with the greatest impact on surgical planning (Albrecht T, 2005: Sahani DV et al, 2004). Sensitivity is over 95% and specificity 98%, detecting 10-32% more metastases than CT and MRI (Albrecht T, 2005: Sahani DV et al, 2004; Bluemke DA et al, 2000).

Ultrasound detection of a focal lesion depends on size, location, echogenicity and mass effect on intrahepatic vessels and liver contour (Albrecht T, 2005). Echogenicity is highly variable: hyperechoic lesions with peripheral hypoechoic halo, hypoechoic or mixed lesions "bulls eye" (Fig.1.19 a, b). Without a strict correlation between the US aspect and the primary tumor, some aspects are more commonly associated with a particular tumor: hyperechoic metastases in colon cancer, neuroendocrine tumors, kidney cancer, choriocarcinoma; hypoechoic metastases in breast, lung, pancreatic cancer; calcified metastases in mucinous adenocarcinomas (colon, ovary, stomach, breast).
Contrast behavior is evaluated in the three phases: the arterial phase differentiates hypovascular metastases (hypoechoic) from hypervascular ones, which become intensely and homogeneously hyperechoic, while in the portal and late phases all metastases become hypoechoic compared to liver parenchyma, which remains enhanced (Albrecht T, 2005). Thus, the last two phases improve the detection of lesions below 1 cm in diameter and isoechoic lesions (Albrecht T, 2005).

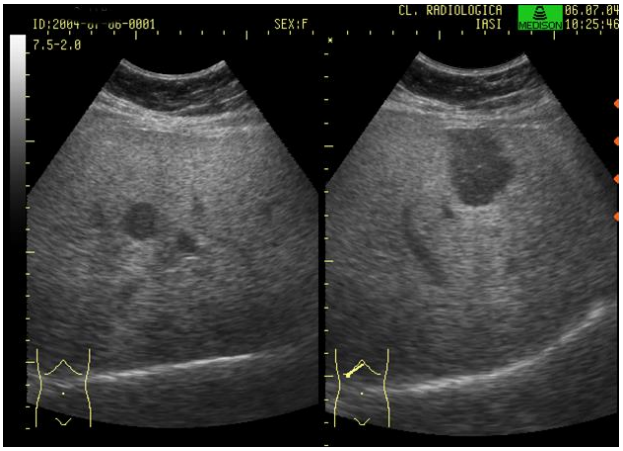

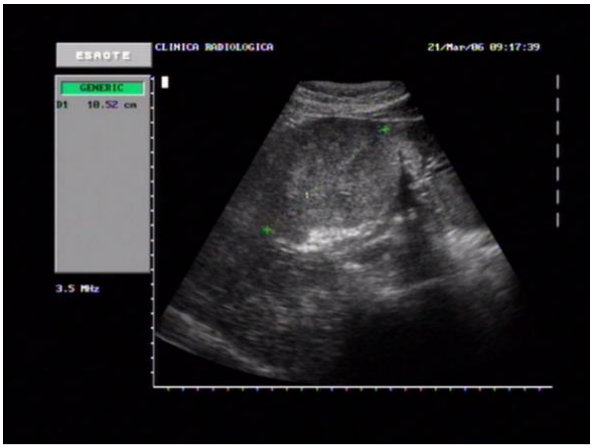

Fig. 1.19 a) Liver ultrasound: multiple hypoechoic lesions – metastases; b) isoechoic metastasis

B. CT examination

It is used for the detection and characterization of secondary lesions, being the gold-standard for pre-therapeutic staging, as well as for detection of recurrence after chemotherapy or ablation techniques. It is also the standard method for volumetry and to guide percutaneous procedures (biopsy, alation).

The protocol includes 3 mm slices, with 3-phases acquisition after intravenous injection of contrast medium to differentiate hypervascular metastases and benign lesions from malignant. The characteristic CT appearance is native hypodense nodular lesions, with variable enhancement in arterial time (homogeneous, heterogeneous or peripheral, depending on the degree of vascularization), and hypodense in portal phase (Fig. 1.20, 1.21).

The rate of detection is 75-85% compared to the results of intraoperative exploration (intraoperative US and pathological examination) (Valls C, et al, 2001; C. Kulinna et al, 2005).

False negative results are due to small size (lesion smaller than 1 cm, difficult to detect and characterize). False positive results are associated with benign liver lesions (hemangiomas, biliary adenomas, biliary hamartomas, periportal fibrosis) (Valls C et al, 2001).

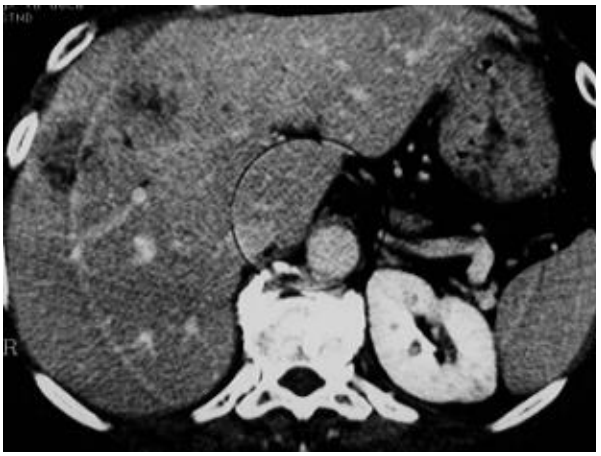

Fig. 1.20. Abdominal CT – hypodense liver metastases in the portal phase

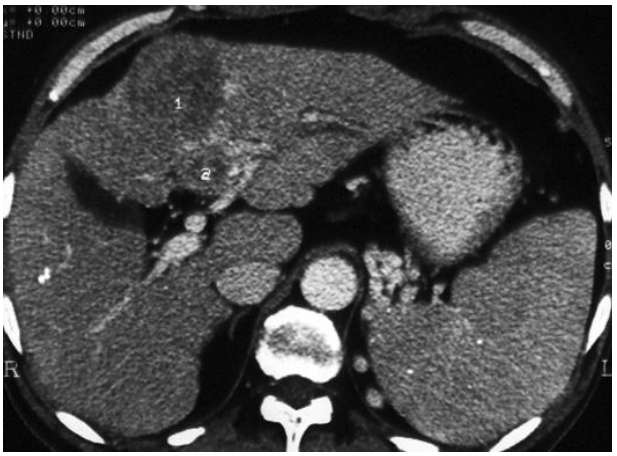

Fig. 1.21. CT of the abdomen – liver metastases: characterization of the relationship with vascular structures

C. MRI

It is considered the best method for detecting secondary lesions. The standard protocol includes native and post-contrast T1- and T2-weighted sequences (Sahani DV et al, 2004; Kulinna C et

al, 2005). T1-weighted, gradient echo (GRE) fast sequences are useful for detecting fat infiltration of the parenchyma. For T2-weighted sequences, preference is given to turbo-spin echo (TSE) (Kulinna C et al, 2005).
Liver metastases are generally slightly hypointense on T1-w images, excepting those with hemorrhage and melanin (melanoma metastases) - hyperintense. On T2-w sequences, metastases are slightly hyperintense, the signal being accentuated by edema and necrosis. Postcontrast sequences are essential in detecting and characterizing lesions. The type and dose of contrast medium, and the scanning time are decisive factors for diagnostic accuracy (Kulinna C et al, 2005). There are three types of contrast agents used in MRI:

a) extracellular contrast (gadolinium chelate), which provides information identical to that given by iodinated contrast on CT: hypervascular metastases enhance early, intensely and short-term in the arterial phase, and hypovascular enhance lately; the maximum contrast between the liver parenchyma and the lesions is reached in the portal phase;
b) contrast specific for reticuloendothelial system (superparamagnetic), also called negative contrast, which decrease the intensity of the liver parenchyma on T2-weighted sequences, therefore metastases, not having Kupffer cells, appear hyperintense on postcontrast sequences.
c) contrast specific with hepatocyte uptake and biliary excretion, which determine increased intensity of the parenchyma late postcontrast, while metastases, which do not contain hepatocytes, remain hypointense (Kulinna C et al, 2005).

MRI allows for better characterization of lesions, especially small ones, compared to CT, as well as better, but still limited, detection for infracentimeter lesions (5, 7, 9). Better characterization decreases the rate of false positives, so diagnostic accuracy increases towards 93-95% with new sequences and use of superparamagnetic contrast (Bluemke DA et al, 2000; Kinkel K et al, 2002)..
Dynamic sequences also provide functional information on tumor tissue, since tumor vascularization is a predictive factor for therapeutic response and is used to monitor this response (Laarhoven H et al, 2005).

D. PET-CT

Unlike cross-sectional imaging methods, offering mainly morphological information, PET-CT adds functional information. PET was already recognized as the most sensitive method in detecting liver metastases from digestive cancers and differentiating active lesions, and combination with CT allows better location (Kinkel K et al , 2002; Kulinna C et al, 2005; Barker DW et al, 2005).
It is used for detection and functional characterization of secondary lesions, in order to predict and assess the therapeutic response to chemotherapy, by assessing the degree of vascularization or hypoxia of the tumor tissue.
PET-CT is also useful for assessing recurrence after ablation, allowing the identification of the high metabolic activity areas within tumor, not always accurately identified by contrast-enhanced CT or MRI (Barker DW et al, 2005). This information allows biopsies or ablation techniques to be accurately guided, especially for lesions not detectable by other imaging methods (Barker DW et al, 2005; Prior JO et al, 2007).
The method has the disadvantage of the high dose of radiation.

Therefore, the radiological report in a patient with known neoplasia should include the following information regarding a liver lesion:

1. Identification and characterization of lesions

The ideal imaging method for achieving this goal should have good spatial resolution, optimal contrast between lesion and parenchyma, lesion-specific signal or density (Ward J et al, 2005).

Also, a characteristic contrast behaviour would allow better characterisation of lesion and avoids false positive results. The detection of liver metastases is essential for choosing the therapeutic option, and for reducing the rate of recurrence.
Both CT and MRI accurately meet these criteria. Information should be specified about number, location, size, relationship with the surrounding structures (vascular involvement, bile duct dilation).

2. Assessment of resectability

Precise localization in liver segments, characterization of the relationship with hepatic veins, portal vein, hepatic hilum and diaphragm are essential elements for choosing the optimal therapeutic option (liver resection vs. percutaneous or laparoscopic thermal or chemical ablation). Postcontrast CT and MRI examination and multiplanar reconstruction/ acquisitions are necessary to optimal assess these elements. Intraoperative US remains the imaging method that often influences the surgeon's decision (Sahani DV et al, 2004).

3. The volumetry, concerning two aspects:

- the volume of metastatic liver lesions, an important element that decides the optimal therapeutic method (surgery/ ablation/ chemotherapy), and useful for follow-up. The volume is estimate on cross-sectional methods (CT, MRI), either by measuring the 3 diameters or by using algorithms (Yim PJ et al, 2003; Pfeifer T et al, 1992);
- the volume of estimated remnant liver to assess the risk of liver failure (Dinant S et al, 2007).

4. Features useful for image-guided interventional techniques

- intraarterial: embolisation of hypervascularised metastases (arterial feeders: number, origin, anatomical variants);
- percutaneous biopsy: identification of the lesion easiest to approach, with minimum risk for complications.
- ultrasound or CT guided percutaneous ablation: size, relation with major vessels.

Conclusions

Imaging assessment of liver metastases is essential for selecting and planning the optimal therapeutic attitude. There is no one single optimal imaging method, therefore indications, advantages, and limits of each method should be well known by the radiologist.

1.2.3 Interventional radiology for liver beyond oncological procedures

1.2.3.1 Percutaneous treatment of hepatic hydatid cyst

Introduction

Human echinococcosis is a zoonotic infection caused by larval forms (metacestodes) of the tapeworm of the genus echinococcus found in the small intestines of carnivores. Human infection is acquired from ingestion of the parasite eggs from infected animals. Humans are only incidentally infected, Echinococcus granulosus causing cystic echinococcosis (Milicevic M, 1994). Hippocrates recognized hydatid disease 2000 years ago. The disease remains endemic in sheep raising areas of the world, including the Mediterranean region of Europe, and Romania. Dogs are the definitive hosts for E. granulosus, and sheep are the major intermediate host. The liver is the most frequent site for cystic lesions, followed by the lung, the brain, and other viscerae (Smego RA et al, 2003). Surgery is the recommended treatment for hepatic hydatid cysts, but drug therapy and percutaneous drainage have been introduced as alternative treatments. Two benzimidazoles (mebendazole and albendazole) have scolicidal activity but are clinically effective in less than 30 percent of patients with hepatic hydatidosis. Percutaneous drainage is minimally invasive and very effective in the treatment of hepatic hydatidosis.

Material. Method

The cases diagnosed with liver hydatid cyst were selected for Percutaneous Aspiration-Injection-Reaspiration Drainage (PAIR) based on their imaging features (ultrasound, CT). All cases presented well-defined cystic mass on ultrasound, with homogeneous low-density mass on CT (Fig. 1.22). Criteria of exclusion were calcification of the pericyst, overt communication with the biliary tree, or ruptured cysts. The volume of the cysts was evaluated by ultrasound. The patients were previously treated by Albendazole 800 mg/day for 22 days; the treatment was discontinued 14 days before the PAIR procedure. The PAIR procedure was performed under ultrasound guidance, after local anesthesia. A CHIBA needle of 18 Gauge was used for percutaneous transhepatic puncture of the cyst. A sample of fluid (10 mL) was sent for bacteriological and histopathological examination. The cystic fluid was drained in a close system until the ultrasound conformed the collapse of the cavity. Hypertonic serum 20 ‰ was then introduced in the cavity and left for about 20 min, followed by reaspiration of the fluid with membrane fragments (Fig. 1.23). The ultrasound followed-up the size of the cavity during the procedure.

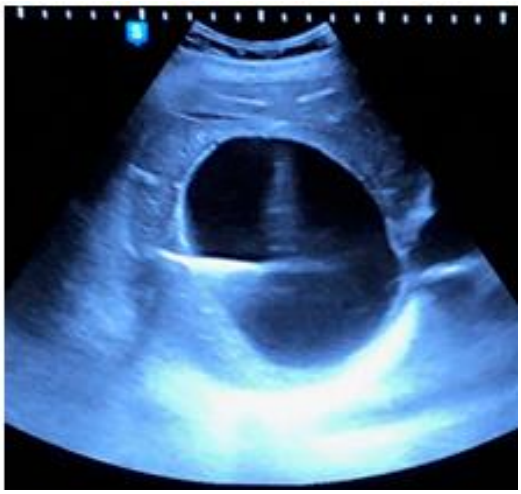

Fig. 1.22 Large cystic mass in the right lobe of the liver

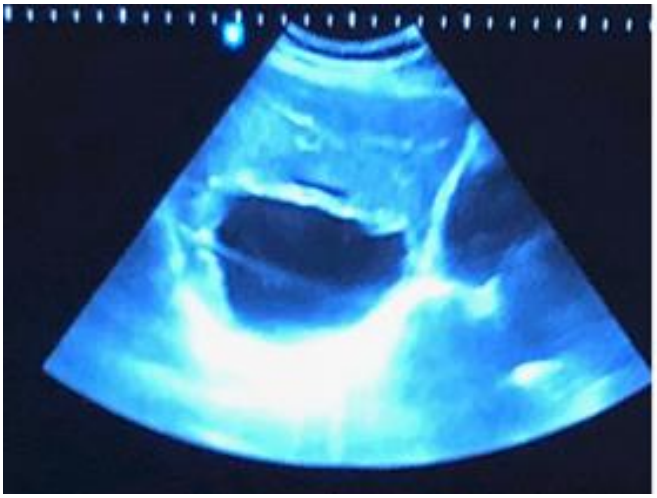

Fig. 1.23 US- after instillation of the hypertonic serum

Results

After the drainage, the remaining cavity was mainly hyperechoic, with a maximum diameter of 2 cm (Fig. 1.24). Ultrasound was used to follow-up the patient after the procedure. The Abendazole treatment was continued in a dose of 800 mg per day for 2 weeks.

There were no complications related to PAIR procedure.

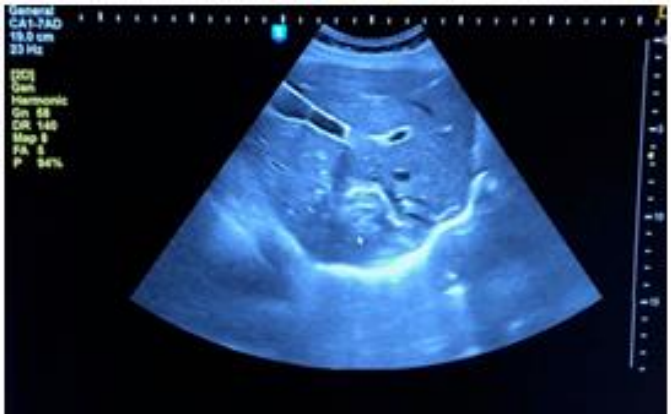

Fig. 1.24 US – the collapsed cystic lesion in the segment VII of the liver with folted membranes inside

Discussion

Percutaneous treatment of liver hydatid cysts introduced in the mid-1980s has become an attractive alternative to surgery and medical management. Percutaneous drainage is minimally invasive and very effective in the treatment of hepatic hydatidosis. The PAIR technique was proposed in 1986 by a Tunisian team (Ben Amoor N et al, 1986). Studies with patients treated by PAIR procedure and followed for up to five years have shown that the risk of anaphylaxis is negligible, and regrowth of cysts does not occur (Mohammad SK et al, 1997).
The main concern about percutaneous aspiration of liver hydatid cyst was related to the risk of leakage of cyst contents, which can lead to anaphylaxis and seeding of intraperitoneal structures. Since the advent of drug therapy effective against Echinococcus species, many health care centers advocated an approach based on pre- and postoperative chemotherapy (Albendazole or Mebendazole) combined with PAIR (WHO 2001; Eckert J, 2001; Mueller PR et al, 1985;Bret PM et al 1988; Khuroo MS et al, 1991).
The PAIR meets the goals of surgery in hydatid disease: to inactivate the cestode parasites and the germinal layer, to evacuate the cyst cavity, and to obliterate the residual cavity, but substitutes surgical removal of the germinal membrane with sclerosing. Since its introduction, despite some controversies, this technique has become widely used and its safety and efficacy have been reported in the literature (Ben Amoor N, 1986;Yaghan R et al, 2004; Giogio A et al, 1992; Khuroo MS et al, 1997; Kabaalioglu A et al, 2006). Nowadays, it is increasingly accepted as a treatment option for hydatid disease, and the World Health Organization (WHO) currently supports PAIR as an effective alternative to surgery, based on an accurate selection of cases. The indications and contraindications according to the WHO guidelines are summarized in table 1.VIII. (WHO).

Table 1.VIII The indications and contraindications of PAIR according to the WHO guidelines

Indications for PAIR	Contraindications for PAIR
- Non-echoic lesion ≥ 5 cm in diameter; • Cysts with daughter cysts, and/or with detachment of membranes; • Multiple cysts if accessible to puncture; • Infected cysts ;	Non-cooperative patients and inaccessible or risky location of the cyst in the liver; • Inactive or calcified lesion; • Cysts communicating with the biliary tree; • Cysts open into the abdominal cavity, bronchi and urinary tract;
- Patients who refuse surgery/ with contraindications for surgical treatment; - Cysts who relapse after surgery; - Patients who fail to respond to chemotherapy alone; - Children over 3 years; - Pregnant women.	

Patients should be followed clinically after PAIR treatment. Recurrence is increased in complicated cysts, including those with multiple daughter cysts. PAIR should only be performed in highly specialized centers with appropriately trained and experienced staff. In addition, an anaesthesiologist should be present for monitoring and treatment in case of anaphylactic shock. Surgeons should be notified immediately in case of complication (Yagci G et al, 2005).
The advantages of percutaneous drainage include a shorter hospital stay and a lower complication rate (Yagci G ey al, 2005). Khuroo et al (Khuroo MS et al, 1997) reported 88% disappearance of cysts with percutaneous drainage which was preceded by Albendazole therapy (10 mg/kg body

weight) for 8 weeks. He showed that the efficacy of percutaneous drainage is similar to that of standard treatment with cystectomy, in terms of reducing the size of the cyst and causing its disappearance over a period of up to two years. Combined PAIR under ultrasonography or CT guidance, with chemotherapy is as effective as open surgical drainage with fewer complications and less cost (Yorganci K et al, 2002). Yagci et al from Turkey reported a single-center experience comparing surgery, laparoscopic surgery, and percutaneous treatments in 355 patients of liver hydatid cyst over a period of 10 years and concluded that PAIR is an effective and safe option (Yagci G et al, 2005). Failure of PAIR was reported in multivesiculated cysts (Giorgio et al, Kabaalioglu et al). Theefore, our selection criteria included unilocular cysts.

Other percutaneous techniques are generally reserved for cysts that are difficult to drain or tend to relapse after PAIR (multivesiculated cysts or cysts with predominantly solid content and daughter cysts). Percutaneous evacuation (PEVAC), modified catheterization technique (MoCaT), and dilatable multifunction trocar (DMFT) are some of the devices used for aspiration of the solid content of the liver hydatid cyst, the germinal and the laminated layer. Another technique, still under evaluation, is thermal ablation by radiofrequency (RF) (Saricik B et al, 2019). Preliminary reports are rather disappointing because nearly all the treated cysts relapsed after a few months (Yorganci K et al, 2002)..

The major risks of percutaneous techniques are anaphylactic shock, spillage of cystic fluid with secondary echinococcosis, and chemical cholangitis by contact of the scolicidal agent with the biliary tree. Major complications, such as anaphylactic shock, are rare (0.1 - 0.2%). Major complications are reported to be only 0.38% and secondary echinococcosis as a result of spillage of fluid is reported to up to 1.27% in the literature available. It is unclear whether this is because of spillage-free puncture, Albendazole prophylaxis, or underreporting because of incomplete follow-up regarding length and imaging techniques used. Minor complications (urticaria, itching, hypotension, fever, infection, fistula and rupture in biliary system) range from 10 -30% (Akhan O et al, 1999). Cyst-biliary communications (biliary rupture and fistula formation) developing after PAIR and caused by cyst decompression, can usually be handled endoscopically (Smego RA et al, 2005) or, in case of inability or recurrence, by cyanoacrylate infusion (Kuran S et al, 2006). Cystography and cholangiographyby ERCP are recommended to assess any biliary communication. The overall mortality has been lowered to 0.1% in a meta-analysis (Smego RA et al, 2005). Mortality factors are associated with perioperative complications, patient's age, and infection of the remaining cyst cavity. Hospitalization period is approximately 3 days in uncomplicated cases, whereas in complicated cases it ranges from 17–20 days (Ormeci N et al, 2001).

In a recently published meta-analysis comparing surgery with PAIR in 1721 patients, the latter has been shown to have fewer major (25.1% vs 7.9%) and minor (33.0% vs 13.1%) complications and fewer recurrence rates (6.3% vs 1.6%) (Smego RA et al, 2005).

The efficacy of percutaneous treatment has also been documented in pediatric cases, because it has been proved that the long-term results of the method are in accordance with the results of adults (Goktay et al, 2005). Where indicated, percutaneous drainage is the most effective and reliable minimally invasive interventional procedure, which is associated with low mortality, morbidity, and recurrence and short hospitalization (Akhan O et al, 1999).

Conclusions

The PAIR is an effective and safe method of interventional radiology to treat large univesicular cyst in the liver, allowing a short period of hospitalization and outpatient follow up with benefits for social integration.

1.2.3.2. Percutaneous drainage of liver abscess

Introduction

Liver abscesses are rare but potentially fatal disease, consequence of a suppurative processes affecting hepatic parenchyma by different pathways. The septic process is followed by the formation of intrahepatic, single or multiple purulent collections (Krige JE et al, 2001). The pathogenic agent involved in the development of liver abscesses may be fungal, bacterial or parasitic (Huang CJ et al, 1996). The main bacterias isolated in liver abscess are Escherichia coli, Klebsiella pneumoniae, Staphylococcus aureus or Enterococcus faecalis, all associated with solitary or multiple abscesses (Webb GJ et al, 2014). The incidence is 8-16 cases per 100,000, with a death rate of 2-12 % in the developed countries (Ahmed S et al, 2016; Du ZQ et al, 2016). Different paths of bacterial dissemination were described, the ascendent route through the biliary tract or portal flow, via hepatic artery, from the surrounding organs or idiopathic causes (Yu SC et al, 2004).

The therapeutic strategies for liver abscesses are not standardized. Intravenous antibiotherapy is the gold standard but may be insufficient as a single treatment (Webb GJ et al, 2014). The efficiency of percutaneous treatment (aspiration combined or not with catheter drainage depending on abscess size) was proved in partially liquefied liver abscesses (Ahmed S et al, 2016; Du ZQ et al, 2016; Kulhari M et al, 2019). The main drawback is the slow resolution of the abscess, incomplete evacuation, and the risk of recurrence (Malik AA et al, 2010). The cut-off size for a liver abscess to be successfully drained percutaneously is between 3 and 6 cm (Singh P et al, 2019). Multiple or multiloculate abscesses are recognized complex situations, making the drainage more technical difficult, with lower chances of success, and longer time for resolution (Dariushnia SR et al, 2020). For these situations, the use of adjunct fibrinolytic agents was advocated (Dariushnia SR et al, 2020).

The Use of Mucolytic Agent in Percutaneous Drainage of Liver Abscess: A Case-Series Analysis

Material and Methods

Our department database was searched for the period 2015–2020, to identify the patients admitted with liver abscess and treated by ultrasound-guided percutaneous drainage.

From these, cases with intracavitary instillation of mucolytic agent were selected, and data regarding imaging appearance (abdominal ultrasound or computed tomography), drainage technique, inflammatory markers and clinical course were reviewed and assessed.

The initial imaging work-up was done by abdominal ultrasound and computed tomography, to determine the location, number, and size of the abscess.

After coagulation profile assessment and coagulopathy correction, an informed written consent was signed by the patient. All drainage procedures were performed in the radiology department, under ultrasound and fluoroscopically guidance and local anesthesia with lidocaine 1%. The shorter transparenchymal path to the abscess was chosen, aiming the gravity-dependent part of the collection and the avoidance of vascular structures. The percutaneous puncture was made with a Chiba needle (sized 18 to 21 Gauge) and abscess fluid was aspirated for bacteriological exam. A Seldinger technique was used to place a self-locking pigtail catheter (sized 10, 12 or 14 French; the catheter diameter was chosen by the interventional radiologist according to the viscosity and the appearance of the material resulted from the initial

needle aspiration). Once the position of the catheter was verified by injection of contrast medium, abscess fluid was aspirated.
The catheter was then secured to the skin and a 3-way stopcock was adapted to ensure the continuous external drainage in a drainage bag and catheter flushing (Fig..1.25).

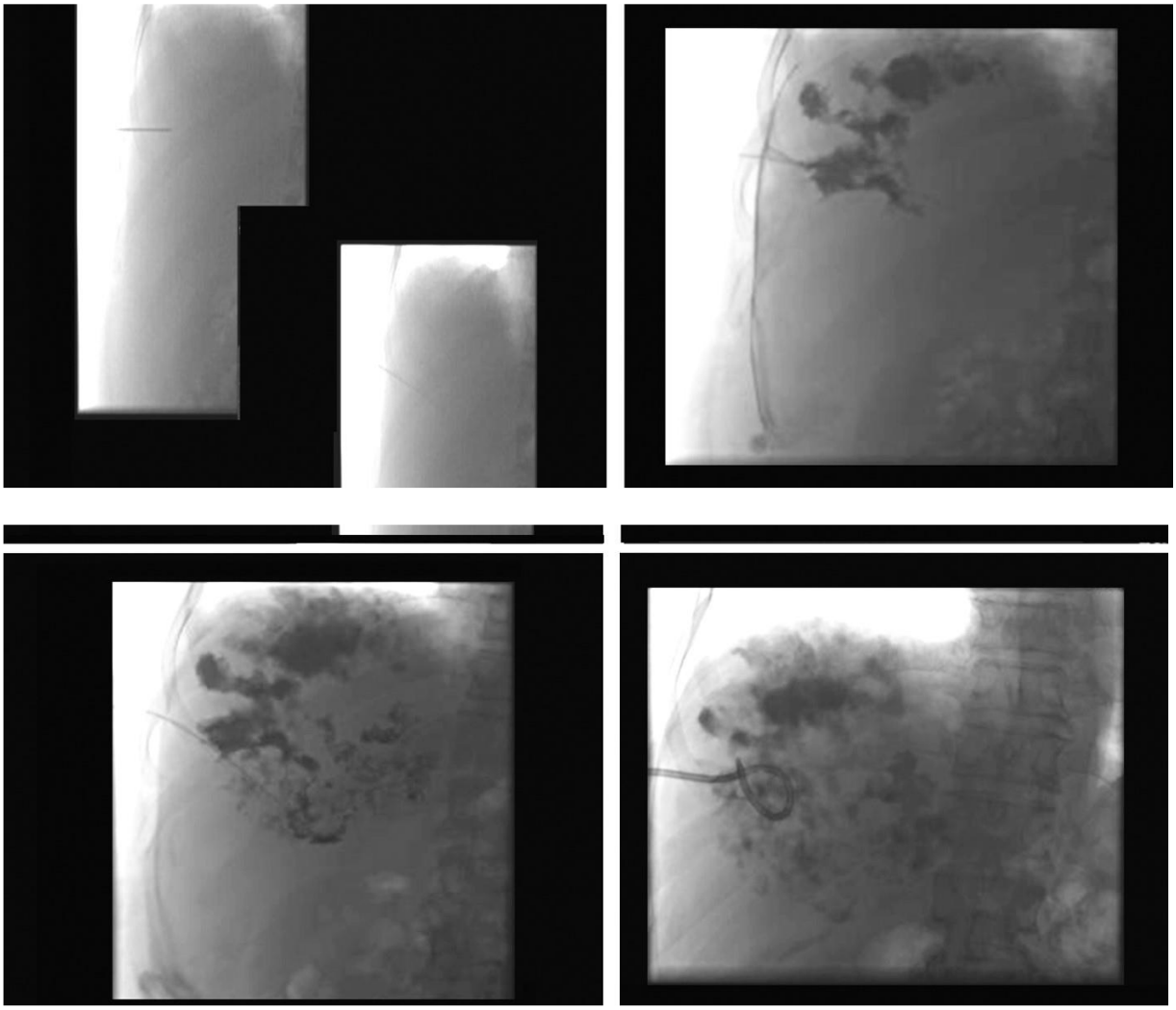

Fig 1.25 Percutaneous drainage of liver abscess by Seldinger technique

Drainage catheter was flushed every 8 hours with 5-10 mL of saline solution to ensure its patency and once a day with 10 mL acetylcysteine in dilution 1:1 with saline to increase fluidity of the abscess content. Catheter management was performed both by the interventional radiologist and the referring surgical team, with the radiologist following up periodically the position of the catheter and the size of the cavity by ultrasound. Specific antibiotherapy was administered according to bacterial or fungal sensitivity.
The effectiveness of this procedure was assessed by the amount of drainage and by the evolution of the cavity. When catheter output decreased under 10 mL per day and ultrasound confirmed resolution of the fluid collection, the catheter was removed.

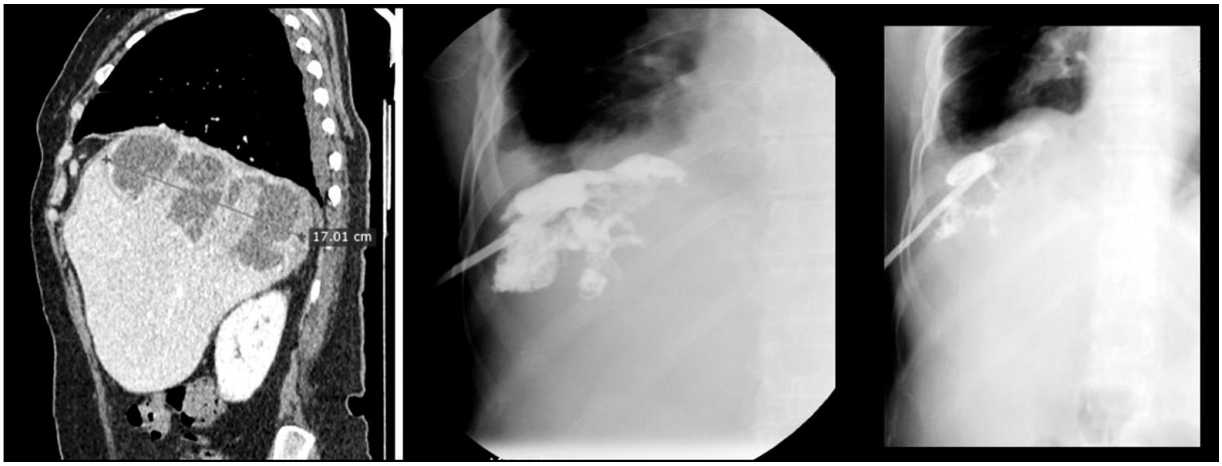

Fig. 1.26 Drainage of a multiloculate abscess – follow-up: CT before drainage – large collection in the right lobe; contrast-medium injection into the cavity 5 days and 12 days after percutaneous placement of catheter showing decreasing of the cavity and of the number of septae

Results

A total of 21 patients were treated for complex liver abscess with ultrasound-guided percutaneous drainage and intracavitary acetylcysteine between 2015 and 2021 in Surgical Clinic I-II, St. Spiridon Hospital, Iasi.

A total number of 28 lesions were diagnosed by CT in both lobes; 23 abscesses, sized 8 to 17 cm, were drained, mainly in the right lobe; 4 lesions in the left lobe and one in segment I were under 4 cm and responded to the medical treatment. The patient parameters are presented in table 1.IX.

Table 1.IX. Patient characteristics

Age	59.3±13.8
Gender, male	14 (66.6)
Coexisting diseases - Type 2 diabetes mellitus - Neoplasia (breast, colon, rectum, gastric) - Arterial hypertension - Severe anemia (HGB< 70 g/L)	 9 (42.8) 5 (23.8) 7 (33.3) 3 (14.2)
Presenting symptoms - Fever - Abdominal pain - Weakness	n (%) 19 (90.4) 15 (71.4) 7 (33.3)
Abscess size (mm)	8-17 (mean 11.6)
Abscess number Single Two Three	28 18 (85.7) 1 (7.15) 2 (7.15)
Abscess location Right lobe Left lobe	n (%) 17 (80.9) 4 (19.1)

In all cases, the fluid aspirated from the abscess was analysed in the Department of Bacteriology; fungal infection was isolated in 2 patients, and bacterial infection in 19 patients, predominantly by Klebsiella pneumoniae (8), followed by Escherichia coli (6), Staphylococcus (3), and Streptococcus (2). All patients with fever had blood specimen taken during fever followed by blood culture and in 5 patients was confirmed a positive blood culture with the same bacteria isolated from the pus.

Clinical and radiological resolution was achieved within 14 to 29 days, as a primary success in 19 cases (Fig. 1.26). Follow-up CT imaging was performed in 2 patients who were not improving their clinical status, and the residual non-drained cavity was shown. These two cases required supplementary drainage of the non-communicating residual cavity, performed in the same session with the extraction of the first catheter, day 7 and 12, respectively. Both achieved secondary success, no additional surgical treatment being necessary. There were no complications, periprocedural deaths or relapse at 3 months follow-up.

Discussion

The first description of the surgical approach of liver abscess was made in 1938, but this type of drainage was associated with high rates of mortality, 60-80% (Ochsner A, et al, 1938). The developments in antibiotic therapy, radiology techniques, and interventional radiology, with percutaneous aspiration of a sample necessary for the microbiological examination and to establish the targeted antibiotic reduced the death rates to 5-30% (Qian Y et al, 2016). Multiple or multiloculated abscesses are still considered complex situations both for surgery and interventional radiology, lowering the chances of success (Dariushnia SR et al, 2020). But the lower rate of complications and mortality of percutaneous drainage has made the surgical approach less atractive and reserved for the unaccessible positions in the right hepatic lobe, limitation of the maneuverality due to duodenal angulation or multiple abscesses (Ivanina E et al, 2012).

Image-guided percutaneous drainage of a hepatic collection is the treatment of choice for lesions larger than 4 cm, in the absence of contraindications (severe coagulopathy, severe cardiopulmonary disfunction, hemodynamic instability, lack of a safe pathway to the abscess, patient refusal of procedure (Dariushnia SR et al, 2020). A curative drainage is defined by the complete resolution of the infection, with no further need for surgery (Dariushnia SR et al, 2020).

The ultrasound guidance has many advantages, making this technique a gold standard procedure for single liver abscesses, due to clear localization of abscess and needles, real-time and direct demarcation of liver structures and the path of the needle into the cavity (Medrado BF et al, 2013). A limit of the ultrasound guidance is represented by the monomicrobial Klebsiella pneumoniae abscesses, when the lesion may appear solid and, therefore, the choice of the larger compartment to drain is difficult (Hui JY et al, 2007).

The decision of percutaneous drainage of multiloculated abscesses must be tailored by some factors, as the size, the patient comorbidity or guided accessibility. For complex multiloculated collections refractory to simple catheter drainage, the use of adjunct fibrinolytic agents may increase the rate of succes (Beland MD et al, 2008).

Our study assessed the use of a mucolytic agent in the management of percutaneous drained multiloculated liver abscesses as an accelerator for an efficient drainage. The chemical debridement of intracavitary detritus ascertained a progressive and more rapidly decrease of this type of collection, to the ultrasound and radiological control. Acetylcysteine (N-acetyl-L-cysteine) exerts an intense mucofluidizing action at the mucus and mucopurulent secretions, by depolymerization of mucoprotein complexes and nucleic acids that increase the viscosity of the aqueous and purulent component of secretions (Abdel-Daim MM et al, 2019).

Additional properties are reduction of induced hyperplasia of mucosal cells, direct antioxidant action, consisting of a nucleophilic thiol group (-SH) capable of direct interaction with electrophilic groups of oxygen free radicals (Aldini AG et al, 2018). Moreover, the molecular structure allows acetylcysteine to easily cross the cell membrane (Bhatti J et al, 2018). Acetylcysteine also exerts an indirect antioxidant effect through its role as a GSH precursor. GSH is a highly reactive, ubiquitous peptide, spread in various tissues of animals, essential for maintaining the functional capacity and morphological integrity of the cell. This is the most important intracellular defense mechanism, both exogenous and endogenous against oxygen free radicals and numerous cytotoxic substances, including paracetamol (Ahmed S et al, 2016; Amaral EP et al, 2016).

Finding techniques which can increase the rate of resorption of the abscess content and cavity, reduce the duration of the drainage and of the hospital stay represent a point of interest.

The usage of lithic substances which can lower the viscosity of the content and dislocates the intracavitary septa may extend the indications for percutaneous drainage of complex liver abscess. Our study showed that the instillation of acetylcysteine is associated with a length of drainage less than 30 days even for large complex abscesses, a rate of success of 100%, without complications and recurrences after catheter removal.

Conclusion

Percutaneous drainage is recommended by its simplicity, effectiveness, and fewer procedural-related complications in the management of complex liver abscess and association with intracavity instillation of mucolytic substances is increasing the rate of success and is accelerating the healing of liver abscesses. Further studies are required to compare the efficacy of acetylcysteine with other fibrinolytic substances in quality improvement of the drainage of the multiloculate liver abscess.

1.2.4. Interventional radiology for biliary system

Introduction

Modern management of unresectable neoplasic obstructive jaundice includes interventional radiological techniques. The main objective in these cases is the alleviation of symptoms and improvement of the quality of life, by effective drainage of bile ducts (Zerem E et al, 2022). The access to the bile ducts is either percutaneous transhepatic or endoscopic transpapillary or combined (rendez-vous technique). Under fluoroscopic guidance, external bile drainage (EBD), external-internal bile drainage (EIBD) or biliary endoprosthesis (percutaneous, endoscopic or rendezvous) can be achieved. Percutaneous Bile Drainage (PBD) is the interventional radiological technique that aims to reduce jaundice by decompression of the bile duct; the drainage catheter is introduced into dilated bile ducts percutaneously through the liver parenchyma. The first EBD was described by Kaude et al in the early 70s (Kaude JV et al, 1969), its results being confirmed by other studies [Burcharth F et al, 1976;, Hansson JA et al, 1979).. Hoevels et al (Hoevels J, et al, 1979) in Europe and Nakayama (Nakayama T et al, 1973) in Japan subsequently carried out the first internal drainage. Other authors later confirmed the usefulness of the method for bile duct decompression and developed the materials and technique (Ring EJ et al, 1978; Ferrucci JT et al, 1983; Mueller PR et al,1982). In Romania, the first transhepatic percutaneous bile drainage was performed in Iasi, at St. Spiridon Hospital (Daniil C, Stanciu C), in 1982 (Stanciu C et al, 1984; Daniil C et al, 1986).

By EIBD, the transhepatic drainage catheter is placed into the duodenum surpassing the biliary stricture; the percutaneous access is maintained and converted, if necessary, into an external drainage or later replaced with a prosthesis.

Bile duct plastic or metal endoprosthesis is placed inside the bile ducts, percutaneously, endoscopically or by rendez-vous technique. This technique was first performed in 1978 by Burchard and Pereiras, who used plastic prostheses (Burcharth F et al, 1981; Pereiras RV Jr et al, 1978). Metal prostheses were introduced by Carrasco and Wallace in 1985, when they performed the first animal tests using expandable prostheses (Carrasco CH et al, 1985). Metal prostheses have been in current clinical practice since 1989. In Romania, the first percutaneous transhepatic endoprostheses of the bile ducts were also performed in the Iasi Radiological Clinic, in 1984 (Stanciu C et al, 1984; Daniil C et al, 1986).

Percutaneous biliary drainage in malignant obstructive jaundice

The present study aimed to evaluate the value of PBD in the management of patients with neoplastic obstructive jaundice.

Material and method

The retrospective study included a group of 35 patients with neoplastic unresectable obstructive jaundice, treated by PBD in the Department of Radiology, St. Spiridon Hospital Iasi between March 2004 and March 2008. Demographic characteristics, risk factors, drainage types and patient survival were analyzed. The selection of patients was made based on the clinical-imaging diagnosis of neoplastic obstructive jaundice, and the inoperability criteria confirmed by diagnostic laparoscopy; all patients were admitted in Surgical Clinics of "St. Spiridon" Hospital. The endoscopic stenting was not considered as a first option in these cases because of difficulties of biliary cannulation (obstructions close to or above the hilum), or inaccessible papilla (duodenal stenosis caused by tumour invasion, previous gastric surgery). The interventional procedures were performed on a Philips Tele diagnost radiological equipment with angiography options, under fluoroscopic guidance and with local anesthesia. The right transhepatic percutaneous approach was preferred to avoid working position into the beam direction. For biliary drainage, hydrophilic and SuperStiff guide wires, and 8, 10 and 12 F dedicated biliary catheters were used. Percutaneous stenting was performed with Carey-Coons prostheses of 12 F, 15 cm and double pigtail of 8 F.

Results

The patients' age ranged 27-77 years, with an average of 56 years and 45% (16 patients) over 60 (Fig. 1.27), and a slight predominance of male sex (54.3%).

The etiology of obstructive jaundice and types of drainages are presented in tables 1.X and 1.XI. Three patients with percutaneous endoprosthesis had obstructive jaundice caused by lymphadenopathy (due to breast cancer, pancreatic cancer, and gastric cancer) and one by periampullary tumor (Fig. 1.28). Two endoscopic endoprostheses were placed in a distal cholangiocarcinoma with ascites, after failure of the percutaneous attempt, and in a case of gallbladder tumor with hilum and right segmental bile ducts invasion thar prevent the percutaneous drainage. Both EIBD were performed for Klatskin tumor. External drainages were performed in the remaining cases, mostly for Klatskin tumors. Patients were referred for interventional radiology after failure of curative or palliative surgery, including surgical prosthetics

The clinical and metabolic response after decompression is predictable and fairly rapid. Bilirubin levels decreased by 2-3 mg/dL in the first 24 hours. The decrease in bilirubin up to 20 mg/dL was generally achieved within 1-2 weeks, dropping to near normal levels, depending on the volume of decompressed liver as well as the presence of cytolytic syndrome.

Acute complications encountered were minimal. The pain during the procedure was reported at the entrance site or as a result of reflux of bile into the peritoneum and was classified as mild in 10 cases, average in 5 cases, and severe 1 case; one case required the intervention of an

anesthesiologist for sedation and analgesia, due to the extremely intense pain (the patient had a history of surgery for liver trauma and the passage of the materials through the liver was very difficult). Minor haemobilia was noted in 3 patients (8.5%) and resolved immediately after the procedure. Intraperitoneal hemorrhage was noted in one case (2.8%), as well as acute pancreatitis (2.8%). There was no peri-procedural mortality.

.

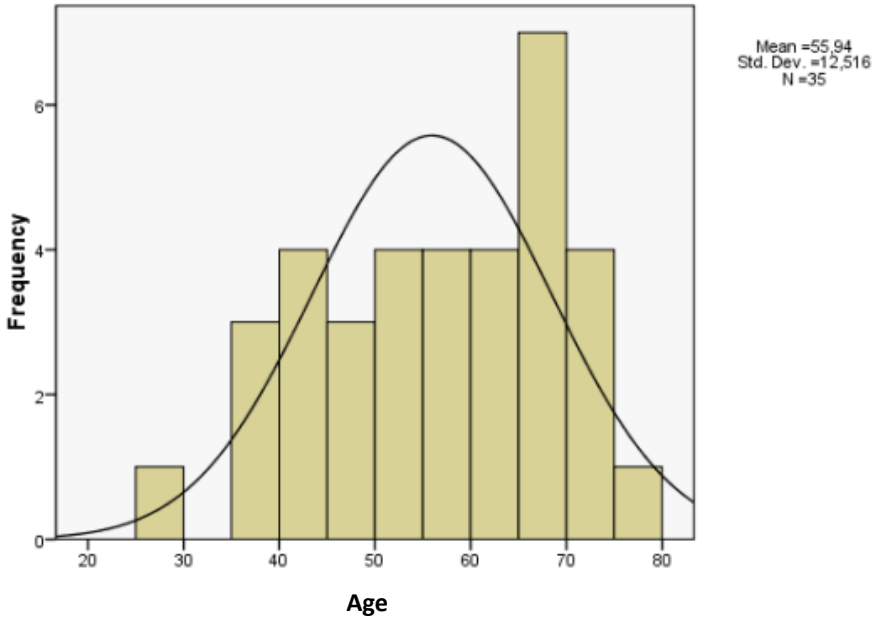

Fig. 1.27. Distribution of patients by age

Table 1.X Etiology of obstructive jaundice

Etiology of obstructive jaundice	No patients/ %
Cholangiocarcinoma extrahepatic Perihilar Distal	15 / 42.85% 13 / 37.14% 2 / 5.71%
Gallbladder carcinoma with perihilar invasion	3 / 8.57%
Local and lymph nodes recurrence of gastric cancer	10 / 28.57%
Pancreatic cancer	4 / 11.42%
Liver cancer	1 / 2.9%
Lymphadenopathy	2 / 5.71%

Table 1.XI Types of drainage procedure

Percutaneous procedure	No patients/ %
EBD - Definitive treatment - Before biliary-digestive anastomosis	27 / 77.14% 25 / 71.42% 2 / 5.71%
EIBD	2 / 5.71%
Endoprosthesis Percutaneous Rendez-vous/endoscopically	6 / 17.14% 4 / 11.42% 2 / 5.71%

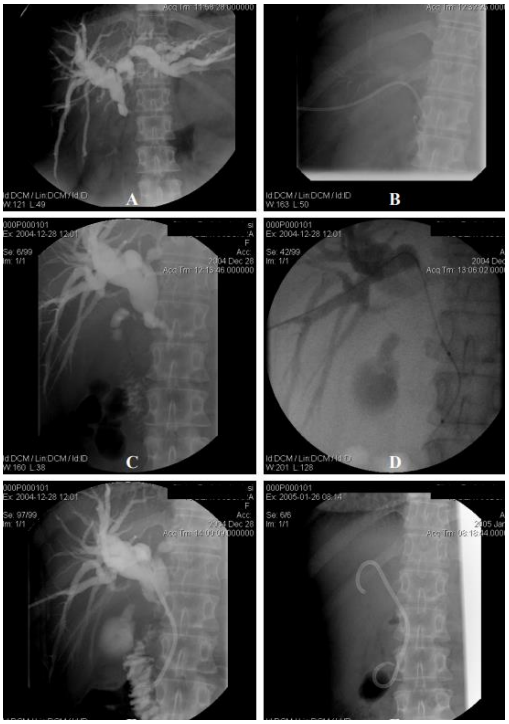

Fig. 1.28. Two-steps drainage and prosthetic placement in a perihilar obstruction. A. B. EIBD as a first step C. D. Cholangiography at 2 months shows the passage of the contrast medium into the duodenum; dilation of the stenosis is achieved; E.F. A 8 F - double "pigtail" prosthesis is advanced through stenosis, with distal end into the duodenum

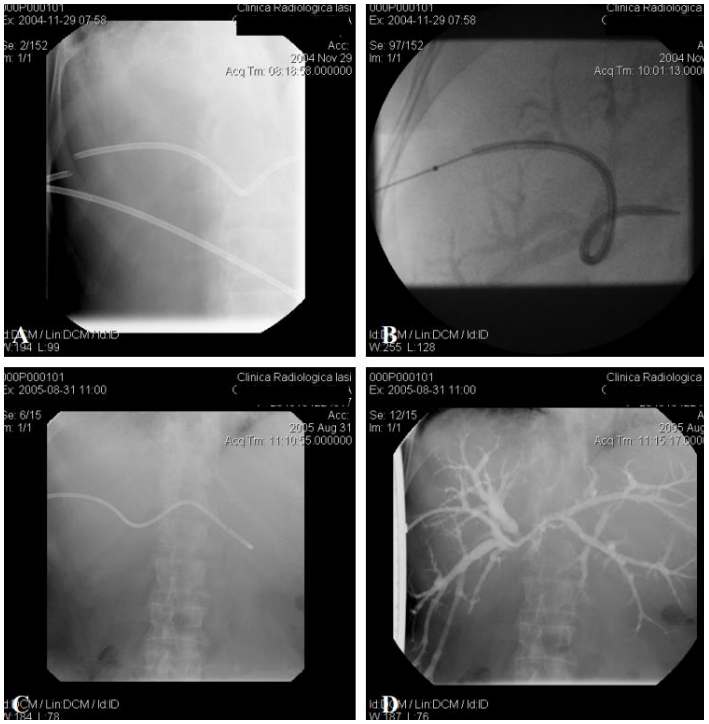

Fig 1.29.Fracture and replacement of the drainage catheter: A. Right upper quadrant X-ray: Catheter fracture. B. Extraction with a balloon catheter. C. catheter replacement; D. Cholangiography to check the position of the catheter.

Thirty-day mortality was 8.5% (no.=3), all elderly patients with advanced stages of the disease and prolonged jaundice; in these cases, jaundice remission does not improve hepato-renal function.

Late complications were mainly related to the catheter malfunction (slip or occlusion), clinically diagnosed by leakage of bile around catheter, increased bilirubin level and cholangitis. The interval of catheter patency in EBD and EIBD ranged between 3 and 6 months, therefore replacement of the catheter was required at 3-6 months. Other complications of biliary drainage were fracture of the catheter (1 case) (Fig.1.30) and slippage of the catheter, requiring reinsertion (6 cases). It should be noted that all patients with EBD reported a major discomfort, due to the permanent care of the catheter, limitations in terms of lifestyle (bathing for example), and to the necessity of compensation of hydro-electrolyte losses. If the catheter were properly cared for (i.e. periodic washing, change at regular intervals), the hydro-electrolyte losses were well-compensated and the patient managed to overcome the psychological obstacle of permanent catheter presence, spectacular survivals were be obtained related to the underlying pathology. Maximum survival in our group of EBD was 30 months, with a mean of 6 months. In all our patients, the biliary drainage lasted until the end of the patient's life.

The interval of stent patency ranged between 3 to 9 months, but 3 patients died within the first 6 months due to the progression of the disease.

Discussion

PBD is an established method used to relieve jaundice, with clinical success rates ranging between 75% and 98% in various reports (Zerem E et al, 2022). The advanced inoperable malignancies represent a group of indications with technical difficulties and poor prognosis.
The complication rate of PBD is reported to range between 7.8% and 42% (Zerem E et al, 2022). Current practice guidelines of the Society of Interventional and Cardiovascular Radiology (SCVIR) place the total of these complications at 10% (Lewis CA et al, 1996). Important acute complications occur in 5-10% of patients and are mainly represented by intra-abdominal hemorrhage, cholangitis, bile peritonitis due to bile leakage, pancreatitis, pneumothorax, liver abscesses, patient discomfort related to the catheter, and body fluid loss with electrolyte imbalance (Zerem E et al, 2022; Lammer J, 1999). Haemobilia is reported in the literature with a frequency of 3-10% (Madoff DC et al, 2002).
Late complications occur due to catheter dysfunction (slippage or occlusion) and is reported in 40-50% of patients; their rate decrease with increased catheter size (preferably 12 F), softer catheters, and the presence of the locking loop (Lammer J et al, 1999). Catheter replacement can be performed in one-day hospitalization, except in cases with severe cholangitis. The catheters placed for EBD or EIBD require periodic check-up, catheter repositioning (especially in patients with ascites due to peritoneal carcinomatosis) or replacement (periodically, every 3-6 months).
To avoid hydro-electrolyte imbalances and to eliminate the need for a drainage bag, external-internal drainage is preferred. Also, EIBD allows easier access to change the internal drainage than the endoprostheses. Endoprostheses are the best options, both for patient comfort and for the body's homeostasis. Generally, larger gauges are preferred, both for catheter drainage and for prosthesis, though there are studies demonstrating no major improvements in stent patency and life at gauges beyond 10F (Cowling MG et al, 2001). There is a general consensus that plastic stents should only have side holes at the ends (Cowling MG et al, 2001). Stent efficacy in malignant biliary obstructions is difficult to assess, because survival period of the malignant pathology is often shorter than the stent patency period. According to several studies, the average survival interval is 7-10 months, regardless of the type of stent used (Lee BH et al, 1997; Lammer J et al, 1996; Davids PH et al, 1992; Gordon RI et al, 1992; Mathieson JR et al, 1994).
Considering that our study group consisted of seriously ill patients, with advanced unresectable neoplasia, the survival time and the overall complication rates confirmed PBD is safe and effective in the management of obstructive jaundice in these cases. The 30-day mortality rate ranges in the literature between 0.9% and up to 30%, higher in patients with hepato-renal syndrome (Lammer J et al, 1999; Zerem E et al, 2022). Survival correlations could not be made according to the type of drainage due to the small group of advanced stage of disease of patients. However, survival appears to be poorer in alcohol-using patients, probably due to pre-existing liver damage (median survival 4.5 months for drinkers versus 6.5 months for others). Otherwise, survival appears to depend on disease stage and performance status at the time of presentation. For this reason, the only differences we noticed depending on the type of drainage are those in terms of quality of life.

Conclusions
PD is an effective procedure to reduce symptoms associated with jaundice, to improve liver performance and survival. The quality of life is an important factor to consider, so whenever is possible, the stents and external-internal bile drainage are preferred. However, EBD can be used as a temporary or definitive solution, with remission of symptoms but with a reduced quality of life.

1.2.5. Imaging follow-up after hepatic and biliary surgery

Introduction

Liver surgery is the primary curative option for primary malignancies of the liver and can remarkably improve overall survival. One essential condition for a good outcome is that the remaining liver can provide sufficient function (Kishi Y et al, 2009). There is no recommended standardised surveillance program for patients after curative hepatectomy for HCC. Contrast-enhanced CT or MRI are the recommended imaging for post-hepatectomy surveillance but the ideal imaging interval is unknown (Lee KF et al, 2018). Many centres employed an imaging interval of 3 months in the first 2 years and 6 months thereafter (Lee KF et al, 2018). Inadequate postoperative surveillance imaging may delay diagnosis of recurrent disease and deprive patients chance of curative retreatment. For other types of hepatic resection, the postoperative follow-up is also tailored according to the underlying pathology and type of surgery.
We focused on two specific types of hepatic surgery, for hepatic hydatid cyst and liver transplantation.

1.2.5.1. Imaging follow-up after surgery for hepatic hydatid cyst

Material. Method
The study presented the spectrum of imaging findings in the postoperative period and assessed the role of ultrasound and contrast studies in postoperative follow-up after surgical treatment for hepatic hydatid cyst. It was a retrospective study that included 69 patients with surgical treatment for hepatic hydatid cyst, 59 patients with conservative surgical procedures (puncture – inactivation - external drainage, partial perichistectomy, and filling of the remaining cavity) and 10 patients with radical ones (ideal cystectomy, atypical or anatomic liver resection). The imaging follow-up was based on abdominal ultrasound (69 cases, 1 to 5 examinations/ patient) and cavity control with contrast media (46 cases, 1 to 4 examinations/patient); CT was indicated only in complications (3 cases). Both early and late postoperative period, up to one year, were included in the study. The following aspects were assessed: cavity evolution (size, content, walls); drains position; biliary fistula; peritoneal or pleural fluid effusion; wound healing; hydatid disease relapse.

Results
Cavity evolution was favorable for 52 patients. Four patterns of evolution were identified:

a) the closure of the cavity, with minor structural disorder (hypoecoic, inhomogeneous scar) at the level of the former cavity; this ultrasound aspect was highlighted in 29 cases, of which 22 required a single ultrasound examination in the postoperative period (fig.1.30);
b) progressive reduction in size of the cavity is the ultrasound aspect highlighted in 23 cases (fig.1.31); in 18 cases, the reduction was obvious and significant since the first ultrasound examination, with no further examinations necessary, and in the other cases, the reduction was followed-up by successive examinations (2 examinations in 5 cases, 3 examinations in 2 cases and 4 examinations, respectively, 5 examinations in one case);
c) a stability of the cavity size was revealed in 7 cases;
d) initial increase in cavity dimensions was certified in 10 cases, examined by ultrasound up to 5 times during the longer hospital stay.

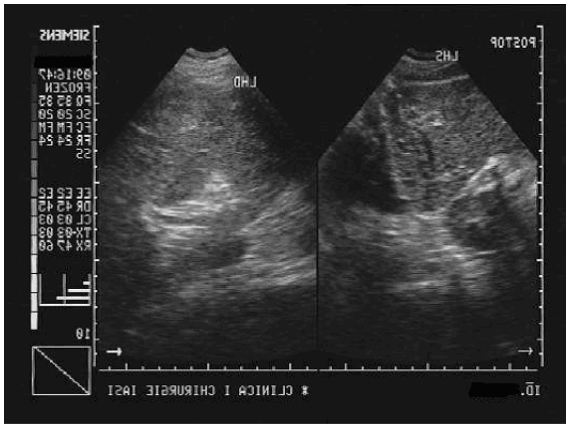

Fig. 1.30 Postoperative US follow-up: closure of the cavity

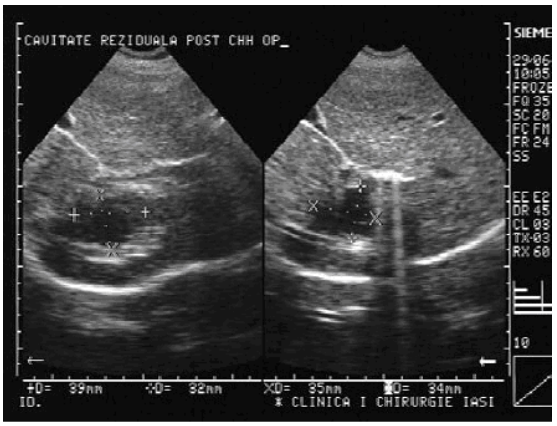

Fig.1.31 US: cavity shrinkage

For the last 2 categories, the following complications were associated: infected cyst cavity in 8 cases (with thick internal septa and fluid-fluid level at ultrasound) (fig.1.32), eccentrically placed drains (8 cases), biliary fistula (14 cases, all after conservative interventions; contrast injection by drains into the cavity shows the simultaneously opacification of the bile ducts) (fig.1.33). Pleural effusion was also associated in 7 cases. Although the unfavorable evolution of the dimensions and the inhomogeneous content of the cavity are elements of semiology suggestive for cavity superinfection, they are not specific to this complication. The inhomogeneous opacification of the cavity was also revealed in multivesicular cysts or in retention of hydatid material (fig. 1.34).

The late complication noted in our group was the hydatid disease relapse (2 cases).

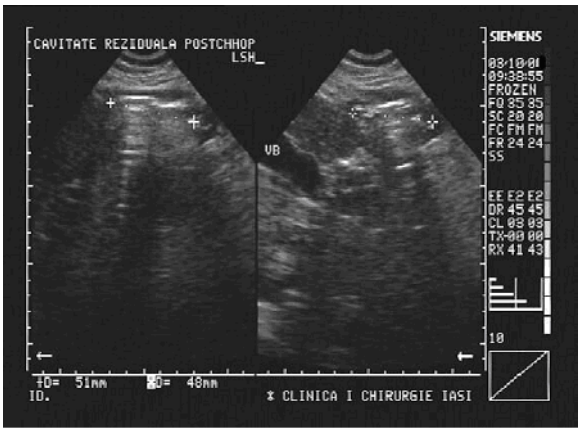

Fig. 1.32 Postoperative US : non-homogeneous cavity suggesting infection

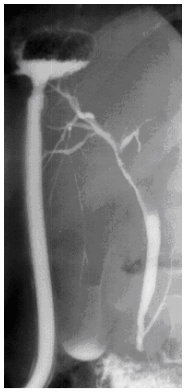

Fig 1.33 Contrast injection into the cavity through the drainage tube with simultaneous opacification of the biliary tree – biliary fistula

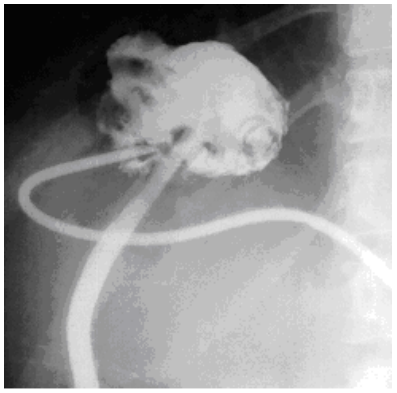

Fig. 1.34 Non-homogeneous cavity content in hydatid material retention

Discussion

Conservative treatment was the most common choice due to the multiplicity and location of cysts. This type of treatment requires longer postoperative monitoring compared to radical procedures (Chautems R et al, 2003). The postoperative imaging follow-up frequently included ultrasound and contrast studies, CT being necessary especially in case of recurrence, and endoscopic retrograde cholangiography being reserved for cases with biliary fistula. The most common postoperative complications are pleural effusion, parietal infections, biliary fistulas or perihepatic transient collections, complications that frequently resolve under conservative treatment or drainage.

Both methods (abdominal ultrasound and contrast studies) aimed primarily at assessing the dimensions of the remaining cavity. The contrast study of the postoperative cavity assessed more accurately the size of the cavity than ultrasound. The evolution of cavity size correlated significantly on the study group with the postoperative evolution: stationary aspect, cavity growth or fluctuating evolution were suggestive of unfavorable evolution, the frequency of postoperative complications in this group being significantly higher than in the group of patients with cavity closure. Therefore, when we appreciate the aspect of the postoperative cavity, the constant evolution towards reducing and closing is significant for a favorable postoperative evolution, while the stationary, variable or progressive dimensions are elements suggestive for complicated postoperative evolution. Although the unfavorable evolution of the size and the inhomogeneous content of the cavity are suggestive of superinfection of the cavity, they are not specific to this complication. The inhomogeneous opacification of the cavity was also evident in the case of multivesicular cyst or in the case of hydatid material retention. Conversely, for the evaluation of the remaining liver parenchyma, the size of the bile ducts, the peritoneal cavity and the other abdominal viscera ultrasound is a reliable method, being useful in the diagnosis of most postoperative complications. Biliary fistulas are the most common complication of CHH interventions, being described in 10-27% of cases (Moreno Gonzale E et al, 1991; Krug et al, 1997). The ultrasound reveals only non-specific elements (minimal dilation of the bile ducts, persistence of the postoperative cavity), but the contrast examination of the cavity directly reveals communication with the bile ducts.

The rate of recuherence varies from 0 to 12%, being determined by hydatid vesicle retention, peritoneal or retroperitoneal dissemination

Conclusions: Ultrasound and contrast studies are necessary to follow-up the patients with operated hepatic hydatid disease, both to certify the normal evolution and to identify the complications.

1.2.5.2. Imaging follow-up after liver transplantation

Liver transplantation (LT) has become even in Romania the treatment of choice for end-stage liver disease (irreversible hepatic failure, liver cancer). More than 27.000 procedures are performed annually over the world, with more than 7.000 LT yearly in Europe. The history of LT in Romania began at Fundeni Institute, Bucharest (Prof. Irinel Popescu) in April 2000 with the first successful LT, followed in the same year by live-donor LT (child), and by domino and split-liver transplantation (adult and child; 2001), live-donor LT (adult; 2003), adult and adult split liver transplantation (2011) and dual graft life-donor LT (2012). Since 2016, a second center of LT in Romania was opened in Iasi, as a territorial center meant to use harvested organs mainly from Moldavia. Forty-five whole graft LT (all from cerebral death donors) were performed during this period in Iasi.

Indications for LT are well established and include viral C and B hepatitis, alcoholic liver disease, idiopathic/autoimmune liver disease, primary biliary cirrhosis, primary sclerosing cholangitis, acute liver failure, metabolic liver disease (eg, inborn errors of metabolism), hepatocellular carcinoma, neuroendocrine tumor metastases.
Contraindications to LT are represented by active extrahepatic malignancy, hepatic malignancy with macrovascular or diffuse tumor invasion, active and uncontrolled infection outside of the hepatobiliary system, active substance or alcohol abuse, severe cardiopulmonary or other comorbid conditions, psychosocial factors that would likely preclude recovery after transplantation.
Imaging assessment is crucial both for donor and recipient evaluation.

Early Spontaneous Graft Intra- and Perihepatic Hematoma after Liver Transplantation

Introduction
Liver allograft hematoma after OLT, although rare, is a serious underreported condition, requiring prompt management to avoid any devastating consequence (Massarolo PC et al, 2004; Kim DS et al, 2006; Kasahara M et al, 2004). Asymptomatic bleeding can be detected onimaging follow-up, whereas significant bleeding may lead to shock, expanding hematoma, hepatic rupture (Gorok D et al, 2008; Hong SS et al, 2009), graft loss with need of retransplantation or even death (Kasahara M). Early spontaneous liver graft hematoma is uncommon and the association between intra- and exprahepatic hematoma may even worsen the postoperative course after transplantation.

Case Report
A 62-year-old caucazian male with a past history of decompensated cirrhosis due to alcohol abuse (MELD 18), with negative viral, autoimmune serologies and metabolic marquers , had been listed for transplantation and he was transplanted within 6 moths. He received a full-sized liver allograft from a female donor after brain death occured as a consequence of a cerebrovascular accident. The donor had no significant past medical history. The surgical procedure was uneventful, the hepatectomy to the recipient being performed without the use of the veno-venous bypass. A large cavo-cavostomy was tailored by triangulation to secure adequate outflow to the graft. Portal, arterial and biliary reconstructions were undertaken according to the standard techniques, respectively. Intraoperative Doppler ultrasound evaluation of the vascular anastomoses confirmed normal inflow, outflow and resistivity index. Immunosuppression was initiated intraoperatively with methylprednisolone 1g and simulect (basiliximab) 20 mg and continued with tacrolimus and mycophenolic acid (MMF) afterwards. Valgancyclovir was used for prevention of viral infection in the day 2 postoperatively.
Patient initial recovery was marked by a moderate anemia and persistent thrombocytopenia Despite, anticoagulation therapy with enoxaparine (Clexane) 0,4 ml/24 h was carried on throughout the hospital stay. In the 7-th postoperative day patient's hemoglobin level dropped to 7,7 mg/dl, serum C-reactive protein rose to 25 mg/dl, and total bilirubin to 4,95 mg/dl.
The abdominal MDCT disclosed bilateral moderate pleural effusion, normal vascular anastomotic flow, a subcapsular liniar laceration 6/37 mm (thickness/caudal extension) in the segment VII of the allograft, paracaval and subhepatic hematoma 58/61/65 mm (AP/T/CC) with active bleeding but without overt arterial feeder (Fig. 1.35). White blood cell, platelet count, prothrombin time, hepato-renal function and patient's hemodynamic were stable. The patient was treated conservatively with analgesia, intravenous antibiotics and fluids, red cell blood (RCB) (2 units) and human albumin. He remained stable (including abdominal ultrasound findings) until the 18-th postoperative day when he presented an episode of acute diarrhoea, followed by another

decline in the hemoglobin levelto 6,6 mg/dl and Ht to 19 %. The test for Clostridium difficile toxins A and B in stools was positive.

Abdominal Doppler ultrasound examination showed a huge intrahepatic hematoma, 11 cm in diameter, ill defined, located in the right hemiliver, with moderate compression over the right segmental portal branches and right hepatic vein, associated with perihepatic hematoma (pre-hepatic, right subphrenic and posterior paracaval) and right flank hematoma. A significant amount of free intraabdominal fluid was also noted. The peritoneal drain inserted under ultrasound guidance in the lower right quadrant removed hemorrhagic ascites. Bacteriologic test of the ascites identified enteroccocus faecalis and pseudomonas aeruginosa requiring specific systemic antibiotherapy.

Thoracoabdominal MDCT showed moderate right pleural effusion with passive collaps of the lower right lobe, non-homogeneous structure of the right hemiliver with hematic densities associated to a subphrenic hematoma with hematic level (consistent with a recent bleeding), 10/6/10 cm (AP/T/CC) in diameter, 8/10 cm right flank hematoma fused to the previous reported paracaval hematoma, and a prehepatic collection with fluid density, 4 cm in thickness. No active bleeding was noticed (Fig. 1.36). Vascular anastomosis of the graft as well as their intrahepatic branches were patent. The patient presented respiratory distress, increased abdominal pressure with tenderness and right lower limb oedema without thrombosis. Laboratory tests revealed sudden increase in liver enzymes (up to 5000 UI/dl) raising the issue of hepatic necrosis and surgical revision. However, the hemodynamic stability, the patency of the graft inflow and outflow, absence of intrahepatic vascular flattening, normal coagulation tests, rapid improval of the hepatic function, allowed a conservative treatment combined with ultrasound-guided drainages of the right pleural cavity to evacuate the hemorrhagic efusion and of the prehepatic collection (with very thin, central enous catheter), due to the loculated appearence on US, in order to rule out a secondary infection and to decrease the compression on the hepatic parenchyma.

Intermitent pleural and peritoneal drainage were maintained for the next three weeks. Patient condition slowly improved.

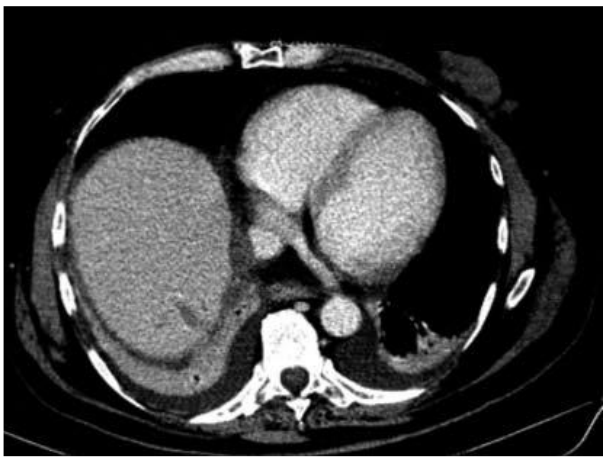

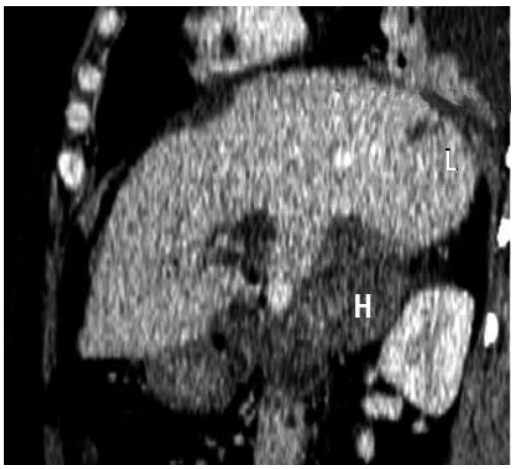

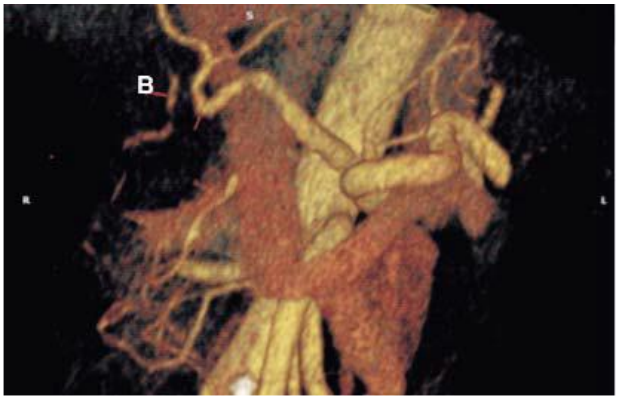

Fig. 1.35 MDCT - 7th postoperative day after liver transplantation: thin subcapsular laceration in the segment VII of the liver graft (L) is not related to the arterial anastomosis nor to the pancreatico-duodenal vessels (d)

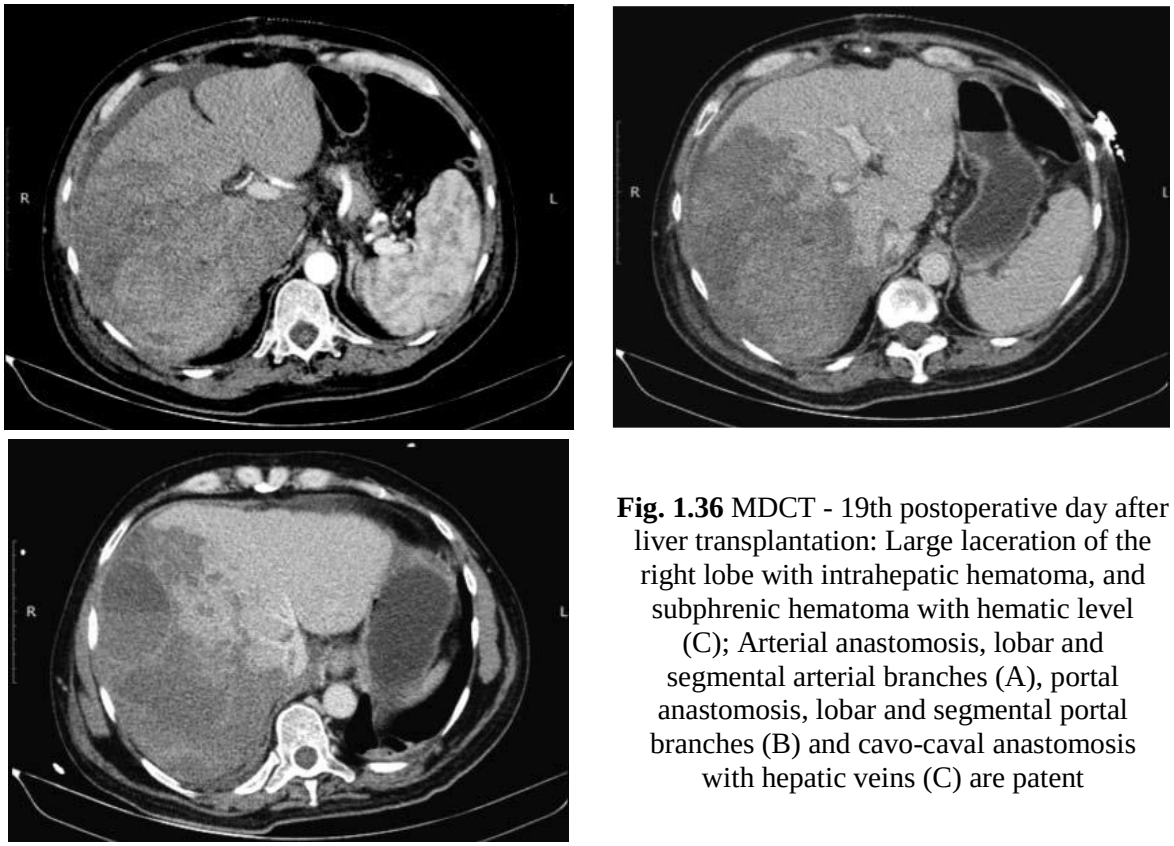

Fig. 1.36 MDCT - 19th postoperative day after liver transplantation: Large laceration of the right lobe with intrahepatic hematoma, and subphrenic hematoma with hematic level (C); Arterial anastomosis, lobar and segmental arterial branches (A), portal anastomosis, lobar and segmental portal branches (B) and cavo-caval anastomosis with hepatic veins (C) are patent

Close imaging follow-up (daily Doppler US) revealed progressive left hemiliver hypertrophy with slow resorbtion of the right intraparenchimal and perihepatic hematomas, also confirmed by MDCT examination performed after 2 weeks (Fig. 3). He was discharged on the 50-th postoperative day with good clinical and metabolic status. Six months after LT the patient has normal clinical, metabolic and imaging findings.

Discussion

Hematoma of the liver allograft is scarcely reported in the literature, but is a serious complication of liver transplantation (Massarolo PC et al, 2004; Kim DS et al, 2006; Kasahara M et al, 2004; Gorok D et al, 2008). It may present as intrahepatic, subcapsular or both and may develop spontaneously or subsequently to parenchimal injuries, either intraoperative (parenchimal laceration by compression) (Hong SS et al, 2009; Shin CH et al, 2017) or after percutaneous transhepatic invasive procedures, such as endoscopic retrograde cholangiopancreatography (Cardenas A et al, 2008) or liver biopsy (Nissen NN et al, 2010). Likewise, it may occur either

after full-sized or partial-liver graft transplantation (Massarolo PC et al, 2004; Kim DS et al, 2006; Kasahara M et al, 2004; Gorok D et al, 2008). Whether this rare phenomenon is more likely to occur after either whole or live donor liver transplantation remains unknown. The liver graft may be more sensitive to microtrauma and to blood flow compromise than a native liver as a consequence of loss of vascular autoregulation and of collateral flow (Nissen NN et al, 2010). Therefore, the liver graft must be handled with special care to prevent potential mechanical injuries, either during organ procurement or transplantation procedure (Hong SS et al, 2009; Shin CH et al, 2017).

This case described a large spontaneous intra- and perihepatic hematoma of a liver allograft occured in the early course after LT. The US and MDCT initially described a paracaval and subphrenic hematoma with active bleding but with no overt arterial feeder, which rendered the selective transarterial embolisation useless. Likewise, a subcapsular linear laceration in the segment VII of the allograft was described which was likely to result in the huge intra- and extrahepatic hematomas subsequently. As far as we didn't recognise any graft intraoperative damage, we should consider it a spontaneous occurence.

Another plausible contributing factor might be the presence of the low platelet count during the perioperative period. The patient was in significant respiratory and abdominal distress, however the vital functions were stable. Major intraparenchimal and perihepatic hematomas with sudden highly elevated liver enzymes (AST), even non specific, would have been consistent for liver cell necrosis and acute liver damage. Moreover, lack of traumatic element and of the active bleeding on the follow-up CT scan, would suggest rather necrosis than expanding hematoma. This was in fact the main diagnostic and therapeutic dilemma along with the balance between hemorrhage and risk of thrombosis, increased in septic conditions, our patient having ongoing anticoagulation therapy throughout the hospital stay. Hepatic capsule has been certainly damaged in the affected area whereas several large perihepatic hematomas have occured. However, an intact capsule would led to an increased intrahepatic pressure by the expanding hematoma, resulting in hepatic vascular compromise and hepatic necrosis. In our reported case, it is likely that perihepatic large hematomas behaved like a „perihepatic packing" with compressive effect on the liver but without vascular intrahepatic compromise or thrombosis. Minimal ultrasound-guided drainage was undertaken to reduce pressure and to exclude the infection of the hematoma. On the contrary, the „liver compartment syndrome" (Nissen NN) leads to acute hepatic failure, usually requiring retransplantation.

Conclusions

This was, to our knowledge, the first reported case of early spontaneous huge intra-and perihepatic hematoma, after OLT. Timely diagnosis, close clinical and imaging follow-up and suitable management including vital function support, antibiotics, percutaneous US -guided drainage can successfully salvage the patient and the liver allograft. Our emphasis is that patients who develop even massive intraparenchymal and perihepatic hematomas in the early course post OLT can be treated nonsurgically provided they are hemodinamically stable, they have patent graft inflow and outflow, no compression over the hepatic vasculature and stable hepato-renal function.

Chapter 2.
PRE- AND POSTOPERATIVE IMAGING DIAGNOSIS IN SURGICAL DISEASES OF THE PANCREAS

2.1. CONTEXT AND RATIONALE OF THE RESEARCH TOPIC

This second theme of research emerged naturally since hepato-biliary and pancreatic pathology are intricated. Moreover, diagnostic of pancreatic diseases is often challenging and requires combination of several imaging methods. CT and MR provide an excellent spatial resolution of the pancreatic anatomy and are the modalities of choice when considering the pancreas.
Pancreatic cancer is the fourth leading cause of cancer-related deaths in the United States and Europe (Malvezzi M et al, 2018). Surgical resection is considered to be the only potentially curative treatment for pancreatic cancer, but the majority of pancreatic cancer patients are diagnosed in locally advanced or metastatic status, therefore careful imaging interpretation is required to select the only 15% to 20% of pancreatic cancer patients who are candidates for surgical resection (ressectable and borderline resectable). These two categories are defined by anatomical, biological and clinical elements, and imaging is crucial for anatomic assessment. The role of imaging has been evolving in line with the development of pancreatic cancer treatment, and imaging plays a crucial role in the screening, diagnosis, preoperative staging, postoperative surveillance, and treatment response evaluation of pancreatic cancer. The postoperative imaging after pancreatic surgery is also a captivating subject, due to continuous evolution of surgical techniques, to their complexity, but also to the great variety of postoperative complications and to their severity, with major impact on survival. All these reasons prompt for an accurate and rapid postoperative imaging diagnosis to improve the management of complications.
The research continued the collaboration with surgical team from our tertiary center for hepato-biliar and pancreatic surgery, begun during my PhD training. During the last years, the radiologist proved to be a valuable member of the multidisciplinary team managing pancreatic diseases, both in the preoperative and the postoperative period.

2.2. SCIENTIFIC ACHIEVEMENT IN THE FIELD OF RESEARCH

Below is presented the research carried out in this field and the results published in original articles to which I contributed as main author or co-author.
I have divided the research I have conducted on pancreatic imaging in three main subdivisions:

1. **Staging of pancreatic tumors and diagnosis of vascular involvement/variant**s
2. **Postoperative imaging and its implications in management of the complications**;
3. **Rare lesions of the pancreas**.

2.2.1 Staging of pancreatic tumors and diagnosis of vascular involvement/ anatomical variants

Articles

1. Lupascu C, Trofin A, Zabara M, Vornicu A, Cadar R, Vlad N, Apopei O, Grigorean V, **Lupascu-Ursulescu C**. Emergency Backwards Whipple for Bleeding: Formidable and Definitive Surgery. Gastroenterol Res Pract. 2017;2017:2036951. doi: 10.1155/2017/2036951 (IF 2017 – 1,859)

2. Trofin AM, Vlad N, Zabara M, Rusu-Andriesi D, Bradea C, Vornicu A, Cadar R, Târcoveanu E, **Lupascu-Ursulescu C**, Lupascu CD. Pancreaticoduodenectomy in patients with hepatic artery, anatomic variants: tailoring, perioperative care and surgical outcomes. Rev.Med. Chir. Soc.Med.Nat. 2016; 120 (4):874-879
3. Lupașcu C, Andronic D, Grigorean VT, **Ursulescu C**. Mesopancreas first dissection during pancreaticoduodenal resection; selective approach or paradigm? Hepato-Gastroenterology 2014; 61(130): 463-468
4. Georgescu S, **Ursulescu C,** Grigorean VT, Lupascu C. Hind right approach pancreaticoduodenectomy: From skill to indications. Gastroenterology Research and Practice. Volume 2014 (2014), Article ID 210835, 8 pages ISSN 1687-6121 (factor de impact 2014– 1,502)
5. Lupașcu C, **Ursulescu C,** Dănilă N, Grigorean V, Târcoveanu E, Andronic D. Early retroportal lamina dissection during pancreaticoduodenectomy resection: how, when and why? Rev Med Chir Soc Med Nat Iasi 2013; 117 (1): 137-143
6. Lupașcu C, **Ursulescu C,** Andronic D. Emergency pancreaticoduodenectomy for bleeding pancreatic pseudoaneurysm in patient with common mesentery and replaced right hepatic artery. Chirurgia (Bucur). 2013;108(6): 907-911
7. Lupaşcu C, Moldovanu R, Andronic D, **Ursulescu C**, Vasiluţă C, Răileanu G, Fotea V, Târcoveanu E. Posterior approach pancreaticoduodenectomy: best option for hepatic artery anatomical variants. Hepatogastroenterology. 2011; 58 (112):2112-4
8. Lupașcu C, Andronic D, **Ursulescu C**, Vasiluta C, Vlad N. Technical tailoring of pancreaticoduodenectomy in patients with hepatic artery anatomic variants. Hepatobiliary Pancreat Dis Int. 2011;10(6):638-43 ISSN 1499-3872

Introduction

The continuous development of imaging techniques (CT equipment with large number of detectors, allowing the reconstruction of very fine sections, but also fast and three-dimensional MRI sequences), has allowed the permanent and dynamic amplification of the role of the radiologist, as a member of the multidisciplinary team, in the diagnosis and monitoring of pancreatic adenocarcinoma treatment. The decision of clinical resectability is based on the integrated analysis of anatomical and biological factors and general condition, and imaging is an essential factor in establishing the degree of anatomical resectability.

Evaluation of peripancreatic vessels is an essential step in this respect.

Regarding the relationship with portal vein and superior mesenteric vein (SMV) we should assess the length and patency of SMV, anatomical variants (such as double trunk), the gastrocolic trunk (formed by the confluence of the inferior right pancreaticoduodenal vein, on the anterior face of the head of the pancreas, with the right gastroepiploic veins and superior right colic; it drains into the VMS at the lower edge of the pancreatic isthmus, being frequently involved by tumors in this location). Venous invasion is assessed by imaging depending on the percentage of vein circumference that is in contact with the tumor, contour and shape irregularities of the vein or thrombosis.

Celiac trunk and SMA are the two pancreatic arterial sources commonly involved in pancreatic tumors extension. Arterial invasion is assessed similarly to venous involvement.

Moreover, knowledge of the hepatic artery anatomy is essential to prevent unnecessary surgical complications during pancreaticoduodenectomy (PD). Since the first description of the hepatic artery (HA) variants by Haller in 1756, several reports have been published about hepatic artery anatomy. Nowadays, Michels' and Hyatt's classifications of hepatic artery variants are commonly used Michels NA, 1955; Hiatt JR et al, 1994). PD is usually performed backward, with transection of the pancreatic neck before retroportal lamina dissection close to the superior mesenteric artery (SMA). Therefore, early retroportal lamina approach allows a better assessment

of the variant pattern of the arterial blood supply to the liver, proper mobilization of the specimen from the vessels before pancreatic division and, if necessary, safe venous clamping. Therefore several "artery-first" surgical approaches were described, and the choice of the surgical technique depends, along with experience of the surgical team, on the degree of vascular involvement by the pancreatic tumor and the presence of HA variants that should be preserved during the surgical resection.

In our tertiary-center hospital, several studies and case reports were carried out in patients with pancreatic surgical diseases, especially adenocarcinoma and other malignant tumors, emphasizing the importance of correct identification of celio-mesenteric vessels by preoperative CT, with direct impact on tailoring the surgical procedure.

2.2.1.1 Technical tailoring of surgical treatment in patients with hepatic artery anatomic variants

Results

In the surgical department of our high-volume university hospital, 134 consecutive patients underwent PD for periampullary and pancreatic head tumors between January 1, 2007, and November 30, 2010. Among them, 42 (31%) (23 females and 19 males, age range 41-76 years) who were preoperatively assessed by contrast-enhanced CT had HA anatomic variants and underwent a retroportal lamina dissection during PD, as a standard procedure performed by a single team.

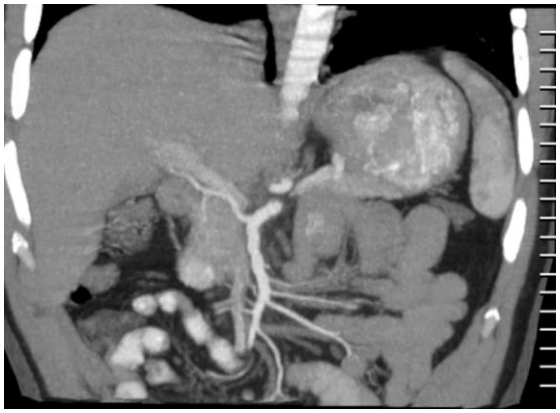

Fig 2.1 CT: Replaced common HA from SMA in a patient with pancreatic head insulinoma

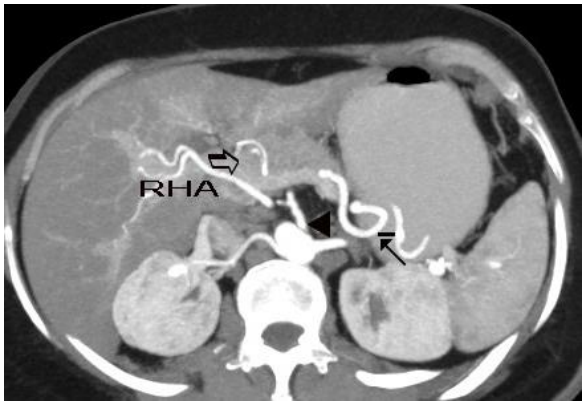

Fig 2.2 CT: replaced RHA from celiac trunk with dorsolateral position within porta hepatis; open arrow – PV, arrow – splenic artery, arrowhead – celiac trunk

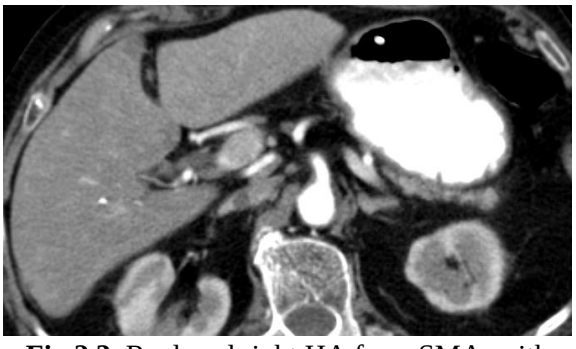

Fig 2.3. Replaced right HA from SMA, with retroportal position in the hepatic hilum; proper HA is located anterior to the portal vein

Patients' characteristics are detailed in table 2.I. Thirty-seven patients with preoperatively detected HA anatomic variants had malignant tumors of the pancreatic head or periampullary region and 5 had neuroendocrine tumors of the inferior pancreatic head (4 insulinomas and 1 malignant neuroendocrine tumor). Thirty-two patients had an accessory or replaced right hepatic artery arising from the SMA or celiac trunk. Ten patients had a replaced common HA originating in the SMA. In two patients with a replaced common HA originating from the SMA, the abnormal vessel was involved with an enlarged lymph node mass behind the pancreatic head (Fig. 2.1, 2.2, 2.3). Segmental resection of the involved artery and arterial reconstruction were performed, using the reversed splenic artery in both patients. Five patients with HA variants and adenocarcinoma involving the portomesenteric vein required en bloc vascular resection, and mobilization of the right colon and mesentery root followed by mesentericoportal end-to-end anastomosis and reimplantation of the splenic vein. Anastomotic patency with normal blood flow was confirmed by Doppler ultrasonography at the end of the procedure.

Table 2.I Patients characteristics

CHARACTERISTICS			**No**	**%**
MEDIAN AGE (ys)			58.7	
DISEASES (Pathologic entity)				
MALIGNANT DISEASE	**TOTAL**		**29**	**64,45**
	PANCREATIC ADK		19	65.51
	AMPULLARY ADK		4	13.79
	DISTAL CBP ADK		3	10.34
	DUODENAL ADK		2	6.89
	NEUROENDOCRINE PANCREATIC TUMOURS		1	3.45
BENIGN DISEASE	**TOTAL**		**13**	**35.55**
	INSULINOMA		4	25
	CHRONIC PANCREATITIS		3	38.5
	IMPT		6	46.5
HEPATIC ARTERY ANATOMIC VARIANT	**TOTAL**		**42**	
	1) ABERRANT RIGHT HEPATIC ARTERY (RHA)		**32**	
	ORIGIN	From the SMA	27	
		From the CT	5	
	TYPE	Replaced RHA	25	
		Accessory RHA	7	
	2) ABERRANT COMMON HEPATIC ARTERY (CHA) - Replaced CHA		**10**	
	ORIGIN	From the SMA	8	23.33
		From the aorta	2	3.33

Discussion

One of the difficulties of pancreaticoduodenectomy is the variability of peripancreatic vessels anatomy. Assessment of variant patterns of the arterial supply to the liver in patients who are about to undergo this procedure is a challenging but mandatory procedure, that can avoid or minimize unnecessary complications, such as fatal hepatic injury (Varty PP et al, 2005; Yang F et al, 2008) Accidental ligation of a HA anatomic variant may result in hepatic necrosis, ischemic biliary injury or anastomotic complications.(Yamamoto S et al, 2005; Yang SH et al, 2007). The importance of sparing it lies not so much in preventing hepatic ischemia, but in preventing a breakdown of bilioenteric anastomosis,

because the blood supply to the cranial part of the bile duct is entirely dependent on the right hepatic artery after PD. Preoperative assessment of peripancreatic vascular patterns (variants, strictures) by imaging methods is of upmost importance for the surgeon. Contrast-enhanced CT with acquisitions in arterial and venous phase is the method of choice, since it enables rapid acquisition of thin-slice high-resolution images of the abdominal arteries, as well as 3D reconstructions (Koops A et al, 2004). The accuracy of CT angiography compared with conventional angiography for detecting hepatic arterial variants is 97-98% (Winston C et al, 2007).

Anatomic variations in the hepatic artery occur in 25 to 75% cases (Michels NA, 1955; Hiatt JR et al, 1994). Although there are different classifications, the most used are Michel's classification, which establish the difference between an accessory and a replaced artery (Table 2.II) and Hiatt classification (Table 2.III)

Table 2.II Classification of hepatic arterial variants by Michels (1955)

Anatomic variant	Average	Range
I: standard anatomy	~60%	55-61%
II: replaced LHA	~7.5%	3-10%
III: replaced RHA	~10%	8-11 %
IV: replaced RHA and LHA	~1%	
V: accessory LHA from LGA	~10%	8-11%
VI: accessory RHA from SMA	~5%	1.5-7%
VII: accessory RHA and LHA	~1%	
VIII: accessory RHA and LHA and replaced LHA or RHA	~2.5%	
IX: CHA replaced to SMA	3%	2-4.5%
X: CHA replaced to LGA	0.5%	
Unclassified CHA separate origin from aorta double hepatic artery PHA replaced to SMA; GDA origin from aorta	 2% 4% <0.5%	

Table 2.III Classification of hepatic arterial variants according to Hiatt

Type	Anatomical variants
I	Normal anatomy
II	Replaced left hepatic artery originating from the left gastric artery Accessory left hepatic artery originating from the left gastric artery
III	Replaced right hepatic artery originating from the superior mesenteric artery Accessory right hepatic artery originating from the superior mesenteric artery
IV	Co-existence of Type II and III Accessory left hepatic artery originating from the left gastric artery and accessory right hepatic artery originating from the superior mesenteric artery Accessory left hepatic artery originating from the left gastric artery and replaced right hepatic artery originating from the superior mesenteric artery
V	Common hepatic artery originating from the superior mesenteric artery
VI	Common hepatic artery directly originating from the aorta

The most likely HA anatomic variant expected during planning or performing PD is a replaced or accessory right hepatic artery (10%-11%) (Yang SH et al, 2007) followed by a replaced

common hepatic artery arising from the SMA (2%-3%). These vessels may course behind, within the pancreas head or along its ventral side. (Yang SH et al, 2007). A right hepatic artery or replaced common hepatic artery coursing within pancreas parenchyma is preserved by dividing this parenchyma. In our study group, 31 such vascular variants coursed along the posterior side and 11 within the pancreas. Before dissecting the variant HA, we could not confirm its course, therefore preoperative imaging is crucial. Ductal carcinoma with limited venous involvement can be resected with a long-term survival similar to that after radical resection without venous involvement. In case of tumoral arterial involvement, arterial resection and reconstruction of a replaced hepatic artery can be done using the splenic artery.

Conclusion

Knowledge of the aberrant hepatic artery blood supply in patients who are about to undergo PD is essential in order to avoid and minimize unnecessary surgical complications such as fatal hepatic injury. Intraoperative early control of the SMA by "artery-first" approach enables easier safeguarding of a HA anatomic variant and an early selection of patients, avoiding the "point of no return" (in terms of resectability).

2.2.1.2 Pancreatic vascular pathology as an indication for emergency surgery

Introduction

Pancreatic pseudoaneurysm (PPA) is a rare vascular complication of acute and chronic pancreatitis, resulting from erosion of the pancreatic or peripancreatic arteries into a pseudocyst (PPC). It differs from a true aneurysm because its wall does not contain the components of a vessel but consists of fibrous tissue which usually continues to enlarge, creating a pulsating malformation, an extravascular hematoma, communicating with the intravascular space (Hsu JT et al, 2006; Chu KE et al, 2012; Carr JA, et al, 2000). Accordingly, a communication between the peripancreatic vessels and the PPC is formed. PPA forms when enzymes-rich peripancreatic fluid, often within a PPC leads to autodigestion and weakening of the walls of adjacent arteries (Hsu JT et al, 2006; Chu KE et al, 2012; Carr JA, et al, 2000). The splenic artery is the most frequently involved, up to 50 % cases; less frequently the gastroduodenal artery (GDA), the pancreaticoduodenal artery (PDA), the superior mesenteric artery (SMA), the left gastric artery and the hepatic artery (HA) (Hsu JT et al, 2006; Chu KE et al, 2012; Carr JA, et al, 200are involved. Though rather uncommon, PPA is accompanied by life-threatening complications, mainly rupture and bleeding, with mortality rates as high as 12.5% even in treated patients and > 90 % if patients are left untreated arteries (Hsu JT et al, 2006; Chu KE et al, 2012; Carr JA, et al, 2000). CT and selective angiography are the standard tools for the diagnosis of PPA and for treatment planning, with sensitivity and specificity up to 90 and 95 % respectively (5 Balthazar EJ et al, 2001). Pancreaticoduodenectomy (PD), a complex surgical procedure, is routinely performed as an elective procedure, emergency PD representing less than 2 % of the indications and implying an added challenge for the surgical team (Ionescu M et al, 2003). No evidence-based guidelines exists regarding the optimal treatment modality for PPA as limited data is available (Bergert H et al, 2005; Flati G et al, 2003; Udd M et al, 2007). The current major controversy is whether selective transcatheter arterial embolization (TAE) should be the conclusive treatment or whether it should be only a previous approach for further elective surgery (Balachandra S et al, 2005).

We reported the case of a sudden PPA rupture in a patient with multiple comorbid conditions, common mesentery and replaced right hepatic artery (rRHA). Whereas the patient has suddenly become hemodynamically unstable, an emergency PD had to be performed as single and final therapeutic management. To our knowledge, related reported cases are scarce.

Bleeding pancreatic pseudoaneurysm

A 65 year-old man, former miner, occasionally drinker, with a medical record of pulmonary silicosis, CPOD, myocardial infarcts, angor pectoris and recent aorto-coronary by-pass under antiplatelet therapy with clopidogrel, presented at the emergency room subfebrile, with mild dyspnea, asthenia, moderate to intense epigastric pain, anorexia and intermittent melena in the past 3 weeks. The pain had not decreased by the usual analgesics and had worsened in the past 4 days. Physical examination revealed normal heart sounds (88/min) and arterial pressure (135/85 mmHg). Rectal examination showed traces of melena. Laboratory tests indicated leukocytosis (11 400/mm3), low hemoglobin level (9,4 g/dl), normal platelet count (36,4×104/mm3), normal serum creatinin and bilirubin level, glucose 136 mg/dl, lipase 325 IU/l, amylase 171 IU/l, LDH 285 IU/l, aspartate aminotransferase 44 IU/l.

A chest X-ray film disclosed small amount of right pleural effusion. Abdominal ultrasound showed a hydropic gallbladder, a 9.6 mm common bile duct, and a 49/48 mm hypoechoic structure in the pancreatic head with upstream enlarged main pancreatic duct.

Contrast-enhanced abdominal CT described a common mesentery and a 5 cm-sized mass of the pancreatic head, including a well delimited cystic structure, enhancing similarly to the aorta and suggesting a PPC complicated with PPA (fig. 2.4). An enlarged pancreatic duct (9.5 mm) was noticed in the body of the pancreas, with possible communication in between. No overt biliary tree dilatation was seen. The reconstructed coronal plan of the arterial sequence ascertained the PPA as a vascular structure related to the inferior PDA (fig. 2.5). A replaced right HA originating from the right-sided SMA (consistent with common mesentery) was described as well (fig. 2.5) in retroportal position.

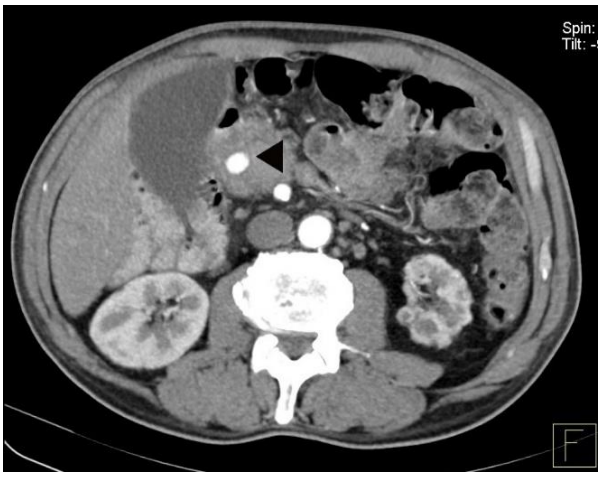

Fig. 2.4 CT-arterial aquisitionn: Pancreatic head pseudoaneurysm (black arrowhead), right-sided superior mesenteric artery and duodenojejunal angle (suggestive for common mesentery)

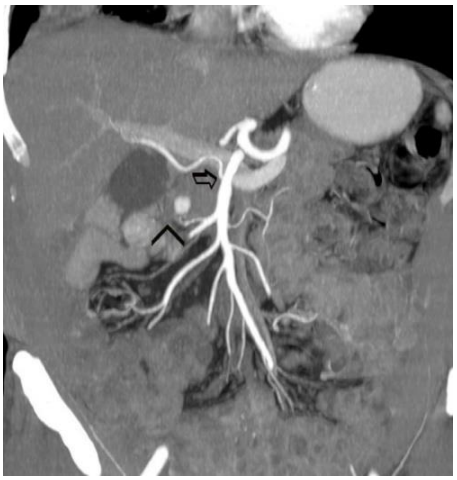

Fig. 2.5 CT- pancreatic head pseudoaneurysm related to the inferior pancreaticoduodenal artery (open arrowhead) and replaced right hepatic artery arising from the superior mesenteric artery (arrow)

Upper endoscopy examination revealed small amount of blood in the second part of the duodenum but with no overt transpapillar bleeding.

The conclusive diagnosis was chronic pancreatitis with cepuncturelic PPC and PPA formation, common mesentery, replaced right HA arising from the SMA, right pleural effusion.

Due to recent aorto-coronary by-pass, angor pectoris, CPOD, and pulmonary silicosis, and to the acceptable clinical course, the patient was considered at risk for surgery and scheduled for TAE.

On the 2nd day of hospitalization, the patient presented a sudden, sharp epigastric pain associated with general pallor, sweating, tachycardia, abdominal tenderness and systolic arterial pressure dropped at 80 mmHg. Hemoglobin level and hematocrit dropped to 6, 2 g/dl and 17 % respectively. Color Doppler imaging showed turbulent blood flow inside the PPC structure. Emergent endoscopy revealed transpapillar hemorrhage, so a sudden rupture of the PPA with active bleeding inside the PPC was highly suspected. Since an interventional radiology gesture was no more of choice in this poor-risk and rapidly deteriorating patient, hemodynamically unstable, emergency surgery was necessary as single life-salvage treatment. The laparotomy confirmed the pancreatic head tumor of about 5 cm diameter, well delimited, with no sign of bleeding into the peritoneal cavity. According to these intraoperative findings likewise, a PD was decided, with both hemostatic and curative intent. Considering the PPA vascular sources and HA variant, a backwards Whipple was performed with mesopancreas first dissection, allowing rapid exposure of the right side of the SMA (ever more readily in case of common mesentery) with the rRHA. Early control over PPA bleeding was achieved by exposure and ligation of the GDA and inferior PDA outside the PPC, before any digestive or pancreatic transection and removal of the specimen. Early postoperative outcome was uneventful and the patient was discharged on the 11th postoperative day. Three months after PD, the patient presented a normal clinical and imaging status.

The pathological examination of the operative specimen confirmed the diagnosis of PPC and PPA (fig. 2.6) .

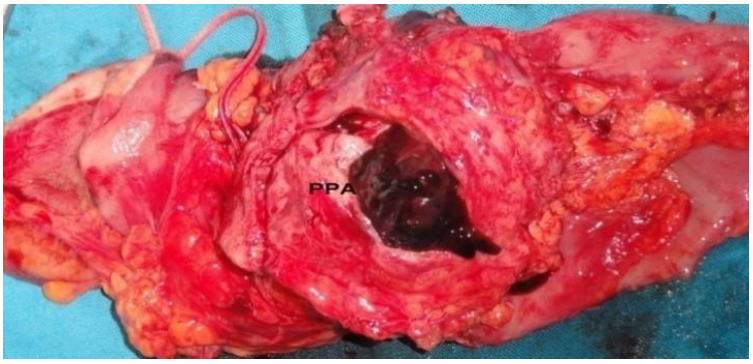

Fig 2.6. Pancreaticoduodenal resection specimen with pancreatic pseudoaneurysm (PPA) inside the pseudocyst.

Discussion

PPA formation is a rare yet lethal complication of chronic pancreatitis, with a prevalence less than 10 %, but a severe outcome with a mortality rate over 90 % in untreated patients. Spontaneous thrombosis of the PPA has been reported but this is a very rare event (Hsu JT et al, 2006; Chu KE et al, 2012; Carr JA, et al, 2000). Complications like rupture and bleed into the biliary tree (hemobilia), pancreatic duct ("hemosuccus pancreaticus"- as in our reported case), gastrointestinal tract, peritoneal cavity and retroperitoneum are more frequent, with 12, 5 % mortality rate even in treated patients (Hsu JT et al, 2006; Chu KE et al, 2012; Carr JA, et al, 2000). The hemorrhage is usually associated with a very poor prognostic. Localization of PPA by preoperative imaging studies is crucial to further treatment. Plain abdominal ultrasound is of little diagnostic value. Doppler ultrasound, contrast-enhanced US and contrast-enhanced CT are widely used as non-invasive techniques to detect bleeding PPA inside a PPC as it has been proved in our case (Hsu JT et al, 2006; Chu KE et al, 2012; Carr JA, et al, 2000; Balachandra S et al, 2005). However, angiography remains the definitive modality to precisely locate and evaluate

the PPA with a sensitivity rate of 100 %, and its major advantage is the opportunity to treat the lesion by embolization (44-51).

The spectrum of therapeutic methods provided for PPA includes thrombin injection, embolization or stent placement, and surgical repair (Hsu JT et al, 2006; Chu KE et al, 2012; Carr JA, et al, 2000; Balachandra S et al, 2005).

There are some reports of percutaneous ultrasound-guided thrombin injection to treat pseudoaneurysm, mainly for postcatheterization femoral artery pseudoaneurysms (Krueger K et al, 2005). When organ infarction is of concern, a stent can be used to maintain the patency of the involved vessel. TAE is more reliable and widely used method of treatment for large PPA with a success rate of 70 to100 % and a reported rate of mortality of 12-33% (Tessier DJ et al, 2003; Udd M et al, 2007). Most authors agree that TAE is appropriate when bleeding is diffuse or emanating from the pancreatic head, for unsuccessful surgery or postoperative bleeding. Its use is however quite limited in the case of patient`s hemodynamic instability (Tessier DJ et al, 2003; Udd M et al, 2007).

A complex surgical procedure as PD performed in emergency is quite exceptional (less than 2%), being reported mainly for trauma (Ionescu M et al, 2003). The most commonly reported cases of non-trauma emergency PD are: severe complication after therapeutical endoscopies (perforation or bleedings), intractable duodenal or ampullary bleedings (ulcer or tumors). Surgery-related complications after emergent PD are reported to be quite similar to those after elective PD, although the overall morbidity is higher due to the altered general status of the patient with emergency indications.

Some authors consider surgery as the best option for bleeding PPA complicating chronic pancreatitis (Hsu JT et al, 2006; Chu KE et al, 2012; Carr JA, et al, 2000). Nevertheless, selection of the best surgical procedure is still a matter of debate. The major controversy surrounding the operative management of bleeding PPA is whether to perform arterial ligation or pancreatic resection. Location of the PPA is a major issue when selecting the surgical procedure. Patient outcome is better for lesions in the pancreatic body and tail (16 % mortality) than for those with lesions in the pancreatic head (43 % mortality) event (Hsu JT et al, 2006; Chu KE et al, 2012; Carr JA, et al, 2000). In our case, a bleeding PPA complicating a pancreatic head PPC required emergent surgery due to patient hemodynamic instability. Even in this high operative risk patient, an emergent Whipple was the procedure of choice as far as it provided either early control over the bleeding vessel and complete removal of the pancreatic head lesion. Posterior approach was preferred because it allowed mesopancreas first dissection with early isolation of the right-sided SMA and rRHA (close to the SMA origin) alongside early isolation and ligation of the inferior PDA and GDA, as vascular sources of the PPA. Handling likewise, the rRHA could be spared and steady hemostasis of the bleeding PPA was provided before any digestive or pancreatic transection and removal of the specimen.

Conclusion

Preoperatively imaging identification of arterial variants and arterial pathology relatd to the pancreas is crucial for appropriate management. Even in poor surgical risk patient, as soon as the patient becomes hemodynamically unstable, the interventional radiology is no longer indicated and surgery, particularly the pancreatic resection, is the only certain way to provide both definitive hemostasis and removal of the lesion. Backwards Whipple is a good approach to the bleeding pancreatic head pseudoaneurysm as it allows early control over peripancreatic vasculature and sparing HA variants within early mesopancreas approach.

2.2.2 Postoperative imaging and its implications in management of the complications

Articles

1. Savin ML, Gheorghe L, **Lupașcu Ursulescu C**, Negru D, Trofin AM, Zabara M, Nuțu V, Cadar R, Blaj M, Lovin O, Crumpei F, Lupașcu C. Applications using artificial intelligence in predicting the risk of postoperative pancreatic fistula using preoperative CT images. Journal of Surgery [Jurnalul de chirurgie]. 2022; 18(3): 215 - 223,
2. Rusu-Andriesi D, Trofin AM, Zabara M, Vlad N, Vasiluta C, Vasilescu A, Blaj M, Spiridon I, Cadar R, Lovin O, Crumpei F, Tarcoveanu E, **Lupascu-Ursulescu C**, Lupascu C. Does the Overall Survival of the Resectable Periampullary Carcinomas Correlate with High Expression of p53 and ki67? Chirurgia 2022; 117: 423-430.
3. Savin ML, Mihai F, Gheorghe L, **Lupascu Ursulescu C**, Negru D, Trofin AM, Zabara M, Nutu V, Cadar R, Blaj M, Lovin O, Crumpei F, Lupascu C. Proposal of a Preoperative CT-Based Score to Predict the Risk of Clinically Relevant Pancreatic Fistula after Cephalic Pancreatoduodenectomy. Medicina (Kaunas). 2021 Jun 24;57(7):650
4. Vasilescu AM, Andriesi Rusu DF, Bradea C, Vlad N, **Lupascu-Ursulescu C**, Cianga Spiridon IA, Trofin AM, Tarcoveanu E, Lupascu CD. Protective or Risk Factors for Postoperative Pancreatic Fistulas in Malignant Pathology. Life 2021, 11, 1216.
5. Andriesi-Rusu FD, **Lupascu-Ursulescu C**, Trofin AM, Vlad N, Vasilescu A, Zabara M, Lozneanu L, Bradea C, Bejan V, Lupascu C. The impact of obesity on the risk of postoperative pancreatic fistula in malignant surgical pathology. Journal of Surgery, 2021; 17 (2): 112-118
6. Trofin AM, Zabara M, Cadar R, Nastase A, Palaghia M, Blaj M, **Lupascu-Ursulescu C** (corespondent), Lupascu C. Pain Management After Pancreatic Resections for Cancer. Biomed J Sci & Tech Res 32(2)-2020. BJSTR. MS.ID.005228
7. Trofin AM, Lupascu C, Cianga Spiridon I, **Lupascu Ursulescu C**, Zabara M, Grigorean V, Brasoveanu V. The implications of e-cadherin expression in pancreatic cancer. Rev.Chim. (Bucharest); 2018; 69 (8): 2291-2294 FI 2017/2018 1,412
8. Rusu Andriesi D, Trofin AM, Cianga Spiridon IA, **Lupascu Ursulescu C**, Lupascu C. Non-operative risk factors and the implications of sandostatin for postoperative pancreatic fistula in malignant pancreatic surgery. Rev. Chim.(Bucharest) 2017; 68 (12): 2875-2878
9. **Ursulescu C**, Negru D, Grigoraş M, Moisii L, Fotea V, Reuţ R, Jari I. Evaluarea CT a pancreasului operat. Imagistica Medicală, 2006, 1-2, p.28-32

Books

Buzea C, Eva L, Doroftei B, **Lupașcu Ursulescu C**, Iancu D, Iancu RI, Cojocaru ID, Agop M. Probleme actuale ale medicinei moderne din perspectiva inteligentei artificiala, Ars Longa 2019 ISBN 978-973-148-336-8

Introduction

Pancreatic surgery consists of various procedures (large or limited resections, drainage or cystogastrostomy for pancreatitis) to treat benign and malignant pancreatic and periampular

tumors and pancreatitis. In addition, pancreas transplantation has become a viable treatment alternative for patients with diabetes, ensuring blood glucose control and stabilization or even reversibility of complications associated with this disease.
Although surgical techniques and postoperative therapy have been continuously improved, leading to decreased mortality rates, the number of postoperative complications remains high as increasingly complex procedures are practiced in patients with advanced diseases. Postoperative imaging, especially CT, plays an important role for an early and correct diagnosis of complications, with direct impact to management.
We present the main postoperative CT aspects after pancreatic surgery, including normal aspects, which should be identified to avoid interpretation pitfalls, and characteristic aspects for complications.

2.2.2.1 Normal postoperative aspects and imaging diagnosis of complications

The acquisition protocol
The CT protocol changed over time in close relation to the evolution of equipment which allows nowadays faster acquisition. Moreover, it is tailored depending on the interval from surgery (early or late postoperative) and the clinical diagnosis.
The volume examined extended from 2 cm above the diaphragm to the level of the pubic symphysis in majority of cases, or is extended to the thorax if lung complications are suspected.
In our institution, a tertiary care center, we have a standard dynamic scan protocol for pancreas. If a fistula is suspected and the patient is able to ingest fluids, we give diluted oral contrast scan (up to 500 mL) to facilitate the distension of the digestive tract, the identification of anastomoses, and the assessment of potential collections. The nasogastric tube is clamped 1 h before the procedure. In the early postoperative period, CT exam can be performed immediately after an upper digestive tract contrast study, without additional oral contrast administration, to improve detection of perianastomotic contrast and differentiate a fistula-associated collection from a seroma (Tamm EP et al, 2003).
After a native acquisition and injection of iodine contrast media (with a flow rate of 3 mL/s, 100 mL, and bolus tracker monitorization in the abdominal aorta at the level of celiac trunk), we made two acquisitions in arterial time (at 15 s after start of injection - the threshold of 150 HU) and portal venous time (at 40 s). A delayed scan at 3 min is not necessary in the postoperative period, unless intravenous or oral contrast extravasation need to be confirmed.
The CT report should include data about postoperative anatomical aspects in accordance with surgical protocol (identification of anastomoses and remnant digestive segments, size and structure of pancreatic parenchyma), for a correct definition of pathological aspects.

Pancreatoduodenectomy (PD)
Major pancreatic resections, especially indicated for malignant tumors, are dominated by PD. The classical Whipple procedure (fig. 2.7) consists of a radical resection of the head of the pancreas, duodenum and gastric antrum, followed by restoration of digestive continuity by gastro-enterostomy, choledocojejunostomy and pancreaticojejunostomy (Zollinger RM Jr, 1993). There are some technical variants: PD with pylorus preservation (duodeno-jejunal anastomosis), pancreatico-gastric anastomosis (with lower frequency of fistulas compared to pancreatic-jejunal anastomosis due to better vascularization of the gastric wall), and Wirsung duct occlusion without pancreatic-digestive anastomosis (Zins M, 1999, Tamm EP et al, 1995).

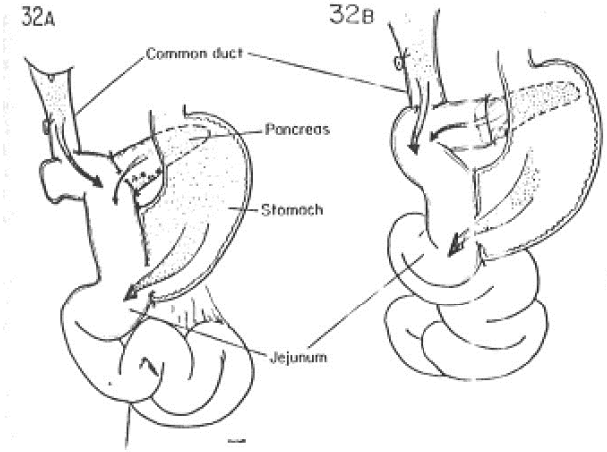

Fig.2.7 PD Whipple (after Zollinger). Drawing of the anatomy after Whipple procedure.

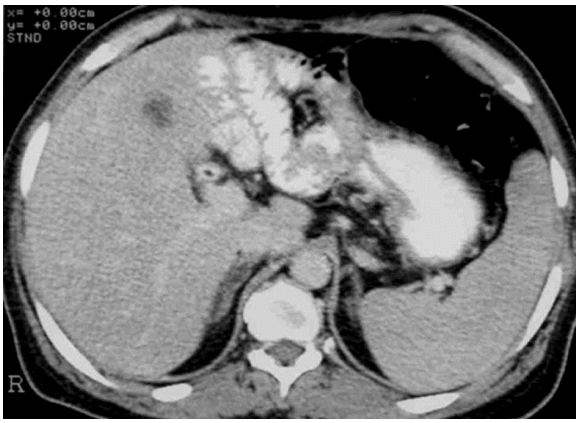

Fig. 2.8 Gastrojejunal anastomosis after Whipple procedure: normal CT appearance

Anatomical elements to be identified on CT images after PD are:

a) digestive anastomosis, gastro-jejunal or duodeno-jejunal, are identified by changes of digestive folds near the stomach (Fig. 2.8). Two situations may rise difficulties in correct identification leading to false positive diagnosis of complication: nondistended jejunal loops in the PD area and hepatic hilum may mimic lymphadenopathy or local recurrence, and the first jejunal loop located posteriorly to mesenteric vessels can simulate a retroperitoneal recurrence (Zins M, 1999; Coombs RJ et al, 1990; Di Carlo V et al, 1999; Furukawa H et al, 1997).
b) pancreatic anastomosis: the pancreatic-jejunal anastomosis is located to the right of the remaining pancreas, anterior to the mesenteric vessels, at the level of the splenic vein, sometimes presenting a pseudointussusception of the pancreas in the jejunal loop, while the pancreatic-gastric anastomosis is located on the posterior face of the stomach, with pancreatic stump oriented anteriorly (fig. 2.9) (Zins M, 1999; Trerotola SO, 1989). The remaining pancreas is frequently atrophic or involutes on successive examinations, but experimental studies have shown that the pancreas can regenerate after major pancreatectomy, the administration of growth factors and peptides intensifying this process or preventing atrophy (Zins M, 1999; Tsiotos CG 1999; Jang JY et al, 2003; Sumi S et al, 2000).
c) biliary anastomosis, choledoco-jejunal or hepato-jejunal, are located in the hepatic hilum, anterior to the portal vein, being easily identified due to pneumobilia. It should be noted that aerobilia is present only in 60-80% of cases, and its absence does not necessarily mean anastomotic obstruction, as contrast reflux in the bile ducts, seldom seen in CT, is not significantly associated with colangitis (Zins M, 1999; Bluemke DA 1997).

In the early postoperative period, the presence of drains may facilitate the finding of anastomosis: drain in the pancreatic duct through pancreatic-digestive anastomosis (Fig. 2.10), external biliary drain through bilio-digestive anastomosis, and external jejunal drain for anastomotic jejunal loop. There are some *transient changes* in the early postoperative period: fluid collections (3-6 weeks), in the PD area, interhepato-renal, and right paracolic space; infiltration of mesenteric fat, especially around the upper mesenteric artery; inflammatory mesenteric lymph nodes, hepatic steatosis.

The most common postoperative *complication* after PD is pancreatic anastomotic fistula, especially from pancreatic-jejunal anastomosis, found in 3-13% of cases and responsible for 50% of the mortality rate after PD (Tamm EP et al, 1995; Schlitt HJ et al, 2002; Watanabe M et al, 2004). The CT signs for pancreatic fistula are perianastomotic extravasation of the oral contrast,

ill-defined large collection in contact with pancreatic anastomosis, without regression on successive examinations (fig. 2.11). In uncertain cases, CT-guided percutaneous puncture allows biological assessment of the fluid (Zins M, 1999; Lepanto L et al, 1994).
The differential diagnosis with an abscess is often difficult based only on imaging criteria; the abscess is usually more heterogeneous, with air-fluid level and peripheral enhancement (Zins M, 1999).

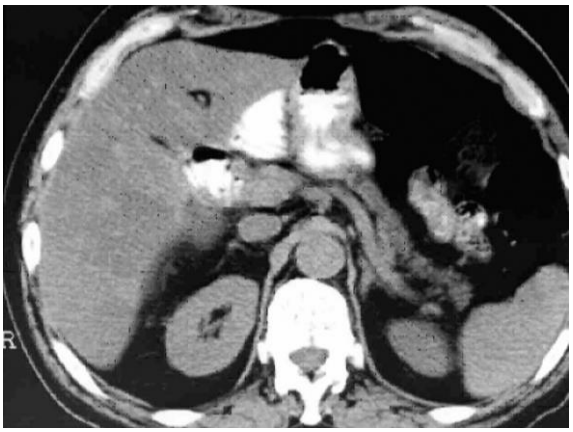

Fig. 2.9 Pancreato-gastric anastomosis after Whipple procedure: normal CT appearance

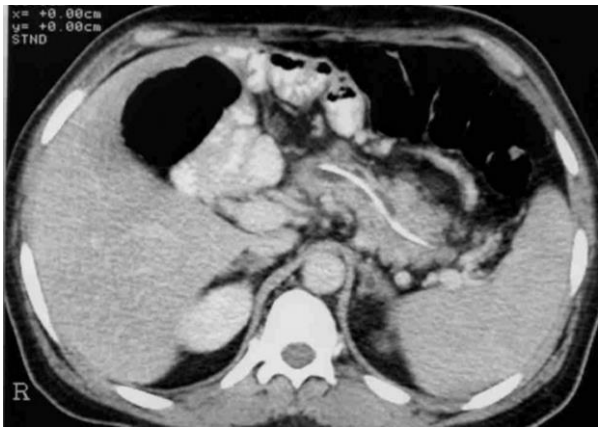

Fig. 2.10 Postoperative CT after PD: pancreatic drain

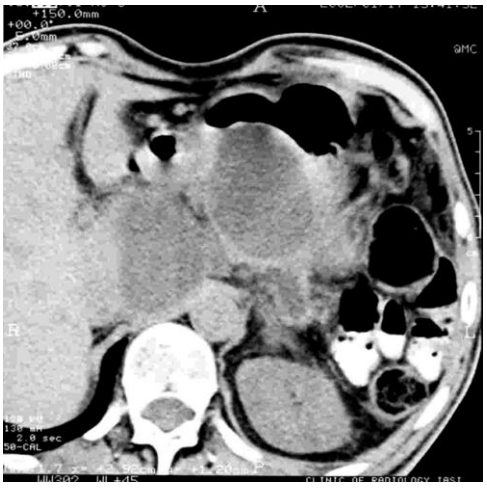

Fig. 2.11 Abdominal CT 11 days after PD: perianastomotic fluid collections suggestive for pancreatic fistula.

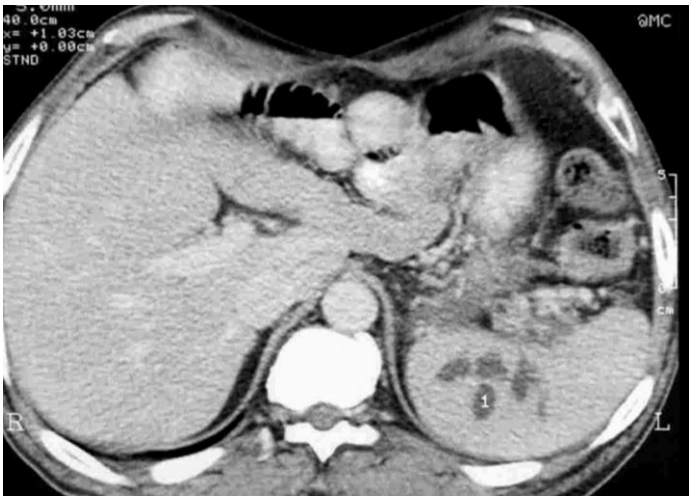

Fig. 2.12 Postoperative pancreatitis: peripancreatic and splenic fluid collections.

Postoperative pancreatitis is a clinical and biological diagnosis, CT allowing the assessment of parenchymal necrosis and extrapancreatic extension (fig. 2.12).
Intraperitoneal hemorrhage or hematoma is a rare complication (1% of PD); it can be secondary to an arterial pseudoaneurysm, diagnosed at CT by synchronous enhancement with arterial structures and ovoid shape.
Anastomotic strictures (biliary, gastric) are due to edema in the early postoperative period and CT can exclude other perianastomotic changes. In late postoperative period, tumor recurrence is a frequent cause, diagnosed by segmental dilation of the pancreatic duct, segmental dilation of bile ducts, dilation of jejunal loops) associated with infiltration in perivascular fat, solid masses, adenopathy, liver metastases.

Left pancreatectomy

Also a major pancreatic resection, left pancreatectomy is performed for lesions located in the body and tail of the pancreas, and may associate splenectomy. The pancreatic stump is sutured or anastomosed with a jejunal loop.
Postoperative anatomical aspects are easily identified on CT, the pancreatic resection line being located to the right of the midline, sometimes near the gastroduodenal artery. Infiltration of peripancreatic or left upper quadrant fat persists for 2 weeks postoperatively (fig. 2.13)
The main postoperative complication is pancreatic fistula (5-10% of cases). The CT diagnosis of this complication, as well as of acute cephalic pancreatitis or intraperitoneal haemorrhage, are identical to those described in PD. Portal thrombosis can be secondary to local inflammation.
Tumor recurrence, local or distant, is similar as CT features to PD (fig. 2.14).

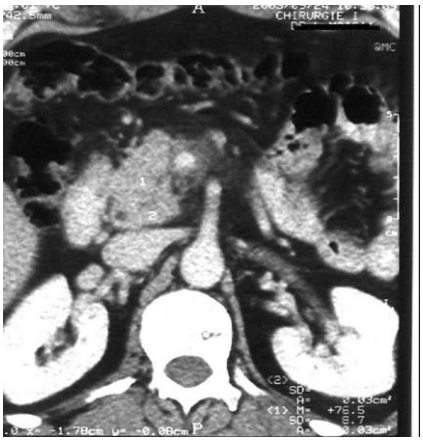

Fig. 2.13 Left pancreatectomy: normal postoperative findings with increased density of the fat around mesenteric vessels

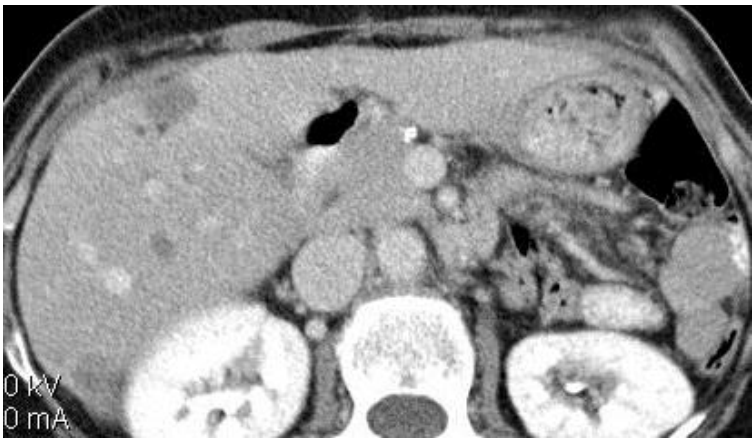

Fig. 2.14 Left pancreatectomy for pancreatic adenocarcinoma: liver metastases

Total pancreatectomy
It involves resection of the whole pancreas, together with antropyloric region, duodenum, distal main bile duct and spleen. The digestive continuity is restored by gastro-jejunal and biliary drainage by choledoco-jejunal anastomosis.
After total pancreatectomy, the pancreatic area is filled by digestive structures (stomach, jejunal loops) (Fog. 2.15). The main complications are hemorrhage, abscesses and collections. Tumor recurrence is common, local, distant or by adenopathy.

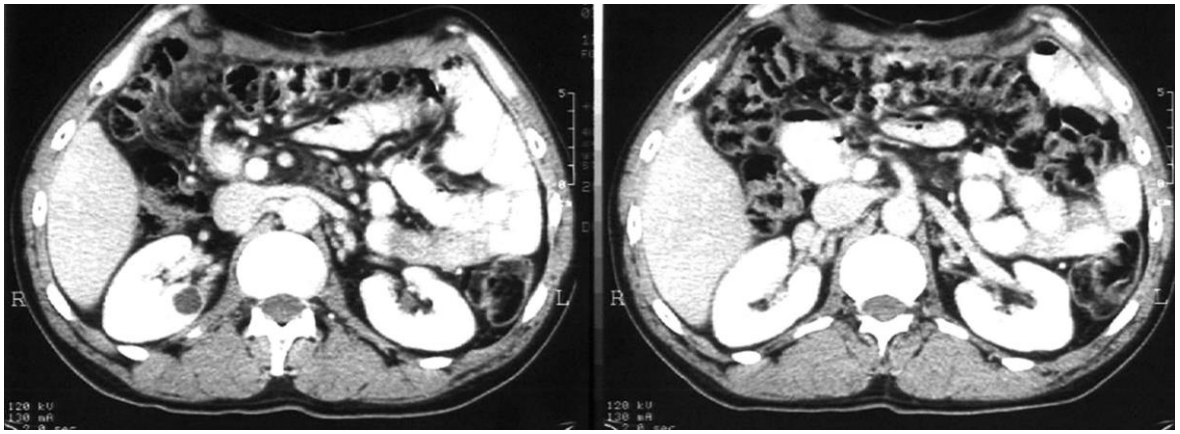

Fig. 2.15 Total pancreatectomy – normal postoperative findings: the pancreatic bed is filled by stomach and jejunal loops.

Pancreas transplantation

It is frequently a simultaneous reno-pancreatic transplant. The pancreatic graft is placed in the right iliac fossa, extra- or intraperitoneally. Pancreatic exocrine secretions are drained into the bladder or intestine, through a duodenal segment, and vascularization is provided by anastomoses between the iliac vessels of the recipient and the splenic artery, superior mesenteric artery and portal vein of the donor (Dachman AH et al, 1998; Moulton JS et al, 1989; Pozniak MA et al, 1995).
The early postoperative imaging follow-up is done by ultrasound. CT is indicated in the presence of complications (fever, increased amylase, large fluid collections) (Pozniak MA et al, 1995). The size and structure of pancreatic graft, density of the peripancreatic fat, patency of vascular anastomosis, and associated collections should be evaluated.
The pancreatic graft appears as a parenchyma round on the axial plan, located in the lower abdomen, with the head oriented downwards in the pelvis. The diameter is, on average, 3 cm at tail, 3.8 cm corporeal and 5 cm in cephalic region (Moulton JS et al, 1989). The examination performed 1week after surgery already reveals a homogeneous structure and a clear contour (Moulton JS et al, 1989). When exocrine secretions are drained into the bladder, there is a change in the shape of the bladder, which is attracted to anastomosis, and a focal thickening of the wall. The most feared complication is rejection, associated with variable degree of inflammatory changes in peripancreatic fat and nonhomogeneous parenchyma, which can evolve to fluid structure in case of necrosis. The CT aspect should be correlated with biological status (Moulton JS et al, 1989).
Other complications are vascular (thrombosis of venous or arterial anastomosis, arterial pseudoaneurysms), digestive anastomotic leak, with peritonitis, abdominal or intrapancreatic abscesses, acute pancreatitis, parietal or abdominal hematomas (Moulton JS et al, 1989).

Conclusions
The interpretation of postoperative CT examinations in patients with pancreatic surgery requires a good knowledge of surgical protocole and normal postoperative variants, as well as a correct examination technique. Evaluating both postoperative anatomical aspects and the presence of complications or tumor recurrence, CT examination is the reference method in the study of the operated pancreas.

2.2.2.2 Postoperative pancreatic fistula

Introduction
Pancreaticoduodenectomy (PD) is the only curative treatment for malignant tumors located in the pancreatic head, periampullary area, or distal bile duct. Although, in recent years, postoperative mortality has dropped considerably (below 5%), the rate of postoperative complications remains high (Hashimoto, Y et al, 2010). The most common postoperative complications are bleeding, infectious complications, delayed gastric emptying syndrome, and pancreatic fistulas (Harada, N.; et al, 2014). The postoperative pancreatic fistula (POPF) remains the main and feared complication, with an important impact on the quality of life, causing high morbidity (i.e., high risk of acute pancreatitis, hemorrhage, sepsis, and multiple organ failure) and a prolonged hospital stay [Maleo G et al, 2014; Tien YW et al, 2005; Gouma DJ et al, 2000). Patients with postoperative pancreatic fistulas have an increased risk of local tumor recurrence and a double risk of death (Butturini, G et al, 2008; Allen, P.J et al, 2014; Vin, Y et al, 2008). The presence of postoperative pancreatic fistulas has an indirect impact on postoperative

survival, being an important cause of delayed initiation of adjuvant therapy (Denbo, J.W et al, 2012).
In 2016, ISGPS (International Study Group for Pancreatic Surgery) introduced a standard definition for postoperative pancreatic fistulas and new criteria for determining its severity. The major change was the replacement of grade A fistula with the term "biochemical leak", corresponding to asymptomatic pancreatic leak. Grade B includes the cases necessitating invasive procedures for drainage of abdominal collections and angiographic procedures. Grade C of POPF included the patients with organ failure, surgical reinterventions, or death (Pulvirenti, A et al, 2017).
Previous studies identified several risk factors for PF, including a soft pancreas (lipomatosis), hard pancreas (fibrosis),Wirsung duct caliber and obesity (Hashimoto Y et al, 2010; Lin JW et al, 2004).
The consistence of the pancreas is a subjectively assessed intraoperative parameter that is determined by the balance between the lipomatosis and fibrosis and affects the quality of the pancreatoenteric suture (Mathur A et al, 2007; Harada N et al, 2014). Although the pathologic assessment is the most accurate in determining the parameters of the texture of the pancreas, a preoperative CT can determine the degree of fatty infiltration of the pancreas and the fibrosis, based on the unenhanced density and the pattern of enhancement of the pancreas (Tajima Y et al, 2004; Takahashi N et al, 2009; Kim SY et al, 2014; Hashimoto Y et al, 2011).
A high caliber of the main pancreatic duct favors a good pancreaticojejunal anastomosis and reduces the risk of PF, provided there is a duct-to-mucosa anastomosis (Kajiwara T et al, 2010).
The pancreatic remnant volume has been proven to independently predict the risk of clinically relevant pancreatic fistula (Kanda M et al, 2014).
A multidisciplinary team in our hospital, including surgeons, radiologists, and pathologists conducted several studies in order to identify the protective factors, the risk factors and a preoperative image-based score allowing the prediction of POPF and improving the postoperative management.

Protective or Risk Factors for Postoperative Pancreatic Fistulas in Malignant Pathology

The aim of the study was to identify a series of factors which can be assessed by objective methods: factors that can be used to identify the patients with a high risk for the development of postoperative pancreatic fistulas.

2. Methods

A retrospective study included a series of 109 consecutive patients with pancreatic resections for malignant pancreatic and periampullary tumors. Selection criteria were: patients with pancreatic resections (PD, distal pancreatectomy, pancreatic biopsy) for pancreatic ductal adenocarcinomas and periampulary adenocarcinomas, histologically confirmed. Patients with malignant neuroendocrine tumors, mucinous carcinomas, or other carcinomas were excluded from the study. All patients included in the study had signed, at the time of hospitalization, the consent for publication and the surgical procedure, and an agreement to participate in clinical trials and research. We analyzed the incidence of POPF, its association with peritumoral fibrous tissue and areas of acute pancreatitis, and the distribution of these histological aspects, depending on the diagnosis.
Resected tumors were fixed and embedded in paraffin to obtain tissue preservation in a reproducible manner. Each tissue fragment was initially fixed in formalin, then processed

according to the standard protocol for histological examination. The sectioning of the blocks with tissues embedded in paraffin were made with the microtome, obtaining sections of 4–5 μm. The sections thus obtained were fixed on the slides, and subsequently subjected to hematoxylin eosin staining. Hematoxylin-eosin-stained slides of the resection specimens were reviewed by a pathologist specialist, who was blinded to all clinical data, and the diagnosis was reconfirmed by a histopathology physician.

Patients' clinical data were obtained from observation sheets. Information was selected, such as age, gender, comorbidities, symptomatology, laboratory analyzes followed in dynamics, preoperative and postoperative imaging, operating protocol, and postoperative evolution.

The diagnosis of POPF was established in patients who had three times the value of amylases in the fluid in the drain tube compared to the normal value, or a persistence of drainage. The quantification of the drainage was both in terms of quantity (drainage measured in mL) and in terms of duration (measured in days).

Statistical Analysis

To perform statistical analysis, the SPSS v.24 was used, with statistical significance established at $p < 0.05$. Continuous variables were reported as mean with standard deviation. Comparisons between the analyzed groups were performed using the t-Student test, ANOVA, Kruskal–Wallis, or Mann–Whitney U Test for continuous variables. The homogeneity of the series was verified regarding the statistical differences between the variances of the series by the Levene test (Levene Test of Homogeneity of Variances). The correlations between certain parameters were tested using the Pearson test, by evaluating the correlation coefficient r. Qualitative variables were presented as absolute (n) and relative (%) frequencies, and comparisons between groups were made based on the results of non-parametric M-L, Yates, or PearsonChi-square tests. Univariate and multivariate analysis of prognostic factors for complications was performed using the Logistic regression model. The power of univariate prediction of risk factors was assessed using the ROC curve based on the value of the area under the curve (Area Under the Curve: AUC).

Results

Our study group included 109 patients (55 males and 54 females) aged between 37 and 79 years. The median age of patients with pancreatic ductal adenocarcinoma was 60.5 ± 10.52, and that of patients with periampullary adenocarcinomas was 59.49 ± 9.04. According to the histological diagnosis, 35 patients had periampullary adenocarcinomas, and 74 pancreatic ductal adenocarcinomas.

PD was the procedure of choice (n = 89), followed by pancreatic biopsy (n = 12) and distal pancreatectomies (n = 8).

Both groups, with pancreatic ductal adenocarcinoma and periampullary adenocarcinomas, have a series of associated comorbidities, but without a significant difference in their distribution (Table 2.IV). Hypertension predominated in both groups of patients. The incidence of diabetes was almost three times higher in the group of patients with pancreatic ductal adenocarcinoma, and the incidence of obesity was almost double in the group of patients with periampullary adenocarcinomas.

Table 2.IV The comorbidities.

Comorbidities	Diagnostic		*p*-Value
	Pancreatic Ductal Adenocarcinoma (Absent/Present) (*n* = 74)	Periampullary Adenocarcinoma (Absent/Present) (*n* = 35)	(95% CI)
Obesity	64/10	27/8	0.224
	86.5%/13.5%	77.1%/22.9%	
Diabetes	57/17	32/3	0.066
	76.7%/23.3%	91.4%/8.6%	
Hypertension	52/19	20/9	0.702
	73.2%/26.8%	69%/31%	
Other cardiac pathologies	55/16	21/8	0.625
	78.6%/21.4%	72.4%/27.6%	

The incidence of POPF on the entire study group was 11.01%. Most patients had grade B POPF (n = 8), one patient had grade A POPF after a pancreatic biopsy, and two patients had grade C POPF. For the two patients with grade C POPF, surgical reoperation was required, with the restoration of the pancreato-jejunal anastomosis.

No significant association was found between postoperative pancreatic fistulas and the gender (p = 0.606) or age (p = 0.605) of the patients.

No statistically significant association was found in our study group between the risk of POPF and the type of surgical resection (p = 0.537). The occurrence of POPF predominated in the group of patients with PD, where the incidence was 12.4%. In this group, the operating team preferred pancreato-jejunal anastomosis "duct to mucosae". In only three cases, a pancreato-gastric anastomosis was performed. In the group of patients with distal pancreatic resections, closure of the pancreatic trance was performed by manual suturing.

The lowest incidence of pancreatic fistulas was observed in the group of patients with pancreatic ductal adenocarcinomas (4.06% vs. 25.72% in the periampullary adenocarcinomas, with p = 0.002).

According to statistical analysis, histological diagnosis demonstrated an increased accuracy in predicting the occurrence of postoperative pancreatic fistulas (AUC = 0.741, p = 0.007, 95% CI: AUC → 0.590–0.892) (Fig. 2.16).

The presence of peritumoral fibrous tissue was objectified in 56.14% of patients with pancreatic ductal adenocarcinomas, and 37.04% in those with periampullary adenocarcinomas, without a statistically significant difference in fibrous tissue distribution according to histological diagnosis (p = 0.08). The group of patients with peritumoral fibrosis included patients who underwent microscopic examination of tumors delimited by desmoplastic stroma and fibrous tissue. The incidence of pancreatic fistulas was 11.9% in the group of patients without peritumoral fibrosis, and 14.3% in the group with peritumoral fibrosis, without a statistically significant difference in the two groups (p = 0.5). The calculated value of the area under the ROC curve demonstrates that the presence of peritumoral fibrous tissue has a weak predictive power on the occurrence of postoperative pancreatic fistula ROC (AUC = 0.526, p = 0.781, 95% CI: AUC → 0.343–0.710).

The coexistence of areas of acute pancreatitis with adenocarcinomas on the resection specimen was associated with a 7.8-fold increase in the incidence of POPF (30% vs. 3.8%, with a p = 0.026). Areas of acute pancreatitis, associated with adenocarcinomas, demonstrated a good

accuracy in predicting the risk of occurrence of pancreatic fistulas (AUC = 0.739, p = 0.079, 95% CI: AUC → 0.474–0.998) (Fig. 2.17).

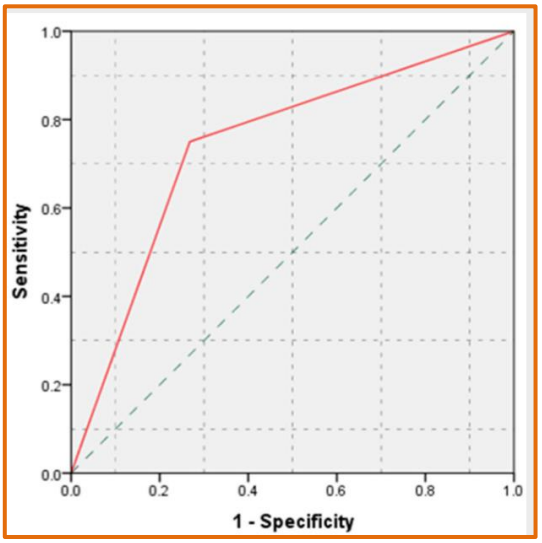

Fig 2.16 ROC curve: histological diagnosis versus pancreatic fistula.

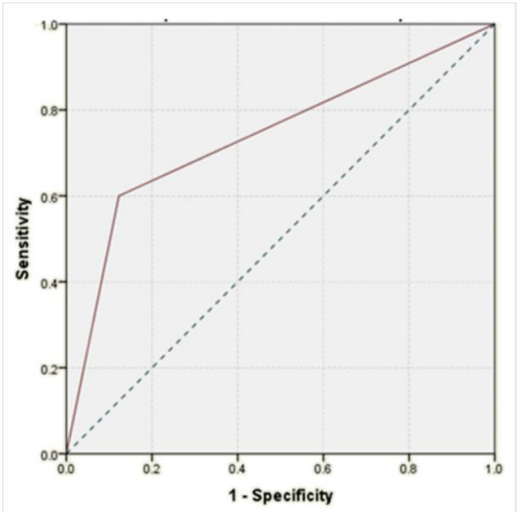

Fig. 2.17 ROC curve: areas of acute pancreatitis associated with adenocarcinomas vs. pancreatic fistula.

Multivariable analysis showed that the histological diagnosis and the areas of acute pancreatitis associated with adenocarcinomas were independently associated with postoperative pancreatic fistulas (Table 2.V).

Table 2.V Multivariable logistic regression model results for the association with pancreatic fistula.

Pancreatic Fistula	OR (Odds Ratio)	OR 95% CI Min	OR 95% CI Max	*p*-Value
Sex	0.248	0.033	1.88	0.178
Histological diagnosis	12.84	1.29	127.29	0.029
Peritumoral fibrosis	4.68	0.605	36.32	0.139
Adenocarcinomas associated with acute pancreatitits	11.34	1.34	95.66	0.026

Discussions

The risk factors involved in the production of POPF can be grouped into modifiable and unchangeable risk factors. In order to eliminate the biases related to the surgeon's experience, the subjective interpretation of the pancreas texture, the surgical technique adopted, or the possible intraoperative complications that may occur, in the current study, we turned our attention to unchangeable risk factors.

Studies in the literature have shown that pancreatic resections for malignant tumors have been associated with a reduced incidence of POPF (Addeo, P et al, 2014; Kang WS et al, 2018), comparing with traumatic pancreatic surgery, where the incidence of POPF can reach up to 38% (Kang WS et al, 2018).

Our study analyzed the incidence of pancreatic fistulas according to the histological type of malignant tumors, finding a significant difference between the group of patients with periampullary adenocarcinomas and the group of patients with pancreatic ductal adenocarcinomas (6.3-fold lower incidence in later group).

The hard pancreatic structure due to the peritumoral fibrous tissue is thought to reduce the risk of pancreatic fistulas for patients with pancreatic ductal adenocarcinomas (Søreide K et al, 2019) but

this was not confirmed in our study group, where there were no statistically significant differences in distribution of peritumoral fibrous tissue according to histological report.

A soft structure of the pancreas can increase the risk of pancreatic fistula up to 10 times compared to a hard gland (Wang H et al, 2017). A series of factors can be responsible for a decrease in the incidence of pancreatic fistulas in patients with a hard structure of the pancreas: (1) the prolonged pancreatic duct obstruction, which leads to a dysfunction of exocrine pancreatic function; (2) pancreatic fibrosis; (3) low risk of injury of pancreatic tissue (Hu BY et al, 2016). Patients with a soft pancreas present an insecure suturing and knotting of the pancreatico-jejunal anastomosis, and a higher risk of the damage to the pancreatic tissue (Hu BY et al, 2016).

A multicentre study of the French Surgical Association confirmed that the rate of pancreatic fistulas was significantly higher in patients with normal or soft pancreatric parenchyma than in hard or fibrous pancreatic tissue. Also, the study concluded that the pancreatic texture can predict the occurence of pancreatic fistulas in patients with adenocarcinomas (Addeo P et al, 2014)

In his study, Callary observed that the soft gland texture and narrowed pancreatic duct diameter demonstrate that exocrine function is generally preserved, which is more susceptible to ischemia and injury (Callery, M.P et al, 2013).

The gland structure is a subjective factor that depends on the surgeon's experience, and there is not a unitary standard (Wang H et al, 2017), but our study eliminated this bias by microscopic confirmation of peritumoral fibrous tissue that contributes to a hard texture.

The results of our study showed that the occurrence of postoperative pancreatic fistulas did not depend on the structure of the pancreas. Martin et al. also concluded in their study that the pancreatic texture and the duct size were not associated with the development of pancreatic leak after distal pancreatectomy (. Martin AN et al, 2018)

The process involved in the development of POPF is a complex one, which includes a multitude of factors that can interact. One of the most important factors involved in this process is the exocrine hypersecretion of the pancreas, which plays a decisive role in producing this postoperative complication (Wang H et al, 2017). Pancreatic exocrine hypersecretion is found in acute pancreatitis, triggering and maintaining pancreatic fistulas.

To our knowledge, there are no studies that have found correlations between the association of adenocarcinomas and areas of acute pancreatitis with an increased risk of POPF. The results of our study showed that when malignant tumors were associated with areas of acute pancreatitis, the incidence of pancreatic fistulas had a significant increase of 7.8 times. Cases with histologically confirmed areas of acute pancreatitis had no specific clinical symptoms and imaging. Histological confirmation of areas of acute pancreatitis associated with adenocarcinomas is an important predictive factor and can be considered one of the most important independent risk factors involved in the occurrence of postoperative pancreatic fistulas.

A study published in 2015 looked at the long-term effects of the association of pancreatic cancer with acute pancreatitis, but this study included patients with clinically relevant, moderate, and severe acute pancreatitis. Thus, Feng et al. found that pancreatic cancer associated with clinically relevant acute pancreatitis had a poor survival time and early recurrence within 12 months (Feng Q et al, 2019).

Some studies show that up to 13.8% of cases of pancreatic cancer may be associated with acute pancreatitis (Feng Q et al, 2019). Feng affirms that the onset of acute pancreatitis may be due to cancer progression itself or to complications of the diagnostic and therapeutic interventional procedures used in pancreatic carcinoma treatment, such as endoscopic retrograde cholangiopancreatography, surgery, and chemotherapy (Feng Q et al, 2019). Acute pancreatitis is a frequent complications after retrograde cholangiopancreatography, and one-third of these patients develop moderate or severe forms of acute pancreatitis (Feng Q et al, 2019; Cheng CL et al, 2006).

Risk factors for pancreatic fistulas differ depending on the type of pancreatic resection. In the case of distal pancreatic resections, emphasis is placed on how to close the pancreatic trance of the remaining pancreas. The way to reduce the appearance of fistulas is to close the distal pancreas using a stapler (Kitahata, Y et al, 2016). Clinical trials have not demonstrated the superiority of the use of a hemostatic adhesive in the distal pancreatic trance (Kitahata, Y et al, 2016). Jiwani et al. affirm that the risk of pancreatic fistula increases considerably when distal pancreatic resections also involve multiorgan resections (Jiwani A et al, 2019). On the contrary, Xia et al. consider that extended lymphadenectomy increases the incidence of pancreatic fistulas after distal pancreatic resections (Xia W et al, 2018).

For pancreatoduodenectomies, a major role in the development of postoperative pancreatic fistulas is the type of pancreato-digestive anastomosis. Pancreato-gastric anastomosis offers a series of advantages that reduce the risk of fistula, such as: (1) the location of the stomach in the proximity of the remaining pancreas; (2) rich vascularization of the stomach; and (3) gastric acid environment. Gastric acid environment has the role of inhibiting the activation of pancreatic enzymes, the rich vascularization of the stomach reduces the risk of ischemia in the pancreato-gastric anastomosis, and the anatomical location of the stomach and pancreas provides a decrease in tension of the anastomosis (Kitahata, Y et al, 2016). However, the use of pancreato-gastric anastomosis has a major disadvantage: it is associated with an increase in postoperative bleeding (Kitahata, Y et al, 2016; Pedrazzolo S, 2017). In a clinical study that observed the long-term effects of pancreato-digestive anastomosis, Benini et al. found that exocrine pancreatic function was much more affected after pancreato-gastric anastomosis, and was also associated with a decrease in vitamin D levels, and with malabsorption of fats (Benini L et al, 2019).

For these reasons, pancreato-jejunal anastomosis was preferred in our surgery department, and in most cases, it was “duct to mucosae”.

A controversial topic is the use of internal stents versus no stents for pancreato-jejunal anastomosis, but the majority of reviews did not report any differences in fistula rate, mortality, or morbidity (Pedrazzoli S, 2017).

Conclusions

Peritumoral fibrous tissue is not a factor involved in the development of POPF. The association of adenocarcinoma with areas of acute pancreatitis has led to a significant increase in POPF, as a significant and independent risk factor. Factors such as age, gender, and type of pancreatic resection had no role in the development of pancreatic fistulas.

2.2.2.2.2 Proposal of a Preoperative CT-Based Score to Predict the Risk of Clinically Relevant Pancreatic Fistula after Cephalic Pancreatoduodenectomy

The aim of the study was to assess the capability of independent parameters evaluated on a preoperative CT scan to predict the clinically relevant pancreatic fistula and to draw up a score based on a logistic regression analysis to detect high-risk patients.

Materials and Methods

Study Design and Patients

This retrospective study was approved by the Bioethics Committee of “Gr. T. Popa”, University of Medicine Iasi. We searched our prospectively maintained database for patients who underwent PD between 2015 and 2020 that also had an available preoperative multisequence CT scan of the abdomen.

The PD was performed for preoperative high suspicion of pancreatic head cancer or periampullary tumors. No distant metastases or borderline resectable tumors were noted preoperatively. We excluded patients where the marked atrophy of the pancreas did not allow the drawing of a sufficiently large region of interest (ROI) to determine the density of the pancreas and where the pancreatic resection was not performed at the level of the left margin of the superior mesenteric vein (SMV).
All the patients included in the study were represented by randomized numeric codes, and all personal data were hidden.

Surgical Procedure for PD
The surgical procedure consisted of a backwards Whipple (right posterior SMA-first approach), including a pylorus resection. All the patients had pancreaticojejunal temporarily stented "duct-to-mucosa" end-to-side anastomosis, hepaticojejunal end-to-side anastomosis and a side-to-side gastrojejunostomy. A standard lymphadenectomy was undertaken in all cases. The procedures were performed by the same surgical team. The mean operating time was about 5.5 h, with a mean blood loss of ~350 mL, consistent with the reported values in other centers. The patients were administered antibiotherapy up to the 3rd day after surgery, as far as no sign of infection was noted. All patients received a single dose of intraoperative Octreotide injection and intravenous H2 receptor antagonists each 12 h throughout the period of absent oral intake.
Peritoneal drainage was measured daily. An early postoperative CT scan was performed at days 8–12, followed by the removal of the draining tubes if no fistula or other complications were noticed.

Clinically Relevant Pancreatic Fistula
The pancreatic fistula is defined as a peritoneal drainage at more than 3 days after surgery of any quantity of fluid, with an amylase content of more than 3 times the seric amylase. The 2016 ISGPF classification and grading of pancreatic fistula makes a clear distinction between a biochemical leak (grade A) and clinically relevant fistula (grades B and C) (Bassi C et al, 2017). Grade B pancreatic fistula requires adjusting the clinical management with antibiotherapy, nutritional supplements, Somatostatin analog and percutaneous drainage. Grade C pancreatic fistula can result in sepsis, abdominal hemorrhage, multiorgan failure and even death.
Early postoperative CT images were assessed for the presence of fistulas, seen as fluid collections with or without gas, adjacent to the pancreatojejunal anastomosis (Hashimoto M et al, 2007).
MDCT Acquisition Protocol
For 55 of the 78 patients, the preoperative examination was performed using the 16-slice computed tomography (CT) scanner Somatom Sensation 16 (Siemens Medical Solutions, Erlangen, Germany) at a tube voltage of 140 kV, tube current of 150 mA, standard convolution kernel, mean reconstruction field of view of 37 cm and matrix size of 512 x 512.
The scanned volume extended from 2 cm above the diaphragm to the level of the pubic symphysis. Since our institution is a tertiary care center, 23 patients had preoperative CT acquisitions performed in other hospitals using nonstandard dynamic scan protocols. To minimize the effect of different slice thickness and reconstruction filters, we reformatted the images with a slice thickness of 5 mm and an increment of 4 mm, using the diagnostic capabilities of the diagnostic console Intellispace Philips 10 available at our institution.
The preoperative scan was performed after the patients ingested 500 mL of diluted contrast solution to facilitate the assessment of the anastomoses and the visualization of potential collections. When a nasogastric tube was present, it was clamped 1 h before the procedure.

Standard scan protocol included an unenhanced scan, an injection of iodine contrast media at a rate of 3 mL/s with bolus tracker monitorization in the upper abdominal aorta, followed by two scans timed at 15 s and 40 s after the threshold of 150 HU. An additional delayed scan was performed at 3 min after the injection of the contrast in most patients.

Investigated Parameters and Rationale:
Our study investigated the possibility of using imaging-only parameters for the assessment of the risk of clinically relevant pancreatic fistula, objectively quantifiable on widely available preoperative CT scans without taking into account the intraoperative parameters (blood loss, operative time and vascular resections) or disease-specific parameters (TNM staging and neoadjuvant therapy).
Liver steatosis, as a possible indication of associated metabolic disorders, was assessed using the density of the liver during unenhanced preoperative scans. For each patient, we acquired three measurements with a region of interest (ROI) of 1 cm2 and noted the mean value.
The density of the pancreas is useful both for the evaluation of the degree of lipomatosis and for the identification of the degree of fibrosis. The pancreatic density was measured with a ROI of 1 cm2 placed at the estimated level of resection, excluding vascular structures, tumoral tissue, calcifications and ductal ectasias while minimizing partial volume effects from the surrounding structures; three measurements were performed, and we noted the mean value on the unenhanced scans and in the arterial, venous and late scans (Fig. 2.18A).
We also investigated the difference between the density of the pancreas in the arterial phase and delayed phase as a possible indicator of fibrosis of the pancreas but were limited by the availability of the scans (not part of the standard protocol) or the inconsistency of the timing of the delayed scans (3, 4 and 10 min). The caliber of the main pancreatic duct was considered, as it is potentially useful in estimating the quality of the pancreaticojejunal -anastomosis. We noted the caliber of the duct at the estimated site of pancreatic resection (Fig. 2.18 B). An estimated remnant pancreatic volume was considered, as it can potentially influence the risk of pancreatic fistula, patients at a high risk having a greater pancreatic volume, with a greater surface area of the pancreato-entero anastomosis. Volume estimation was performed using the volumetric tools in Intellispace 10 software (Philips) using a clipping plane at the left of the superior mesenteric vein (Fig. 2.18 C,D).

Statistical Analysis
The statistical analysis began by inspecting the continuous variables for the normality of distribution using the Shapiro–Wilk test ($p > 0.05$), histogram analysis and z score. For the analysis of the correlation of the continuous numeric independent parameters with the clinically relevant pancreatic fistula (CRPF), we used a univariate analysis. Statistically significant independent parameters were used in the multiple logistic regression to evaluate the contribution of independent risk factors in the univariate analysis.
The predictive power of the models was analyzed using the area under the receiver operating characteristic curve (AUC) method. A concordance index > 0.8 was considered reliable In all statistical tests, a value of $p < 0.05$ was considered statistically significant.
All statistical tests were performed with SPSS version 23. To compare the strength of the proposed models, we first verified the correlation with the alternative fistula risk score (aFRS)using Spearman's correlation and then assessed the difference between them using the DeLong test in MedCalc Statistical software version 20.006.

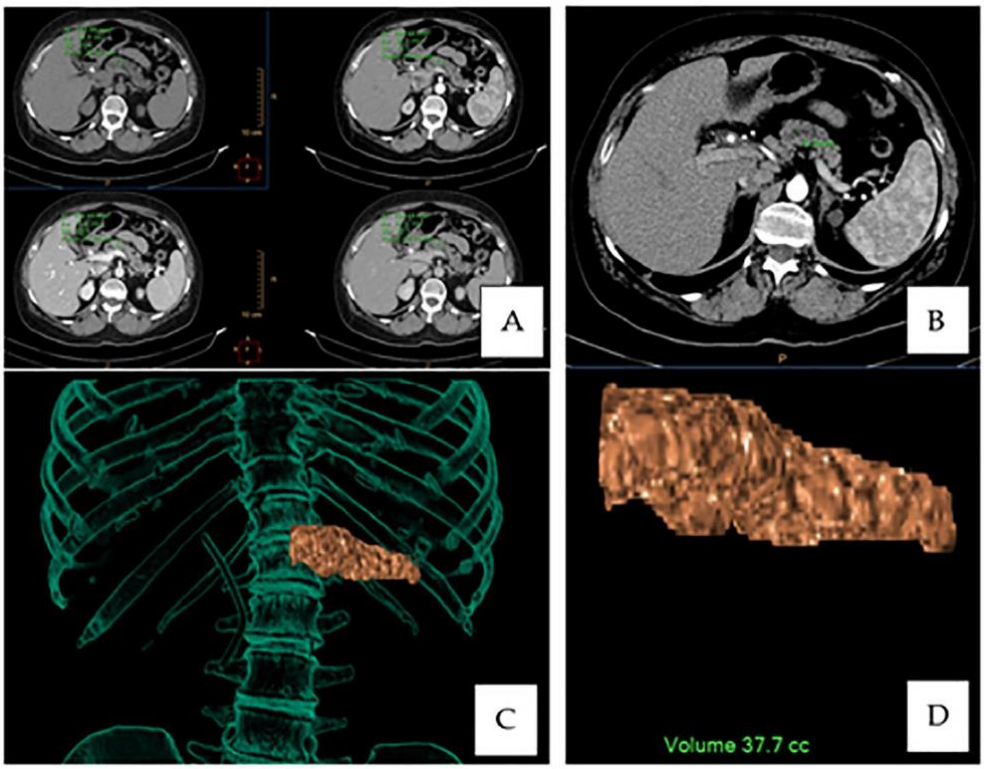

Fig. 2.18 Parameter acquisitions: (A) Pancreatic density on a multisequence CT scan at the site of resection. (B) Main pancreatic duct measurement. (C,D) Volumetric rendering overlay and estimated pancreatic remnant volume

Results

In total, 78 patients were enrolled in the study: 40 females (51.3%) and 38 males (48.7%), with a mean age of 59.33 years (SD 11.47) and a median body mass index (BMI) of 21 (IQR: 19–23) Kg/m2 (Table 2.VI).

A total of five independent parameters were found to be significantly different in the group with CRPF compared to the non-CRPF group: the unenhanced density of the liver (UDL), the unenhanced pancreatic density (UPD), the delayed scan density of the pancreas, the main pancreatic duct (MPD) diameter and the estimated pancreatic remnant volume (EPRV). Due to the unavailability of the delayed scan of the pancreas in all patients and the differences in the scan protocols between different centers (the timing of the delayed scans varied at 3, 4 or 10 min after the injection of contrast, which could potentially alter the validity of the acquired values), we excluded this parameter from further analysis. Additionally, because of the low number of cases, we tried to restrict the model to three parameters.

Table 2.VI Baseline characteristics of the retrospective group

Age, Mean (SD)	59.33 (11.47)	Disease, *n* (%)	
Sex (male), *n* (%)	38 (48.7%)	Pancreatic ductal adenocarcinoma	19 (24.35)
BMI, median (IQR) Kg/m^2	21 (19–23)	Chronic pancreatitis	7 (8.97)
ASA classification		Neuroendocrine tumor	4 (5.12)
I	18 (23.07%)	Cholangiocarcinoma	6 (7.69)
II	46 (58.97%)	Ampullary carcinoma	24 (30.76)
III-IV	13 (16.66%)	Duodenal carcinoma	12 (15.38)
Comorbidity, *n* (%)		Cystic neoplasms	2 (2.56)
Cardiac	16 (21.79%)	Other	5 (6.41)
Hypertension	17 (21.79%)	Pathology, *n* (%)	
Pulmonary	9 (11.53%)	Malignant	65 (83.33)
Diabetes mellitus	12 (15.38%)	Benign	13 (16.66)

BMI: Body Mass Index; IQR: Interquartile Range; ASA: American Society of Anaesthesiologists Physical Status.

Table 2.VII Univariate analysis of the independent factors and their association with CRPF

Independent Variable	Non-Clinically Relevant Pancreatic Fistula *N* = 56		Clinically Relevant Pancreatic Fistula *N* = 22		*p*-Value
	Mean	SD	Mean	SD	
Unenhanced density of the liver (HU)	50.54	SD 6.31	44.09	6.80	0.008
Pancreatic density (unenhanced)	32.42	11.93	22.24	11.49	0.02
Pancreatic density (arterial) (HU)	81.35	22.66	73.39	18.63	0.308
Pancreatic density (venous) (HU)	79.23	18.29	67.55	19.66	0.087
Pancreatic density (delayed scan) (HU)	61.28	16.55	48.67	18.05	0.045
Difference between the arterial and delayed density of the pancreas (HU)	19.45	20.32	24.7	15.39	0.42
Main pancreatic duct diameter (mm)	3.146	2.95	0.93	0.35	0.02
Total pancreatic volume (cm^3)	76.69	31.49	91.31	26.68	0.185
Estimated remnant pancreatic volume (cm^3)	34.87	12.35	46.37	10.39	0.01

Next, we verified the independence of the factors by analyzing the Pearson/Spearman's correlation of the factors, and we observed a correlation between the unenhanced density of the liver and the unenhanced density of the pancreas (r = 0.29, p = 0.07) and the main pancreatic duct diameter (rs = 0.14, p = 0.37), suggesting the need to exclude one of these parameters.

In the multiple logistic regression, we compared the predictive power of two models by using three factors, using both the MPD and the EPRV and differing in the third independent parameter. The predictive power of the model using the unenhanced pancreatic density preliminary proved to be higher than the one using the unenhanced density of the liver (92.3% compared to 84.6%). Given that marked pancreatic atrophy is frequent in pancreatic head cancers, we proceeded to investigate both models, with the second model potentially being used as an alternative in these patients.

Model 1 (using ERPV, MPD and UPD).

The logistic regression model predicted CRPF after pancreatectomy (Table 2.VIII).

The risk of CRPF was estimated using the formula $y = 1/(1 + e^{-z})$, where z = -1.114 + 0.155 x (EPRV) - 0.787 x (MPD) - 0.16 x (UPD). A result of > 0.5 estimated a significant risk for CRPF.

To create a practical score, we proceeded to the estimation of the cutoff values for the different parameters. Using the Youden method, we established a cutoff value of 41 cm3 for the ERPV (with a sensibility of 81.8% and a specificity of 71.4%) and 30 HU for the unenhanced density of the pancreas (sensibility 90.0% and specificity of 71.4%).

Table 2.VIII Multivariate logistic regression for model 1

	Weight (β)	Odds Ratio	*p*	CI	
				Lower	Upper
ERPV	0.155	1.168	0.02	1.025	1.330
MPD	−0.787	0.455	0.02	0.235	0.881
UPD	−0.160	0.852	0.032	0.736	0.986
Constant	−1.114				

ERPV: the preoperatively estimated pancreatic remnant volume; MPD: the main pancreatic duct diameter; UPD: the values of unenhanced pancreatic density.

We checked the correlation of the BMI with the unenhanced pancreatic density, as an expression of the metabolic status, using Spearman's correlation and found a low correlation, although without statistical significance (rs = -0.155, p = 0.167). Due to the non-gaussian distribution of the data for the pancreatic duct diameter, we proceeded to estimate the cutoff value for the main pancreatic duct by comparing the AUC of the model using different thresholds, starting from the maximum normal diameter (3 mm) and decreasing by 0.5 mm at each step, obtaining an optimum cutoff value of 2.5 mm.
Based on the odds ratio, we allocated points to the score, as shown in Table 2.IX.

Table 2.IX Proposed score for the assessment of risk of pancreatic fistula (Model 1)

Variable	Cutoff Value	Weight (β)	OR	Points Allocated	
ERPV (cm^3)	41 cm^3	0.155	1.168	If <41 cm^3 If ≥41 cm^3	0 points 2.5 points
Unenhanced density of the pancreas (HU)	30 HU	−0.160	0.852	If >30 HU If ≤30 HU	0 points 2 points
MPD diameter (mm)	2.5	−0.787	0.455	If >2.5 mm If ≤2.5 mm	0 points 1 points

ERPV: the preoperatively estimated pancreatic remnant volume; MPD: the main pancreatic duct diameter.

We scored 2.5 points for ERPV higher than 41 cm3, 2 points for UPD lower than 30 HU, 1 point for MPD diameter lower than 2.5 mm and 0 points for each of those conditions when they were not met.
We analyzed the distribution of the scores related to the clinically relevant pancreatic fistula and found that a score greater than 3 could identify patients at risk for CRPF with an AUC of 0.92 (95% CI: 0.828–1, sensibility 90.9% and specificity 67.9%) and with a positive predicting value of 47.82% and a negative predicting value of 100%, which suggests the score could correctly identify low-risk patients, although it could not accurately identify high-risk patients.
Using a cutoff score of 4.5 provided a slightly lower AUC of 0.846 (95% CI: 0.694–0.941), sensibility 72.72% and specificity 96.4%) but with a higher positive predictive value (88.88%) and an acceptable negative predictive value (90%), suggesting a good accuracy for the detection of high-risk patients. The mean probability of CRPF for patients with a score of more than or equal to 4.5 was 76.4% (95% CI: 7.35–21.3), compared with 13.84% (95% CI: 58.01–94.92) for scores below 4.5.
A Spearman's correlation comparison of the score derived from Model 1 to the aFRS showed a good correlation (rs = 0.633, p < 0.001). Next, we performed the DeLong test, showing a minor improvement of the AUC using our score compared to the aFRS (AUC 0.846 vs. 0.808) but without being statistically significantly better (p = 0.661) (Fig. 2.19).
Model 2 (using ERPV, MPD and UDL).

The risk of CRPF in this model was calculated using the formula $y = 1/(1 + e^{-z})$, where z = 7.219 + 0.138 x (EPRV) - 0.870 x (MPD) - 0.256x (UDL). A result of > 0.5 estimated a significant risk for CRPF.

We calculated the cutoff value for the UDL using the Youden method at 45 HU (sensitivity 76.4% and specificity 78.6%). Hepatic steatosis correlated with the BMI with a correlation coefficient rs = -0.130 and p = 0.334. Based on the odds ratio, we allocated points to the alternative score.

Comparison of ROC curves

Variable 1	aFRS (alternative Fistula Risk Score)
Variable 2	Model 1 score with a threshold of 4.5
Classification variable	CRPF (clinically relevant pancreatic fistula)

Sample size	78
Positive group [a]	22 (28.21%)
Negative group [b]	56 (71.79%)

[a] CRPF = 1
[b] CRPF = 0

Variable	AUC	SE [a]	95% CI [b]
aFRS	0.808	0.104	0.651 to 0.916
Model 1 score with a threshold of 4.5	0.846	0.0726	0.694 to 0.941

[a] DeLong et al. 1988
[b] Binomial exact

Pairwise comparison of ROC curves

aFRS - Model 1 score with a threshold of 4.5	
Difference between areas	0.0373
Standard Error [a]	0.0853
95% Confidence Interval	-0.130 to 0.205
z statistic	0.438
Significance level	$p = 0.6615$

[a] DeLong et al. 1988

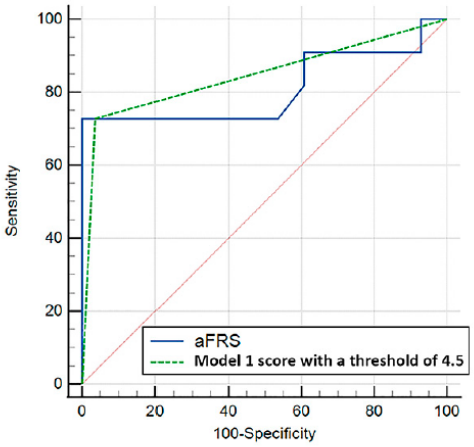

AUC comparison of aFRS and the score in Model 1 for the prediction of CRPF.

Fig. 2.19 Model 1

Table 2.X Alternative score using Model 2

Variable	Cutoff Value	Weight (β)	OR	Points Allocated	
ERPV (cm^3)	41 cm^3	0.138	1.148	If <41 cm^3 If ≥41 cm^3	0 points 3 points
Unenhanced density of the liver (HU)	45 HU	−0.256	0.774	If >45 HU If ≤45 HU	0 points 2 points
MPD diameter (mm)	2.5	−0.870	0.419	If >2.5 mm If ≤2.5 mm	0 points 1 points

ERPV: the preoperatively estimated pancreatic remnant volume; MPD: the main pancreatic duct.

In Model 2, we scored 3 points for ERPV higher than 41 cm^3, 2 points for UDL lower than 45 HU, 1 point for a MPD diameter lower than 2.5 mm and 0 points for each of those conditions when they were not met.

A risk stratification analysis (Figure 6) showed that a score greater than 4 produced an AUC of 0.774 (95% CI 0.599–0.850) with a sensibility of 72.7% and a specificity of 82.1%, a positive predictive value of 61.5% and a negative predictive value of 88.46%. The mean probability for CRPF for patients with a score > 4 was 60% (95% CI 37.87–82.13), compared to 12.3% (95% CI 3.79–20.81) for scores < 4. The correlation of the score model with the aFRS was found to be significant (rs = 0.524, p = 0.001). Comparison with the aFRS using the DeLong test showed no improvement over the aFRS (p = 0.715) (Fig. 2.20).

Comparison of ROC curves

Variable 1	aFRS (alternative Fistula Risk Score)
Variable 2	Model 2 score with a threshold of 4
Classification variable	CRPF (clinically relevant pancreatic fistula)

Sample size	78
Positive group [a]	22 (28.21%)
Negative group [b]	56 (71.79%)

[a] CRPF = 1
[b] CRPF = 0

Variable	AUC	SE [a]	95% CI [b]
aFRS	0.808	0.104	0.651 to 0.916
Model 2 score with a threshold of 4	0.774	0.0795	0.612 to 0.892

[a] DeLong et al. 1988
[b] Binomial exact

Pairwise comparison of ROC curves

aFRS - Model 2 score with a threshold of 4	
Difference between areas	0.0341
Standard Error [a]	0.0934
95% Confidence Interval	-0.149 to 0.217
z statistic	0.365
Significance level	$p = 0.7151$

[a] DeLong et al. 1988

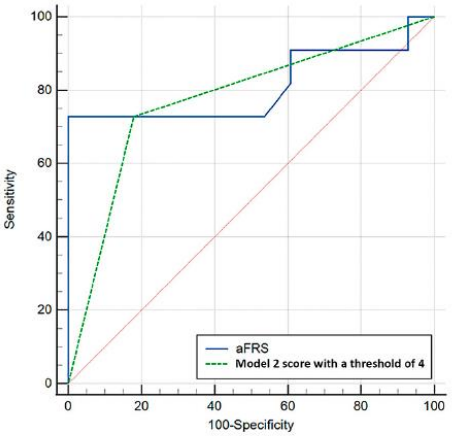

Fig. 2.20 Comparison of the alternative fistula score

Discussion

Predicting the risk of pancreatic fistula remains controversial, with multiple proposed scores in the literature when using pre-, intra- and postoperative parameters with different accuracy levels (AUC between 0.656 and 0.806) (Mungroop TH et al, 2019; Callery MP et al, 2013; El Nakeeh A et al, 2018; Chen JY et al, 2015). Although some studies noted the influence of the surgical technique on the risk of pancreatic fistula, other authors stated that the type of anastomosis and the placement of the pancreatic stent did not influence the risk of pancreatic fistula (Harrell FE et al, 1982)

Our study focused solely on evaluating the contribution of independent imaging parameters derived from preoperative contrast-enhanced computer tomography scans and confirmed a number of parameters correlating with the risk of CRPF: the unenhanced density of the liver (the degree of liver steatosis), the unenhanced density of the pancreas (pancreatic steatosis), the delayed density of the pancreas (a parameter that we further excluded because of the inconsistence and nonuniformity in the timing of the sequence between examinations), the main pancreatic duct diameter and the estimated remnant pancreatic volume. An investigation of the correlation of the metabolic status of the patient (expressed through the BMI) with liver/pancreatic steatosis showed only a mild correlation but did not provide statistically significant results, which could be a consequence of both the small sample size and the particularities of the cohort, as multiple patients had a diagnosis of chronic pancreatitis, caused by alcohol consumption, that can alter the measured density of the pancreas (Sharma P et al, 2020).

We proposed two scores that can be derived from a preoperatively obtained unenhanced CT scan of the abdomen using the following parameters: the unenhanced density of the pancreas at the estimated site of resection (to the left of the superior mesenteric vein) using a cutoff value of 30 HU, the main pancreatic duct diameter at the estimated site of anastomosis using a cutoff value of 2.5 mm, the estimated remnant pancreatic volume using a cutoff value of 41 cm3 and the unenhanced density of the liver using a cutoff value of 45 HU. Although the score using Model 1 (UPD, MPD and ERPV) showed a good performance compared to the aFRS, we derived a second score based on Model 2 (UDL, MPD and ERPV) that did not produce the same performance level but can be a useful alternative in patients with marked atrophy of the pancreas

(for whom the confident and reproductible measurement of the unenhanced pancreatic density can be difficult), a frequent situation in pancreatic head neoplasms.
Both scores showed a good sensibility and specificity for the prediction of clinically relevant pancreatic fistula. Although our data showed a mild improvement in the AUC analysis compared to the aFRS in the first model, it did not have a significant improvement when analyzed with the DeLong test, a situation that could be related to the intrinsic limitations
of the test when the model was developed and deployed on the same dataset (Demler OV et al, 2012)The good negative predicting value of the scores could be used in the selection of low-risk patients, for whom the complication of mitigation strategies could be adjusted- opting, for example, for a no-drain strategy—especially considering the complications that may occur because of the draining tubes (Witzigmann, H.; et al, 2016).
The proposed scores use objective, CT-based independent parameters, irrespective of the intraoperative parameters and histology, and might be an early and useful tool to tailor surgical procedures and postoperative strategies.
The technique employed for the establishment of the cutoff values had a limitation, as they are directly derived from the test set. In our dataset, the threshold value for the pancreatic duct size was found similar to the one found by Xia et al. (Xia W et al, 2018). Additionally, our study obtained a different cutoff value for the estimated remnant pancreatic volume as compared to Miyamoto et al. (Miyamoto V et al, 2018).
Another shortcoming of our study was the small number of patients, necessitating a further study to validate the proposed CT-based pancreatic fistula risk score.

Conclusions
Clinically relevant pancreatic fistula can be predicted using preoperative CT scan of the abdomen when using the following parameters: estimated remnant pancreatic volume, main pancreatic duct diameter, pancreatic steatosis and liver steatosis. We formulated two score-based models, the second one having a lower accuracy but useful as an alternative for patients with marked atrophy of the pancreas.

2.3.4 Artificial intelligence in predicting the risk of postoperative fistula

Pancreatectomy is the optimal treatment for most benign and malignant tumors of the pancreas. The mortality rate after PD, the most common type of pancreatectomy, remains significantly increased, of 10–28%, regardless the technique (with or without pylorus preservation), despite decreasing in recent decades (Richter A et al, 2003; Trede Met al, 1990; Adam U et al, 2004; DeOliveira M et al, 2006). Postoperative pancreatic fistula after PD favors the occurrence of intra-abdominal hemorrhage and severe peritonitis, and remains the leading cause of postoperative morbidity, increased hospitalization costs or even death.
Therefore, the identification of high-risk patients is crucial. Previous studies have recognized some predictive imaging factors: soft pancreas, pancreatic lipomatosis, pancreatic duct caliber, obesity (Hashimoto Y et al, 2010).
The objective of the current study is to validate machine learning models that predict with high accuracy clinically significant pancreatic fistula (grade B and C) after pancreatectomy, using images obtained by CT.
Deep learning based on image can predict postoperative fistula after pancreatectomy with high accuracy using CT images and has high potential for generalized applications in biomedical image interpretation and medical decision-making. Artificial intelligence (AI) has the potential to revolutionize diagnosis and management of diseases by carrying out classifications difficult for human experts and by fast review of huge amounts of images. Despite its potential, clinical interpretation and AI feasibility remain challenging.

The traditional algorithmic approach of image analysis for classification was previously based on (1) object segmentation performed manual, followed by (2) identification of each segmented object using statistical classifiers or superficial neural classifiers of machine learning-type designed specifically for each class of objects, and finally (3) classification images. Creating and perfecting more classifiers required many skilled people and time and it was expensive from computing point of view (Hoover A et al, 2003).
Development of convolutional neural network layers allowed significant gains in the ability to classify images and detect objects in an image (Krizhevsky A et al, 2017). It's about applying analysis filters or convolutions to multiple processing layers.
Abstracted representation of images within each layer is built transforming systematically multiple filters over the image, producing a feature map that is used as input for the next layer. This architecture allows image processing in pixel shape as input and giving desired classification as output. Approaching image-classification in a classifier replaces several stages of previous methods of image analysis.
A method to address data gaps of a particular domain is to use the data from a similar field, a technique known as transfer learning. Transfer learning turned out to be an extremely effective technique, especially in areas with limited data (Yosinski J et al, 2014). Instead of training a completely empty network, we use a feed-forward approach to set weightings at lower levels already optimized to recognize structures found in images in general and to retrain weights on higher levels with back-propagation. The model can recognize the distinctive characteristics of a particular category of images, such as images of the eye, much faster, with much fewer examples of training, and with less computing power.

Material and method.
Preoperative CT examination was performed between 2 and 58 days preoperatively (median = 21). For 28 of the 33 patients, early postoperative scanning was performed with a CT scan with Somatom Sensation 16 rows of detectors (Siemens Medical Solutions, Erlangen, Germany). The scanning field extended from 2 cm above the diaphragm to the level of the pubic symphysis.
We divided our study into 4 subgroups, depending on the sequences acquired (native and venous) and the type of pancreatic fistula (significant and insignificant) and classified them according to a normal state:
- native – significant/normal: train – 200/300, test – 109/113, validated – 8/8
- native – insignificant/normal: train – 300/300, test – 140/113, validated – 8/8
- venous – significant/normal: train – 300/370, test – 92/103, validated – 8/8
- venous – insignificant/normal: train – 400/370, test – 109/103, validated – 8/8.

Transfer learning
The fine-tuning of our model
The fine-tuning implementation consists of truncating the last layer (softmax layer) of the pre-trained network and replacing it with a new softmax layer that is relevant to our analysis.
Several neural network models were evaluated, which are summarised below.
1) MobileNet
MobileNet is an architecture that is more suitable for mobile-based and embedded viewing applications where computing power is lacking. This architecture was proposed by Google.
2) VGG16
Researchers from the Oxford Visual Geometry Group, or VGG for short, developed the VGG network, which is characterized by its simplicity, using only 3 x 3 convolutional layers stacked on top of each other, in increasing depth. Volume size reduction is done by max pooling. Finally, two fully connected layers, each with 4,096 nodes, are then followed by a softmax layer. Pooling is achieved through max pooling layers, which follow some of the convolution layers. Not all convolution layers are followed by max pooling. Max pooling is performed on a window of 2 x

2 pixels, with a pitch of 2. ReLU activation is used in each hidden layer. The number of filters increases with depth in most VGG variants (Fig. 2.21).

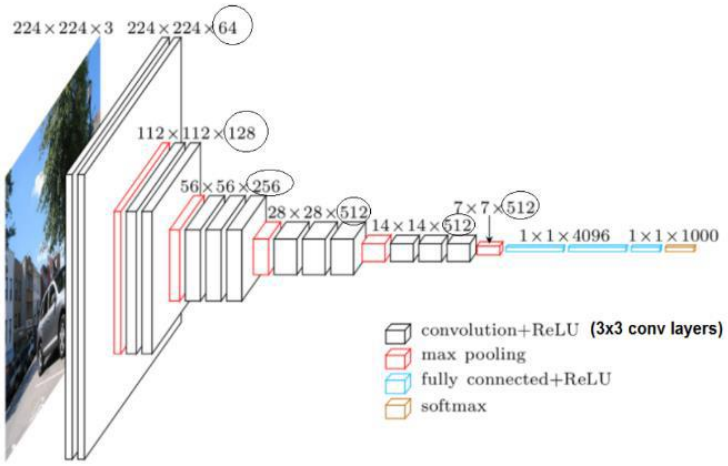

Fig. 2.21

3) CNN Model with 5-Hidden Layers
We apply 5 CNN (convolutional layer) with 3 * 3 kernel and "resume" activations.
4) Custom VGG model

Results
1) MobileNet 1 Model
Accuracy of the test is 85.135 %
Confusion Matrix
[[80 33]
[0 109]]

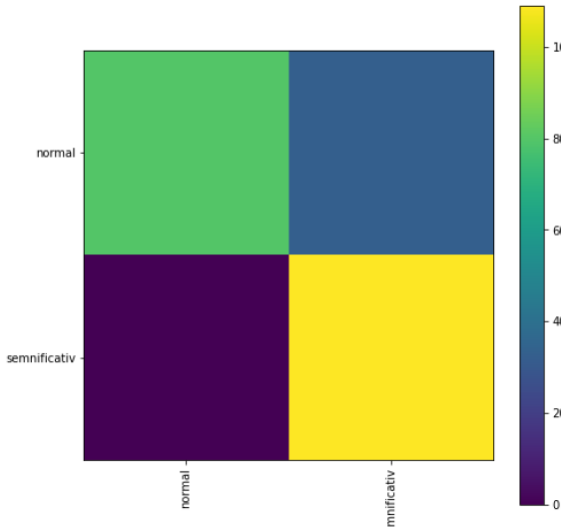

Fig. 2.22 Images that represent the significant fistula can be identified easily compared with normal images.

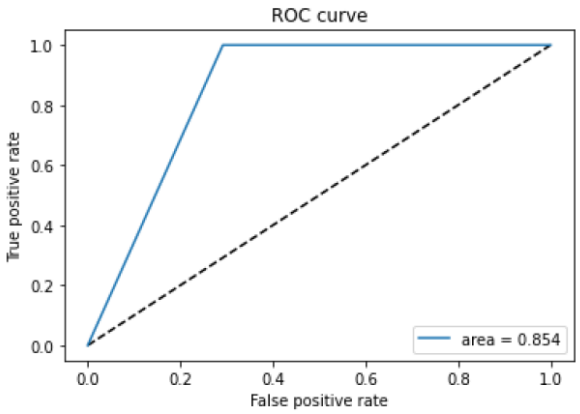

Fig 2.23 The result could be further improved by working with other models.

2) VGG16 model 2
Accuracy of the test is 100.00.
Confusion Matrix
[[113 0]

[0 109]]

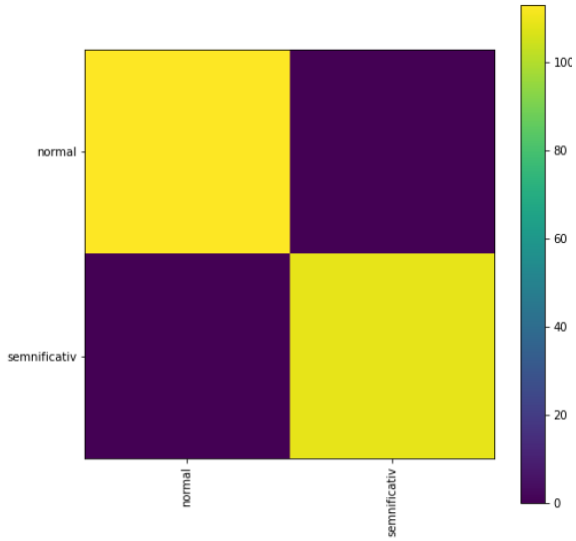

Fig. 2.24 In this model, normal images and those representing significant fistula can be identified easily and with maximum accuracy.

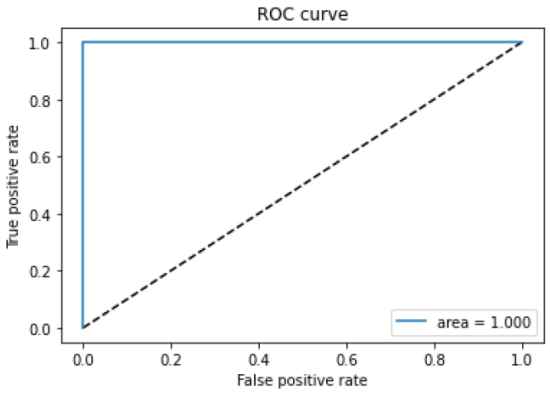

Fig. 2.25 ROC and AUC curve

3) CNN model with 5-Hidden Layers
Accuracy - Test result: 68.018 loss: 3.543
Confusion Matrix
[[113 0]
[71 38]]

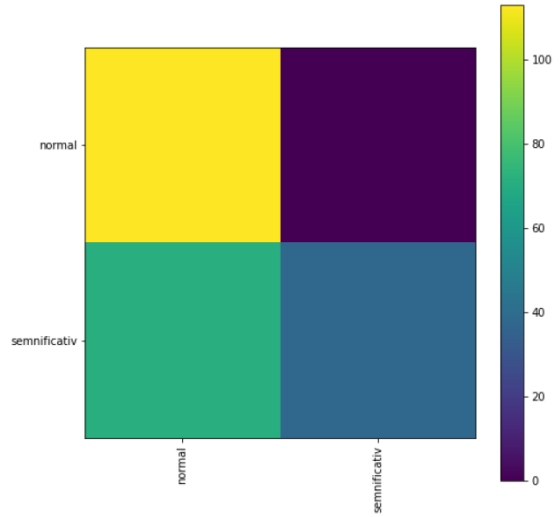

Fig. 2.26.Images that represent the normal state can be identified more easily than those that represent the significant fistula.

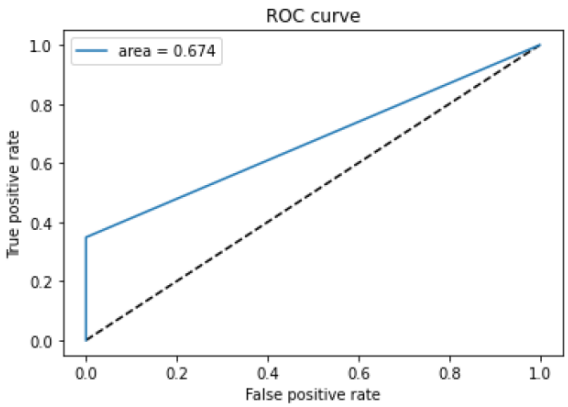

Fig. 2.27 ROC and AUC curves

4) Custom VGG Model
Confusion Matrix
[[0 113]

[0 109]]

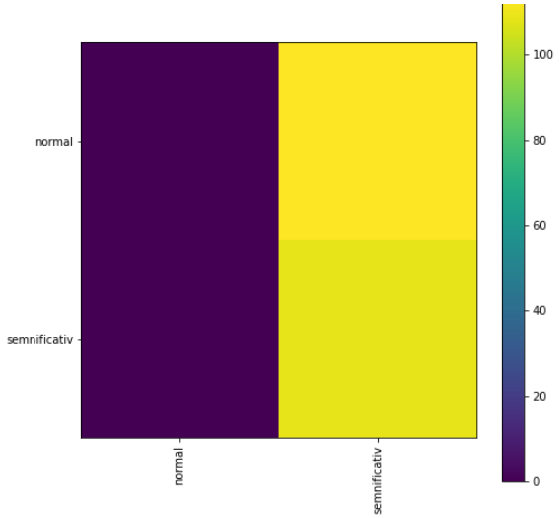

Fig. 2.27 The model correctly predicted all cases of significant fistula but got all normal cases wrong.

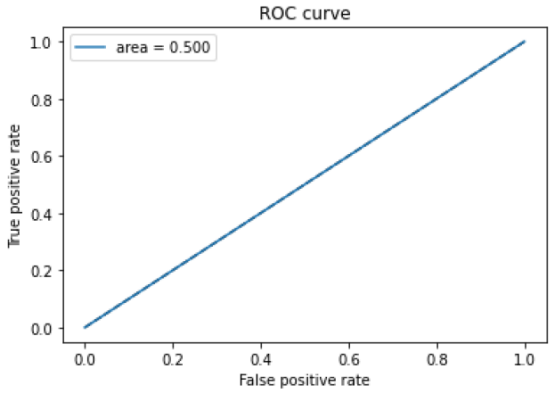

Fig. 2.28 ROC and AUC curves

Discussions

There are multiple scores aiming to quantify the risk of clinically significant pancreatic fistula. The score formulated by Callery in 2013 (fistula risk score FRS) uses intraoperative parameters, namely the presence of soft pancreas, diameter of the pancreatic duct, the presence of pathology other than adenocarcinoma and chronic pancreatitis, as well as intra-operative hemorrhage (Callery et al, 2013). Mungroop formulated an alternative score (a-FRS) based on simpler to estimate parameters, namely pancreas texture, Wirsung duct diameter, and body mass index Mungroop et al, 2019). The same author created an updated score, mainly for minimally invasive pancreatic surgery, but later validated for open surgery, which includes male gender as an additional factor (Mungroop TH et al, 2021). Kantor formulated in 2017 a similar score, also externally validated, which takes into account sex, body mass index, preoperative bilirubin level, diameter of the Wirsung duct and texture of the pancreas.

A meta-analysis published in 2021, based on 108 relevant studies, identified a four-type classification of pancreatic changes in pancreatic risk factors [96]. Type A includes non-soft pancreas with Wirsung duct diameter >3 mm. Type B refers to a non-soft pancreas <3 mm in diameter. Type C refers to a soft pancreas with a diameter of the Wirsung duct >3 mm. Type D includes patients with soft pancreas and Wirsung duct <3 mm. The risk of fistula increases substantially in type D (23.2%) versus type A (3.5%).

Recently, nomograms with high specificity have been created based on laboratory samples obtained on postoperative day 1.

The impact of prediction scores starts in the preoperative period, with evidence-based counseling, and continues intraoperatively and in the postoperative period, with adjustment of follow-up and management to minimize the impact of high-risk situations.

The current study investigated several image classification methods to assess the accuracy of the method in pre-operative detection of potential clinically significant pancreatic fistulas.

The prediction was possible using the VGG 16 model, without suffering from overfitting. The current study highlights machine learning-based training models. It is limited by the absence of

a validation study comparing it to traditional scores (fistula risk score and alternative fistula risk score).

Conclusions
Estimation of the risk of clinically significant pancreatic fistula benefits from implementations of machine learning algorithms, but requires validation on larger series and related to other risk scores.

2.2.3 Rare lesions of the pancreas

Articles

1. A Năstase, Ana-Maria Trofin, M Zabara, Ramona Cadar, Anda Năstase, Oana Lovin, Gh Balan, Lorena Marian, **Corina Lupașcu-Ursulescu**, C Lupașcu: Management of intraductal papillary and mucinous pancreatic neoplasms. Journal of Surgery [Jurnalul de chirurgie]. 2022; 18(2): 121 - 128.
2. **Lupascu-Ursulescu C**, Trofin AM, Zabara M, Vornicu A, Cadar R, Apopei O, Stefanescu G, Lupascu C. Bleeding from isolated gastric varices as complication of a mucinous cystic neoplasm of the pancreas. A case report. Medicine 2017; 96:47(e8775) (IF 2017 – 2,028)
3. Bar C, Negru D, **Ursulescu C,** Crumpei F, Georgescu Ș. Metastază pancreatică unică de la un carcinom renal cu celule clare. Prezentare de caz. Rev. Med. Chir. Soc. Med. Nat., 2006;110 (3), 646-649 (Index Medicus, Medline) ISSN: 0048-7848

2.2.3.1 Pancreatic metastasis

Pancreatic metastases are rare, generally found in patients with advanced tumors. A wide variety of primary non-lymphomatous tumors can metastasize into the pancreas; The most common sources are cancers of the lung, breast, kidney, gastrointestinal tract and, rarely, malignant melanoma, hepatocellular carcinoma and osteosarcoma (Scatarige JC et al, 2001; To'o KJ et al, 2005).
Due to their slow growth (Fritscher-Ravens A et al, 2001), most patients do not show specific symptoms when metastases are discovered incidentally by imaging during a regular check-up. Symptomatic cases may present weight loss, abdominal or lumbar pain, pancreatic endocrine or exocrine insufficiency, jaundice, gastrointestinal bleeding, signs of upper digestive tract obstruction. Pancreatic metastases can directly invade the ductal epithelium and thus mimic a pancreatic adenocarcinoma or, very rarely, induce acute pancreatitis (Peschaud F et al, 2002). Metastases from kidney cancer are commonly localized to the lung, liver, or bone (Law CH et al, 2003).
Secondary pancreatic lesions occur via the lymphatic route, but hematogenous spreading is also possible (Nagakawa T et al, 1994). Most of them are solitary, metachronous with the primary tumor (their occurrence was reported up to 16.5 years after nephrectomy). No predilection for a particular region of the pancreas was reported ((Law CH et al, 2003)).
Pancreatic metastases are commonly solitary mass, with large size at diagnosis, round or oval shape, relatively well defined; compression or obstruction of the main bile duct or pancreatic duct may occur. The hypervascular character of these nodules guides the imaging diagnosis toward renal origin.
Case report

We presented the case of a patient aged 51 years, with right nephrectomy performed 3 years ago for a stage II clear cell renal carcinoma, who was hospitalized in emergency for an episode of upper digestive bleeding (hematemesis and melena). Endoscopy revealed a friable tumor located at the level of the duodenal papilla. Clinical and biological examinations revealed severe anemia, with no signs of cholestasis. Abdominal ultrasound identifies in the head of pancreas the presence of a voluminous mass, with mixed echostructure (predominantly solid, hypoechogenic but with centrally located transonic, liquid areas). The mass has mass effect on the inferior vena cava and aorta (fig. 2.29). At the upper pole of the lesion, the corporeocaudal pancreas is identified, with upstream dilatation of the pancreatic duct. The bile ducts are non-dilated.

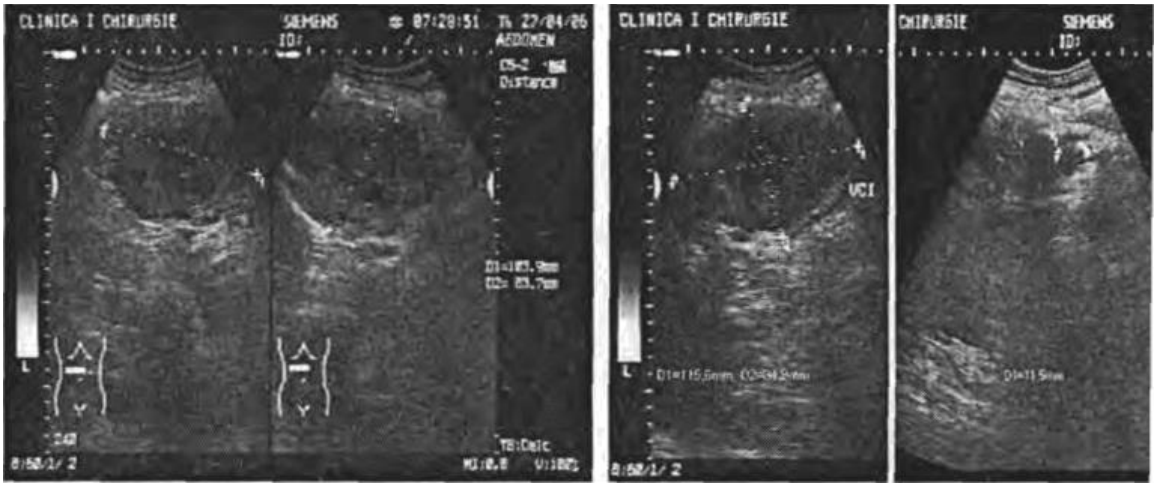

Fig. 2.29 Abdominal US: hypoechoic lesion with mass effect in the inferior vena cava.

Eso-gastroduodenal barium study revealed enlarged duodenal loop and multiple marginal lacunar images.

CT certifies the presence of solid mass anterior to large abdominal vessels, in the region of the cephalic pancreas, with intense enhancement after iodinated contrast medium injection and central necrosis. The lesion invades the walls of the second and third parts of the duodenum, the mass protruding into the lumen. The superior mesenteric vessels are deviated and partial thrombosis of the superior mesenteric vein was identified distally (fig. 2.30). The pancreatic duct is dilated in the body and tail of the pancreas ; the main bile duct is normal (Fig. 2.31).

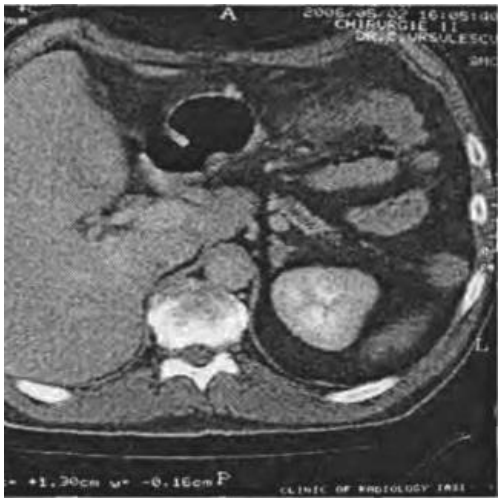

Fig. 2.30 CT: dilation of the pancreatic duct in the distal part of the pancreas.

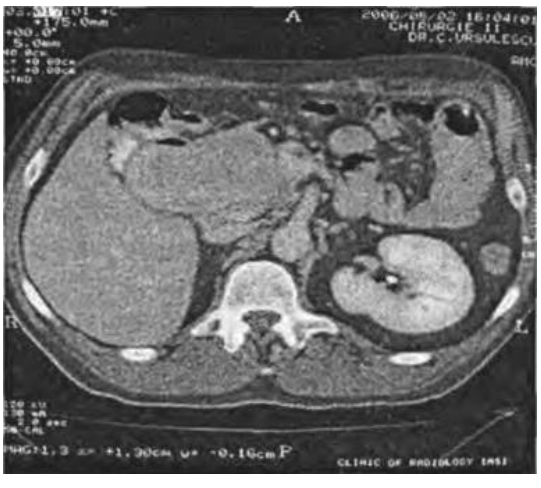

Fig. 2.31 CT: hypervascular mass in the region of the pancreatic head.

The hypervascular character of the lesion oriented the CT diagnosis towards a unique pancreatic metastasis from renal cell carcinoma. The patient received surgical treatment (pancreatoduodenectomy). The pathological examination of the resected specimen confirms the diagnosis.

Discussion

Pancreatic metastases of renal cell carcinoma can raise problems for diagnostic imaging. Gray-scale ultrasound has difficulties in exploring the pancreatic gland and has no specificity for these secondary lesions. Doppler ultrasound has a better sensitivity highlighting their hypervascular character. Eso-gastroduodenal barium study, like ultrasound, lacks specificity. CT shows a hypervascular mass (intense and early uptake in the arterial phase), nonhomogeneous by areas of central necrosis in large lesions. Eco-endoscopy is difficult to perform in the presence of a bulky mass or in the case of a caudal pancreatic localization. Biopsy of the lesion is not routinely done due to the potentially severe bleeding.

Early diagnosis enables a curative surgical resection (depending on the topography of the lesion), the only treatment with impact on survival of these patients (Law CH et al, 2003). Chemotherapy and immunotherapy may play a role, after resection, in case of lymph node invasion or tumor remnant (Peschaud F et al, 2002).

2.2.3.2 Management of intraductal papillary and mucinous pancreatic neoplasms

Introduction

Pancreatic cystic lesions are clinically challenging, and the management of these lesions is controversial to this day. Prevalence of pancreatic cystic lesions range between 2 and 45% (Ip IK et al, 2011; Girometti R et al, 2011) in the general population by age. The most common cystic pancreatic lesions are intraductal papillary and mucinous neoplasms (IPMN), mucinous cystic tumors, serous cystadenoma and pseudocyst (Feixiang Hu et al, 2022). Risk of malignant degeneration depends on the type of lesion. An accurate diagnosis is important for a correct management, to establish the risk of malignant degeneration and decide the need for surgery. European Study Group on Cystic Tumours of the Pancreas published in 2018 the European recommendations, one year after the Revisions of international consensus Fukuoka guidelines for the management of IPMN of the pancreas pulished by Masao Tanaka (Tanaka M, et al, 2017).

Imaging protocole

Prevalence of pancreatic cystic lesions range from 2.1 to 2.6% for CT studies and between 13,5 and 45% for MRI (Girometti R, 2011; Lee KS, et al, 2010). This discrepancy between the two examinations is due to higher resolution of MRI. The accuracy of imaging is relative low in determining the type of cyst, or establishing the reports with the pancreatic ductal system, both for single imaging exams as well as for association of multiple exams. Thin-slice CT with three-phase injection (dedicated protocol for pancreas) and pancreatic MRI examination (with sequences for pancreatic ducts) provides information of similar accuracy in characterization of pancreatic cysts (Chaudhari VV et al, 2007; de Jong K et al, 2012). However, MRI is more sensitive than CT in terms of identification of communication with pancreatic ductal system, as well as detection of a mural nodule or septa. In addition, MRI is very sensitive to identify multiple cysts, multiplicity being in favor of IPMN (Sahani DV et al, 2013). Patients diagnosed with IPMN may require lifelong imaging surveillance, and MRI is preferred to avoid repeated exposure to radiation (Chaudhari VV et al, 2007; de Jong K et al, 2012).

However, CT is routinely used to detect intracystic calcifications and for the loco-regional and distant staging of malignant cystic tumors (Curry CA et al, 2000; Soloff EV et al, 2018).

The typical appearance of a branch-duct IPMN is of a cystic dilation communication with pancreatic duct. On MRI, this lesion has hypersignal on T2-weighted sequences. It is necessary however, to avoid overestimation of the communications between the cystic lesion and the pancreatic duct on MRI, when the communication is not obvious. A diffuse dilation more than 5 mm in diameter of the main pancreatic duct evokes an IPMN of the main duct (MD-IPMN) (Crippa S et al, 2020).
A honeycomb appearance on CT and MR with a central scar that associates calcifications is suggestive of a serous cystadenoma.
High risk factors for degeneration (high risk stigma) are (Gut, 2018):
- Inclusion of the main pancreatic duct dilated more than 10 mm;
- The presence of a tissular pancreatic mass;
- The presence of an intracystic mural nodule over 5 mm with contrast enhancement;
- Jaundice caused by the mass effect;
- Positive cytology for dysplasia of high-grade or adenocarcinoma in fine needle aspiration by endoscopic ultrasound.

Conclusion
Pancreatic mucinous and papillary cystic neoplasm represent a pathology controversial both for diagnosis and for management. There are today effective criteria and diagnostic modalities (endoscopic, imaging and histopathological). High risk factors should be identified to select the appropriate treatment.

SECTION II

FORTHCOMING PROJECTS AND DEVELOPMENT IN MY ACADEMIC CAREER

II. 1. PROJECTS IN THE ACADEMIC FIELD

The main goal of the academic career is to create a high-quality teaching interaction with medical students. This quality depends upon several factors, such as high-quality information (according to the newest information available, confirmed by evidence-based medicine) presented in interesting manners, easy to understand and intriguing the student's interest, correlated with information from other fields of medicine (anatomy, internal medicine, surgery, pathology). All these should guarantee the success of the knowledge transfer towards the future generations of doctors. I will continue to prioritize this objective in my future academic activity. The means to accomplish this objective are:

- Updating the teaching resources (such as presentations, printed manual, practical guides);
- Improving the student-centered teaching method, more interactive and participative for students;
- Improving the accessibility of scientific language, especially of radiology-specific terms, through explanation, examples and conclusive correlations;
- Use of various technological tools (computer, web sites, etc.) for teaching/ training;
- More dynamic assessment of knowledge and skills, allowing a personalize improvement during the semester;
  Involvement of students in case reports for clinical sessions and case series presentation for medical students' congresses; this activity can be criteria of selection for undergraduate students who want to elaborate their license theses in radiology;
- Organizing more workshops based on image interpretation during medical students congresses and conferences, even outside the basic curriculum for the 4^{th} year, which proved to be a very useful experience in the last years not only for Romanian students, but also for students from French series and English series;
- Introduction of a new optional course for the 5th year French series, to enlarge the possibility of discussing cross-sectional imaging in various fields of medicine.

Another objective of my teaching activity is to re-establish at our University a line of study dedicated to technicians in radiology. Over the past 20 years, we have witnessed a continuous development of radiology and medical imaging techniques, especially cross-sectional and hybrid imaging. This unprecedented development of techniques has been matched by one of radiology and imaging equipment, as well as an impressive increase in the number of radiology and medical imaging equipment used both in our university center and in the North-East Region. Radiology technicians handle this equipment for acquisition of quality examinations, enabling an optimal diagnosis by the radiologist. Therefore, extensive knowledge of conventional radiology, ultrasonography, cross-sectional techniques (computed tomography and magnetic resonance imaging, and of hybrid techniques (PET-CT, PET-MRI) is required and can be achieved only in an academic environment.

An important compound of teaching activity is post-graduated teaching. We have large series of well-trained residents in Radiology, already selected by a rigorous exam (in the last years,

radiology was among the first 5 specialties chosen by the students with high score at the national exam of residency). We follow the national curricula during the 5 years of training, but we also encourage the participation to international courses and congresses. To improve the assimilation of knowledge during the training period in Radiology, I will continue to encourage individual work, but also to organize the residents in work teams, with the purpose of developing the team spirit, the capacity of others' analysis and self-assessment, of encouraging the research projects and the elaboration of presentation for national congresses and conferences and for international congresses. I would also like to conduct regular sessions, once a week, to discuss latest studies/ articles published in the national/ international scientific flow, especially the guidelines regarding the indications of imaging, the algorithm of examination, the standardization of reporting image studies, and new developed techniques. Also, I will stress more the importance of interdisciplinary approach and the participation in multidisciplinary teams as a necessary step to validate the results of imaging studies and to improve treatment efficiency and patient care. A special attention will be focused on study and exam preparation according to recommended learning resources (permanent updating of course and bibliography based on scientific literature – books, articles, websites etc.). In the last years, I started, and I will continue the guidance of foreign students that perform internships within the department or began a residency program as non-EU citizens. I believe that this is a very useful way of exchange information on the level of training and education in radiology around the world. It was also a way to achieve certain important external links.

I will further participate as course director or a guest lecturer at CME and post-graduate courses for specialists, under the auspices of University and Medicine "Grigore T. Popa" Iasi, to permanently inform our former residents about recent developments and advances in radiology.

As a future PhD and post-doctoral tutor, I will be actively involved in selecting the appropriate doctoral research topic for each PhD student, identifying funding sources for conducting research, supervising research and dissemination of the results through presentations at conferences and full text articles. I will guide the elaboration of the doctoral thesis at high standards that may allow graduation and obtaining the title of Doctor in medicine.

II.2 PERSPECTIVES IN MEDICAL PRACTICE

Concerning my medical professional area, I will continue to be a dedicated radiologist, both in the field of diagnostic imaging and of interventional radiology. Medical imaging is a continuously evolving branch of medicine, with new development every year. Being connected to the latest recommendations of radiological societies, as well as to ever-changing demands of medical practice is therefore a necessity.

I will be permanently involved in updating the imaging protocols in our hospital and improving daily medical practice.

I will continue my activity in the multidisciplinary team involved in liver transplantation in St. Spiridon Hospital Iasi and I will propose the creation of a multidisciplinary team to manage focal liver lesions in our hospital.

As a coordinator for residency program in Radiology, I will continue to improve the practical activities of residents, who are already involved in all practical aspects of our specialty. A permanent feed-back from senior radiologist supervising their activity is mandatory to make personalized improvements.

Developing the interventional radiology in our country is an important goal of the Romanian Society of Neuroradiology and Interventional Radiology and I intend to contribute through my efforts to develop the techniques in St. Spiridon Hospital Iasi, one pioneer-center in this field in Romania. As a local coordinator of a National Health Program in Interventional Radiology, I intend to enlarge the type of procedures of interventional radiology practiced in our hospital, as

well as to better disseminate information about indications, patient selection, contraindications of various interventional procedures to our colleagues from other specialties.
Clinical activity is also the base of my research activity and, both, improves the results of teaching activity.

II.3 PROJECTS FOR SCIENTIFIC RESEARCH

Radiology is interconnected with almost all medical and surgical disciplines and the clinical research is usually multidisciplinary. I will continue my future scientific activity integrated in research groups from St. Spiridon Hospital Iasi and "Grigore T. Popa" University, within I have elaborated my main studies so far and I will be opened to new opportunities for research.
As I mentioned in first section, my capacity to work in multidisciplinary teams and to coordinate research teams, to organize and manage research activities was developed over the last 18 years as a member of national and international research projects.
Research work involves time, talent, teachers, training, team, often sophisticated hardware, and financial support. With all these resources targeted, my future directions of study will be focused on :

1. <u>Development of new techniques for focal lesions ablation, especially thermal ablation, under imaging guidance.</u>
Image-guided focal lesion ablation, especially thermal ablation has become the standard practice in some well-defined situations, like treatment of malignant liver tumors, but also a practice with indications that are permanently extending to other organs (kidney, metastatic lung tumors) or other medical situations (pain management, etc). CT is widely used for guiding ablation procedures.
This type of activity is not well-developed in the medical university center of Iasi and our multidisciplinary hospital has many situations who are treated only by alternative methods.

2. <u>Imaging studies and interventional radiology in liver transplantation</u>
Since 2016, a Regional Centre of Liver Transplantation developed in St. Spiridon Hospital Iasi. A multidisciplinary team of gastroenterologists, immunologists, pathologists, surgeons, anesthesiologists, and radiologist is involved in management of patients on the waiting list and those receiving a liver graft. Pre-, intra- and postoperative imaging is required for optimal selection of patients, assessment of vascular anastomosis and postoperative follow-up. With more than 40 patients who benefited from this definitive solution for treatment of liver cirrhosis in our center, experienced has gained also in liver transplant imaging. I had the opportunity to be involved mainly in intraoperative imaging and postoperative follow-up, especially in the early postoperative period. The majority of acute complications appeared in the early postoperative period and requires prompt diagnosis and management, imaging being essential for diagnosis. Long-term results are influenced by appearance of steatosis after liver transplantation and of neoplasia. Non-alcoholic liver disease is not only an increasing cause of liver transplantation, but it also might occur after transplantation, as recurrence of the disease or de novo hepatic steatosis, with a prevalence ranging from 30–60% in different studies (Kappus and Abdelmalek, 2017; Eshraghian et al., 2020). Some imaging methods are now used to quantify hepatic steatosis. Chemical shift–encoded MRI is now established as the most accurate and precise method for liver fat quantification. CT is important for the detection and quantification of incidental steatosis and may play an increasingly prominent role in risk stratification, particularly with the emergence of CT-based screening and artificial intelligence. Quantitative imaging methods are increasingly used for diagnostic work-up and management of steatosis, including treatment monitoring.
We are planning several prospective studies in liver transplantation:

- a prospective study to quantify liver graft steatosis (measured by MRI) in our group of patients, and correlate it to metabolic risk factors.
- a study on sarcopenia before and after liver transplantation, measured by L3 Skeletal Muscle Index Dynamics.
- a prospective study on pleural effusion in early postoperative period (based on image features and characterization of fluid by image-guided puncture);
- a prospective study on changes of Doppler ultrasound parameters during the sepsis, applied to the vascular anastomosis of the graft, especially for vascular inflow;

3. **Standardization of the results of chemoembolization for hepatocellular carcinoma by** creating a more comprehensive score based on complex imaging and biological parameters to predict its outcome.

TACE has been associated with a wide range of practice pattern, with variations for HCC between different medical centers and different countries. There is even considerable variability among the physicians practicing within the same institution, reported in the literature and a daily concern of our practice (Marrero JA et al, 2018; Kokudo N et al, 2015). This considerable ambiguity may lead to the heterogeneous quality in treatment and have a negative impact on the role of TACE in the overall multidisciplinary HCC treatment system. Some consensus statements were organized concerning patients' selection, procedural
technique, TACE outcomes, repeat TACE and TACE failure/refractory, and TACE-based combination treatments.

To deal with this great variability and to improve selections of patients with real benefit from this treatment, several scores were developed and are used in medical practice.

We intend to identify from our database the clinical, biological or technical elements that can predict the outcome after the procedure and to create a comprehensive score.

4. Development of Artificial intelligence in hepatobiliary and pancreatic imaging

Even if artificial intelligence (AI) was developed in the sixth decade of the past century, its importance has rapidly increased in medicine in the last ten years, with various clinical applications. Radiology has become a main field of interest for AI, because of the very large number of images and time-consuming interpretation process. Several programs were developed first to assist the radiologist for diagnosis and then to diagnose some specific diseases. Such programs are now in use for pulmonary embolism, detection of lung nodules, identification of abnormalities on chest X-ray, etc.

Computer models were developed, and several deep learning models were also proposed for other pathology. One of the limits of AI is the result of differences in digital resources and economic status of countries, which decide the access to the latest progresses. Moreover, the results given by AI should be continuous and firmly validated, so large teams of radiologist and computer scientists are working together and permanently to improve the algorithm. Supplementary studies and new data are necessary to give AI a valuable place and to ensure the right balance between AI as a useful and a dominating tool.

The pilot study we performed with AI in predicting the risk for pancreatic fistula was a promising step.

Therefore, we will actively continue this project, aiming to validate the created score for postoperative pancreatic fistula risk and to incorporate it into a soft that can produce a report of fistula risk in the same time with staging report. Moreover, AI can be used to improve selection of patients for chemoemolisation, and we intend to correlate these two projects (development of a valid score and of a computer program to select patients who will benefit from this procedure).

In **conclusion**, throughout my career I will continuously be concerned on developing new skills, knowledge and aptitudes for research and education. Taking into account the above selected scientific, academic and research postdoctoral works in two fields of interest, the main future guide marks of my career, can be synthetized as follows:

- as a teacher with an impact in the academic community, I will improve my skills, including a solid scientific education, communication abilities, coordinating functional entities.
- preferential support and maximal exploitation, efficient interdisciplinary and interprofessional use of equipment and human experience.
- encouragement and improvement of the participation of the residents, PhD and post PhD researchers in different programs, as well as in the translation of research results in daily practice.
- development of the research infrastructure of the Department of Radiology, University of Medicine and Pharmacy "Gr. T. Popa" Iasi.
- development of new research teams, based on national and international priorities, human and technical possibilities.
- assessment and research new directions according to European trends and with financing opportunities through national and international grants.

SECTION III

REFERENCES

Abdel-Daim MM, Dessouki HG, Abdel-Rahman R, Eltaysh AA, Alkahtani S. Hepatorenal protective effects of taurine and N-acetylcysteine against fipronilinduced injuries: The antioxidant status and apoptotic markers expression in rats. Sci Total Environ. 2019;650 (Pt 2):2063-2073.

Adam U, Makowiec F, Riediger H, Schareck WD, Benz S, Hopt UT. Risk factors for complications after pancreatic head resection. Am J Surg. 2004;

Addeo, P.; Delpero, J.R.; Paye, F.; Oussoultzoglou, E.; Fuchshuber, P.R.; Sauvanet, A.; Cunha, A.S.; Le Treut, Y.P.; Adham, M.; Mabrut, J.; et al. Pancreatic fistula after a pancreaticoduodenectomy for ductal adenocarcinoma and its association with morbidity: A multicentre study of the French Surgical Association. HPB 2014, 16, 46–55.

Ahmed S, Chia CL, Junnarkar SP, Woon W, Shelat VG. Percutaneous drainage for giant pyogenic liver abscess--is it safe and sufficient. Am J Surg. 2016;211(1):95–101.

Ahmed S, Chia CL, Junnarkar SP, Woon W, Shelat VG. Percutaneous drainage for giant pyogenic liver abscess: is it safe and sufficient? Am J Surg. 2016;211(1):95-101.

Akhan O, Ozmen MN. Percutaneous treatment of liver hydatid cysts. Eur J Radiol. 1999;32(1):76–85

Albrecht T, Oldenburg A, Hohmann J, et al (2003a) Imaging of liver metastases with contrast-specific low-MI realtime ultrasound and SonoVue. Eur Radiol 13(Suppl 3): N79–86

Albrecht T. Sonography of Liver Metastases. In R. Lencioni, D. Cioni, C. Bartolozzi (Eds.) Focal Liver Lesions. Detection, Characterization, Ablation. Springer-Verlag Berlin Heidelberg 2005, 261-274

Aldini AG, Altomare, Baron G, Vistoli G, Carini M, Borsani M, et al. NAcetylcysteine as an antioxidant and disulphide breaking agent: The reasons why. Free Radic Res.2018;52(7): 751-762.

Alghamdi, A.A.; Jawas, A.M.; Hart, R.S. Use of octrotide for the prevention of pancreatic fistula after elective pancreatic surgery: A systematic review and meta-analysis. Can. J. Surg. 2007, 50, 459–466.

Allen, P.J.; Gönen, M.; Brennan, M.; Bucknor, A.A.; Robinson, L.M.; Pappas, M.M.; Carlucci, K.E.; D'Angelica, M.I.; DeMatteo, R.P.; Kingham, T.P.; et al. Pasireotide for Postoperative Pancreatic Fistula. Ne. Engl. J. Med. 2014, 370, 2014–2022

Al-Osaimi AMS, Caldwell SH. Medical and endoscopic management of gastric varices. Semin Intervent Radiol 2011;28:273–82

Amaral EP, Conceição EL, Costa DL, Rocha MS, Marinho JM, Cordeiro-Santos M, et al. N-acetyl-cysteine exhibits potent anti-mycobacterial activity in addition to its known anti-oxidative functions. BMC Microbiol. 2016;16(1):251.

Asrani, S.K.; Devarbhavi, H.; Eaton, J.; Kamath, P.S. Burden of liver diseases in the world. J. Hepatol. 2019, 70, 151–171.

Awaya, H.; Mitchell, D.G.; Kamishima, T.; Holland, G.; Ito, K.; Matsumoto, T. Cirrhosis: Modified Caudate–Right Lobe Ratio. Radiology 2002, 224, 769–774.

Bachofner, J.A.; Valli, P.V.; Kröger, A.; Bergamin, I.; Künzler, P.; Baserga, A.; Braun, D.; Seifert, B.; Moncsek, A.; Fehr, J.; et al. Direct antiviral agent treatment of chronic hepatitis C results in rapid regression of transient elastography and fibrosis markers fibrosis-4 score and aspartate aminotransferase-platelet ratio index. Liver Int. 2017, 37, 369–376.

Badea R. Ficatul În: Dudea S, Badea R (ed): Ultrasonografie vasculară. Ed. Medicală București, 2004

Balachandra S, Siriwardena AK. Systemic appraisal of themanagement of the major vascular complications of pancreatitis.Am J Surg. 2005;190(3):489-95

Balthazar EJ, Fisher LA. Hemorrhagic complications of pancrea-titis: radiologic evaluation with emphasis on CT imaging.Pancreatology. 2001;1(4):306-13.

Barker DW, Zagoria RJ, Morton KA, Kavanagh PV, Shen P. Evaluation of liver metastases after radiofrequency ablation: utility of 18F-FDG PET and PET/CT. AJR Am J Roentgenol. 2005 Apr;184(4):1096-102.

Bassi, C.; Marchegiani, G.; Dervenis, C.; Sarr, M.; Abu Hilal, M.; Adham, M.; Allen, P.; Andersson, R.; Asbun, H.J.; Besselink, M.G.; et al. The 2016 update of the International Study Group (ISGPS) definition and grading of postoperative pancreatic fistula: 11 Years After. Surgery 2017, 161, 584–591.

Bassi, C.; Molinari, E.; Malleo, G.; Crippa, S.; Butturini, G.; Salvia, R.; Talamini, G.; Pederzoli, P. Early versus late drain removal after standard pancreatic resections: Results of a prospective randomized trial. Ann. Surg. 2010, 252, 207–214.

Beland MD, Gervais DA, Levis DA, Hahn PF, Arellano RS, Mueller PR. Complex abdominal and pelvic abscesses: efficacy of adjunctive tissue-type plasminogen activator for drainage. Radiology. 2008;247(2):567-73.

Ben Amor N, Gargouri M, Gharbi HA, Golvan YJ, Ayachi K, Kchouck H. Trial therapy of inoperable abdominal hydatid cysts by puncture. Ann. Parasitol. Hum. Comp., 61, 1986, p. 689-692.

Benini, L.; Gabbrielli, A.; Cristofori, C.; Amodio, A.; Butturini, G.; Cardobi, N.; Sozzi, C.; Frulloni, L.; Mucelli, R.P.; Crinó, S.F.; et al. Residual pancreatic function after pancreaticoduodenectomy is better preserved with pancreaticojejunostomy than pancreaticogastrostomy: A long-term analysis. Pancreatology 2019, 19, 595–601.

Bergert H, Hinterseher I, Kersting S, Leonhardt J, BloomenthalA, Saeger HD. Management and outcome of hemorrhage due toarterial pseudoaneurysms in pancreatitis. Surgery. 2005;137(3):323-8.

Bernardino M.E. Percutaneous biopsy. AJR, 1984, 142: 41-45.

Bhatti J, Nascimento B, Akhtar U, Ghind SG, Tien H, Nathens A, et al. Systematic review of human and animal studies examining the efficacy and safety of Nacetylcysteine (NAC) and N-acetylcysteine amide (NACA) in traumatic brain injury: Impact on neurofunctional outcome and biomarkers of oxidative stress and inflammation. Front Neurol. 2018;8:744.

Bluemke DA, Abrams RA, Yeo CJ, Cameron JL, Fishman EK. Recurrent pancreatic adenocarcinoma: Spiral CT evaluation following the Whipple procedure. Radiographics 1997; 17 (2): 303-313

Bluemke DA, Paulson EK, Choti MA, et al (2000) Detection of hepatic lesions in candidates for surgery: comparison of ferumoxides-enhanced MR imaging and dual-phase helical CT. AJR Am J Roentgenol 175:1653–1658

Boggi, U.; Del Chiaro, M.; Croce, C.; Amorese, G.; Signori, S.; Vistoli, F.; Di Candio, G.; Campatelli, A.; Morelli, L.; D'Imporzano, S.; et al. Vascular complications of pancreatectomy. JOP J. Pancreas 2007, 8 (Suppl. 1), 102–113.

Boutin, R.D.; Yao, L.; Canter, R.J.; Lenchik, L. Sarcopenia: Current Concepts and Imaging Implications. Am. J. Roentgenol. 2015, 205, W255–W266.

Bray F, Ferlay J, Soerjomataram I et al. Global cancer statistics 2018: GLOBOCAN estimates of incidence and mortality worldwide for 36 cancers in 185 countries. CA Cancer J Clin 2018; 68:394-424

Bret PM, Fond A, Bretagnolle M, Valette PJ, Thiesse P, Lambert R, Labadie M. Percutaneous aspiration and drainage of hydatid cysts in the liver. Radiology. 1988 Sep;168(3):617–620

Brown JL. Interferon therapy reduces the risk for hepatocellular carcinoma. Gut. 2000;47(5):610-1.

Burcharth F, Efsen F, Christiansen LA, Hancke S, Jensen LI, Nielsen OV, Pedersen JH, Pedersen G. Nonsurgical internal biliary drainage by endoprosthesis. Surg Gynecol Obstet. 1981;153(6): 857-860.

Burcharth F, Nielbo N: Percutaneous cholangiography with selective catheterization of the common bile duct. AJR Am J Roentgenol. 1976; 127(3): 409-412.

Butturini, G.; Daskalaki, D.; Molinari, E.; Scopelliti, F.; Casarotto, A.; Bassi, C. Pancreatic fistula: Definition and current problems. J. Hepato-Biliary-Pancreat. Surg. 2008, 15, 247–251.

Cacoub P, Comarmond C, Domont F, Savey L, Desbois AC, Saadoun D. Extrahepatic manifestations of chronic hepatitis C virus infection. Ther Adv Infect Dis, 2016, 3(1):3–14.

Cacoub P, Poynard T, Ghillani P, Charlotte F, Olivi M, Piette JC, Opolon P. Extrahepatic manifestations of chronic hepatitis C. MULTIVIRC Group. Multidepartment Virus C. Arthritis Rheum, 1999, 42(10):2204–2212.

Callery, M. P., Pratt, W. B., Kent, T. S., Chaikof, E. L., & Vollmer, C. M. (2013). A prospectively validated clinical risk score accurately predicts pancreatic fistula after pancreatoduodenectomy. Journal of the American College of Surgeons.

Callery, M.P.; Pratt, W.B.; Kent, T.S.; Chaikof, E.L.; Vollmer, C.M. A prospectively validated clinical risk score accurately predicts pancreatic fistula after pancreatoduodenectomy. J. Am. Coll. Surg. 2013, 216, 1–14.

Callery, M.P.; Pratt,W.B.; Kent, T.S.; Chaikof, E.L.; Vollmer, C.M., Jr. A Prospectively Validated Clinical Risk Score Accurately Predicts Pancreatic Fistula after Pancreatoduodenectomy. J. Am. Coll. Surg. 2013, 216, 1–14.

Cameron, J.L.; Riall, T.S.; Coleman, J.; Belcher, K.A. One thousand consecutive pancreaticoduodenectomies. Ann. Surg. 2006, 244, 10–15.

Cardenas A, Crespo G, Balderramo D, Bordas JM, Sendino O, Llach J. Subcapsular liver hematoma after endoscopic retrograde cholangiopancreatography in a liver transplant patient. Ann Hepatol. 2008;7(4):386-8.

Carr JA, Cho JS, Shepard AD, Nypaver TJ, Reddy DJ. Visceral pseudoaneurysms due to pancreatic pseudocysts: rare but lethal complications of pancreatitis. J Vasc Surg. 2000;32(4):722-30

Carrasco CH, Wallace S, Charnsangavej C, Rich li W, Wright KC, Fanning T, Gianturco C. Expandable biliary endoprostheses: an experimental study. AJR Am J Roentgenol. 1985; 145(6):1279-1281.

Chaudhari VV, Raman SS, Vuong NL, et al. Pancreatic cystic lesions: discrimination accuracy based on clinical data and high resolution CT features. J Comput Assist Tomogr 2007; 31:860–7.

Chaudhuri S, Chatterjee S, Katz N, Nelson M, Goldbaum M. Detection of blood vessels in retinal images using two-dimensional matched filters. IEEE Trans Med Imaging. 1989;

Chautems R, Bubler L, Gold B, Chilcott M, Morel P, Mentha G. Long term results after complete or incomplete surgical resection of liver hydatid disease. Swiss Med Wkly 2003; 133: 258-262

Chen J, Peng J, Zheng Y, Li S, Yang P, Wu X, Tian H, Liu H, Yang S, Wang W, Wu B. Primary renal lymphoma: a populationbased study in the United States, 1980–2013. Sci Rep, 2019, 9(1):15125.

Chen X, Hu D, Fang L, Chen Y, Che X, Tao J, Weng G, Ye X. Primary renal lymphoma: a case report and literature review. Oncol Lett, 2016, 12(5):4001–4008

Chen, J.-Y.; Feng, J.; Wang, X.-Q.; Cai, S.-W.; Dong, J.-H.; Chen, Y.-L. Risk scoring system and predictor for clinically relevant pancreatic fistula after pancreaticoduodenectomy. World J. Gastroenterol. 2015, 21, 5926–5933.

Chen, Z.; Li, W.-Y.; Ho, M.; Chau, P.-H. The Prevalence of Sarcopenia in Chinese Older Adults: Meta-Analysis and Meta-Regression. Nutrients 2021, 13, 1441.

Cheng, C.-L.; Sherman, S.;Watkins, J.L.; Barnett, J.; Freeman, M.; Geenen, J.; Ryan, M.; Parker, H.; Frakes, J.T.; Fogel, E.L.; et al. Risk Factors for Post-ERCP Pancreatitis: A Prospective Multicenter Study. Am. J. Gastroenterol. 2006, 101, 139–147.

Chu KE, Sun CK, Wu CC, Yang KC. Complete remission ofpancreatic pseudoaneurysm rupture with arterial embolization nin a patient with poor risk for surgery: a case report. Case Rep Gastroenterol. 2012;6(2):254-9.

Cioni D, Lencioni R, Bartolozzi C. Therapeutic effect of transcatheter arterial chemoembolization on hepatocellular carcinoma: evaluation with contrast-enhanced harmonic power Doppler ultrasound. Eur.Radiol.2000; 10: 1570-1575

Conti F, Buonfiglioli F, Scuteri A, Crespi C, Bolondi L, Caraceni P, et al. Early occurrence and recurrence of hepatocellular carcinoma in HCV-related cirrhosis treated with direct-acting antivirals. J Hepatol. 2016;65(4):727-33.

Coombs RJ, Zeiss J, Howard JM, Thomford NR, Merrick HW. CT of the abdomen after the Whipple procedure: Value in depicting postoperative anatomy, surgical complications, and tumor recurrence. AJR 1990; 154 (5): 1011-1014

Cowling MG, Adam AN. Internal stenting in malignant biliary obstruction. World J Surg. 2001;25: 355-361.

Crippa S, Arcidiacono PG, De Cobelli F et al. Review of the diagnosis and management of intraductal papillary mucinous neoplasms United European Gastroenterol J. 2020 Apr; 8(3): 249–255.

CT/MRI LI-RADS v2018 | American College of Radiology (acr.org)

Curry CA, Eng J, Horton KM, et al. CT of primary cystic pancreatic neoplasms: can CT be used for patient triage and treatment? AJR Am J Roentgenol 2000; 175:99–103.

Cyriac S, Rejiv R, Shirley S, Sagar GT. Primary renal lymphoma mimicking renal cell carcinoma. Indian J Urol, 2010, 26(3):441–443.

Dachman AH, Newmark GM, Thistlethwaite JR Jr, Oto A, Bruce DS, Newell KA. Imaging of pancreatic transplantation using portal venous and enteric exocrine drainage. AJR 1998; 171(1):157-63

Daniil C, Balan G, Stanciu C et al. Percutaneous Biliary drainage and Endoprosthesis for malignant obstructive jaundice. In vol. 3th Congress of the Hungarian Radiol. Society (Budapesta): 1986. p. 121

Daniil C, Stanciu C, Balan G, Frasin M, Strat V, Târcoveanu E, Diaconescu MR, Dolinescu C, Burcoveanu C, Dragomir C, Stoian M. Radiologia intervenţională în icterele obstructive. RevMed Chir Soc Med Nat (Iaşi). 1986; 2: 361-365.

Dariushnia SR, Mitchell JW, Chaudry G, Hogan MJ. Society of Interventional Radiology Quality Improvement Standards for Image-Guided Percutaneous Drainage and Aspiration of Abscesses and Fluid Collections. J Vasc Interv Radiol. 2020;31(4):662-666.e4.

Davids PH, Groen AK, Rauws EA, Tytgat GN, Huibregtse K. Randomised trial of self-expanding metal stents versus polyethylene stents for distal malignant biliary obstruction. Lancet. 1992; 340(8834-8835): 1488-1492.

de Jong K, Nio CY, Mearadji B, et al. Disappointing interobserver agreement among radiologists for a classifying diagnosis of pancreatic cysts using magnetic resonance imaging. Pancreas 2012; 41:278–82.

de Sanjose S, Benavente Y, Vajdic CM, Engels EA, Morton LM, Bracci PM, Spinelli JJ, Zheng T, Zhang Y, Franceschi S, Talamini R, Holly EA, Grulich AE, Cerhan JR, Hartge P, Cozen

W, Boffetta P, Brennan P, Maynadié M, Cocco P, Bosch R, Foretova L, Staines A, Becker N, Nieters A. Hepatitis C and non-Hodgkin lymphoma among 4784 cases and 6269 controls from the International Lymphoma Epidemiology Consortium. Clin Gastroenterol Hepatol, 2008, 6(4): 451–458.

Demler, O.V.; Pencina, M.J.; D'Agostino, R.B. Misuse of DeLong test to compare AUCs for nested models. Stat. Med. 2012, 31, 2577–2587.

Demler, O.V.; Pencina, M.J.; D'Agostino, R.B. Misuse of DeLong test to compare AUCs for nested models. Stat. Med. 2012, 31, 2577–2587.

Denbo, J.W.; Orr, W.S.; Zarzaur, B.L.; Behrman, S.W. Toward defining grade C pancreatic fistula following pancreaticoduodenectomy: Incidence, risk factors, management and outcome. HPB 2012, 14, 589–593.

DeOliveira ML, Winter JM, Schafer M, Cunningham SC, Cameron JL, Yeo CJ, et al. Assessment of complications after pancreatic surgery: A novel grading system applied to 633 patients undergoing pancreaticoduodenectomy. Ann Surg. 2006;

Desmet, V.J.; Roskams, T. Cirrhosis reversal: A duel between dogma and myth. J. Hepatol. 2004, 40, 860–867.

Di Carlo V, Zrebi A, Balzano G (1999) Pylorus-preserving pancreaticoduodenectomy versus conventional Whipple operation. World J Surg 23: 920-925

DiMartini, A.; Cruz, R.J., Jr.; Dew, M.A.; Myaskovsky, L.; Goodpaster, B.; Fox, K.; Kim, K.H.; Fontes, P. Muscle mass predicts outcomes following liver transplantation. Liver Transpl. 2013, 19, 1172–1180.

Dinant S, Graaf W, Verwer BJ, Bennink RJ, van Lienden K, Gouma DJ, van Vliet A, van Gulik TM Risk Assessment of Posthepatectomy Liver Failure Using Hepatobiliary Scintigraphy and CT Volumetry. J Nucl Med 2007 May;48(5):685-92.

Donahue J, Jia Y, Vinyals O, Hoffman J, Zhang N, Tzeng E, et al. DeCAF: A deep convolutional activation feature for generic visual recognition. In: 31st International Conference on Machine Learning, ICML 2014. 2014.

Du ZQ, Zhang LN, Lu Q, Ren YF, Lv Y, Liu XM, et al. Clinical Charateristics and outcome of pyogenic liver abscess with different size: 15-year experience from a single center. Sci Rep. 2016;6:35890. Sci Rep. 2016;6:35890.

Du, Y.; Wang, X.; Xie, H.; Zheng, S.; Wu, X.; Zhu, X.; Zhang, X.; Xue, S.; Li, H.; Hong, W. Sex differences in the prevalence and adverse outcomes of sarcopenia and sarcopenic obesity in community dwelling elderly in East China using the AWGS criteria. BMC Endocr. Disord. 2019, 19, 109.

Durand T, Di Liberto G, Colman H, Cammas A, Boni S, Marcellin P, Cahour A, Vagner S, Féray C. Occult infection of peripheral B cells by hepatitis C variants which have low translational efficiency in cultured hepatocytes. Gut, 2010, 59(7):934–942

Ecker BL, McMillan MT, Allegrini V, Bassi C, Beane JD, Beckman RM, et al. Risk Factors and Mitigation Strategies for Pancreatic Fistula after Distal Pancreatectomy: Analysis of 2026 Resections from the International, Multi-institutional Distal Pancreatectomy Study Group. Ann Surg. 2019;

Eckert J (ed.). OIE Manual on Echinococcosis in Humans and Animals. Geneva: HO/OIE, 2001.

El Nakeeb, A.; El Sorogy, M.; Ezzat, H.; Said, R.; El Dosoky, M.; El Gawad, M.A.; Elsabagh, A.M.; El Hanafy, E. Predictors of long-term survival after pancreaticoduodenectomy for peri-ampullary adenocarcinoma: A retrospective study of 5-year survivors.Hepatobiliary Pancreat. Dis. Int. 2018, 17, 443–449.

El-Serag HB. Hepatocellular carcinoma. N Engl J Med 2011; 365:1118-1127

Eshraghian A, Taghavi A, Nikeghbalian S, Malek-Hosseini SA. Reduced rate of hospital admissions for liver-related morbidities during the initial COVID-19 outbreak. Lancet Gastroenterol Hepatol. 2020 Sep;5(9):803-804.

Feixiang Hu, Yue Hu, Dan Wang et al. Cystic neoplasms of the pancreas: Differential diagnosis and radiology correlation. Front Oncol . 2022 Mar 1;12:860740

Feng, Q.; Li, C.; Zhang, S.; Tan, C.-L.; Mai, G.; Liu, X.-B.; Chen, Y.-H. Recurrence and survival after surgery for pancreatic cancer with or without acute pancreatitis. World J. Gastroenterol. 2019, 25, 6006–6015.

Ferrucci J.T.Jr., Wittenberg J., Mueller P.R., Simeone J.F., Kirkpatrick R.H., Taft P.D. Diagnosis of abdominal malignancy by radiologic fine-needle biopsy. AJR, 1980, 134: 323-330.

Ferrucci JT Jr, Adson MA, Mueller PR, Stanley RJ, Stewart ET. Advances in the radiology of jaundice. AJR Am J Roentgenol. 1983; 141(1): 1-20.

Flati G, Andren-Sandberg A, La Pinta M, Porowska B, Carboni M. Potentially fatal bleeding in acute pancreatitis:pathophysiology, prevention, and treatment. Pancreas. 2003;26(1):8-14.

Freed KS, Paulson EK, Frederick MG, Keogan MT, Pappas TN. Abdomen after a Puestow Procedure: Postoperative CT Appearance, Complications and Potential Pitfalls. Radiology 1997; 203 (3), 790-794

Fritscher-Ravens A, Sriram PV, Krause C, Atay Z, Jaeckle S, Thonke F, Brand B, Bohnacker S, Soehendra N. Detection of pancreatic metastases by EUS-guided fine-needle aspiration. Gastrointest Endosc. 2001 Jan;53(1):65-70

Furukawa H, Kosuge T, Shumada K, Yamamoto J, Ushio K. Helical CT of the abdomen after pancreaticoduodenectomy: usefulness for detecting postoperative complications. Hepato-Gastroenterology 1997; 44: 849-855

Ganeshan D, Iyer R, Devine C, Bhosale P, Paulson E. Imaging of primary and secondary renal lymphoma. AJR Am J Roentgenol, 2013, 201(5):W712–W719.

Gaujoux, S.; Cortes, A.; Couvelard, A.; Noullet, S.; Clavel, L.; Rebours, V.; Lévy, P.; Sauvanet, A.; Ruszniewski, P.; Belghiti, J. Fatty pancreas and increased body mass index are risk factors of pancreatic fistula after pancreaticoduodenectomy. Surgery 2010, 148, 15–23.

Geetha N, Shahid A, Rajan V, Jacob PM. Primary renal lymphoma – a case report. Ecancermedicalscience, 2014, 8: 466

Geschwind JFH, Artemov D, Abraham S et al. Chemoembolization of Liver Tumor in a Rabbit Model: Assessment of Tumor Cell Death with Diffusion-Weighted MR Imaging and Histologic Analysis. JVIR 2000; 11: 1245-1255

Gheorghe, L.; Iacob, S.; Curescu, M.; Brisc, C.; Cijevschi, C.; Caruntu, F.; Stanciu, C.; Simionov, I.; Sporea, I.; Gheorghe, C.; et al. Real-Life Use of 3 Direct-Acting Antiviral Regimen in a Large Cohort of Patients with Genotype-1b HCV Compensated Cirrhosis. J. Gastrointest. Liver Dis. 2017, 26, 275–281.

Gill K, Ghazinian H, Manch R, Gish R. Hepatitis C virus as a systemic disease: reaching beyond the liver. Hepatol Int, 2016, 10(3):415–423.

Giorgio A, Tarantino L, Francica G. Unilocular hydatid liver cysts: treatment with US-guided, double percutaneous aspiration and alcohol injection. Radiology. 1992;182:705–710

Girometti R, Intini S, Brondani G, et al. Incidental pancreatic cysts on 3D turbo spin echo magnetic resonance cholangiopancreatography: prevalence and relation with clinical and imaging features. Abdom Imaging 2011; 36:196–205

Goktay AY, Secil M, Gulcu A, et al. Percutaneous Treatment of Hydatid Liver Cysts in Children as a Primary Treatment: Long-term Results. J. Vasc Interv. Radiol., 16, 2005, p. 831.

Gordon RL, Ring EJ, LaBerge JM, Doherty MM. Malignant biliary obstruction: treatment with expandable metallic stents–follow-up of 50 consecutive patients. Radiology. 1992; 182: 697-701.

Gorok D, Fehervary I, Doros A, Nemes B, Mathe Z, Kobori L. Subcapsular hematoma and rupture of the liver graft, Magy Seb 2008;61(4):230-3.

Gouma DJ, Van Geenen RCI, Van Gulik TM, De Haan RJ, De Wit LT, Busch ORC, et al. Rates of complications and death after pancreaticoduodenectomy: Risk factors and the impact of hospital volume. Ann Surg. 2000;

Gouma DJ.; Van Geenen R.C.I.; Van Gulik T.M.; De Haan R.J.; De Wit L.T.; Busch O.R.C.; Obertop, H. Rates of complication ns and death after pancreaticoduodenectomy: Risk factors and the impact of hospital volume. Ann. Surg. 2000, 232, 786–795.

Haaga J.R., Alfidi R.J. Precise biopsy localization by computed tomography. Radiology, 1976,118:603-607.

Hansson JA, Hoevels J, Simert G, Tylén U, Vang J. Clinical aspects of nonsurgical percutaneous transhepatic bile drainage in obstructive lesions of the extrahepatic bile ducts. Ann Surg. 1979;189(1): 58-61.

Harada, N.; Ishizawa, T.; Inoue, Y.; Aoki, T.; Sakamoto, Y.; Hasegawa, K.; Sugawara, Y.; Tanaka, M.; Fukayama, M.; Kokudo, N. Acoustic radiation force impulse imaging of the pancreas for estimation of pathologic fibrosis and risk of postoperative pancreatic fistula. J. Am. Coll. Surg. 2014, 219, 887–894.e5.

Harbin, W.P.; Robert, N.J.; Ferrucci, J.T. Diagnosis of cirrhosis based on regional changes in hepatic morphology: A radiological and pathological analysis. Radiology 1980, 135, 273–283.

Harrell, F.E.; Califf, R.M.; Pryor, D.B.; Lee, K.L.; Rosati, R.A. Evaluating the Yield of Medical Tests. J. Am. Med. Assoc. 1982, 247, 2543–2546.

Harrell, F.E.; Califf, R.M.; Pryor, D.B.; Lee, K.L.; Rosati, R.A. Evaluating the Yield of Medical Tests. J. Am. Med. Assoc. 1982, 247,

Hashimoto Y, Traverso LW. Incidence of pancreatic anastomotic failure and delayed gastric emptying after pancreatoduodenectomy in 507 consecutive patients: Use of a web-based calculator to improve homogeneity of definition. Surgery. 2010;

Hashimoto, M.; Koga, M.; Ishiyama, K.; Watarai, J.; Shibata, S.; Sato, T.; Yamamoto, Y. CT features of pancreatic fistula after pancreaticoduodenectomy. Am. J. Roentgenol. 2007, 188, W323–W327.

Hashimoto, Y.; Sclabas, G.M.; Takahashi, N.; Kirihara, Y.; Smyrk, T.C.; Huebner, M.; Farnell, M.B. Dual-Phase Computed Tomography for Assessment of Pancreatic Fibrosis and Anastomotic Failure Risk Following Pancreatoduodenectomy. J. Gastrointest. Surg. 2011, 15, 2193–2204.

Hashimoto, Y.; Traverso, L.W. Incidence of pancreatic anastomotic failure and delayed gastric emptying after pancreatoduodenectomy in 507 consecutive patients: Use of a web-based calculator to improve homogeneity of definition. Surgery 2010, 147, 503–515.

Hiatt JR, Gabbay J, Busuttil RW. Surgical anatomy of the hepatic arteries in 1000 cases. Ann Surg. 1994 Jul;220(1):50-2

Hirakawa M, Nishie A, Asayama Y, et al. Clinical outcomes of symptomatic arterioportal fistulas after transcatheter arterial embolization. World J Radiol 2013; 5:33–40.

Hoevels J, Lunderquist A, Ihse I. Percutaneous transhepatic intubation of bile ducts for combined internal/external drainage in preoperative and palliative treatment of obstructive jaundice. Gastrointest Radiol. 1978; 3(1): 23-31.

Hong SS, Kim AY. Early postoperative bleeding after living donor liver transplantation. Abdom Imaging. 2009;34(3):565-70.

Honselmann, K. C., Antoine, C., Frohneberg, L., Deichmann, S., Bolm, L., Braun, R., Lapshyn, H., Petrova, E., Keck, T., Wellner, U., & Bausch, D. (2021). A simple nomogram for early postoperative risk prediction of clinically relevant pancreatic fistula after pancreatoduodenectomy. Langenbeck's Archives of Surgery.

Hoover A, Goldbaum M. Locating the optic nerve in a retinal image using the fuzzy convergence of the blood vessels. IEEE Trans Med Imaging. 2003;

Hsu JT, Yen CN, Hung CF, Chen HM, Hang TL, Jan YY, Chen MF. Management and outcome of bleeding pseudoaneurysm sassociated with chronic pancreatitis. BMC Gastroenterol. 2006;6:3

Hu BY, Wan T, Zhang WZ, Dong JH. Risk factors for postoperative pancreatic fistula: Analysis of 539 successive cases of pancreaticoduodenectomy. World J. Gastroenterol. 2016, 22, 7797–7805.

Huang CJ, Pitt HA, Lipsett PA, Osterman Jr FA, Lillemoe KD, Cameron JL, et al. Pyogenic hepatic abscess. Changing trends over 42 years. Ann Surg. 1996;223(5):600-7; discussion 607-9.

Huang MS, Lin Q, Jiang ZB, et al. Comparison of long-term effects between intra-arterially delivered ethanol and Gelfoam for the treatment of severe arterioportal shunt in patients with hepatocellular carcinoma. World J Gastroenterol. 2004; 10: 825-829

Huber, A.; Ebner, L.; Montani, M.; Semmo, N.; Roy Choudhury, C.; Heverhagen, J.; Christe, A. Computed tomography findings in liver fibrosis and cirrhosis. Swiss Med. Wkly. 2014, 144, w13923.

Hui JY, Yang MK, Cho DH, Li A, Loke TKL, Chan JCS, et al. Pyogenic liver abscesses caused by Klebsiella pneumoniae: US appearance and aspiration findings. Radiology. 2007;242(3):769-76.

Ionescu M, Stroescu C, Bubuta S, Ciurea S, Popescu I.Pancreaticoduodenectomy - the rutin surgery? Chirurgia (Bucur)2003;98 (2):103-8

Ip IK, Mortele KJ, Prevedello LM, et al. Focal cystic pancreatic lesions: assessing variation in radiologists' management recommendations. Radiology 2011;259:136–41.

Ishii H, Sonoyama T, Nakashima S, et al. Surgical treatment of hepatocellular carcinoma with severe intratumoral arterioportal shunt. *World J Gastroenterol* 2010; 16: 3211-3214

Ito, K.; Mitchell, D.G.; Gabata, T. Expanded Gallbladder Fossa: Simple MR Imaging Sign of Cirrhosis. Radiology 1999, 211, 723–726

Ivanina E, Mayer I, Li J, et al. EUS-guided drainage of hepatic abscess. Gastrointest Endosc 2012; 75(4): AB114.

Izaki K, Sugimoto K, Sugimura K, Hirota S. Transcatheter arterial embolization for advanced tumor thrombus with marked arterioportal or arteriovenous shunt complicating hepatocellular carcinoma. Radiat Med. 2004; 22: 155-162.

Jang JY, Kim SW, Han JK, Park SJ, Park YC, Joon Ahn Y, Park YH. Randomized prospective Trial of the Effect of Induced Hypergastrinemia on the Prevention of Pancreatic Atrophy After Pancreatoduodenectomy in Humans. Ann Surg. 2003; 237: 522-529

Janjua NZ, Chong M, Kuo M, Woods R, Wong J, Yoshida EM, et al. Long-term effect of sustained virological response on hepatocellular carcinoma in patients with hepatitis C in Canada. J Hepatol. 2017;66(3):504-13.

Jepsen P, Vilstrup H, Schønheyder HC, Sørensen HT. A nationwide study of the incidence and 30-day mortality rate of pyogenic liver abscess in Denmark, 1977-2002. Aliment Pharmacol Ther. 2005;21(10):1185–8.

Jiwani, A.; Chawla, T. Risk Factors of Pancreatic Fistula in Distal Pancreatectomy Patients. Surg. Res. Pract. 2019, 2019, 1–6.

Johns TN, Evans BB. Collateral pathways in portal hypertension. Ann Surg 1962;155:838–45.

Jutric, Z.; Johnston, W.C.; Grendar, J.; Haykin, L.; Mathews, C.; Harmon, L.K.; Shen, J.; Hahn, H.P.; Coy, D.L.; Cassera, M.A, et al. Preoperative computed tomography scan to predict pancreatic fistula after distal pancreatectomy using gland and tumor charactersitics. Am. J. Surg. 2006, 211, 871–876.

Kabaalioglu A, Ceken K, Alimoglu E, Apaydin A. Percutaneous imaging-guided treatment of hydatid liver cysts: Do long-term results make it a first choice? Eur J Radiol. 2006;59:65–73

Kajiwara, T.; Sakamoto, Y.; Morofuji, N.; Nara, S.; Esaki, M.; Shimada, K.; Kosuge, T. An analysis of risk factors for pancreatic fistula after pancreaticoduodenectomy: Clinical impact of bile juice infection on day 1. Langenbeck's Arch. Surg. 2010, 395, 707–712.

Kanda, M.; Fujii, T.; Suenaga, M.; Takami, H.; Hattori, M.; Inokawa, Y.; Yamada, S.; Nakayama, G.; Sugimoto, H.; Koike, M.; et al. Estimated pancreatic parenchymal remnant volume accurately predicts clinically relevant pancreatic fistula after pancreatoduodenectomy. Surgery 2014, 156, 601–610.

Kang, W.S.; Park, Y.C.; Jo, Y.G.; Kim, J.C. Pancreatic fistula and mortality after surgical management of pancreatic trauma: Analysis of 81 consecutive patients during 11 years at a Korean trauma center. Ann. Surg. Treat. Res. 2018, 95, 29–36.

Kappus, Matthew R. and Manal F. Abdelmalek. "De Novo and Recurrence of Nonalcoholic Steatohepatitis After Liver Transplantation." Clinics in liver disease 21 2 (2017): 321-335 .

Kasahara M, Kozaki I, Yoshida T, Yamamoto H, Ogawa K, Ogura Y, et al. Subcapsular hematoma after right-lobe living-donor liver transplantation. J. Hepatobiliary Pancreas Surg. 2004;11(5):330-2.

Kaude JV, Weidenmier CH, Agee OF. Decompression of bile ducts with the percutaneous technique. Radiology. 1969; 93(1): 69-71.

Ke, Z.; Cui, J.; Hu, N.; Yang, Z.; Chen, H.; Hu, J.; Wang, C.; Wu, H.; Nie, X.; Xiong, J. Risk factors for postoperative pancreatic fistula. Analysis of 170 consecutive cases of pancreaticoduodenectomy based on the updated ISGPS classification and grading system. Medicine 2018, 97, e12151.

Khuroo MS, Wani NA, Javid G, et al. Percutaneous Drainage Compared with Surgery for Hepatic Hydatid Cysts. N Engl J Med 1997; 337:881-887

Khuroo MS, Zargar SA, Mahajan R. Echinococcus granulosus cysts in the liver: management with percutaneous drainage. Radiology 1991;180(1):141-5

Kim DS, Lee SG, Sung GB, Ko GY, Park KM, Kim KH, et al. Management of subcapsular hematoma of the graft after living donor-liver transplantation, Liver Transpl. 2006;12(7):1124-8

Kim, H.Y.; Jang, J.W. Sarcopenia in the prognosis of cirrhosis: Going beyond the MELD score. World J. Gastroenterol. 2015, 21, 7637–7647.

Kim, S.Y.; Kim, H.; Cho, J.Y.; Lim, S.; Cha, K.; Lee, K.H.; Kim, Y.H.; Kim, J.H.; Yoon, Y.-S.; Han, H.-S.; et al. Quantitative assessment of pancreatic fat by using unenhanced CT: Pathologic correlation and clinical implications. Radiology 2014, 271, 104–112.

Kinkel K et al. Detection of Hepatic Metastases from Cancers of the Gastrointestinal Tract by Using Noninvasive Imaging Methods (US, CT, MR Imaging, PET): A Meta-Analysis. Radiology 2002; 224:748–756

Kishi Y, Abdalla E.K., Chun Y.S.. et al. (2009) Three hundred and one consecutive extended right hepatectomies: evaluation of outcome based on systematic liver volumetry. Ann. Surg. 250, 540–548

Kitahata, Y.; Kawai, M.; Yamaue, H. Clinical trials to reduce pancreatic fistula after pancreatic surgery—review of randomized controlled trials. Transl. Gastroenterol. Hepatol. 2016, 1, 4.

Kogiso, T.; Sagawa, T.; Kodama, K.; Taniai, M.; Katagiri, S.; Egawa, H.; Tokushige, K. Hepatocellular carcinoma after direct-acting antiviral drug treatment in patients with hepatitis C virus. JGH Open 2018, 3, 52–60.

Kokudo N, Hasegawa K, Akahane M, et al. Evidencebased Clinical Practice Guidelines for Hepatocellular Carcinoma: The Japan Society of Hepatology 2013 update (3rd JSH-HCC Guidelines). Hepatol Res 2015

Koops A, Wojciechowski B, Broering DC, Adam G, Krupski- Berdien G. Anatomic variations of the hepatic arteries in 604 selective celiac and superior mesenteric angiographies. Surg Radiol Anat 2004;26:239-244.

Krige JE, Beckingham IJ. ABC of diseases of liver, pancreas, and biliary system. BMJ. 2001;322(7285):537-40.

Krizhevsky A, Sutskever I, Hinton GE. ImageNet classification with deep convolutional neural networks. Commun ACM. 2017;

Krueger K, Zaehringer M, Lackner K. Percutaneous treatmentof a splenic artery pseudoaneurysm by thrombin injection. JVasc Interv Radiol. 2005;16(7):1023-5

Krug B, Zieren HU, Jung G, Hemme A, Heindel W, Krings F. Late results after resection of benign hepatic tumors: clinical and radiological findings. Eur Radiol 1997; 7(3): 327-32

Kudo, M.; Zheng, R.Q.; Kim, S.R.; Okabe, Y.; Osaki, Y.; Iijima, H.; Itani, T.; Kasugai, H.; Kanematsu, M.; Ito, K.; et al. Diagnostic Accuracy of Imaging for Liver Cirrhosis Compared to Histologically Proven Liver Cirrhosis. Intervirology 2008, 51, 17–26.

Kulemann, B.; Fritz, M.; Glatz, T.; Marjanovic, G.; Sick, O.; Hopt, U.T.; Hoeppner, J.; Makowiec, F. Complications after pancreaticoduodenectomy are associated with higher amount of intra- and postoperative fluid therapy: A single center retrospectie cohort study. Ann. Med. Surg. 2017, 16, 23–29.

Kulhari M, Mandia R. Prospective randomized comparative study of pigtail catheter drainage versus percutaneous needle aspiration in treatment of liver abscess. ANZ J Surg. 2019;89(3):E81–6.

Kulinna C., Schima W.: Imaging Features of Hepatic Metastases: CT and MR. In R. Lencioni, D. Cioni, C. Bartolozzi (Eds.) Focal Liver Lesions. Detection, Characterization, Ablation. Springer-Verlag Berlin Heidelberg 2005, 275-294

Kuran S, Disieeyaz S, Parlak E et al. Biliocutaneous Fistula Following Alveolar Hydatid Disease Surgery Treated Successfully With Percutaneous Cyanoacrylate. Dig. Dis. Sci. 2006;1: 18-20.

Kuroda C, Sakurai M, Monden M, Marukawa T, Hosoki T, Tokunaga K, Wakasa K, Okamura J, Kozuka T. Limitation of transcatheter arterial chemoembolization using iodized oil for small hepatocellular carcinoma. A study in resected cases. Cancer 1991, 67, 81–86

Laarhoven H et al. Gadopentetate Dimeglumine and FDG Uptake in Liver Metastases of Colorectal Carcinoma as Determined with MR Imaging and PET. Radiology 2005; 237:181–188

Lammer J, Hausegger KA, Flückiger F, Winkelbauer FW, Wildling R, Klein GE, Thurnher SA, Havelec L. Common bile duct obstruction due to malignancy: treatment with plastic versus metal stents. Radiology. 1996; 201(1): 167-172.

Lammer J, Mueller PR, Ferrucci JT. The biliary ducts: interventional techniques. In: Ferrucci JT (ed) Radiology on CD-ROM. New York: Lippincott Williams & Wilkins; 1999.

Laursen TL, Sandahl TD, Kazankov K, George J, Gronbaek H. Liver-related effects of chronic hepatitis C antiviral treatment. World J Gastroenterol. 2020;26(22):2931-47.

Law CH, Wei AC, Hanna SS, Al-Zahrani M, Taylor BR, Greig PD, Langer B, Gallinger S. Pancreatic resection for metastatic renal cell carcinoma: presentation, treatment, and outcome. Ann Surg Oncol. 2003 Oct;10(8):922-6

Lee BH, Choe DH, Lee JH, Kim KH, Chin SY. Metallic stents in malignant biliary obstruction: prospective long-term clinical results. AJR Am J Roentgenol. 1997; 168(3): 741-745.

Lee KF, Chong CCN, Fong AKW, Fung AKY, Lok HT, Cheung YS, Wong J, Lai PBS. Pattern of disease recurrence and its implications for postoperative surveillance after curative hepatectomy for hepatocellular carcinoma: experience from a single center. Hepatobiliary Surg Nutr. 2018 Oct;7(5):320-330

Lee KS, Sekhar A, Rofsky NM, et al. Prevalence of incidental pancreatic cysts in the adult population on MR imaging. Am J Gastroenterol 2010; 105:2079–84.

Lepanto L, Gianfelice D, Dery R, dagenais M, Lapointe R, Roy A. Postoperative changes, complications and recurrent disease after Whipple's operation: CT features. AJR 1994; 163: 841-846

Lewis CA. Standards of Practice Committee. Quality improvement guidelines for percutaneous transhepatic cholangiography and biliary drainage. SCVIR, Draft 3, 1996.

Lin JW, Cameron JL, Yeo CJ, Riall TS, Lillemoe KD. Risk factors and outcomes in postpancreaticoduodenectomy pancreaticocutaneous fistula. J Gastrointest Surg. 2004;

Lin, J.W.; Cameron, J.L.; Yeo, C.J.; Riall, T.S.; Lillemoe, K.D. Risk factors and outcomes in postpancreaticoduodenectomy pancreaticocutaneous fistula. J. Gastrointest. Surg. 2004, 8, 951–959.

Lindgren P.G., Andersson T. Invasive ultrasound. În Goldberg B., Pettersson H. (eds) Ultrasonography. The Nicer Yearbook, 1996, 641-669.

Liu, P.; Li, P.; He, W.; Zhao, L.-Q. Liver and spleen volume variations in patients with hepatic fibrosis. World J. Gastroenterol. 2009, 15, 3298.

Lizardi-Cervera J, Poo JL, Romero-Mora K, Castañeda B, Pichardo-Bahena R, Morán S, Uribe M. Hepatitis C virus infection and non-Hodgkin's lymphoma: a review and case report of nine patient. Ann Hepatol, 2006, 5(4):257–262.

Llovet JM, Real MI, Montana X, Planas R, Coll S, Aponte J, et al. Arterial embolisation or chemoembolisation vs. symptomatic treatment in patients with unresectable hepatocellular carcinoma: a randomised controlled trial. Lancet 2002;359:1734–1739

Lo CM, Ngan H, Tso WK, Liu CL, Lam CM, Poon RT, et al. Randomized controlled trial of transarterial lipiodol chemoembolization for unresectable hepatocellular carcinoma. Hepatology 2002;35:1164–1171.

Lundstedt C, Andren-Sandberg A. CT of liver steatosis after total pancreatectomy. Acta Radiol, 1991, 32: 30-33

Luo MY, Shan H, Jiang ZB, Liang WW, Zhang JS, Li LF. Capability of multidetector CT to diagnose hepatocellular carcinoma-associated arterioportal shunt. *World J Gastroenterol* 2005;11: 2666-2669

Madoff DC, Wallace MJ. Palliative treatment of unresectable bile duct cancer Which stent? Which approach? Surg Oncol Clin N Am. 2002; 11: 923-939.

Makuuchi M., Hasegawa H., Yamazaki S., Takayasu K., Moriyama N. The use of operative ultrasound as an aid to liver resection in patients with hepatocellular carcinoma. World.J.Surg., 1987,11: 615-621.

Malik AA, Bari SU, Rouf KA, Wani KA. Pyogenic liver abscess: changing patterns in approach. World J Gastrointest Surg. 2010;2(12):395–401.

Malleo, G.; Pulvirenti, A.; Marchegiani, G.; Butturini, G.; Salvia, R.; Bassi, C. Diagnosis and management of postoperative pancreatic fistula. Langenbeck's Arch. Surg. 2014, 399, 801–810.

Malvezzi M, Carioli G, Bertuccio P, Boffetta P, Levi F, La Vecchia C, et al. European cancer mortality predictions for the year 2019 with focus on breast cancer. Ann Oncol. 2019;30:781–787

Marrero JA, Kulik LM, Sirlin CB, et al. Diagnosis, Staging, and Management of Hepatocellular Carcinoma: 2018 Practice Guidance by the American Association for the Study of Liver Diseases. Hepatology 2018;68:723-50.

Marrero JA, Kulik LM, Sirlin CB, Zhu AX, Finn RS, Abecassis MM, Roberts LR, Heimbach JK. Diagnosis, Staging, and Management of Hepatocellular Carcinoma: 2018 Practice Guidance by the American Association for the Study of Liver Diseases. Hepatology, 2018; 68 (2): 723-750

Martin, A.N.; Narayanan, S.; Turrentine, F.E.; Bauer, T.W.; Adams, R.B.; Zaydfudim, V.M. Pancreatic duct size and gland texture are associated with pancreatic fistula after

pancreaticoduodenectomy but not after distal pancreatectomy. PLoS ONE 2018, 13, e0203841.

Martino C.R., Haaga J.R., Bryan P.J. CT guided liver biopsies: eight years experience. Radiology, 1984, 152: 755-757.

Massarolo PC, Shiroma FM, Rodriguez AJ Jr, Mies S. Subcapsular hematoma of the graft after liver transplantation, Transplant proc. 2004;36(4):964-6

Mathieson JR, McLoughlin RF, Cooperberg PL, Prystai CC, Stordy SN, MacFarlane JK, Schmidt N. Malignant obstruction of the common bile duct: long-term results of Gianturco-Rosch metal stents used as initial treatment. Radiology. 1994; 192(3): 663-667

Mathur, A.; Pitt, H.A.; Marine, M.; Saxena, R.; Schmidt, C.M.; Howard, T.J.; Nakeeb, A.; Zyromski, N.J.; Lillemoe, K.D. Fatty pancreas: A factor in postoperative pancreatic fistula. Ann. Surg. 2007, 246, 1058–1064.

Mauro, E.; Crespo, G.; Martinez-Garmendia, A.; Gutierrez-Acevedo, M.N.; Diaz, J.M.; Saidman, J.; Bermudez, C.; Ortiz-Patron, J.; Garcia-Olveira, L.; Zalazar, F. Cystatin C and Sarcopenia Predict Acute on Chronic Liver Failure Development and Mortality in Patients on the Liver Transplant Waiting List. Transplantation 2020, 104, e188–e198.

Mauro, E.; Crespo, G.; Montironi, C.; Londoño, M.C.; Hernández-Gea, V.; Ruiz, P.; Sastre, L.; Lombardo, J.; Marino, Z.; Diaz, A.; et al. Portal pressure and liver stiffness measurements in the prediction of fibrosis regression after sustained virological response in recurrent hepatitis C. Hepatology 2018, 67, 1683–1694.

McGahan J.P., Brant W.E. Principles, instrumentation and guidance systems. În McGahan J.P. (ed) Interventional Ultrasound, Wiliams and Wilkins, 1990, 1-21.

Medrado BF, Carneiro FOAA, Vilaca TG, Gouveia TS, Frazão MSV, de Moura EGH, et al. EUS-guided drainage of giant liver abscess associated with transgastric migration of a self-expandable metallic stent. Endoscopy. 2013; 45 Suppl 2:E331-2.

Michels NA. Blood supply and anatomy of the upper abdominal organs: with a descriptive atlas. Philadelphia: J. B. Lippincott, 1955.

Mihai, F.; Trifan, A.; Cuciureanu, T.; Negru, D.; Sîngeap, A.M. Role of computed tomography in the evaluation of the patients with hepatitis C-related liver cirrhosis. Rev. Med. Chir. 2017, 121, 535–547.

13. Sangster, G.P.; Previgliano, C.H.; Nader, M.; Chwoschtschinsky, E.; Heldmann, M.G. MDCT Imaging Findings of Liver Cirrhosis: Spectrum of Hepatic and Extrahepatic Abdominal Complications. HPB Surg. 2013, 2013, 1–12

Milicevic M. Hydatid disease. In: Blumgart LH, ed. Surgery of the liver and biliary tract. 2nd ed. Vol. 2. Edinburgh, Scotland: Churchill Livingstone, 1994, p. 1121.

Miyamoto, R.; Oshiro, Y.; Sano, N.; Inagawa, S.; Ohkohchi, N. Three-Dimensional Remnant Pancreatic Volumetry Predicts Postoperative Pancreatic Fistula in Pancreatic Cancer Patients after Pancreaticoduodenectomy. Gastrointest. Tumors 2018, 5, 90–99.

Mohammad SK, Nazira W, Guljav D, Bashia K, Ghulamn Y, Altafh S, Samoong J. Percutaneous Drainage Compared with Surgery for Hepatic Hydatid Cysts. N. Engl. J. Med.1997; 337: 881.

Molnar W, Stockum AE. Relief of obstructive jaundice through percutaneous transhepatic catheter: A new therapeutic method. Am J Roentgenol Radium Ther Nucl Med. 1974; 122(2):356-367.

Montano-Loza, A.J.; Duarte-Rojo, A.; Meza-Junco, J.; Baracos, V.E.; Sawyer, M.B.; Pang, J.X.; Beaumont, C.; Esfandiari, N.; Myers, R.P. Inclusion of Sarcopenia Within MELD (MELD-Sarcopenia) and the Prediction of Mortality in Patients with Cirrhosis. Clin. Transl. Gastroenterol. 2015, 6, e102.

Moreno Gonzales E, Selas R, Martinez B. Results of surgical treatment of hepatic hydatidosis: current therapeutic modifications. World J Surg, 1991, 15: 254-263

Moulton JS, Munda R, Weiss MA, Lubbers DJ. Pancreatic Transplants: CT with Clinical and Pathologic Correlation. Radiology 1989; 172: 21-26

Mueller PR, Dawson SL, Ferrucci JT, Nardi GL. Hepatic echinococcal cyst: successful percutaneous drainage. Radiology, 155, 1985, p. 627.

Mueller PR, Ferrucci JT Jr, Teplick SK, vanSonnenberg E, Haskin PH, Butch RJ, Papanicolaou N. Biliary stent endoprosthesis: analysis of complications in 113 patients. Radiology. 1985;156(3): 637-639.

Muggli, D.; Müller, M.A.; Karlo, C.; Fornaro, J.; Marincek, B.; Frauenfelder, T. A simple method to approximate liver size on cross-sectional images using living liver models. Clin. Radiol. 2009, 64, 682–689

Mungroop, T. H., Klompmaker, S., Wellner, U. F., Steyerberg, E. W., Coratti, A., D'Hondt, M., de Pastena, M., Dokmak, S., Khatov, I., Saint-Marc, et al. (2021). Updated Alternative Fistula Risk Score (ua-FRS) to Include Minimally Invasive Pancreatoduodenectomy: Pan-European Validation. Annals of Surgery.

Mungroop, T. H., van Rijssen, L. B., van Klaveren, D., Smits, F. J., van Woerden, V., Linnemann, R. J., de Pastena, M., Klompmaker, S., Marchegiani, G., Ecker, B. L.,et al.. (2019). Alternative Fistula Risk Score for Pancreatoduodenectomy (a-FRS): Design and International External Validation. Annals of Surgery.

Mungroop, T.H.; Van Rijssen, L.B.; Van Klaveren, D.; Smits, F.J.; Van Woerden, V.; Linnemann, R.J.; de Pastena, M.; Klompmaker, S.; Marchegiani, G.; Ecker, B.L.; et al. Alternative Fistula Risk Score for Pancreatoduodenectomy (a-FRS): Design and International External Validation. Ann. Surg. 2019, 269, 937–943.

Munigala, S.; Kanwal, F.; Xian, H.; Scherrer, J.; Agarwal, B. Increased Risk of Pancreatic Adenocarcinoma After Acute Pancreatitis. Clin. Gastroenterol. Hepatol. 2014, 12, 1143–1150.e1.

Murakami Y, Uemura K, Hayashidani Y, Sudo T, Hashimoto Y, Nakagawa N, et al. No mortality after 150 consecutive pancreatoduodenctomies with duct-to-mucosa pancreaticogastrostomy. J Surg Oncol. 2008;

Muzica CM, Stanciu C, Huiban L, Singeap AM, Sfarti C, Zenovia S, et al. Hepatocellular carcinoma after direct-acting antiviral hepatitis C virus therapy: A debate near the end. World J Gastroenterol. 2020;26(43):6770-81

Nagakawa T, Kobayashi H, Ueno K, Ohta T, Kayahara M, Miyazaki I. Clinical study of lymphatic flow to the paraaortic lymph nodes in carcinoma of the head of the pancreas. Cancer. 1994 Feb 15;73(4):1155-62

Nakao Y, Hashimoto S, Abiru S, Komori A, Yamasaki K, Nagaoka S, et al. Rapidly growing, moderately differentiated HCC: A clinicopathological characteristic of HCC occurrence after IFN-free DAA therapy? J Hepatol. 2018;68(4):854-5.

Nakayama T, Ikeda A, Ikuda K. Percutaneous transhepatic drainage of the biliary tract. Gastroenterology. 1973; 74: 554-561

Naveed S, Qari H, Banday T, et al. Mucinous cystic neoplasms of pancreas. Gastroenterology Res 2014;7:44–50

Ngan H, Lai C, Fan S et al. Transcatheter arterial chemoembolization in inoperable hepatocellular carcinoma: four year follow-up. JVIR 1996; 7: 419-425

Ngan H, Peh WC. Arteriovenous shunting in hepatocellular carcinoma: its prevalence and clinical significance. *Clin Radiol* 1997; 52: 36-40

Nguyen DD, Rakita D. Renal lymphoma: MR appearance with diffusion-weighted imaging. J Comput Assist Tomogr, 2013, 37(5):840–842

Nissen NN, Geller SA, Klein A, Colquhoun S, Yamini D, Tran TT, et al. Percutaneous liver biopsy after living donor living transplantation resulting in fulminant hepatic failure: The first reported case of hepatic compartment syndrome. J Transplant. 2010; 273578.

Ochsner A, DeBakey M, Murray S. Pyogenic abscess of the liver II. An analysis of forty-seven cases with review of the literature. Am J Surg 1938; XL:292-319.

Okuno SH, Hoyer JD, Ristow K, Witzig TE. Primary renal non-Hodgkin's lymphoma. An unusual extranodal site. Cancer, 1995, 75(9):2258–2261

Origuchi N, Kimura W, Sawabe M, Muto T, Esaki Y. The development of a pancreatic abscess, suppurative pylethrombosis, and multiple hepatic abscesses after a pancreatojejunostomy for chronic pancreatitis: report of a case. Surg Today 1999; 29(4):358-60

Ormeci N, Soykan I, Bektas A, Sanoğlu M, Palabiyikoğlu M, Hadi Yasa M, Dökmeci A, Uzunalimoğlu O. A new percutaneous approach for the treatment of hydatid cysts of the liver. Am. J. Gastroeneterol., 2001; 96(7):2225-2230

Pagani J.J. Biopsy of focal liver lesions: comparison of 18 and 22 gauges needles. Radiology, 1983, 147: 673-675

Paternostro, R.; Lampichler, K.; Bardach, C.; Asenbaum, U.; Landler, C.; Bauer, D.; Mandorfer, M.; Schwarzer, R.; Trauner, M.; Reiberger, T.; et al. The value of different CT-based methods for diagnosing low muscle mass and predicting mortality in patients with cirrhosis. Liver Int. 2019, 39, 2374–2385.

Pedrazzoli, S. Pancreatoduodenectomy (PD) and postoperative pancreatic fistula (POPF). A systematic review and analysis of the POPF-related mortality rate in 60,739 patients retrieved from the English literature published between 1990 and 2015. Medicine 2017, 96, e6858.

Peláez V, Kugler C, Correa D, Del Carpio M, Guangiroli M, Molina J, Marcos B, Lopez E (2000) PAIR as percutaneous treatment of hydatid liver cysts. Acta Trop 75:197–202

Peng, Y.-P.; Zhu, X.-L.; Yin, L.-D.; Zhu, Y.; Wei, J.-S.; Wu, J.-L.; Miao, Y. Risk factors of postoperative pancreatic fistula in patients after distal pancreatectomy: A systematic review and meta-analysis. Sci. Rep. 2017, 7, 1–8.

Pereiras RV Jr, Rheingold OJ, Huston D, Mejia J, Viamonte M, Chiprut RO, Schiff ER. Relief of malignant obstructive jaundice by percutaneous insertion of a permanent prosthesis in the biliary tree. Ann Intern Med. 1978; 89(5 Pt 1): 589-593.

Peschaud F, Cheynel N, Hagry O, Tremeaux JC, Rat P, Favre JP. Traitement chirurgical des métastases pancréatiques des cancers du rein [Surgical treatment of pancreatic metastases from renal carcinoma]. Ann Chir. 2002 Sep;127(7):527-31.

Peveling-Oberhag J, Arcaini L, Hansmann ML, Zeuzem S. Hepatitis C-associated B-cell non-Hodgkin lymphomas. Epidemiology, molecular signature and clinical management. J Hepatol, 2013, 59(1):169–177.

Pfeifer T, Häussler MD, Tomczak R, Rilinger N, Zeitler H, Laasch HU, Friedrich JM, Safi F. The value of tumor volumetry as opposed to bidimensional determination of tumor size during follow-up of hepatic metastases from colorectal carcinoma Rofo. 1992 Dec;157(6):548-51.

Pinggera GM, Peschel R, Buttazzoni A, Mitterberger M, Friedrich A, Pallwein L. A possible case of primary renal lymphoma: a case report. Cases J, 2009, 2:6233.

Pollock TW, Ring ER, Oleaga JA, Freiman DB, Mullen JL, Rosato EF. Percutaneous decompression of benign and malignant biliary obstruction. Arch Surg. 1979; 114(2): 148-151.

Ponziani, F.R.; Gasbarrini, A. Sarcopenia in Patients with Advanced Liver Disease. Curr. Protein Pept. Sci. 2018, 19, 681–691.

Poon RTP, Fan ST, Lo CM, Ng KK, Yuen WK, Yeung C, et al. EXternal drainage of pancreatic duct with a stent to reduce leakage rate of pancreaticojejunostomy after pancreaticoduodenectomy: A prospective randomized trial. Ann Surg. 2007;

Pozniak MA, Propeck PA, Kelcz F, Sollinger H. Imaging of pancreas transplants. Radiol Clin of North Am 1995; 33 (3), 581-594

Pratt WB, Maithel SK, Vanounou T, Huang ZS, Callery MP, Vollmer CM. Clinical and economic validation of the international study group of pancreatic fistula (ISGPF) classification scheme. Ann Surg. 2007;

Pratt, W.B.; Maithel, S.K.; Vanounou, T.; Huang, Z.S.; Callery, M.P.; Vollmer, C.M. Clinical and Economic Validation of the International Study Group of Pancreatic Fistula (ISGPF) Classification Scheme. Ann. Surg. 2007, 245, 443–451.

Prior JO, Kosinski M, Delaloye AB, Denys A Initial report of PET/CT-guided radiofrequency ablation of liver metastases. J Vasc Interv Radiol. 2007 Jun;18(6):801-3

Pulvirenti, A.; Ramera, M.; Bassi, C. Modifications in the International Study Group for Pancreatic Surgery (ISGPS) definition of postoperative pancreatic fistula. Transl. Gastroenterol. Hepatol. 2017, 2, 107.

Qian Y, Wong CC, Lai S, Chen H, He X, Sun L, et al. A retrospective study of pyogenic liver abscess focusing on Klebsiella pneumoniae as a primary pathogen in China from 1994 to 2015. Sci Rep. 2016;6:38587.

Razavian AS, Azizpour H, Sullivan J, Carlsson S. CNN features off-the-shelf: An astounding baseline for recognition. In: IEEE Computer Society Conference on Computer Vision and Pattern Recognition Workshops. 2014.

Reig M, Marino Z, Perello C, Inarrairaegui M, Ribeiro A, Lens S, et al. Unexpected high rate of early tumor recurrence in patients with HCV-related HCC undergoing interferon-free therapy. J Hepatol. 2016;65(4):719-26.

Renzulli M, Buonfiglioli F, Conti F, Brocchi S, Serio I, Foschi FG, et al. Imaging features of microvascular invasion in hepatocellular carcinoma developed after direct-acting antiviral therapy in HCV-related cirrhosis. Eur Radiol. 2018;28(2):506-13.

Richter A, Niedergethmann M, Sturm JW, Lorenz D, Post S, Trede M. Long-term results of partial pancreaticoduodenectomy for ductal adenocarcinoma of the pancreatic head: 25-Year experience. World J Surg. 2003;

Ring EJ, Oleaga JA, Freiman DB, Husted JW, Lunderquist A. Therapeutic applications of catheter cholangiography. Radiology. 1978; 128(2): 333-338.

Roberts, K.J.; Hodson, J.; Mehrzad, H.; Marudanayagam, R.; Sutcliffe, R.P.; Muiesan, P.; Isaac, J.; Bramhall, S.R.; Mirza, D.F. A preoperative predictive score of pancreatic fistula following pancreatoduodenectomy. HPB 2014, 16, 620–628.

Sahani DV, Kalva SP, Tanabe KK, Hayat SM, O'Neill MJ, Halpern EF, Saini S, Mueller PR. Intraoperative US in Patients Undergoing Surgery for Liver Neoplasms: Comparison with MR . Radiology 2004; 232:810–814

Sahani DV, Kambadakone A, Macari M, et al. Diagnosis and management of cystic pancreatic lesions. AJR Am J Roentgenol 2013; 200:343–54.

Sakamori, R.; Yamada, R.; Shinkai, K.; Doi, A.; Tahata, Y.; Shigekawa, M.; Kodama, T.; Hikita, H.; Yamada, T.; Tatsumi, T.; et al. Improvement of Skeletal Muscle Mass after Ledipasvir and Sofosbuvir Treatment for Hepatitis C Virus in Decompensated Liver Cirrhosis. Intern. Med. 2021, 60, 745–750.

Sarıcık B, Kartal A, Esen H, Demircili ME. The Use of Radiofrequency Thermal Ablation Method in The Treatment of Hepatic Hydatid Cysts: Ex vivo Sheep Study. Turkiye Parazitol Derg. 2019 Mar 28;43(1):10-15

Scatarige JC, Horton KM, Sheth S, Fishman EK. Pancreatic parenchymal metastases: observations on helical CT. AJR Am J Roentgenol. 2001 Mar;176(3):695-9

Schlitt HJ, Schmidt U, Simunes D, Jager M, Aselmann H, Neipp M, Piso P. Morbidity and mortality associated with pancreatogastrostomy and pancreatojejunostomy following partial pancreatoduodenectomy. Br J Surg 2002; 89: 1245-1251

Schuh, F., Mihaljevic, A. L., Probst, P., Trudeau, M. T., Müller, P. C., Marchegiani, G., Besselink, M. G., Uzunoglu, F., Izbicki, J. R., Falconi, M., Fernandez-del Castillo, C., et al.

(2021). A Simple Classification Of Pancreatic Duct Size and Texture Predicts Postoperative Pancreatic Fistula. Annals of Surgery.

Scialpi M, Scaglione M, Volterrani L, Lupattelli L, Ragozzino A, Romano S, Rotondo A. Imaging evaluation of post pancreatic surgery. Eur J Radiol. 2005;53(3):417-24

Sebastiani, G.; Gkouvatsos, K.; Pantopoulos, K. Chronic hepatitis C and liver fibrosis. World J. Gastroenterol. 2014, 20, 11033–11053.

Senokuchi T, Baba Y, Hayashi S, Nakajo M. Embolization of hepatic arteriovenous shunt with absolute ethanol in a patient with hepatocellular carcinoma. Cardiovasc Intervent Radiol 2011; 34 Suppl 2:S154-156.

Shafiee, G.; Keshtkar, A.; Soltani, A.; Ahadi, Z.; Larijani, B.; Heshmat, R. Prevalence of sarcopenia in the world: A systematic review and meta-analysis of general population studies. J. Diabetes Metab. Disord. 2017, 16, 21.

Shaikh AB, Waghmare S, Koshti-Khude S, Koshy AV. Unusual presentation of non-Hodgkin's lymphoma: case report and review of literature. J Oral Maxillofac Pathol, 2016, 20(3): 510–517.

Sharma, C.; Eltawil, K.M.; Renfrew, P.D.; Walsh, M.J.; Molinari, M. Advances in diagnosis, treatment and palliation of pancreatic carcinoma: 1990–2010. World J. Gastroenterol. 2011, 17, 867–897.

Sharma, P.; Arora, A. Clinical presentation of alcoholic liver disease and non-alcoholic fatty liver disease: Spectrum and diagnosis. Transl. Gastroenterol. Hepatol. 2020, 5, 19.

Sharma, P.; Arora, A. Clinical presentation of alcoholic liver disease and non-alcoholic fatty liver disease: Spectrum and diagnosis. Transl. Gastroenterol. Hepatol. 2020, 5, 19 2543–2546

Sheth S, Ali S, Fishman E. Imaging of renal lymphoma: patterns of disease with pathologic correlation. Radiographics, 2006, 26(4):1151–1168

Shin CH, Ashok T, Kin SP, Chun CY, Te HK, Horn RY, et al. Management of liver allograft trauma resulting in massive subcapsular hematoma after living donor liver transplantation: can we salvage the liver allograft? Ann Transplant. 2017;22:1-8.

Sieghart W, Hucke F, Peck-Radosavljevic M. Transarterial chemoembolization: Modalities, indication, and patient selection. Journal of Hepatology 2015;62: 1187–1195

Silverman S.G., Bloom D.A., Seltzer T.E., Tempany C.M.C., Adamus D.F. Needle-tip localization during CT guided abdominal biopsy: Comparison of conventional and spiral CT. AJR, 1992, 159:1095-1097.

Sinclair, M.; Gow, P.J.; Grossmann, M.; Angus, P.W. Review article: Sarcopenia in cirrhosis—Aetiology, implications and potential therapeutic interventions. Aliment. Pharmacol Ther. 2016, 43, 765–777.

Singh P, Tapasvi C, Kaur R, Aggarwal S, Nagpal N, Kaur R. Prospective Randomized Comparison of Ultrasound-Guided Percutaneous Needle Aspiration with Percutaneous Catheter Drainage of Liver Abscesses. J Med Sci. 2019;39(2):67–73.

Smego R.A, Bhatti S, Khaliq A.A, Beg M.A. Clinical Infectious Diseases, 37, no. 8, 2003, p. 1073. DOI: 10.1086/378275.

Smego RA, Seanego P. Treatment options for hepatic cystic echinococcosis. Int. J. Infect. Dis. 2005, 9 (2): 69-76.

Soloff EV, Zaheer A, Meier J et al. Staging of pancreatic cancer: resectable, borderline resectable, and unresectable disease. Abdom Radiol (NY). 2018;43(2):301-313.

Søreide, K.; Healey, A.J.; Mole, D.J.; Parks, R.W. Pre-, peri- and post-operative factors for the development of pancreatic fistula after pancreatic surgery. HPB 2019, 21, 1621–1631.

Stanciu C, Daniil C, Strat V, Târcoveanu E. Drenajul biliar percutan extern in icterul obstructiv. Rev Med Chir Soc Med Nat (Iaşi). 1984; 3: 371-374.

Stanciu, C.; Trifan, A. Hepatitis C Virus Treatment Revolution: Eastern European Story. Hepat. Mon. 2015, 15, e28969.

Sumi S, Tamura K. Frontiers of pancreas regeneration. J Hepatobiliary Pancreat Surg. 2000; 7: 286-294

Sung H, Ferlay J, Siegel RL, Laversanne M, Soerjomataram I, Jemal A, et al. Global cancer statistics 2020: GLOBOCAN estimates of incidence and mortality worldwide for 36 cancers in 185 countries. CA Cancer J Clin. 2021;71(3):209-49

Tajima, Y.; Matsuzaki, S.; Furui, J.; Isomoto, I.; Hayashi, K.; Kanematsu, T. Use of the time–signal intensity curve from dynamic magnetic resonance imaging to evaluate remnant pancreatic fibrosis after pancreaticojejunostomy in patients undergoing pancreaticoduodenectomy. Br. J. Surg. 2004, 91, 595–600.

Takahashi S, Murakami T, Takamura M, Kim T, Hori M, Narumi Y, Nakamura H, Kudo M. Multi-detector row helical CT angiography of hepatic vessels: depiction with dual-arterial phase acquisition during single breath hold. Radiology. 2002 Jan;222(1):81-8

Takahashi, N.; Fletcher, J.G.; Hough, D.M.; Fidler, J.L.; Kawashima, A.; Mandrekar, J.N.; Chari, S.T. Autoimmune pancreatitis: Differentiation from pancreatic carcinoma and normal pancreas on the basis of enhancement characteristics at dual-phase CT. Am. J. Roentgenol. 2009, 193, 479–484.

Takayasu K, Shima Y, Muramatsu Y, Moriyama N, Yamada T, Makuuchi M, Hasegawa H, Hirohashi S. Hepatocellular Carcinoma: Treatment with Intraarterial Iodized oil with and without Chemotherapeutic Agents. Radiology 1987; 162: 345-351

Tamm EP, Jones B, Yeo CJ, Maher MM, Cameron JL. Pancreaticogastrectomy and the Whipple Procedure: Radiographic Appearence and Complications. Radiology 1995; 196:; 251-255

Tan, K.C. The Right Posterior Hepatic Notch Sign. Radiology 2008, 248, 317–318.

Tanaka M, Fernández-Del Castillo C, Kamisawa T, et al. Revisions of international consensus Fukuoka guidelines for the management of IPMN of the pancreas. Pancreatology 2017; 17:738–53. 10.1016

Terayama N, Miyayama S, Tatsu H et al. Subsegmental Transcatheter Arterial Embolization for Hepatocellular Carcinoma in the Caudate Lobe. JVIR 1998; 9: 501-508

Tessier DJ, Stone WM, Fowl RJ, Abbas MA, Andrews JC,Bower TC, et al. Clinical features and management of splenicartery pseudoaneurysms: case series and cumulative review ofliterature. J Vasc Surg. 2003;38(5):969-74

The European Study Group on Cystic Tumours of the Pancreas. European evidence-based guidelines on pancreatic cystic neoplasms. Gut. 2018 May; 67(5): 789–804

Thrainsdottir H, Petursdottir V, Blöndal S, et al. Pancreatic mass leading to left-sided portal hypertension, causing bleeding from isolated gastric varices. Case Rep Gastrointest Med, Volume 2014, Article ID 956490, 3 pages EASL Clinical Practice Guidelines: Management of hepatocellular carcinoma. J Hepatol 2018 Jul;69(1):182-236

Tien YW, Lee PH, Yang CY, Ho MC, Chiu YF. Risk factors of massive bleeding related to pancreatic leak after pancreaticoduodenectomy. J Am Coll Surg. 2005;

Tien, Y.W.; Lee, P.H.; Yang, C.Y.; Ho, M.C.; Chiu, Y.F. Risk factors of massive bleeding related to pancreatic leak after pancreaticoduodenectomy. J. Am. Coll. Surg. 2005, 201, 554–559.

Tokuchi, Y.; Suda, G.; Kimura, M.; Maehara, O.; Kitagataya, T.; Kubo, A.; Yoshida, S.; Fu, Q.; Yang, Z.; Hosoda, S.; et al. Possible correlation between increased serum free carnitine levels and increased skeletal muscle mass following HCV eradication by direct acting antivirals. Sci. Rep. 2021, 11, 16616.

To'o KJ, Raman SS, Yu NC, Kim YJ, Crawford T, Kadell BM, Lu DS. Pancreatic and peripancreatic diseases mimicking primary pancreatic neoplasia. Radiographics. 2005 Jul-Aug;25(4):949-65

Trede M, Schwall G, Saeger HD. Survival after pancreatoduodenectomy: 118 Consecutive resections without an operative mortality. Ann Surg. 1990;

Trerotola SO, Jones B, Crist DW, Cameron JL. Pylorus-preserving Whipple pancreaticoduodenectomy: postoperative evaluation. Radiology 1989, 171, 735-738

Trifan, A.; Stanciu, C. Checkmate to liver biopsy in chronic hepatitis C. World J. Gastroenterol. 2012, 18, 5514–5520.

Trivedi, H.D.; Lin, S.C.; Lau, D.T. Noninvasive Assessment of Fibrosis Regression in Hepatitis C Virus Sustained Virologic Responders. Gastroenterol. Hepatol. 2017, 13, 587–595.

Tsiotos GG, Barry MK, Johnson CD, Sarr MG. Pancreas regeneration after resection: does it occur in humans? Pancreas. 1999; 19: 310-313

Tummala, P.; Tariq, S.H.; Chibnall, J.T.; Agarwal, B. Clinical Predictors of Pancreatic Carcinoma Causing Acute Pancreatitis. Pancreas 2013, 42, 108–113.

Udd M, Leppäniemi AK, Bidel S, Keto P, Roth WD, HaapiainenRK. Treatment of bleeding pseudoaneurysms in patients withchronic pancreatitis. World J Surg. 2007;31(3):504-10

Valls C, Andı´a E, Sa´nchez A, Guma` A, Figueras J, Torras J, Serrano T . Hepatic Metastases from Colorectal Cancer: Preoperative Detection and Assessment of Resectability with Helical CT. Radiology 2001; 218:55–60

Varty PP, Yamamoto H, Farges O, Belghiti J, Sauvanet A. Early retropancreatic dissection during pancreaticoduodenectomy. Am J Surg 2005;189:488-491..

Vin Y, Sima CS, Getrajdman GI, Brown KT, Covey A, Brennan MF, et al. Management and Outcomes of Postpancreatectomy Fistula, Leak, and Abscess: Results of 908 Patients Resected at a Single Institution Between 2000 and 2005. J Am Coll Surg. 2008;

Vin, Y.; Sima, C.S.; Getrajdman, G.I.; Brown, K.; Covey, A.; Brennan, M.; Allen, P.J. Management and Outcomes of Postpancreatectomy Fistula, Leak, and Abscess: Results of 908 Patients Resected at a Single Institution Between 2000 and 2005. J. Am. Coll. Surg.2008, 207, 490–498.

Wada, K.; Traverso, L.W. Pancreatic anastomotic leak after the Whipple procedure is reduced using the surgical microscope. Surgery 2006, 139, 735–742.

Wang XJ, Pillai AA. Extrahepatic manifestations of chronic hepatitis C infection: a review and update. Curr Hepatol Rep, 2016, 15(3):150–157.

Wang, H.; Xiu, D.; Tao, M. The pancreatic juice length in the stent tube as the predicting factor of clinical relevant postoperative pancreatic fistula after pancreaticoduodenectomy. Medicine 2017, 96, e8451.

Wani ZA, Bhat RA, Bhadoria AS, et al. Gastric varices: Classification, endoscopic and ultrasonographic management. J Res Med Sci 2015;20:1200–7.

Ward J et al. Liver Metastases in Candidates for Hepatic Resection: Comparison of Helical CT and Gadolinium- and SPIO enhanced MR Imaging. Radiology 2005; 237:170–180

Watanabe M, Usui S, Kajiwara H, Nakamura M, Sumiyama Y, Takada T, Nagakawa T. Current pancreatogastrointestinal anastomotic methods: results of a Japanese survey of 3109 patients. Hepatobiliary Pancreat Surg. 2004; 11: 25-33

Webb GJ, Chapman TP, Cadman PJ, Gorard DA. Pyogenic liver abscess. Frontline Gastroenterol. 2014;5(1):60–7.

Wellner, U.F.; Kayser, G.; Lapshyn, H.; Sick, O.; Makowiec, F.; Höppner, J.; Hopt, U.T.; Keck, T. A simple scoring system based on clinical factors related to pancreatic texture predicts postoperative pancreatic fistula preoperatively. HPB 2010, 12, 696–702.

Winston CB, Lee NA, Jarnagin WR, Teitcher J, DeMatteo RP, Fong Y, Blumgart LH. CT angiography for delineation of celiac and superior mesenteric artery variants in patients undergoing hepatobiliary and pancreatic surgery. AJR Am J Roentgenol 2007;189(1):W13-9.

Witzigmann, H.; Diener, M.K.; Kißenkötter, S.; Rossion, I.; Bruckner, T.; Werner, B.; Pridöhl, O.; Radulova-Mauersberger, O.; Lauer, H.; Knebel, P.; et al. No need for routine drainage

after pancreatic head resection: The dual-center, randomized, controlled PANDRA trial (ISRCTN04937707). Ann. Surg. 2016, 264, 528–537.

Witzigmann, H.; Diener, M.K.; Kißenkötter, S.; Rossion, I.; Bruckner, T.; Werner, B.; Pridöhl, O.; Radulova-Mauersberger, O.; Lauer, H.; Knebel, P.; et al. No need for routine drainage after pancreatic head resection: The dual-center, randomized, controlled PANDRA trial (ISRCTN04937707). Ann. Surg. 2016, 264, 528–537.

World Health Organization. (2001). Puncture, Aspiration, Injection, Re-aspiration : an option for the treatment of cystic echinococcosis / WHO Informal Working Group on Echinocossosis. World Health Organization. https://apps.who.int/iris/handle/10665/67207

Xia, W.; Zhou, Y.; Lin, Y.; Yu, M.; Yin, Z.; Lu, X.; Hou, B.; Jian, Z. A Predictive Risk Scoring System for Clinically Relevant Pancreatic Fistula after Pancreaticoduodenectomy. Med. Sci. Monit. 2018, 24, 5719–5728.

Xia, W.; Zhou, Y.; Lin, Y.; Yu, M.; Yin, Z.; Lu, X.; Hou, B.; Jian, Z. A predictive risk scoring system for clinically relevant pancreatic fistula after pancreaticoduodenectomy. Med. Sci. Monit. 2018, 24, 5719–5728.

Yagci G, Ustunsoz B, Kaymakcioglu N, Bozlar U, Gorgulu S, Simsek A, Akdeniz A, Cetiner S, Tufan T. Results of surgical, laparoscopic, and percutaneous treatment for hydatid disease of the liver: 10 years experience with 355 patients World J. Surg.2005; 29: 1670-9.

Yaghan R, Heis H, Bani-Hani K, Matalka I, Shatanawi N, Gharaibeh K, et al. Is fear of anaphylactic shock discouraging surgeons from more widely adopting percutaneous and laparoscopic techniques in the treatment of liver hydatid cyst? Am J Surg. 2004;187(4):533-7.

Yamada, R.; Sato, M.; Kawabata, M.; Nakatsuka, H.; Nakamura, K.; Takashima, S. Hepatic artery embolization in 120 patients with unresectable hepatoma. Radiology 1983, 148, 397–401

Yamamoto S, Kubota K, Rokkaku K, Nemoto T, Sakuma A. Disposal of replaced common hepatic artery coursing within the pancreas during pancreatoduodenectomy: report of a case. Surg Today 2005;35:984-987.

Yamamoto, Y.; Sakamoto, Y.; Nara, S.; Esaki, M.; Shimada, K.; Kosuge, T. A preoperative predictive scoring system for postoperative pancreatic fistula after pancreaticoduodenectomy. World J. Surg. 2011, 35, 2747–2755.

Yang F, Long J, Fu DL, Jin C, Yu XJ, Xu J, et al. Aberrant hepatic artery in patients undergoing pancreaticoduodenectomy.Pancreatology 2008;8:50-54.

Yang SH, Yin YH, Jang JY, Lee SE, Chung JW, Suh KS, et al. Assessment of hepatic arterial anatomy in keeping with preservation of the vasculature while performing pancreatoduodenectomy: an opinion. World J Surg 2007;31: 2384-2391

Yeo CJ, Cameron JL, Maher MM, Sauter PK, Zahurak ML, Talamini MA, et al. A prospective randomized trial of pancreaticogastrostomy versus pancreaticojejunostomy after pancreaticoduodenectomy. In: Annals of Surgery. 1995.

Yim PJ,Foran DJ. Volumetry of Hepatic Metastases in Computed Tomography Using the Watershed and Active Contour Algorithms 6th IEEE Symposium on Computer-Based Medical Systems (CBMS'03) p. 329

Yorganci K, Sayek I. Surgical treatment of hydatid cysts of the liver in the era of percutaneous treatment. Am J Surg 2002; 184:63–69

Yoshida, K.; Matsui, O.; Miyayama, S.; Ibukuro, K.; Yoneda, N.; Inoue, D.; Kozaka, K.; Minami, T.; Koda, W.; Gabata, T. Isolated arteries originating from the intrahepatic arteries: Anatomy, function, and importance in intervention. J. Vasc. Interv. Radiol. 2018, 29, 531–537

Yosinski J, Clune J, Bengio Y, Lipson H. How transferable are features in deep neural networks? In: Advances in Neural Information Processing Systems. 2014.

Yu SC, Ho SS, Lau WY, Yeung DTK, Yuen EHY, Lee PSF, et al. Treatment of pyogenic liver abscess: prospective randomized comparison of catheter drainage and needle aspiration. Hepatology. 2004;39(4):932–8.

Zeiler MD, Fergus R. Visualizing and understanding convolutional networks. In: Lecture Notes in Computer Science (including subseries Lecture Notes in Artificial Intelligence and Lecture Notes in Bioinformatics). 2014.

Zerem E, Imširović B, Kunosić S, Zerem D, Zerem O. Percutaneous biliary drainage for obstructive jaundice in patients with inoperable, malignant biliary obstruction. Clin Exp Hepatol. 2022; 8(1):70-77

Zhang, Y.; Zhang, X.M.; Prowda, J.C.; Zhang, H.L.; Sant'anna Henry, C.; Shih, G.; Emond, J.C.; Prince, M.R. Changes in hepatic venous morphology with cirrhosis on MRI. J. Magn. Reson. Imaging 2009, 29, 1085–1092.

Zignego AL, Bréchot C. Extrahepatic manifestations of HCV infection: facts and controversies. J Hepatol, 1999, 31 31(2):369–376.

Zins M, Sauvanet A. Pancreas et duodenum. În: Zins M, Sauvanet A (eds) Imagerie de l'appareil digestif opéré. Ed.Flammarion, 1999, Paris, p : 39-62

Zollinger RM Jr, Zollinger RM. Atlas of surgical operations (7th ed.). McGraw-Hill Inc., New York, 1993; 1-285, 420-440

*** PAIR: Puncture, Aspiration, Injection, Re-Aspiration- An option for the treatment of Cystic Echinococcosis World Health Organization. Untitled-1 (who.int)